



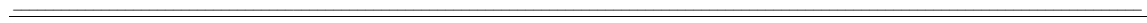
EURISOL DS Project TASK 2: Multi MW target station

Deliverable N°D2 Innovative Waste Management in the Liquid Hg-Loop


Planned Date (month): 39

Achieved Date (month): 52

Lead Contractor(s): P18 (PSI)



Project acronym: *EURISOL DS*
Project full title: *EUROPEAN ISOTOPE SEPARATION ON-LINE
RADIOACTIVE ION BEAM FACILITY*
Start of the Project: *1st February 2005*
Duration of the project: *54 months*

RIDS 515768 TASK: 2	DATE: 25/05/09	
DELIVERABLE: D2	PAGE 1	

Innovative Waste Management in the Mercury Loop of the EURISOL Multi-MW Converter Target

Jörg Neuhausen^a, Dorothea Schumann^a, Rugard Dressler^a, Susanne Horn^a, Sabrina Lüthi^a, Stephan Heinitz^a, Suresh Chiriki^a, Thierry Stora^b, Martin Eller^b

^aRadWaste Analytics
Laboratory for Radio- and Environmental Chemistry
Paul Scherrer Institut
CH-5232 Villigen PSI

^bCERN, ISOLDE
CH-1211 Geneve 23

1. Overview

The EURISOL Design Study (EURISOL-DS) is concerned with the design of a next-generation ISOL facility that should deliver Radioactive Ion Beams (RIB) several order of magnitudes more intense than the facilities that exist now (CERN-ISOLDE [1], TRIUMPH-ISAC [2], SPIRAL [3]) or are in preparation (SPIRAL2) [4]. A schematic view of the facility is shown in figure 1. One important component of the facility is the Multi-MW converter target, where an extremely high flux of fast neutrons is produced in a liquid metal target. These neutrons are then used to produce exotic short lived neutron rich nuclides in surrounding fission targets. The design of this target is illustrated in Figure 2. Mercury has been chosen as the target material for this liquid metal target.

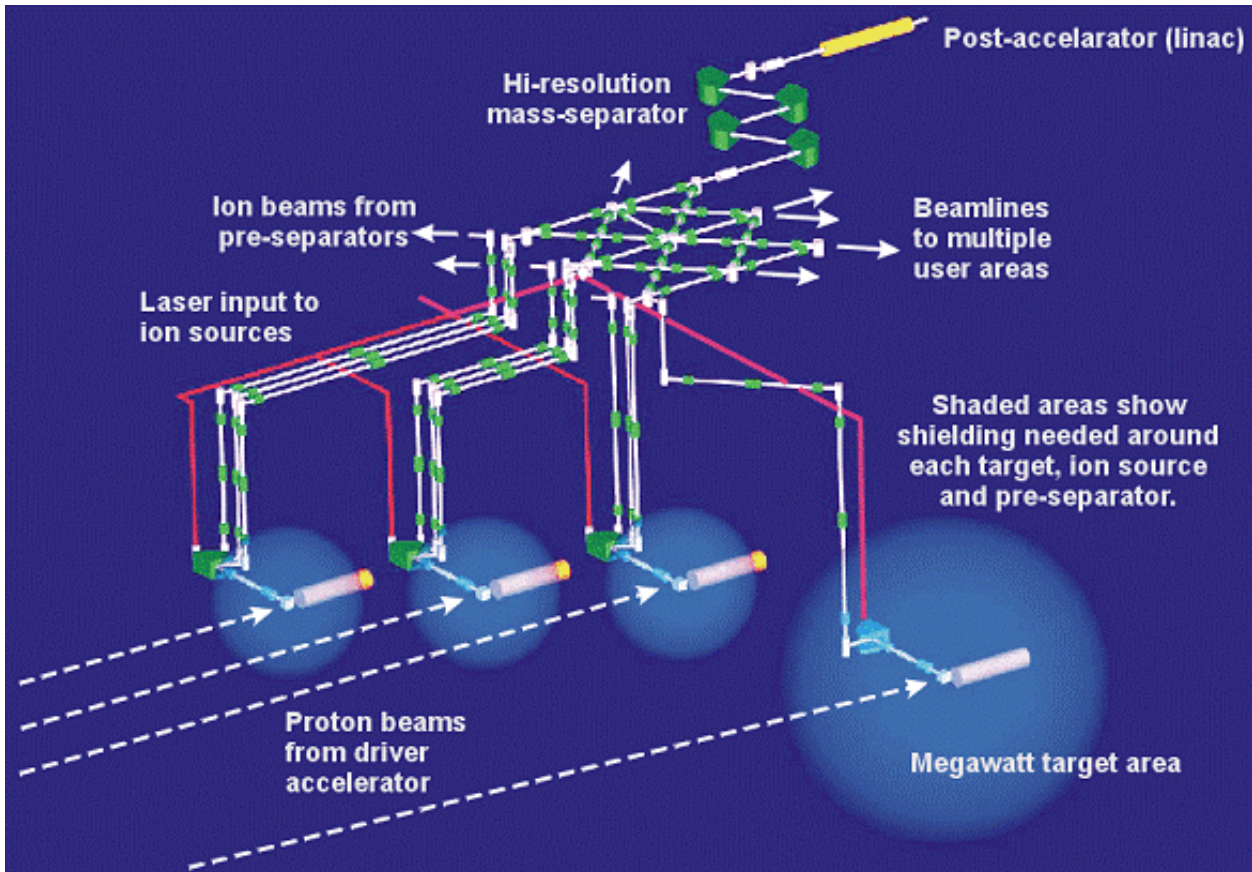


Figure 1: A schematic overview of the planned EURISOL facility comprised of three solid 100 kW target stations and one Multi-Megawatt liquid metal target station as proposed in [5].

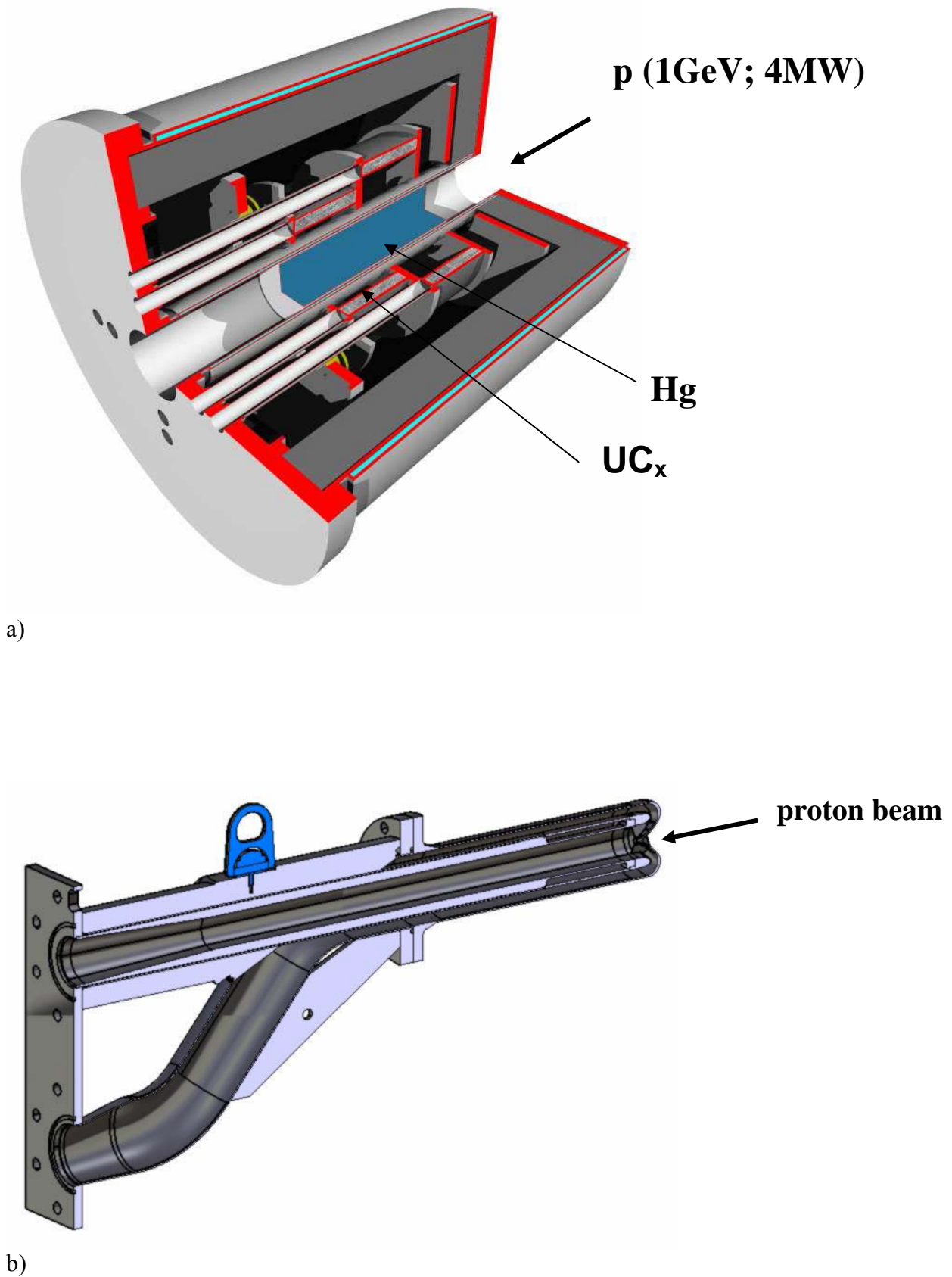


Figure 2: Different views of the EURISOL-DS liquid mercury Multi-MW converter target. a) an earlier design used for neutronics calculations [6] showing the liquid metal target and the surrounding UC_x targets. b) a recent design of the Hg target and its connections to the loop [7].

The choice of mercury as target material imposes various questions concerning the safe operation of such a system that are related to the physical and chemical properties of the target material itself and the nuclear reaction products produced within the target during its life time of several decades. Therefore, a subtask was created within the EURISOL-DS project that is concerned with studying an innovative waste management for the generated radioactivity by chemical means. Such a study strongly depends on the radioactive inventory and its distribution throughout the target and loop system. Radioactive inventory calculations were performed within task 5 [6]. The distribution of nuclear reaction products and their chemical state that can be expected within the target and loop system is one of the topics covered in this report. Based on the results obtained by theoretical studies as well as laboratory scale experiments, the feasibility of waste reduction using chemical methods, both conventional (e.g. leaching, distillation) and innovative (e.g. surface adsorption) are studied experimentally. The results and their implications on separation procedures that can be favourably applied to a spallation target system are discussed with respect to both handling of the radioactive waste and extraction of valuable nuclides for medical, scientific and industrial applications.

1.1. Nuclide inventory

A large amount of radionuclides ranging from atomic number $Z=1$ to 81 will be produced by various nuclear reactions in the liquid mercury target during long term irradiation. Figure 3 illustrates this process and shows the corresponding accumulation of nuclear reaction products - both stable and unstable - in the mercury system calculated using MCNPX [6]. In the graph, the concentrations of nuclear reaction products are given in atom-ppm after 40 years of irradiation with a 1 GeV proton beam of up to 4 MW. For the calculation of the concentrations of the elements, a homogeneous dilution of the produced radionuclides in the 11 tons [7] of mercury is assumed. Details of the nuclear calculations can be found in [6]. It is shown that the concentrations of the elements produced by nuclear reactions reached at the end of irradiation are as high as several hundred ppm. It is immediately clear that the produced radioactivity causes safety problems, both during operation and at the stage of intermediate and final disposal. Moreover, the masses and concentrations of elements that are produced in the liquid metal imply that also chemical effects that are only expected to play a role for macroscopic amounts of impurities have to be taken into account.

In the following sections we discuss the three most important aspects that arise from the consequences of the generation of impurities by nuclear reactions. Generally, we focus on elements that exist in the condensed state under the operation conditions of the target. Gaseous nuclear reaction products such as hydrogen and noble gases have already been treated in studies of the already operating mercury spallation sources [8].

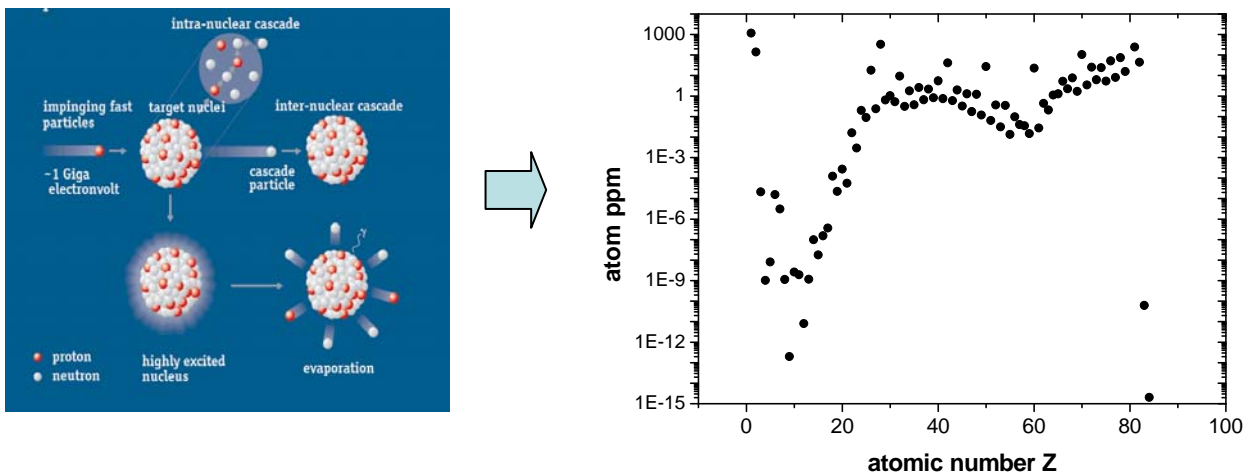


Figure 3: Nuclear reactions leading to the formation of impurities in the mercury.

1.2. Radiation safety aspects

A reliable and safe operation of a high-power liquid target with a foreseen operational time of around 40 years requires careful studies and estimations on all the probable hazards. One of the key issues in this context is the behaviour of the target material and the induced radionuclides during operation and with regard to decommissioning and disposal. Therefore, safety aspects are related to both radiation effects during operation and the long-term behaviour of dangerous radionuclides. Consequently, we have to distinguish between measures taken for reducing the dose rate during operation and conditioning of irradiated material foreseen for a disposal.

Unfortunately, mercury itself is a highly toxic material from the chemical point of view. Additionally, one of the most hazardous of all radionuclides produced in a mercury target (concerning the amount of induced activity as well as the half-life) is ^{194}Hg with a half-life of 520 years. For the dose rates within the operating period, shorter lived mercury isotopes play an important role. A chemical separation of these mercury isotopes is not possible. On the other hand, removal of hazardous nuclides of elements different from mercury (e.g. the α -emitter ^{148}Gd with a half-life of 75 y) before final disposal may be a useful step. This depends on the final disposal strategy, which is also a subject of EURISOL-DS. All considered purification procedures have to be evaluated carefully concerning the two aspects of operational dose rate reduction and conditioning for final disposal.

All radionuclides of elements different from mercury can, in principle, be removed from the liquid metal by chemical means. However, such separations are not straight forward, since they require much effort and cost because known procedures have to be transferred to a highly radioactive environment, and in case of the application of novel methods even more R & D is necessary for the fundamental development of the separation methods and for their transfer to a technical scale.

1.3. Conventional operational safety aspects

Safety aspects that are not directly related to the radioactivity of the nuclear reaction products but result from physical or chemical effects generated by the presence of weighable amounts of impurities are numerous. They may include plugging of tubes or filters, viscosity changes that may be caused by the presence of dissolved material in the liquid metal, changes in the wetting behaviour of the liquid metal and also deposition of material on the walls of the loop. These phenomena have so far been neglected as they seemed to be less important compared to

radiological problems. However, in our view they may have serious consequences on the safe and reliable operation of a liquid metal target system. It is known, for example, that dissolved metals such as iron can drastically change the viscosity of mercury, leading to a “butter-like” texture of the metal at impurity concentrations in the percent range. Obviously, this occurs in technical procedures performed using mercury in steel containers such as chlorine production electrolysis cells using flowing mercury cathodes [9, 10]. While it is not clear whether such phenomena can occur in a spallation target system, the possibility of their occurrence should be kept clearly in mind. Another example is the deposition of material on the walls of the heat exchanger, which may change the heat transfer characteristics significantly.

The first experiences with working mercury spallation sources show that such deposition phenomena actually occur [11]. Of course, as a secondary effect, these depositions also have radiological consequences since radioactive nuclides will be highly enriched in the deposited material. In the Japanese spallation source JSNS that was recently put into operation these deposition phenomena already lead to a change of maintenance procedures that became necessary because of higher radiation doses resulting from radioactive materials sticking to the tubing after draining the mercury [12]. Finally, for the development of a concept for radioactive waste management, knowledge of the distribution of the radioactivity between liquid metal and the walls of target components is mandatory.

1.4. Isolation of medically and industrially interesting isotopes

Commercial production routes for medical and industrial radionuclides are presently reaching their limitations. Consequently, alternative ways for the production of such nuclides, through cooperation between different branches of science at large fundamental physics oriented facilities, are presently being explored. About 80% of the worldwide production of radioisotopes is for medical purposes. Positron Emission Tomography (PET) is an important development in this field and is an excellent illustration of the application of nuclear physics to medicine. The demand for medical isotopes has recently been changing – a trend that will continue in the coming years. New approaches in systemic radioisotope therapy require radionuclides that have different nuclear properties compared to those used for diagnostics. There are a number of radionuclides, especially lanthanides, with great potential for therapeutic application. One of these prospective radionuclides is the α -emitter ^{149}Tb . Additionally, some long-lived isotopes suitable for use in generators, such as $^{188}\text{W}/^{188}\text{Re}$, $^{82}\text{Sr}/^{82}\text{Rb}$ or $^{44}\text{Ti}/^{44}\text{Sc}$ are promising from the medical point of view.

However, medical use is not the only field of application where radioactive isotopes are much-needed. Exotic radionuclides with comparatively long half-lives, such as $^{7/10}\text{Be}$, ^{26}Al , ^{53}Mn , and ^{60}Fe , together with many others, are of great interest in research domains like astrophysics, nuclear structure, geophysics, fundamental nuclear physics and developments in the new nuclear power generation. A large-scale facility like the planned EURISOL implies the possibility to extract these valuable radionuclides for industrial-scale production, due to the high beam intensity and available target material [13]. The radionuclide spectrum of the residues produced in a spallation target is known to be very different from that produced in nuclear reactors. From both a scientific and technological viewpoint many of these isotopes are of great interest for future research and in fact cannot be produced through other means.

Depending on the half-life of the desired isotope, on-line and off-line separation techniques have to be considered. Medical applications additionally require - in any case - a following mass separation (with exception of generator-based nuclides; see later-on). As a result, extremely high-sophisticated, quick and easy-to-handle separation procedures have to be developed, especially for directly produced short-lived radio-labelled pharmaceuticals. One exclusion in the medical sector are the so-called "generator systems", where a long-lived mother nuclide is produced in the

initial nuclear reaction, and the desired daughter nuclide can then be continuously separated by chemical means for a time span depending on the half-life of the mother nuclide [14, 15].

1.5. The scope of this study

The facts collected above show that a reduction of the radioactive inventory by chemical purification of the mercury before disposal does not reduce the dose much, because the main hazardous activity is associated with the mercury itself. Nevertheless, it could be beneficial to remove the non-mercury-carried activity before disposal, since the behaviour of these radioactive species within the disposed material is not known and may cause serious problems. Additionally, a purification of the mercury may make sense to mitigate operational problems caused by the nuclear reaction induced impurities, reduce the dose received during maintenance operations and lower the contamination of replacement components, e.g. the target window. A useful and may be economically interesting “by-product” of the purification of the mercury could be the extraction of useful radionuclides.

The present study is aimed to provide knowledge that is required for a decision if a purification of the mercury used as target material in EURISOL is necessary and useful, both from a technical and an economical point of view.

One of the crucial factors for the development of a working purification procedure is knowledge about the chemical state and the behaviour of the impurities that have to be removed within the system. To make reasonable statements about this chemical behaviour we collect literature data about the properties of mercury itself and the interaction of elements with mercury. Semi-empirical calculation of some thermodynamic data help to fill some gaps in the literature data. A spallation target is a highly complex system with an 80+ elements mixture. For such a system, exact predictions are not possible, but from literature knowledge and theoretical studies it is possible to draw reasonable conclusions on the behaviour of radionuclides in liquid mercury. Furthermore, we study the behaviour of radionuclides in mercury experimentally, using proton irradiated mercury samples as well as mixtures of mercury with activated elements. We also gather knowledge about conventionally applied purification procedures for mercury and study their applicability for the removal of tracer radionuclides experimentally. Additionally, we study innovative purification concepts based on radiochemical separations. Considering the use of irradiated mercury for nuclide production, due to limited resources as well as a lack of basic studies concerning the radionuclide inventory, we will concentrate on only a few examples as models for medical interesting isotopes, with the purpose to give a rough estimation if such a venture could be commercially interesting.

Finally, we summarize the gained information and to our best knowledge comment on the feasibility and economical sensibility of various mercury purification strategies.

2. Review of literature

In this section we will give a short overview of physical and chemical properties and phenomena that play a role for the behaviour of mercury in a spallation environment. We will keep this section rather short, pointing to the large available literature base. Consequently, we will focus on pointing out the influences that impurities can have on these properties and discuss the peculiarities of the spallation target environment. We will not discuss any nuclear properties that are not related to the production of impurities and hence do not have any effect on chemical phenomena.

2.1. Physical properties

2.1.1. State of aggregation

The most important physical property of mercury concerning its application in a liquid metal spallation target is its liquid state of aggregation under ambient conditions. On one hand, this makes heating devices to prevent freezing of the target material unnecessary. On the other hand, the liquid state under ambient conditions poses additional risks for accident cases. Here, mercury remains in the liquid state, which makes the containment of radioactivity and the clean-up more difficult. A target material that solidifies under ambient conditions can act as “first enclosure” for the radioactivity and can be removed more easily. Additionally, mercury has a low boiling point of 357°C and consequently a relatively high vapour pressure [16]. Together with its high chemical toxicity and the large amount of radioactivity associated with it, the volatility of mercury makes it an unfavourable choice concerning the mitigation of accident scenarios.

2.1.2. Surface effects

The surface tension of mercury is of importance with respect to the wetting of construction materials, which on his part has consequences e.g. on corrosion effects and heat transfer. The surface tension of mercury has been studied for more than 200 years. An extensive survey of the results can be found in [17]. This review shows that even for such a fundamental property, the results obtained in about 200 independent studies show a wide range of variation. Possible reasons for these variations are investigated in the paper. One reason found is the accumulation of impurities on the surface. As a related effect, metals dissolved in mercury change the surface tension in an unpredictable way due to formation of complex intermetallic compounds and surface reactions of the dissolved material with the adjacent gas phase. In a spallation target system similar phenomena will occur that will lead to unpredictable surface effects. Apart from the changes in surface tension, the observed effects of impurities indicate that an accumulation of impurities in various chemical forms on the mercury/cover-gas interface of the spallation loop can be expected. Furthermore, dissolved metals are found to be extremely reactive due to their atomic state in solution, and the material accumulated on the surface shows a catalytic effect on mercury oxidation. The consequences of these effects will be discussed in more detail in the chapters covering the chemical behaviour of nuclear reaction generated impurities.

2.1.3. Viscosity

The influence of additives on the viscosity of mercury has mostly been studied for metals that show a relatively high solubility but no strong chemical interaction with mercury (see chemical classification below: Zinc-Type) [18, 19]. For these additive metals, the viscosity of mercury increases with increasing concentrations of the impurities. However, for concentration that are expected to occur within the EURISOL mercury loop, no dramatic changes in viscosity are expected from the production of these elements. However, it is known from experience with the operation of electrolytic cells for the production of chlorine, using mercury as a cathode, that so-called “thick” mercury is formed [9, 10]. This material can contain either large amounts of alkaline metals or large amounts of iron, possibly from corrosion processes of the construction materials. This material has a butter-like consistency and accumulates in regions with low flow rates. This behaviour is known also from fundamental laboratory experience. Mercury sodium mixtures become solid already at sodium concentrations of 1.5 % [20], while mercury iron mixtures become considerably more viscous at concentrations above 1 % and assume the butter-like consistency at 3 % [21]. Naturally, such a behaviour can cause serious problems concerning the mercury flow. Although the concentrations of nuclear reaction produced impurities in the EURISOL spallation loop are lower, it can not be ruled out that a combination of various impurities can lead to dramatic viscosity changes or at least formation of local deposits with increase viscosity. Corrosion of steel components may be enhanced in the high radiation field and complex chemical environment of a spallation loop (see below). Therefore, it cannot be ruled out that rather high concentrations of iron can occur in the liquid metal.

2.2. Chemical behaviour of mercury

Mercury is a noble metal that can easily be obtained from its ores and is also found in elemental form in nature. Pure mercury shows a silvery metallic lustre that remains stable under ambient conditions in air. Mercury which contains impurities oxidizes much more rapidly, leading to the formation of a thin layer of oxide on the surface of the liquid metal. This catalyzing effect of impurities on the oxidation of mercury was already mentioned in chapter (surface tension). The formation of such an oxide film can strongly change the wetting behaviour and also lead to the precipitation of solid materials at unwanted locations. The formation of mercury oxide within a spallation loop will depend on several factors such as the balance between the amount of oxygen present (e.g. in form of oxide layers on the construction materials) and the amount of hydrogen produced by proton irradiation.

Mercury reacts readily with chalcogens and halogens that will be formed by nuclear reactions. In this way, it will compete with other metals generated by nuclear reactions to bind these elements. Generally, many metals form halogenides and chalcogenides that are more stable than those of mercury. However, mercury is present in the target system in a vast excess. During target operation, the distribution of halogens and chalcogens between mercury and other impurity metals will also depend on the reductive potential, which is influenced by the production of hydrogen during irradiation and hydrogen consumption by out-gassing or reduction of oxides.

Mercury dissolves various metals and forms alloys with them. This behaviour is essential for understanding the chemical processes that will occur in liquid mercury that is contaminated with both nuclear reaction and corrosion induced impurities. Therefore, we discuss these topics in more detail in the following chapter.

2.2.1. Solubility of metals in mercury and reactivity of metals with mercury

Both the solutions of metals in liquid mercury as well as solid phases containing mercury and a second metal are referred to in literature as amalgams. Even colloidal solutions of metals in mercury are often designated amalgams. For clarity, we will use the term amalgam in this report for defined compounds of mercury with a certain metal only, while atomically dispersed liquid and solid solutions as well as colloidal solutions will be designated as such.

The available data on the solubility of metals in mercury are reviewed in [22]. In general, the metals can be divided into three groups with respect to their solubility in mercury and their tendency to react with mercury [23]:

- a) Iron-Type: These metals are almost insoluble in mercury and do not form stable alloys (amalgams). For instance, for chromium, iron, and cobalt it is known that the solutions contain the metals in form of suspended particles of the pure metals and not in an atomically dissolved state [24].
- b) Zinc-Type: These metals show high solubility in mercury. In the solid state they form solid solutions rather than defined compounds.
- c) Sodium-Type: Metals of this type show a high chemical affinity to mercury. They form numerous stable stoichiometric compounds (amalgams) with mercury. Their solubility in mercury is generally low, but much higher than that of the metals of the iron-type.

A graphical representation of the classification of the different metals and their arrangement in the periodic table of the elements is shown in Figure 4. From this graph it becomes clear that many of those elements that are formed in rather large amounts by nuclear reactions belong to the less soluble types. Furthermore, it has to be pointed out that the solubility of some of the most important nuclear reaction products formed in a mercury target by both spallation (Ta, W, Re, Os) and fission reactions (Mo, Tc, Ru) have not reliably been determined experimentally, probably because of their extremely low solubility and resulting analytical problems. To overcome this lack of data, we performed an estimation of the solubilities of metals in mercury, based on thermodynamic principles and using thermodynamic data calculated with a semi-empirical cellular method. The method and results are discussed in chapter 3. These results can also serve as an aid for the assessment of the reliability of experimental solubility data, which are often error-prone due to extreme experimental difficulties.

		<div style="display: flex; justify-content: space-around; align-items: center;"> <div style="width: 20px; height: 20px; background-color: red; margin-right: 5px;"></div> Iron type <div style="width: 20px; height: 20px; background-color: green; margin-right: 5px; margin-left: 20px;"></div> Zinc type <div style="width: 20px; height: 20px; background-color: blue; margin-left: 20px;"></div> Sodium type </div>										B	C	N	O																														
Li	Be																																												
Na	Mg											Al	Si	P	S																														
K	Ca	Sc	Ti	V	Cr	Mn	Fe	Co	Ni	Cu	Zn	Ga	Ge	As	Se																														
Rb	Sr	Y	Zr	Nb	Mo	Tc	Ru	Rh	Pd	Ag	Cd	In	Sn	Sb	Te																														
Cs	Ba	La	Hf	Ta	W	Re	Os	Ir	Pt	Au	Hg	Tl	Pb	Bi																															
<table border="1" style="width: 100%; border-collapse: collapse;"> <tr> <td>Ce</td><td>Pr</td><td>Nd</td><td>Pm</td><td>Sm</td><td>Eu</td><td>Gd</td><td>Tb</td><td>Dy</td><td>Ho</td><td>Er</td><td>Tm</td><td>Yb</td><td>Lu</td> </tr> <tr> <td>Th</td><td>Pa</td><td>U</td><td colspan="13"></td> </tr> </table>																Ce	Pr	Nd	Pm	Sm	Eu	Gd	Tb	Dy	Ho	Er	Tm	Yb	Lu	Th	Pa	U													
Ce	Pr	Nd	Pm	Sm	Eu	Gd	Tb	Dy	Ho	Er	Tm	Yb	Lu																																
Th	Pa	U																																											

Figure 4: Classification of metals considering their solubility and their reactivity towards mercury (see text for an explanation).

A spallation target system based on mercury is a highly complex system already considering its composition only (80 impurity elements), for the time being neglecting processes like transport phenomena and radiolytic effects and their influence on chemical processes. Therefore, we limit our discussion of chemical reactions to the very basic classification given above and only give a short overview of more complicated phenomena that have been observed. Naturally, the vast majority of fundamental studies concerned with the chemical reactivity of mercury with other metals deal with binary combinations of one metal with mercury. For these systems, the classification given above gives a good idea on the behaviour of the second metal with mercury. The situation becomes more complicated when one adds one or more components to the binary mixtures. Such mixtures have been investigated concerning the use of mercury as a solvent for the low temperature production of alloys of elements dissolved in mercury [25]. In such systems, both the formation of insoluble binary or ternary mercury-alloys [26] as well as the formation of binary or ternary alloys of the dissolved metals [27-31] was found. Such processes have been applied technically in branches of metallurgy called extractive metallurgy and amalgam metallurgy. Reviews of these reactions and their use for technical processes can be found in [23, 32]. Direct extrapolations of these procedures to a spallation target environment are not possible, but the results of these studies give a hint on the type of reactions that can be expected in a mercury spallation loop, where the complexity rises to an inconceivable degree. In this sense, we consider the understanding of binary interactions a fundamental requirement for an assessment of more complex systems.

2.2.1.1. Physical and chemical properties of solutions of metals in liquid mercury

The physical and chemical properties of diluted solutions of metals in mercury decisively influence the behaviour of nuclear reaction products that are generated in a mercury spallation target. Solutions of the iron-type metals are known that they tend to form colloidal solutions that show aging phenomena, resulting in a slow growth of the particles [32, 33]. With increasing size,

these particles will show a tendency to deposit on the ground or float to the top part of the system, depending on their density. For sure, a part of this material will be continuously carried around in the loop by the flowing liquid metal. More complications arise from the polynary character of the mixture that can cause the formation of particles of complex composition. Furthermore, temperature gradients will influence the dissolution, growth and coagulation processes. The formation of particles can lead to enhanced erosion effects in the liquid metal loop.

Both the elements of the sodium- and zinc-type groups metals are known to be sensitive to oxidation when dissolved in mercury, the former showing a reduced affinity to oxygen compared to the pure metal, while the latter show an increased reactivity towards oxygen. This statement will hold also for the reactivity towards other chalcogen elements such as sulphur, selenium and tellurium and the halogens. Oxygen is present in a spallation system in form of the oxide layers of construction materials, while the higher chalcogens and halogens are formed in concentrations up to some ppm by nuclear reactions. It is probable that the halogens and chalcogens react with the metals of the sodium and zinc groups. However, the extent of these reactions will depend on the reductive potential of the system, which is largely determined by the amount of hydrogen present. The latter will vary with irradiation. There is also a possibility that the oxide layers of construction materials are attacked by those metals showing the highest affinity to oxygen, i.e. the metals of the sodium-type. Overall, these effects will probably lead to the formation of chalcogenides, halogenides and mixed compounds containing more than one type of metal, chalcogens and/or halogen. These compounds will in general be insoluble in mercury and in most cases have a lower density than the liquid metal. Therefore, they will tend to accumulate at the top parts of the loop. As an additional consequence, the attack on the protective oxide layer of the construction materials may enhance corrosion phenomena.

2.2.1.2. Preparation of diluted solutions of metals in mercury

For the preparation of model samples used to study the behaviour of radioactive metals dissolved in liquid mercury, the dissolved component can be introduced to the liquid metal in different ways. The most straight forward technique, favourably applicable to those metals with a high solubility in mercury, involves simply mixing of an appropriate amount of the metal with mercury. More elaborate techniques make use of electrochemical deposition of metals on a mercury cathode or the exchange of metals dissolved in the liquid metal by more noble metals in so-called phase change reactions. A summary of these methods is given in [23].

2.2.2. Wetting and corrosion in Hg

The wetting of various metal surfaces by liquid mercury has been studied in [34]. In a general statement it can be said that metals of the Zinc-Type are normally easily wetted, whereas those of the iron-type can only be wetted by mercury after vigorous etching and intensive chemical or mechanical treatments, followed by an immediate exposure of the newly created metal surface to the liquid metal. In [34] it is shown that surfaces of iron-type metals that are cleaned by ion beam bombardment are wetted by mercury. For the non-cleaned surfaces, impurities such as oxide or adsorbed gas layers inhibit the wetting mechanism, while on the ion bombarded surface an adsorption layer of mercury forms on the surface that facilitates wetting. Similar effects of improved wetting of the surfaces inside the spallation loop due to cleaning effects, caused by the high radiation field, could also occur in parts of the spallation target system, especially at or near the target window.

The corrosion of various metals in mercury has been studied in [35]. As expected, the results indicate that the insoluble metals of the iron-type generally show the best corrosion resistance, while the corrosion resistance of the soluble and reactive metals towards mercury is poor. More interesting for the case of a spallation system are specific studies of steel corrosion in mercury and its inhibition or promotion by additives. It has been shown that small quantities of added metals have an influence on both wetting and corrosion. For example, magnesium or aluminium are typically added as deoxidizer and to promote wetting, while titanium and zirconium additions show an inhibiting effect on the corrosion of some steels in mercury [36]. Others studies show that combinations of different additives may also promote corrosion effects [37] (in this case on titanium surfaces). For a spallation target system, in principle we have to consider the effects of 80 additives combined together. From this, it becomes immediately clear that a reliable prediction of the influence of nuclear reaction induced impurities on wetting and corrosion in a mercury spallation target and loop is impossible. In practice, it may turn out that the cocktail of impurities produced in a spallation target may either promote or inhibit corrosion effects. Even a change in this behaviour during the decades of operation may occur.

Based on the literature knowledge summarized in the preceding sections, we will illustrate the chemical complexity of a liquid mercury spallation target system in the following chapter.

2.3. Liquid metal targets as a chemical system

From a physicochemical point of view, a liquid metal spallation target is an extremely complex heterogeneous multi-component system, comprising macroscopic phases such as construction materials, the liquid metal and the cover gas plenum, as well as many micro-components. The latter can be present in different concentrations and chemical states, depending on operating conditions such as temperature, pressure, liquid metal flow, redox potential and proton dose.

These micro-components are of different origin. Gaseous impurities include oxygen, nitrogen and water. The construction materials contribute oxides, nitrides and carbides, apart from their main components and alloying elements. Furthermore, in a target using liquid mercury as target material, all elements from the periodic table ranging from atomic number 1 (hydrogen) up to 81 (thallium) will be produced in considerable amounts by nuclear reactions such as spallation, fission, fragmentation and activation. These elements can undergo chemical reactions with the macro-components and among each other.

A continuous transport of material is caused by the flow of the liquid metal as well as gradients in temperature and chemical potential. As a result, mobilization, transport and deposition processes can occur in the system. Here, mobilization processes are mainly dissolution processes such as corrosion. Additionally, the fast flowing liquid metal can cause erosion of the construction materials. This effect can be strongly enhanced by the presence of hard solid particles suspended in the liquid that can be formed by precipitation of insoluble phases as well as by breaking-off

crystallites from the construction materials in corrosion processes. Furthermore, gas phase transport processes involving gaseous or volatile species can occur.

Surface properties of the construction materials may be altered by diffusion processes, where materials can be transported from the construction materials to the liquid phase or in opposite direction, i.e. from the liquid to surface layers and/or the bulk solid phase. These diffusion processes are enhanced by the strong radiation field, especially in vicinity of the target window, but also to a lesser extent in the complete target system.

Precipitation processes can include formation of local coatings as well as formation of mobile insoluble particles. As a consequence of the chemical complexity of the system, the nature of precipitations is expected to be equally complex. In principle, formation of metallic or intermetallic platings on metal surfaces have to be considered as well as the precipitation of particles of intermetallic phases, oxides, salts, nitrides or hydrides. These materials, depending on their wetting properties, their density difference compared to the liquid metal and their particle size, can remain suspended in the liquid or accumulate e.g. at the liquid/gas interface, at the walls of the target or liquid metal loop or sediment at the bottom at positions with low flow rate or during maintenance periods when the liquid metal flow is stopped.

Taken as a whole, transport processes cause a continuous chemical stress for the integrity of the complete liquid metal target and loop system. This also includes the degradation of passivating surface layers and embrittlement of construction materials caused by dissolution or incorporation of certain components. The presence of halogens and chalcogens produced by nuclear reactions can have catalyzing effects on degradation and corrosion processes. The hydrogen-water vapour pressure ratio, which is determining the reductive potential, is one parameter that is decisive for the chemical state of different components. This ratio is not known a priori, nor is it constant within the operation period of the target unless special measures such as integration of an oxygen control system are taken.

Overall, an inhomogeneous distribution of nuclear reaction products has to be expected for a liquid metal target system. The implications for operation and maintenance of the systems are numerous: The formation of surface layers throughout the complete target and loop system and the distribution of radionuclides between surfaces and bulk mercury are largely dependent on the operating conditions. At the start-up, the concentration of nuclear reaction and corrosion products is very small. Therefore, homogeneous surface layers cannot be formed. On the other hand, because of the high ratio of adsorption sites on surfaces compared to the number of impurity atoms present at an early stage of operation, it is likely that a substantial fraction of the radionuclides produced are adsorbed on the surfaces. With increasing irradiation time the concentrations of nuclear reaction and corrosion products will get larger and larger. This can lead to an overall increasing ratio of radionuclides carried with the liquid metal, compared to the adsorbed material. Additionally, coatings could be formed, preferably at special positions such as the heat exchanger, where elements or compounds with low solubility could precipitate at the relatively low temperatures present. This could lead to changes in heat conduction, resulting in a change of performance of the heat exchanger. In general, an inhomogeneous distribution of decay heat and radiation has to be taken into account. This has consequences e.g. for shielding calculations or maintenance operations at different components. Furthermore, the accumulation of nuclear reaction products in form of insoluble chemical compounds with lower density compared to the liquid metal at the liquid/gas interface may lead to enhanced evaporation of volatiles, caused by decay heat.

2.3.1. The chemical state of nuclear reaction products in a liquid mercury target

Apart from its function as target material and heat transfer medium, mercury in a liquid metal spallation target acts as a solvent and reaction medium for nuclear reaction and corrosion products. Initially, nuclear reaction products will be present in the target in atomically dispersed form until reaching a certain saturation concentration, unless they react with another chemical species to form a compound. After such a reaction, the solubility of this compound in the liquid metal determines the state of the element under consideration within the system. The solvent mercury, which is present in a large excess, has to be considered to be a principal reaction partner for nuclear reaction products that are present in the system in a highly excited state and hence are very reactive. However, there are compounds that are much more stable than the corresponding compounds of nuclear reaction products with mercury. Consequently, mercury can be displaced from the primary chemical reaction products by other impurities. Therefore, it is expected that finally various other compounds are formed from all the elements present, leading to a minimization of the Gibbs free energy of the system. With increasing irradiation time, reactions of nuclear reaction products among each other become more probable because of the higher concentrations.

From the situation described above, it is concluded that the solubility of elements and compounds plays an important role in the understanding of nuclear reaction product behaviour in liquid mercury. Though there is an extended compilation and review of literature data on the solubility of metals in mercury [22], data for some of the most prominent nuclear reaction products formed in a mercury spallation target are missing. Therefore, we calculate solubility data for elements in mercury, based on thermodynamic relations and data obtained using a semi-empirical method. The method and the results are presented in chapter 3. We compare these results with literature data and discuss the consequences for a liquid mercury target.

Finally, the interaction of nuclear reaction products with the liquid metal and among themselves will have a decisive influence on their chemical state within the target system. In principle, the chemical state of the different components can be evaluated based on thermodynamic data, e.g. using the method of Gibbs free energy minimization. However, this requires a complete and consistent set of thermodynamic data (enthalpies and entropies as well as their temperature dependence) for all possible species/phases/compounds that could be formed in the system. For a system comprised of more or less all elements of the periodic table such as a liquid mercury target, i.e. a system comprising 80 different elements, this seems unrealistic: approximately 3500 binary combinations would have to be considered, whereas the ternary combinations already amount to approximately 95000. We abstain here from giving numbers for more complex systems.

In reality, the number of possible phases or species will be even much larger because there may well be more than one phase/species/compound per binary system. Furthermore, in such a complex system the formation of ternary, quaternary and more complex phases can be expected. Even the formation of hitherto unknown phases is possible. On the other hand, even for binary combinations literature values for thermodynamic data are incomplete. In this respect, dealing with the chemical behaviour of nuclear reaction products in liquid metal targets puts one on the frontier of inorganic chemistry. Consequently, a complete and consistent dataset comprising all possible phases and species, whether obtained from experimental investigations or from first principles calculations, is out of reach. With the Miedema model [38], we have a tool that enables us to calculate approximate values for the standard enthalpies of formation of binary combinations of the elements of group 1 to 16 in the periodic table as well as the partial molar enthalpies of solution in such binary systems. Although the model can give only approximate data, in most cases the results of calculations represent well the periodic behaviour of the elements and in this way can give a foundation for the estimation of the behaviour of different elements in a liquid metal target system. The Miedema model was extended to ternary systems

and has been used for the prediction of their properties such as enthalpy of formation, bulk modulus, hydrogen content etc. [39-41], however, for a system containing about 80 elements, we consider the treatment of ternary combinations as too complex in the moment, given the number of possible combinations. Thus, we propose to try to understand the general behaviour of the different elements formed by nuclear processes in a liquid metal spallation target using a much simplified approach, based on an evaluation of the strength of chemical interaction in binary combinations. As a measure of the strength of chemical interaction we rely on the enthalpies of formation of solid compounds in binary systems. For simplicity, we even confine ourselves to binary compounds of equimolar composition. In this report, we provide the corresponding values of enthalpies of formation for compounds $A_{0.5}B_{0.5}$ (Appendix A) calculated using the Miedema model and discuss their periodicity.

2.4. The purification of mercury

There are an extraordinary number of patents and papers that deal with the purification of mercury. Many of the described processes are adapted and optimized to special applications of the used mercury and the removal of a certain kind of impurities. However, all these processes have a certain strategy in common, which will be outlined here. Only a few examples will be given to illustrate the consequences of different modifications of this general scheme. For more details, the reader is referred to review articles [17, 42, 43] that contain a compilation of several hundred original papers and discuss the purification of mercury in detail. We will discuss the literature focusing on the question if and how the known purification procedures can and should be used for the purification of a mercury spallation target, keeping in mind the general aspects of radiation safety, operational safety and nuclide production outlined in the introduction to this report.

Resulting from its physical and chemical properties, i.e. low melting and boiling point and a noble chemical character, mercury is one of the easiest substances to prepare in a very high degree of purity.

Solid impurities are typically removed from the liquid metal by filtration. Already in the 1st century such filtration techniques were known, using leather as a filter. Since then various types of filtration techniques were developed, most of them for laboratory scale use [42]. For a spallation loop, of course a radiation resistant material has to be chosen. The use of glass, ceramic or metal frits seem most reasonable for this process. Dry scum floating on a mercury surface can also be removed by picking it up with a sticky surface. As a variant, base metals dissolved in the liquid metal can be transformed to the oxides by bubbling air through the mercury before filtration. The precipitated oxides are removed afterwards by the filtration step.

Alternatively, for the removal of base metals mercury can be washed with various aqueous extraction agents. The most popular agent is diluted nitric acid, but other agents of different chemical characteristics such as KOH, acidic $KMnO_4$ -solution, H_2SO_4 etc. have been used as well. By varying the order in which these agents are applied, one can influence the order in which the impurities are removed [44-47]. Another alternative is the electrochemical removal of base metals, where the metals can be removed selectively according to their position in the electrochemical potential series [42]. For all these methods, different methods of agitation were developed to increase the reaction rate.

Finally, mercury can be removed from the noble metals still remaining in solution by distillation. For this process, several variants have been studied that differ mainly in the pressure regime and gas atmosphere that is used. Typical conditions are stagnant air, flow of air under reduced pressure and vacuum [42, 48, 49].

For an assessment of the technical feasibility and economical viability of an application of these conventional techniques for purifying mercury for the activated mercury produced in a spallation target, several technical and economical aspects have to be addressed. We will give here a short

overview on the most important questions to be answered and problems to be solved, before a decision can be taken about if and how a cleaning of the target should be performed. A final discussion including the results of our theoretical and experimental results will be given in the concluding section of this report, where we will answer these questions to the best knowledge available now.

First of all, a decision has to be made if a purification of the target material will be necessary because of radiation safety or operational requirements or if the scientific or economical benefit overcomes the effort and costs involved.

Concerning the radiation safety, we have to differentiate between reducing the radiation hazards during the operation of the system and optimizing the chemical state of the radioactive waste for a final disposal. Keeping the radiation hazard low during operation would require a continuous or at least periodic purification of the target material and probably also a cleaning of the loop components. This of course influences the chosen strategy of purification (the process must be fast and effective). For a periodical cleaning in shut-down periods, it has to be made sure that the target material after purification is in a state that makes its re-introduction to the spallation system possible, making the system available again soon after the cleaning procedure. When only purification before disposal is considered beneficial, the time constraints are released.

Regarding nuclide production, the speed and the periodicity of the processes used will determine the success of the separation procedures applied. Depending on the half-life of the desired nuclides, the optimum separation procedures (online extraction, short term periodic separation, separation after long term irradiation) will vary strongly. Since the separation and purification of radionuclides for medical purposes is a highly cost intensive procedure, we will provide an estimation of the economic benefit that can be gained from radionuclide extraction for a few of the most important medical nuclides with different lifetime.

Furthermore, it has to be clarified if the conventional methods described in the preceding section work efficiently for radiotracers in small concentrations as they are present in a spallation target. We will present the results of corresponding experimental studies below.

The adaptation of the conventional purification techniques to a highly radioactive environment and the operation of the corresponding facilities will be costly. However, from the assumptions about the probable chemical state and behaviour of the radioactive impurities within the spallation system derived above, alternative methods for the cleaning of a target loop could be derived. Therefore, we performed experiments to verify these assumptions on the chemical behaviour of radionuclides and to test novel methods for the removal of radionuclides from liquid mercury.

Based on the information gathered from literature data, the results of our theoretical and experimental studies and from the operators of large scale industrial and scientific facilities dealing with mercury we will derive conclusions for a sensible strategy of chemical mercury handling in a spallation target system.

3. Theoretical studies on nuclear reaction product behaviour in mercury

3.1. Solubility of nuclear reaction products in mercury

Data for the solubility of many elements in mercury that have been extracted from different sources are compiled in [22]. These values are used in this report for comparison with results of our calculations. Generally, the experimental data suffer from deficiencies of experimental solubility measurements and extrapolations over vast temperature ranges that will be discussed in more detail below.

Figure 5 shows a comparison of solubility data derived from [22] for metals in mercury at 463 K (the maximum expected temperature for the most recent target and loop design [7]) and the concentrations that are expected in the Multi-MW converter target of EURISOL after 40 years of irradiation with a 1 GeV proton beam of an average intensity of 2.28 mA, based on nuclide production data resulting from the calculations reported in [6] and assuming, for a start, a homogeneous distribution in the liquid metal. The value for the total amount of mercury of 820 l, i.e. 11111 kg used for the calculation of concentrations was taken from [6]. First of all, it has to be pointed out that there are some elements (Fe ($Z=26$), Ge ($Z=32$), Mo ($Z=42$), Sn ($Z=50$), Nd ($Z=60$), Yb ($Z=70$)) that show an extremely high production at long irradiation periods, compared to the neighbouring elements, thus deviating from the typical functional relationship observed for nuclide production as a function of atomic number. The reasons for these effects are unclear so far. Nevertheless, the production data for the remaining elements seem in good agreement with earlier results obtained within the ESS-study [50] and results obtained in the beginning of EURISOL-DS [51]. Since [6] is to our knowledge the only study dealing with a “recent” EURISOL target and includes the calculation of nuclide decay, we still use it in our evaluation, keeping in mind and discussing the consequences for those elements with the deviating behaviour.

On the first sight, the results seem to indicate that most of the elements will not reach their solubility limit until end of irradiation and thus should remain in solution, unless they undergo some chemical transformation. However, on closer examination it becomes obvious that there is a substantial lack of experimental data, especially for those elements that are primarily produced by spallation and fission reactions. Therefore, in the following, we calculate solubility data for a large range of elements in mercury using thermodynamic data calculated using a semi-empirical method. The calculated values for solubility are compared with the literature data. Based on this comparison, the validity of the calculated results and the possibilities for estimation of unknown elemental solubilities in mercury are discussed, together with the consequences resulting for the operation of liquid mercury targets.

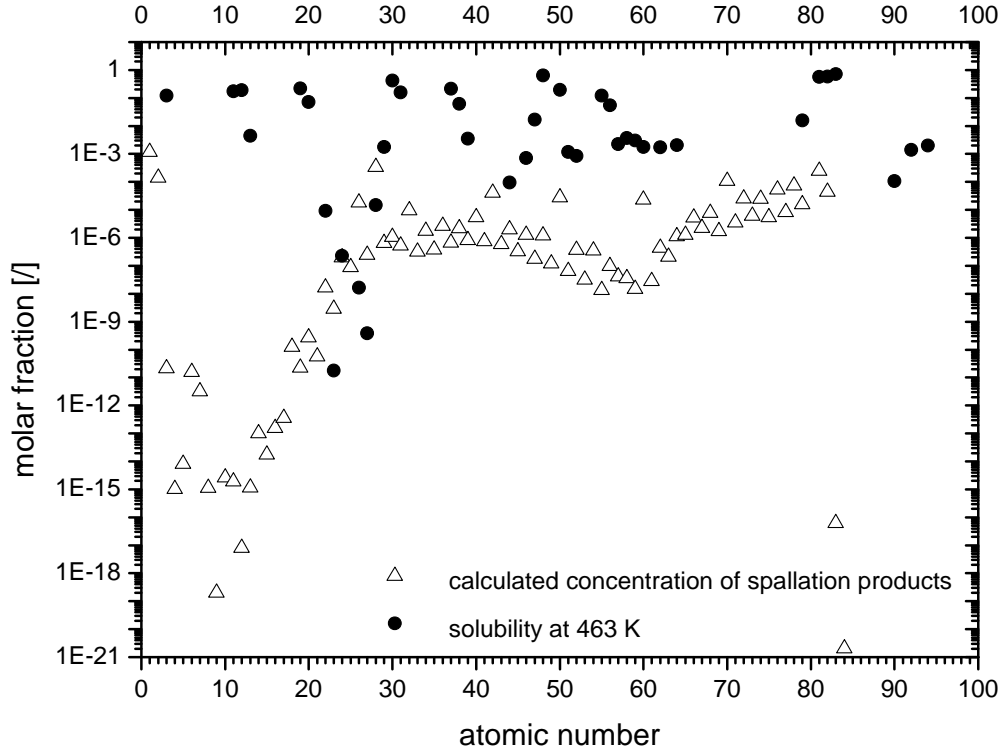
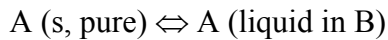


Figure 5: Comparison of literature data [22] on the solubility of elements in Hg at 463 K (solid circles) and the concentrations for homogeneous distribution, derived from the results of nuclear calculations [6] for a 40 year irradiation with 2.28 mA of 1 GeV protons, in a mercury target- and loop-system of 11111 kg mercury (open triangles). Concentrations are given as mole fractions x .

3.1.1. Thermochemical principles for the estimation of solubilities of elements in liquid metals

3.1.1.1. Simplified formulation of the solution equilibrium for pure elements

We consider the heterogeneous equilibrium system of a pure solid element A and a liquid metal B:



Here, we assume that A does not form a solid compound with B and B is insoluble in A. In equilibrium, the chemical potential of the dissolved component A equals the chemical potential of the pure solid element A. Hence, from the equality of the chemical potentials we get:

$$\Delta \bar{G}_{\text{solv}} = 0 \Rightarrow \Delta \bar{H}_{\text{solv}} = T \cdot \Delta \bar{S}_{\text{solv}} \quad (1)$$

with $\overline{\Delta G}_{solv}$ = partial molar Gibbs free energy of the solution process
 $\overline{\Delta H}_{solv}$ = partial molar enthalpy of solution
 $\overline{\Delta S}_{solv}$ = partial molar entropy of solution
T = absolute temperature

Here, $\overline{\Delta H}_{solv}$ is the so-called "last" enthalpy of solution, i.e. it corresponds to the enthalpic effect occurring when one mol A is transferred into the state of saturated solution in B. At low solubility, this state can be approximated with the state of infinite dissolution of A in B. Using this approximation, the enthalpic term can be replaced by the partial molar enthalpy of solution at infinite dilution, $\overline{\Delta H}_{solv}^{\infty}$.

In a simplified approach, the partial molar entropy of solution can be approximated by the partial molar ideal entropy of mixing. This approach neglects the entropy of melting and the partial molar excess entropy, which corresponds to the deviation of the system from ideal behaviour.

With these simplifications, from Eq. (1) follows:

$$\overline{\Delta H}_{solv}^{\infty} = -RT \ln(x) \quad \text{or} \quad \log(x) = \frac{-\overline{\Delta H}_{solv}^{\infty}}{2.303RT} \quad (2)$$

x : mole fraction of the solute A.

In spite of the approximations, this relation facilitates the estimation of the order of magnitude of the solubilities of pure metals [52], given that the values of melting and excess entropies are small. Furthermore, for our calculations we have to rely on the substitution of the partial molar enthalpy of solution at saturation by the partial molar enthalpy of solution at infinite dilution. The latter can be calculated for a vast number of elements ranging from group 1 to 16 of the periodic table, using the semi-empirical Miedema model [38, 53]. This approximation limits the model to systems where the saturation solubility is small.

Table 1 lists the partial molar enthalpies of solution of liquid elements in liquid mercury at infinite dilution, $\overline{\Delta H}_{solv}^{\infty}$ (A in B) (A: solute, B: mercury). These values were calculated with the Miedema model using the parameter set given in [38] for elements of group 1 to 15 and parameters derived in [53] for the chalcogens. For a visualization of the periodicity of these values, partial molar enthalpies of solution in Hg are plotted as a function of the atomic number Z of the solute in Figure 6. This plot clearly shows the periodicity of the chemical interaction with the solvent. This periodicity can be very helpful for the estimation of the strength of interaction between solute and solvent as well as for the critical assessment of literature data.

For the estimation of solubilities using Eq. (2) only systems with values > 0 for the partial molar enthalpy of solution are considered, since these are the systems where the two prerequisites, low solubility and no compound formation, are expected to be fulfilled.

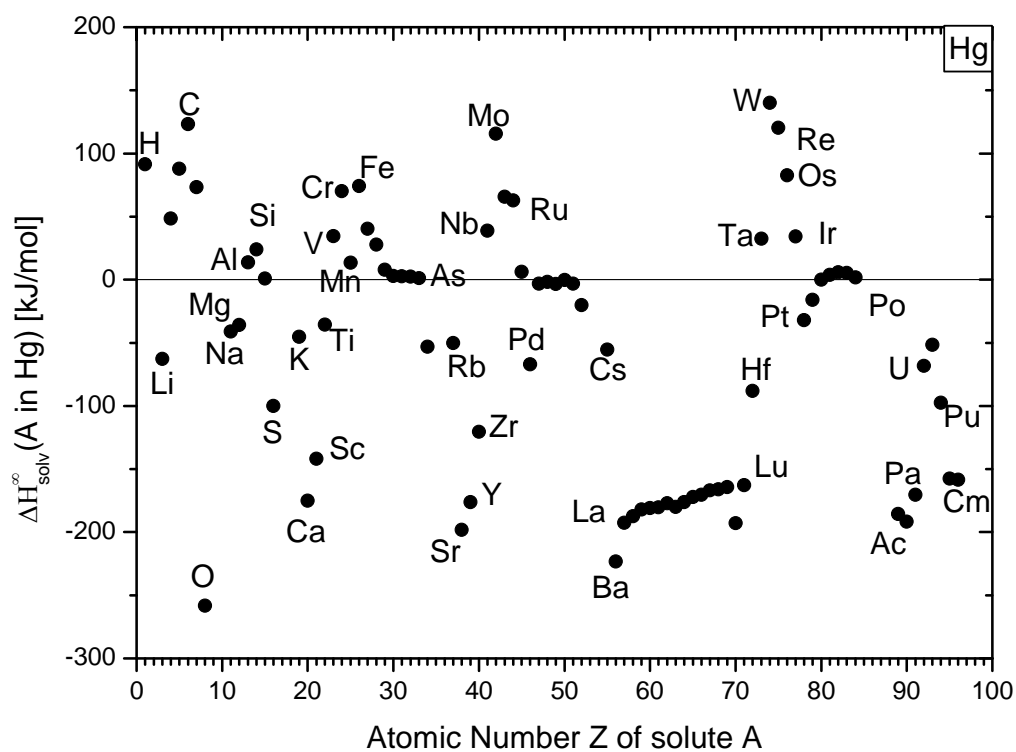


Figure 6: Partial molar enthalpies of solution of elements in liquid mercury as a function of atomic number. Values have been calculated using the Miedema model [38].

Table 1: Values for the partial molar enthalpy of solution of elements in liquid mercury at infinite dilution, $\Delta\bar{H}_{\text{solv}}^{\infty} [\text{kJ/mol}]$, calculated using the Miedema model.

Z	Symbol	$\Delta\bar{H}_{\text{solv}}^{\infty} [\text{kJ/mol}]$ in Hg	Z	Symbol	$\Delta\bar{H}_{\text{solv}}^{\infty} [\text{kJ/mol}]$ in Hg
1	H	91.40	51	Sb	-3.24
3	Li	-62.59	52	Te	-20.18
4	Be	48.50	55	Cs	-55.49
5	B	88.05	56	Ba	-223.19
6	C	123.31	57	La	-192.69
7	N	73.32	58	Ce	-187.23
8	O	-258.24	59	Pr	-182.07
11	Na	-40.99	60	Nd	-180.86
12	Mg	-35.89	61	Pm	-180.38
13	Al	13.81	62	Sm	-176.97
14	Si	24.08	63	Eu(II)	-180.03
15	P	0.88	63	Eu(III)	-80.73
16	S	-100.16	64	Gd	-176.25
19	K	-45.10	65	Tb	-172.19
20	Ca	-174.97	66	Dy	-170.28
21	Sc	-141.79	67	Ho	-167.01
22	Ti	-35.60	68	Er	-166.07
23	V	34.52	69	Tm	-164.17
24	Cr	70.13	70	Yb(II)	-192.86
25	Mn	13.37	70	Yb(III)	-100.93
26	Fe	74.25	71	Lu	-162.78
27	Co	40.41	72	Hf	-88.08
28	Ni	27.75	73	Ta	32.57
29	Cu	8.02	74	W	140.04
30	Zn	2.99	75	Re	120.45
31	Ga	2.54	76	Os	82.60
32	Ge	2.37	77	Ir	34.32
33	As	1.22	78	Pt	-31.93
34	Se	-53.14	79	Au	-15.91
37	Rb	-50.28	80	Hg	0
38	Sr	-198.24	81	Tl	3.74
39	Y	-176.25	82	Pb	5.86
40	Zr	-120.57	83	Bi	5.33
41	Nb	38.95	84	Po	1.69
42	Mo	115.53	89	Ac	-185.69
43	Tc	65.67	90	Th	-191.82
44	Ru	62.93	91	Pa	-170.40
45	Rh	6.16	92	U	-68.32
46	Pd	-67.02	93	Np	-51.63
47	Ag	-3.09	94	Pu	-97.39
48	Cd	-1.63	95	Am	-157.66
49	In	-3.49	96	Cm	-158.34
50	Sn	-0.21			

3.1.1.2. Enhanced formulation of the solubility equilibrium for pure metals

The quantities ΔH and ΔS can be regarded as sums of thermodynamic functions of state for the different steps of the process of solution, e.g. melting of the pure solid component A and subsequent mixing of the liquid component A with liquid solvent B leads to:

$$\overline{\Delta H}_{solv} = \Delta H_{melt}(A(s)) + \overline{\Delta H}_{mix}(AB(l)) \quad (3)$$

with $\Delta H_{melt}(A(s))$: molar enthalpy of melting for pure solid A;
 $\overline{\Delta H}_{mix}(AB(l))$: partial molar enthalpy of mixing of liquid A with liquid B saturated with A

Similarly, $\overline{\Delta S}$ can be expressed as the sum of three terms:

$$\overline{\Delta S}_{solv} = \Delta S_{melt}(A(s)) + \overline{\Delta S}_{ex}(l) + \overline{\Delta S}_{mix}(id) \quad (4)$$

with: $\Delta S_{melt}(A(s))$: molar entropy of melting of pure solid A
 $\overline{\Delta S}_{ex}(l)$: partial molar excess entropy
 $\overline{\Delta S}_{mix}(id)$: partial molar entropy of mixing for an ideal mixture, i.e. B statistically distributed in A

Introducing (3) and (4) in (1) results in:

$$\Delta H_{melt}(A(s)) + \overline{\Delta H}_{mix}(AB(l)) = -T \cdot (\Delta S_{melt}(A(s)) + \overline{\Delta S}_{ex}(l) + \overline{\Delta S}_{mix}(id)) \quad (5)$$

and substituting $\overline{\Delta S}_{mix}(id) = -R \cdot \ln(x)$ (6)

$$\text{results in } \ln(x) = \frac{(\Delta S_{melt}(A(s)) + \overline{\Delta S}_{ex}(l))}{R} - \frac{(\Delta H_{melt}(A(s)) + \overline{\Delta H}_{mix}(AB(l)))}{RT} \quad (7)$$

Entropies and enthalpies of melting for the elements are tabulated in the literature (see e.g. [54]). Some elements undergo one or more phase transitions before melting. As an extension we introduce the sum of the enthalpies $\Sigma \Delta H$ (trans) and entropies $\Sigma \Delta S$ (trans) for the solid state phase transformations of the elements into Eq. (7). With this extension we finally consider a solution process, starting from the elements in the standard state at 298 K, subsequently undergoing solid state phase transformations, melting and mixing with the solvent. This approach seems more sensible for the description of the solution equilibrium of solid elements significantly below their melting point in liquid metals.

Thus, finally we arrive at the following equation for the solubility:

$$\ln(x) = \frac{(\Delta S_{melt}(A(s)) + \Sigma \Delta S_{trans}(A(s)) + \overline{\Delta S}_{ex}(l))}{R} - \frac{(\Delta H_{melt}(A(s)) + \Sigma \Delta H_{trans}(A(s)) + \overline{\Delta H}_{mix}(AB(l)))}{RT} \quad (8)$$

Assuming that the functions of state are independent of temperature, this relationship corresponds to the well known relation for the temperature dependence of solubility:

$$\ln(x) = A + B/T \quad (9)$$

Using Eq. (8), it is in principle possible to approximately determine thermodynamic functions of state from experimentally determined solubility data and their temperature dependence. We go here the opposite way, since we intend to calculate approximate temperature dependent solubility data based on tabulated and estimated thermodynamic functions, using a number of approximations and assumptions. One of these is the assumption that the partial molar excess entropy is small and can be neglected:

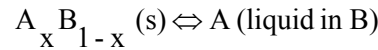
$$\Delta \bar{S}_{\text{ex}}(\text{l}) \cong 0.$$

Another approximation results from the substitution of the partial molar enthalpy of mixing $\Delta \bar{H}_{\text{mix}}(\text{l})$ at saturation with the partial molar enthalpy of solution at infinite dilution with the solvent B.

$$\Delta \bar{H}_{\text{mix}}(\text{AB}(\text{l})) \cong \Delta \bar{H}_{\text{solv}}^{\infty}(\text{AB}(\text{l}))$$

3.1.2. Formulation of the solubility equilibrium for solid compounds

In case the element under consideration forms a stable solid compound with the solvent, the prerequisites for the application of the relations derived above are violated. In this case, a pure solid compound is present as the solid phase in equilibrium instead of the pure solid metal. According to [55-58] we consider the solid compound with the highest stoichiometric content of the solvent B being in equilibrium with the liquid phase. The process of solution can then be formulated in the following way:



For the equilibrium state:

$$\Delta \bar{G}(\text{A}_x \text{B}_{1-x}) = 0 \quad (10)$$

i.e. the chemical potential of $\text{A}_x \text{B}_{1-x}$ in the pure solid state equals that in the saturated solution. Resulting from Eq.(10):

$$\Delta \bar{H}(\text{A}_x \text{B}_{1-x}) = T \cdot \Delta \bar{S}(\text{A}_x \text{B}_{1-x}) \quad (11)$$

Thus, the process of solution of a solid compound can be formulated as a sequence of different steps:

- dissociation of the solid compound, with the respective enthalpy and entropy of formation, $-\Delta H_{\text{form}}(\text{A}_x \text{B}_{1-x})$ and $-\Delta S_{\text{form}}(\text{A}_x \text{B}_{1-x})$.
- melting of the pure solid metals x A and $(1-x)$ B with the corresponding enthalpy and entropy terms, $x \Delta H_{\text{melt}}(\text{A}(\text{s}))$, $(1-x) \Delta H_{\text{melt}}(\text{B}(\text{s}))$, $x \Delta S_{\text{melt}}(\text{A}(\text{s}))$, and $(1-x) \Delta S_{\text{melt}}(\text{B}(\text{s}))$.
- mixing of the pure molten components with the solvent B, involving $(1-x) \Delta \bar{H}_{\text{mix}}(\text{B}(\text{l})) = 0$, $(1-x) \Delta \bar{S}_{\text{mix}}(\text{B}(\text{l})) = 0$, $x \Delta \bar{H}_{\text{mix}}(\text{A}(\text{l}))$, and $x \Delta \bar{S}_{\text{mix}}(\text{A}(\text{l}))$.

For the partial molar enthalpy of solution of the compound $A_x B_{1-x}$ in B at saturation follows:

$$\Delta\bar{H}_{solv}(A_x B_{1-x}) = -\Delta H_{form}(A_x B_{1-x}) + x \Delta H_{melt}(A(s)) + (1-x) \Delta H_{melt}(B(s)) + x \Delta\bar{H}_{mix}(A(l)) \quad (12)$$

and for the partial molar entropy of solution of the compound:

$$\Delta\bar{S}_{solv}(A_x B_{1-x}) = -\Delta S_{form}(A_x B_{1-x}) + x \Delta S_{melt}(A(s)) + (1-x) \Delta S_{melt}(B(s)) + x \Delta\bar{S}_{mix}(A(l)). \quad (13)$$

The last term in Eq. (13) can be substituted:

$$\Delta\bar{S}_{mix}(A(l)) = \Delta\bar{S}_{ex}(A(l)) - R \cdot \ln(x_A)$$

Thus, from Eq. (11), (12) and (13) we obtain:

$$\begin{aligned} \ln(x_A) = & -\frac{1}{xRT} \left[-\Delta H_{form}(A_x B_{1-x}) + x \Delta H_{melt}(A(s)) + (1-x) \Delta H_{melt}(B(s)) + x \Delta H_{mix}(A(l)) \right] \\ & + \frac{1}{xR} \left[-\Delta S_{form}(A_x B_{1-x}) + x \Delta S_{melt}(A(s)) + (1-x) \Delta S_{melt}(B(s)) + x \Delta\bar{S}_{ex}(A(l)) \right] \end{aligned} \quad (14)$$

For the calculation of solubilities of solid compounds $A_x B_{1-x}$ in a liquid metal B we introduce some extensions and approximations to the formulation of the solubility equilibrium, similar to those stated in the section dealing with the solubility of pure metals. First of all, we include the entropies and enthalpies for solid state phase transitions, in case such transitions occur between 298 K and the melting point of A and B, $x \sum \Delta H_{trans}(A(s))$, $(1-x) \sum \Delta H_{trans}(B(s))$, $x \sum \Delta S_{trans}(A(s))$, and $(1-x) \sum \Delta S_{trans}(B(s))$.

This extension transforms Eq. (14) into:

$$\begin{aligned} \ln(x_A) = & \frac{1}{xRT} \left[-\Delta H_{form}(A_x B_{1-x}) + x \Delta H_{melt}(A(s)) + (1-x) \Delta H_{melt}(B(s)) + x \Delta H_{mix}(A(l)) + x \sum \Delta H_{trans}(A(s)) + (1-x) \sum \Delta H_{trans}(B(s)) \right] \\ & + \frac{1}{xR} \left[-\Delta S_{form}(A_x B_{1-x}) + x \Delta S_{melt}(A(s)) + (1-x) \Delta S_{melt}(B(s)) + x \Delta\bar{S}_{ex}(A(l)) + x \sum \Delta S_{trans}(A(s)) + (1-x) \sum \Delta S_{trans}(B(s)) \right] \end{aligned} \quad (15)$$

For the calculations, the enthalpies of formation of ordered solid compounds

$\Delta H_{form}(A_x B_{1-x})$ are separately calculated using the Miedema model [38].

The partial molar enthalpy of mixing $\Delta\bar{H}_{mix}(A(l))$ in B saturated with A is approximated by the partial molar enthalpy of solution of liquid A in B at infinite dilution. The latter is also calculated using the Miedema model (see Table 1). This substitution is only meaningful for small solubilities, as already stated above. Additional approximations are necessary for an assessment of the entropy terms. The entropies of formation of many solid compounds of the elements with mercury are not known. However, typically the formation entropies of solid phases are small and can be neglected.

Values for the partial molar excess entropies $\Delta\bar{S}_{\text{ex}}(A(l))$ of elements in binary systems with mercury are known only in few cases. To a first approximation, they are neglected in our calculations.

Both approximations seem justifiable. In some systems they will even partly compensate for one another.

It has been shown in the literature that solubility estimations based on enthalpy values calculated with the Miedema model can give superior results compared to other methods of estimation [59].

3.2. Solubility of the elements of group 1 to 16 in liquid mercury

For a detailed description of the Miedema model, its applications and limits we refer to the extensive monograph [38]. This monograph also contains the parameters for elements from group 1-15 of the periodic table of the elements used in this work. An extension to the elements of group 16, i.e. the chalcogens, is described in [53]. The elements of groups 17 and 18 (halogens and noble gases) are not covered by the model and are therefore not treated in this work. Using this model we calculate the following quantities required for the application of the relations derived above:

- partial molar enthalpy of solution of elements in mercury at infinite dilution (Table 1)
- integral enthalpy of formation of ordered solid compounds of the elements with mercury

For the latter, we assume that the solid phase in equilibrium with the liquid phase is the phase with the highest content in solvent, i.e. mercury. This is clearly an approximation. From phase diagram data of the binary systems [60, 61] it can be seen that the equilibrium solid phase may change with varying temperature, thus giving rise in changes of the temperature functions of the solubility. Since we are dealing here with a comprehensive view on all binary systems accessible by the Miedema model, we have to restrict ourselves to this simplified approach.

3.2.1. Results of solubility calculations

First of all, a criterion has to be defined to discriminate the systems where stable solid compounds are formed and those systems where the pure metal is present as the solid equilibrium phase. One possible criterion is the experimental evidence on existing compounds that are described in literature. Another possible criterion would be the calculated enthalpies of formation of solid mercury compounds. In systems, where stable compounds are formed, i.e. those with negative enthalpies of formation, the presence of a binary solid phase can be expected in equilibrium, whereas for positive enthalpies of formation the pure solid metal is expected as the solid phase in equilibrium. Within this work we rely on the information on characterized solid compounds of mercury as extracted from the literature [60, 61]. Table 2 contains enthalpies of formation calculated using the Miedema model for the most Hg-rich binary phases described in these references. With very few exceptions the calculated values are negative as expected for a stable compound, thus verifying the similarity of the two approaches described above and the usability of the Miedema model for mercury-metal systems. The two exceptions, i.e. nickel and polonium, may indeed be borderline cases, as shown by the very small positive calculated values for the enthalpies of formation. From experiment it is known that they form binary compounds with mercury, however not very stable ones. In the following, we will treat the binary combinations listed in Table 2 as systems with a solid compound in equilibrium with the liquid, i.e. we use Eq. (15) for calculations of the solubility. The remaining elements are assumed to be present in the pure elemental state in the solubility equilibrium. The solubility of these elements

will be calculated using Eq. (8). For comparison, calculations for these systems have also been performed using the simplified model represented by Eq. (2). The results of the calculations using Eq. (8) generally agreed better with the literature data, as expected for the more sophisticated treatment of the solubility equilibrium. Therefore, in the following only values obtained from Eq. (8) will be given. Generally, from Table 2 one can clearly see the periodicity of the chemical interaction of the elements with mercury. The elements of groups 1 to 4 (with the exception of Be) form stable intermetallic phases. The chalcogens (group 16) also form stable compounds, the stability strongly decreasing when one moves from oxygen to the heavier chalcogens. The elements of groups 5 to 15 generally do not form stable compounds, with a few exceptions (Mn, Pd, Ag, In, Pt, Au). For most of these exceptions, calculated enthalpies of formation are close to zero or at least not highly negative. This behaviour is in good agreement with the classification of the metals considering their chemical behaviour towards mercury as shown in Figure 4.

Table 2: Enthalpies of formation of the most Hg-rich binary phases Hg_xA_{1-x} calculated using the Miedema model.

Z	Element	Hg-Mole fraction	$\Delta H_{\text{form}}(Hg_xA_{1-x})[\text{kJ/mol}]$
3	Li	0.75	-15.21
8	O	0.50	-115.58
11	Na	0.80	-7.98
12	Mg	0.67	-11.23
16	S	0.50	-39.65
19	K	0.92	-3.51
20	Ca	0.91	-16.31
21	Sc	0.75	-39.82
22	Ti	0.75	-15.88
25	Mn	0.50	-5.08
28	Ni	0.80	0.57
34	Se	0.50	-19.90
37	Rb	0.92	-3.92
38	Sr	0.92	-16.42
39	Y	0.80	-39.34
40	Zr	0.75	-37.40
45	Rh	0.83	-3.75
46	Pd	0.80	-18.61
47	Ag	0.57	-2.84
49	In	0.86	-0.47
52	Te	0.50	-6.90
55	Cs	0.86	-7.61
56	Ba	0.92	-18.69
57	La	0.86	-29.98
58	Ce	0.80	-41.69
59	Pr	0.80	-40.59
60	Nd	0.80	-40.32
61	Pm	0.80	-40.20
62	Sm	0.80	-39.50
63	Eu(II)	0.75	-46.25
63	Eu(III)	0.75	-24.93
64	Gd	0.80	-39.34
65	Tb	0.80	-38.49
66	Dy	0.75	-47.27
67	Ho	0.75	-46.45
68	Er	0.75	-46.20
69	Tm	0.75	-45.69
70	Yb(II)	0.80	-40.15
70	Yb(III)	0.80	-23.57
71	Lu	0.80	-36.43
72	Hf	0.75	-29.51
78	Pt	0.80	-12.18
79	Au	0.67	-7.96
84	Po	0.50	0.56
89	Ac	0.80	-41.13
90	Th	0.75	-52.70
91	Pa	0.75	-49.38
92	U	0.80	-19.54
93	Np	0.80	-16.07
94	Pu	0.80	-24.84
95	Am	0.80	-35.48
96	Cm	0.80	-35.70

3.2.1.1. Solubilities for systems with pure elements as solid phase

In this section we compare the calculated solubilities for systems where the pure solid element is present as the solid phase in the solubility equilibrium with literature data taken from [22]. As pointed out above, the calculations were performed using the extended description of the solubility equilibrium incorporating phase transitions in the solid state and melting (Eq. (8)) because of the better agreement with the literature data. Figure 7 shows, as an example, the results of solubility calculations for these elements in mercury at 463 K (the highest temperature expected in the latest design [7]) together with the corresponding literature data.

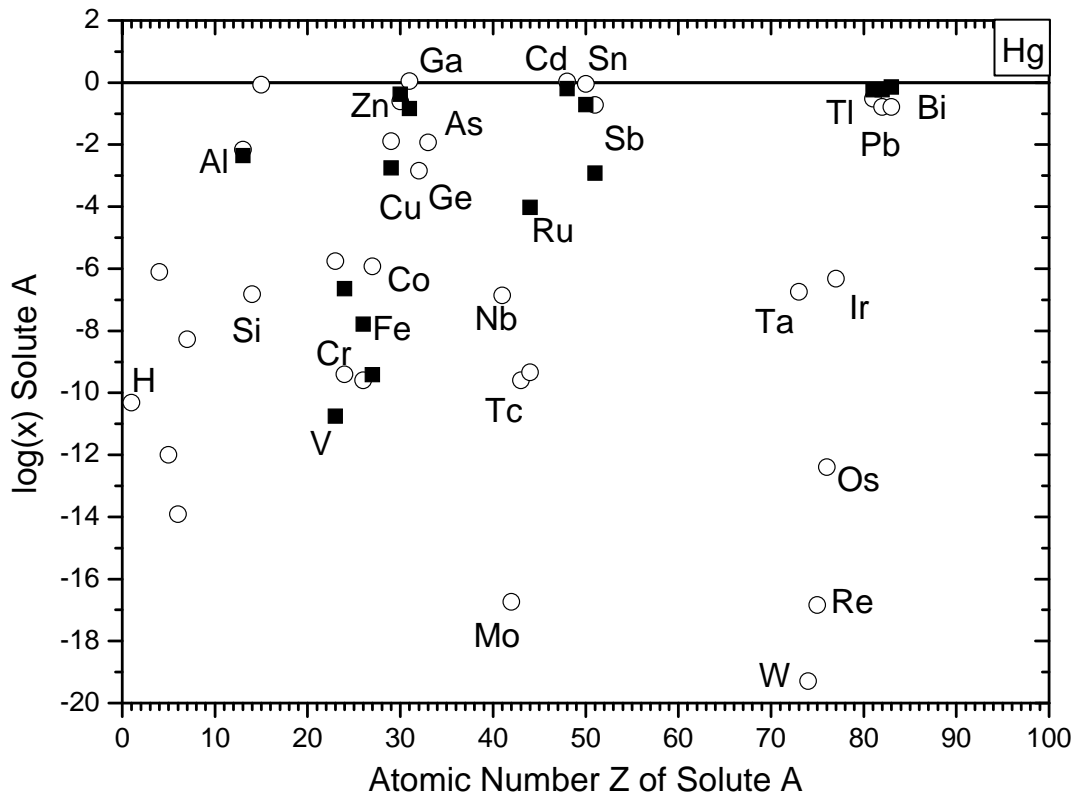


Figure 7: Comparison of calculated solubility of elements in mercury at 463 K and literature data for elements A that are expected to be present as pure solid elements in the solubility equilibrium (squares: literature data; circles: values calculated using Eq. (8)).

Qualitatively, the periodicity of the solubility is well represented by the results of calculations. Metals of groups 5 to 9 (e.g. V, Cr, Fe, Co) show rather low solubility in mercury, whereas the elements of groups 11 to 15 such as Zn, Ga, Cd, Tl, Pb and Bi show large solubility. For the latter elements as well as for Al and Cu, the calculated values also quantitatively agree very well with the experimental findings. However, some large discrepancies are found for other elements. For the elements V and Co differences of several orders of magnitude can be observed between literature data and calculated values. Here, both calculated values are much larger than the experimental data. According to [22] there seem to be large discrepancies between the results of different experimental studies performed on the systems Hg-V and Hg-Co. Finally, the data for these systems are extrapolated from high temperature data and thus may be rather unreliable. Qualitatively, both metals show only small calculated solubility, in agreement with literature data. Opposite behaviour is found for Ru, where the calculations seem to underestimate the solubility. However, there are controversial results found in literature, many papers in fact state a

solubility of Ru in mercury that is under the detection limit, below $x \cong 10^{-7}$. This might be one of the cases where calculations are superior to experimental data because of difficulties to measure the actual concentrations. In any case, it seems that the system mercury-ruthenium requires additional investigation. Another system with a rather large discrepancy is Hg-Sb, where the calculated solubility is about two orders of magnitude higher than the experimentally determined one. For this system, the evaluations given in [22] indicate that there is a lack of clarity in this system concerning the solid phase present in equilibrium. Therefore, the choice of putting Sb in the group of elements where the equilibrium phase is the pure solid metal is questionable. A final decision would require additional work on the antimony-mercury system. Another system with a rather large discrepancy of about two orders of magnitude is iron-mercury, where the calculated solubility is lower than that determined from experimental results. For this system, it is known that colloidal solutions of iron occur that may lead to an overstated solubility determined in the experiments. Overall, there are a lot of systems where plausible explanations for the observed discrepancies are available.

Concerning the predictive power of our calculations we will now look at the results for the elements of group 5 to 8 of the 5th and 6th row of the periodic table, i.e. (Nb-Ru and Ta-Os), where no quantitative data are found in literature. Similar to their lighter homologues they show a minimum of calculated solubility within the corresponding row of the periodic table. This is plausible, since the process of solution involves breaking of chemical bonds in the crystal lattice of the metals. The group of metals considered here is known for their large cohesive energies in the solid state, indicative of extremely strong bonding. Furthermore, for some of the systems Hg-M with M = Nb-Ru and Ta-Os, low solubility or no mutual miscibility has been reported up to high temperatures within the analytical detection limits [22, 61]. The results of our calculations are in good agreement with these facts. Therefore, we believe that the solubilities calculated by us for these metals give at least a useful qualitatively estimation of their solubility in liquid mercury. These elements are prominent spallation and fission products and thus it is especially important to have estimated data on their solubility.

The solubility in mercury for the heavier (rows 5 and 6) elements of group 11 to 15 such as Cd, In, Sn, Sb, Tl, Pb, Bi is calculated to be near unity. This is in agreement with the fact that many of those systems show either large solubility or are even completely miscible. (the exception Sb was discussed above). In fact, numerical values for $\log(x)$ obtained for these elements are slightly larger than 0 in a few cases, which is unphysical because mole fractions by definition have to be numbers between 0 and 1. This probably arises from the approximations and simplifications of the model. As mentioned above, the approximation of the partial molar enthalpy of solution at saturation concentration by the partial molar enthalpy of solution at infinite dilution limits the model to low solubility systems. Considering this fact, the agreement for high solubility binary systems is surprisingly good. We suggest that one can interpret the values of $x > 1$ or $\log(x) > 0$ as “high solubility”.

Overall, we have shown that the results of our solubility calculation for systems where the solute is present in the solid as pure element can give a reasonable estimate for solubility values that have not been determined so far. The temperature dependence of the calculated solubilities is in many cases in reasonable agreement with the experimental data. Generally, solubility increases with increasing temperature, indicative of positive enthalpies of solution. Numerical values for the calculated solubilities of pure metals in mercury are compiled in table 3 together with data from [22] obtained by extrapolation to lower temperatures in cases with low solubility at low temperatures. We give here values for 333 and 463 K, the minimum and maximum temperature of the liquid metal expected for the latest design [7]. Table 4 lists the corresponding coefficients for the temperature functions of the solubilities of these elements calculated using Eq. (8).

Table 3: Literature data [22] and values calculated using Eq. (8) for the solubility of pure elements in Hg at different temperatures.

Z	Element	log(x) (Literature values)		log(x) (calculated)	
		333 K	463 K	333 K	463 K
1	H			-14.34	-10.31142
4	Be			-8.58265	-6.0986
5	B			-16.86833	-11.9971
6	C			-19.34362	-13.91236
7	N			-11.50132	-8.27201
13	Al	-3.37563	-2.35539	-3.24768	-2.1675
14	Si			-10.09603	-6.82426
15	P			-0.13297	-0.06517
23	V	-14.36205	-6.63931	-8.19597	-5.7536
24	Cr	-7.65492	-6.63931	-13.24117	-9.40678
26	Fe	-9.50933	-7.78698	-13.5141	-9.59657
27	Co	-12.56341	-9.41693	-8.4373	-5.92455
29	Cu	-3.80547	-2.74745	-2.82682	-1.88973
30	Zn	-0.95226	-0.37283	-1.06462	-0.61065
31	Ga	-1.26304	-0.83702	-0.31141	0.0467
32	Ge			-4.57294	-2.84128
33	As			-3.20886	-1.93548
41	Nb			-9.7421	-6.86569
42	Mo			-23.55068	-16.74023
43	Tc			-13.53915	-9.59621
44	Ru	-4.55841	-4.02257	-13.17813	-9.33687
48	Cd	-0.72088	-0.1923	-0.17063	0.03016
50	Sn	-1.54286	-0.71107	-0.34234	-0.04216
51	Sb	-4.5229	-2.92373	-1.46106	-0.72848
73	Ta			-9.5687	-6.74089
74	W			-27.0182	-19.29102
75	Re			-23.60493	-16.83606
76	Os			-17.43646	-12.39956
77	Ir			-8.97941	-6.31708
81	Tl	-0.52391	-0.24043	-0.88181	-0.51801
82	Pb	-1.40015	-0.23455	-1.25259	-0.78432
83	Bi	-1.22353	-0.14756	-1.52542	-0.79294

Table 4: Coefficients of the temperature functions $\log(x) = A - B/T$ for the solubility of pure elements in Hg obtained using Eq. (8).

Z	Element	A	B [K]
1	H	0	4774
4	Be	0.2644	2946
5	B	0.4807	5777
6	C	0	6441
7	N	0	3830
13	Al	0.5994	1281
14	Si	1.5565	3880
15	P	0.1085	80
23	V	0.5026	2897
24	Cr	0.4152	4548
26	Fe	0.4383	4646
27	Co	0.5120	2980
29	Cu	0.5107	1111
30	Zn	0.5522	538
31	Ga	0.9640	425
32	Ge	1.5944	2054
33	As	1.3263	1510
41	Nb	0.5024	3411
42	Mo	0.7050	8077
43	Tc	0.5038	4676
44	Ru	0.5027	4556
48	Cd	0.5445	238
50	Sn	0.7268	356
51	Sb	1.1481	869
73	Ta	0.5027	3354
74	W	0.5025	9164
75	Re	0.5027	8028
76	Os	0.5027	5974
77	Pd	0.5026	3157
81	Tl	0.4139	431
82	Pb	0.4152	555
83	Bi	1.0833	869

3.2.1.2. Solubilities for compound forming elements

Solubility calculations for elements that form stable compounds were performed using Eq. (15). The required enthalpies of solution at infinite dilution and enthalpies of formation of the solid compounds with the highest stoichiometric content of mercury, respectively, were calculated using the Miedema model. These values are compiled in tables 1 and 2. Figure 8 shows a plot of the enthalpies of formation of the most Hg-rich compounds, per mole of element A, as a function of the atomic number of A. The plot nicely shows that for practically all of these compounds negative heats of formation are calculated. Only for the two elements Ni and Po slightly positive heats of formation are calculated, indicating that the Miedema model yields at least a qualitatively correct estimation of the interaction of mercury with other elements.

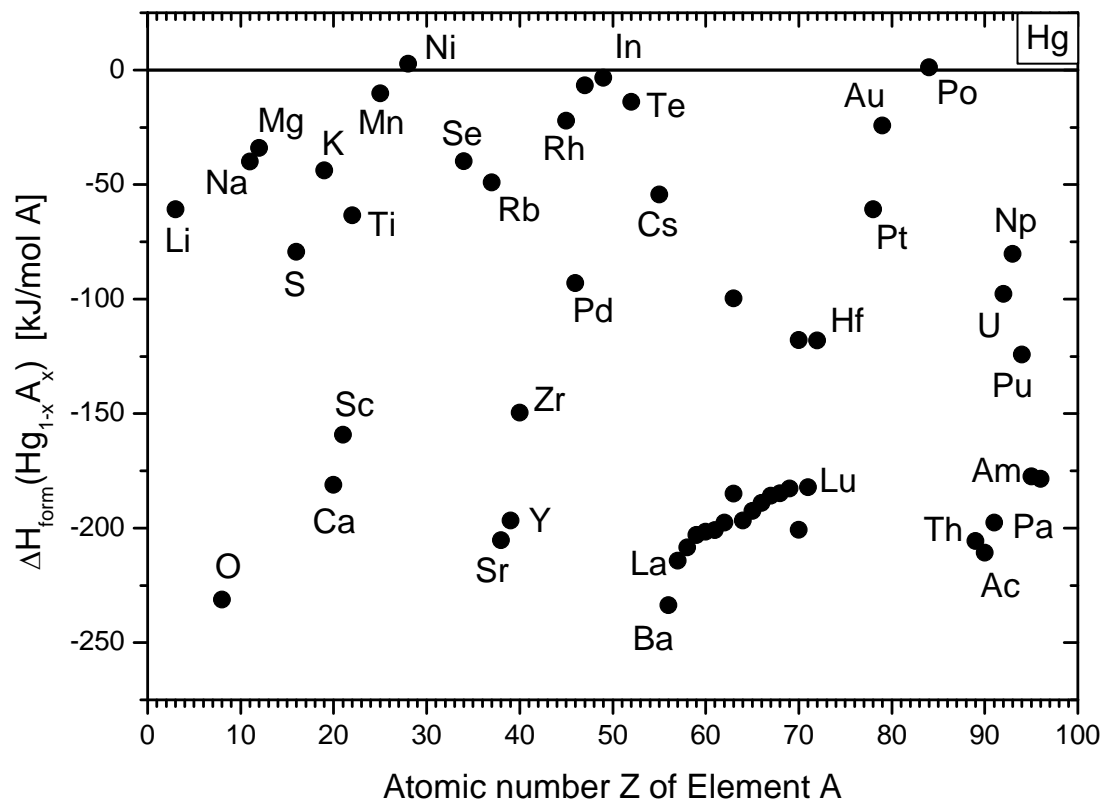


Figure 8: Calculated enthalpies of formation of the most Hg-rich mercury compound of element A, per mole of element A, as a function of the atomic number of A.

Solubilities for these elements in mercury, calculated using Eq. (15), are shown in Figure 9 as a function of Z, together with the available experimental data. The largest discrepancies are observed for the electropositive alkaline and alkaline earth elements. For these systems, mole fractions > 1 or $\log(x) > 0$ are obtained from the calculations. Peculiarities were found when treating alkaline metals using the Miedema model [38], arising from the inability of the model to correctly describe the electron transfer in elements having only one valence electron. Such effects may lead to large errors in the evaluation of enthalpic effects in these systems using the Miedema model.

Similarly, significant problems are encountered in the Hg-chalcogen systems. The calculated solubilities values found for the chalcogens O, S, Se and Te are systematically too high. This may

be caused by the inadequacy of the Miedema model for the quantitative description of systems where a rather polar bonding character is present. While the result of negative enthalpies of formation of mercury chalcogenides yielded by the Miedema model is in qualitative agreement with the experimental evidence on their stability, the accuracy of the quantitative results may be insufficient for a reliable calculation of solubilities.

Another explanation for the discrepancies observed is an uncertainty concerning which solid compound is actually in equilibrium with the liquid phase. The composition of the solid equilibrium phase is certainly a function of temperature. Therefore, the composition of the solid phase may change as a function of temperature, thus giving rise to a kink in the temperature function of the solubility. These effects are neglected in the current treatment. However, especially the binary systems of mercury with alkaline and alkaline earth elements exhibit very complicated phase diagrams with many different mercury-rich compounds and very close stability regions for these phases. This may hamper an estimation of their solubility in liquid Hg with such a simplified approach. Indeed, when one compares the solubilities calculated for these metals at lower temperatures, the discrepancies become much smaller (see Figure 10), indicating that the temperature dependence of the solution equilibrium is not described correctly in our approach, possibly because we neglect the influence of varying equilibrium solid phases with temperature.

We conclude that solubilities of alkaline and alkaline earth metals and chalcogens in mercury should not be calculated using the theoretical approach presented in this work, because of inherent problems of the Miedema model as well as a lack of clarity in the phase relations. For most of these elements, literature data on their solubility exist. Therefore, the deficiency of the model is less problematic in these cases.

Many of the remaining systems, i.e. Pd, Ag, Au, the lanthanides and actinides show a rather good agreement of calculated and experimental solubility.

As a summary of calculations for compound forming systems, it should be noted that the Miedema model, as a semi-empirical model, can generally only give approximated values for thermodynamic data. The shortcomings of the Miedema model in case of combinations with elements of groups 1, 2 and 6 has already been discussed above. For the remaining elements, the accuracy in calculated thermodynamic data is usually better. The general validity of the model is also substantiated by the correct reproduction of the periodic relations within the periodic table of the elements. Because of the uncertainties discussed above, we will not give numerical data for the calculated solubility of alkaline and alkaline earth elements and the chalcogens in this report. Data derived from literature data are compiled in table 5. For the remaining metals, tables 5 and 6 list both calculated and literature data on their solubility in Hg as well as temperature functions of the solubility. For the temperature functions we observe an overestimation of the effect of temperature for most systems, indicating that the overall heats of solution calculated by our approach are slightly too large.

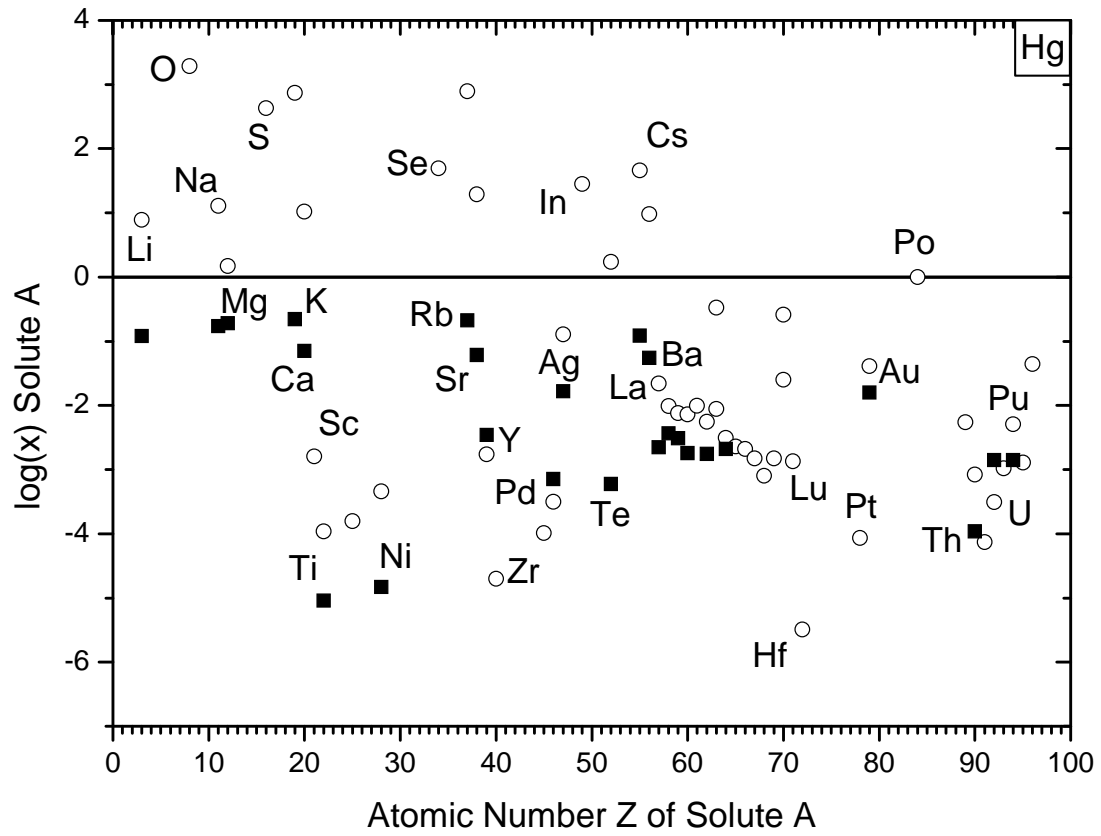


Figure 9: Comparison of calculated solubility in mercury at 463 K and literature data derived from [22] for elements A that are expected to form solid compounds in the solubility equilibrium. Squares: literature data. Circles: values calculated using Eq. (15).

Table 5: Literature data derived from [22] and values calculated using Eq. (15) for the solubility of compound forming elements in Hg at different temperatures.

Z	Element	log(x) (Literature values)		log(x) (calculated)	
		333 K	463 K	333 K	463 K
3	Li	-1.57203	-0.91882		
11	Na	-1.11796	-0.764		
12	Mg	-1.26997	-0.71727		
19	K	-1.14254	-0.65526		
20	Ca	-1.54522	-1.14707		
21	Sc			-4.67426	-2.79317
22	Ti	-6.22322	-5.03856	-6.30811	-3.95945
25	Mn			-5.75001	-3.80392
28	Ni	-7.40277	-4.82922	-5.62303	-3.33845
37	Rb	-1.24223	-0.67359		
38	Sr	-1.52691	-1.21426		
39	Y	-3.34726	-2.4594	-4.80149	-2.7613
40	Zr			-7.3923	-4.70243
45	Rh			-6.68323	-3.98531
46	Pd	-4.50845	-3.14706	-5.83989	-3.50172
47	Ag	-2.73089	-1.77777	-1.68124	-0.89024
55	Cs	-1.23092	-0.91541		
56	Ba	-1.96822	-1.26054		
57	La	-3.47985	-2.65084	-3.67234	-1.65912
58	Ce	-3.57106	-2.43201	-3.73334	-2.00906
59	Pr	-3.57839	-2.51355	-3.8992	-2.11967
60	Nd	-3.79494	-2.74527	-3.91705	-2.13973
61	Pm			-3.68394	-2.00143
62	Sm	-3.43943	-2.7573	-4.09109	-2.25273
63	EuII			-1.41133	-0.47309
63	EuIII			-3.60744	-2.05258
64	Gd	-3.71117	-2.67988	-4.4365	-2.50303
65	Tb			-4.64225	-2.63712
66	Dy			-4.489	-2.67732
67	Ho			-4.71151	-2.82769
68	Er			-5.10816	-3.09327
69	Tm			-4.7024	-2.82823
70	YbII			-1.7645	-0.58452
70	YbIII			-3.17684	-1.60031
71	Lu			-4.96433	-2.87185
72	Hf			-8.47625	-5.48809
78	Pt			-6.62424	-4.06593
79	Au	-2.76194	-1.79667	-2.51515	-1.38832
89	Ac			-4.11751	-2.26357
90	Th	-4.57477	-3.9644	-5.05721	-3.07816
91	Pa			-6.47299	-4.12954
92	U	-3.92293	-2.84855	-5.92528	-3.50528
93	Np			-5.37197	-2.98307
94	Pu	-3.49642	2.70350	-4.29196	-2.29054
95	Am			-5.1024	-2.89079
96	Cm			-2.66171	-1.35702

Table 6: Coefficients of the temperature functions $\log(x) = A - B/T$ for the solubility of compound forming elements in Hg obtained using Eq. (15).

Z	Element	A	B [K]
21	Sc	2.025	2231
22	Ti	2.057	2786
25	Mn	1.181	2308
28	Ni	2.514	2709
39	Y	2.465	2420
40	Zr	2.188	3190
45	Rh	2.926	3200
46	Pd	2.488	2773
47	Ag	1.136	938.1
57	La	3.498	2388
58	Ce	2.408	2045
59	Pr	2.439	2111
60	Nd	2.413	2108
61	Pm	2.308	1995
62	Sm	2.456	2180
63	EuII	1.930	1113
63	EuIII	1.930	1844
64	Gd	2.450	2293
65	Tb	2.499	2378
66	Dy	1.963	2149
67	Ho	1.998	2234
68	Er	2.068	2390
69	Tm	1.973	2223
70	YbII	2.438	1399
70	YbIII	2.438	1870
71	Lu	2.488	2482
72	Hf	2.166	3544
78	Pt	2.487	3034
79	Au	1.498	1336
89	Ac	2.485	2199
90	Th	1.991	2347
91	Pa	1.873	2779
92	U	2.694	2870
93	Np	3.136	2833
94	Pu	2.836	2374
95	Am	2.774	2623
96	Cm	1.985	1547

3.3. Discussion of solubility data and conclusions for the EURISOL target system

The experimental determination of solubilities in liquid metals is an extremely challenging task that requires ultra-pure metals and atmosphere as well as a careful choice of container materials. Furthermore, the separation of solid and liquid phases is difficult. Eventually, sensitive analytic techniques are required. Especially in the case of very low solubility metals and for highly reactive metals such as the strong oxide-, nitride-, carbide- or hydride-formers, experimentally determined solubilities should be regarded critically. This is particularly the case for solubilities lower than < 1 ppm or even < 1 ppb.

One more difficulty in using and interpreting experimental data arises from the fact that in some cases, especially for less soluble elements, those data that are required for estimating the behaviour of a liquid metal target have to be estimated by extrapolation from high temperature experimental data. This procedure naturally leads to errors.

As long as there are missing data, the results of calculations using approximate methods are indispensable. For the combinations of mercury with elements of different chemical characteristics, the corresponding values calculated using the methods described in preceding sections are tabulated in Tables 3 to 6. In cases where there are contradictory or imprecise experimental data only, the calculated values can serve as estimated values for judging the behaviour of the given elements. An assessment of the relevance of the calculated values is obtained based on the periodic behaviour of the elements and the comparison with known experimental data.

Figure 10 gives graphical representations of the results of solubility calculations for elements in mercury obtained for 333 and 463 K, i.e. the lowest and highest temperature expected for the newest design [7]. The figure compares the data derived from experimental studies [22] (solid circles and triangles) with the results of calculations, both for elements that are expected not to form compounds with the target material (open circles) and those that are known as compound formers with mercury (open triangles). The concentrations of nuclear reaction products expected for the final EURISOL irradiation of 40 years with 4 mA of 1 GeV protons as calculated using MCNPX/CINDER90 [6] are indicated by crosses.

Consequences that arise from the consideration of both literature and calculated data affect both the construction materials choice for target systems as well as the assessment of nuclear reaction product behaviour. For the construction materials, their solubility in mercury determines their resistance against dissolution in the liquid metal. Here it becomes clear that iron based alloys are clearly preferable in comparison to nickel alloys. Alloying components can be expected to enhance or decrease corrosion resistance according to their solubility in the liquid metal. One example for this kind of behaviour is the known leaching of nickel from steels in liquid lead bismuth eutectic [62]. Figure 10 indicates that alloying of refractory metals such as molybdenum or tungsten should increase corrosion resistance. Of course, in addition to the fundamental property of solubility in the liquid metal, the kinetics of corrosion processes will be greatly influenced by the presence of surface layers and their stability under the given operating conditions. The influence of alloying components on dissolution processes will also depend on their incorporation in intermetallic phases and its influence on the alloy microstructure. Therefore, the present data can only serve as a base for construction materials choice. Finally, the main group metals are clearly not suitable as construction materials.

Concerning the behaviour of nuclear reaction products, it has to be noted that the operating conditions such as temperature, temperature gradients as well as changes in concentration under continuous irradiation will have a strong influence. Figure 10 indicates that the solubility of some refractory metals such as Nb, Mo, Tc, Ru, W, Re, Os in mercury is very small. Therefore, for these metals the solubility limit can be reached after relatively short irradiation times. For these metals, precipitation is possible, especially at relatively cold spots in the system. Similarly, the

elements V, Cr, Fe and Co show low solubility. For these elements, additional transfer to the liquid metal by corrosion processes has to be considered, leading to even higher concentrations. Therefore, precipitation of these metals can be expected. The form of precipitation however is completely unclear. There could be platings on surfaces, floating material on the free liquid metal surface, deposition on the ground, formation of crystals, particulate material sticking physically to the surfaces or carried with the liquid metal. The latter could enhance erosion processes. A comparison of the solubilities at 333 and 463 K indicate that for some elements such as Hf and Pt a preferred deposition at cold spots could be possible. Concerning the accuracy of our results however, such predictions have to be taken with caution. For many of the remaining elements, especially the main group metals, the solubility limit will not be reached. There is however a group of metals, e.g. Ni, Rh, Pd, Ir and the heavier lanthanides, that will reach concentrations close to their solubility limit according to the calculations. However, regarding the accuracies of our estimations as well as those of the nuclear calculations, we will not try to predict their behaviour here. It should be mentioned however that the consequences discussed here for elements that show questionable results in our nuclide production data [6] are not much influenced by the uncertainties of nuclide production calculations.

Figure 11 shows the situation for the relatively short irradiation time of 1 hour. Here, while for most of the elements the concentrations induced by nuclear reactions are far lower than the solubility limit, for metals such as Mo and W, Re and Os the solubility limit can be reached even at very short irradiation times, indicating the possibility of precipitations already shortly after the start of irradiation. Indeed, e.g. ^{185}Os and ^{188}Ir (close to the solubility limit after 1 h at 333 K) have been detected in depositions on the wall at JSNS after draining the mercury in the start-up phase. The nature of these depositions, i.e. elemental or chemical compound, physisorbed or chemisorbed, is unclear so far. A short account of chemical effects that will influence the nature of precipitates will be given in the next chapter. Finally, the experiences from operating liquid metal targets will give clues on the precision of our predictions.

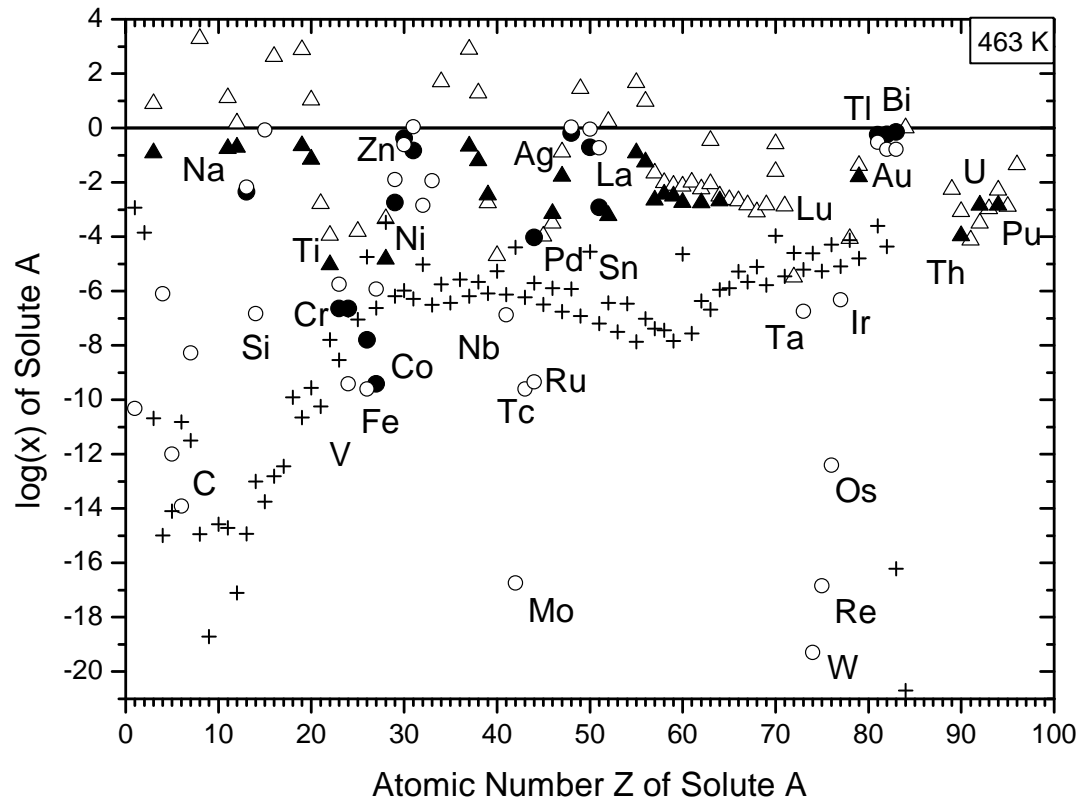
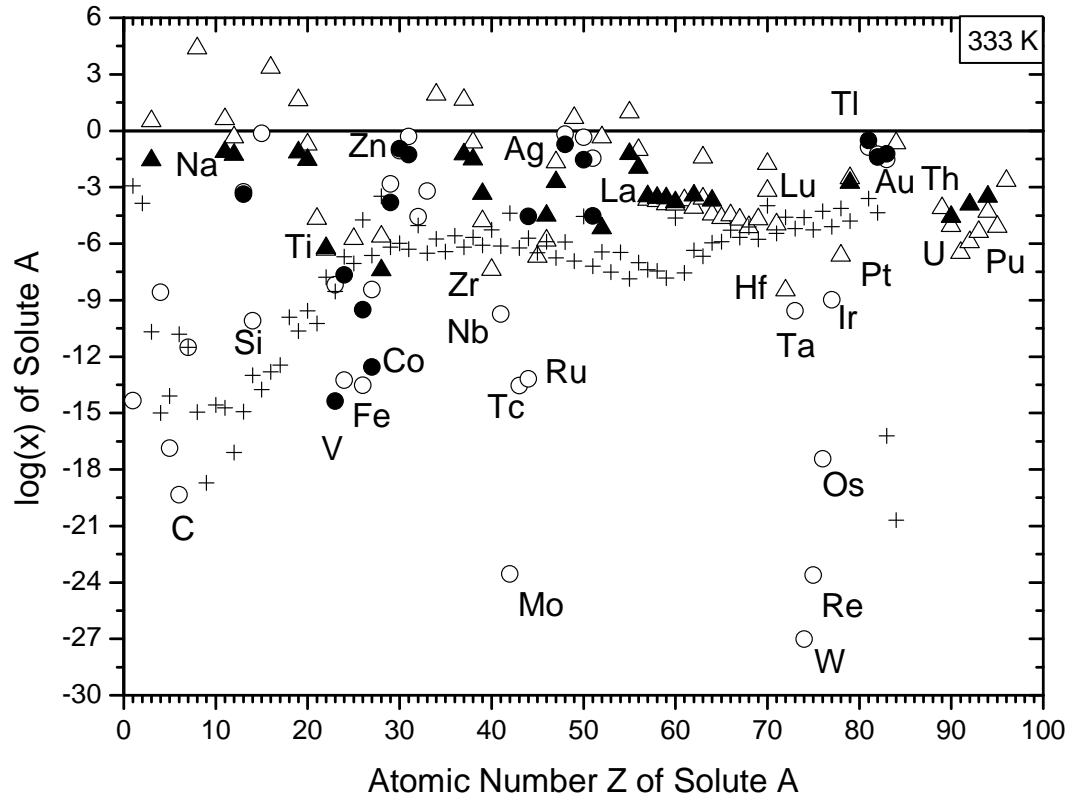


Figure 10: Comparison of literature data (solid circles and triangles) on solubility of elements in mercury [22] with calculated values for non-compound forming (open circles) and compound forming (open triangles) elements at 333 and 463 K. The expected concentrations of nuclear reaction products after 40 y irradiation of the EURISOL target are indicated as crosses [6].

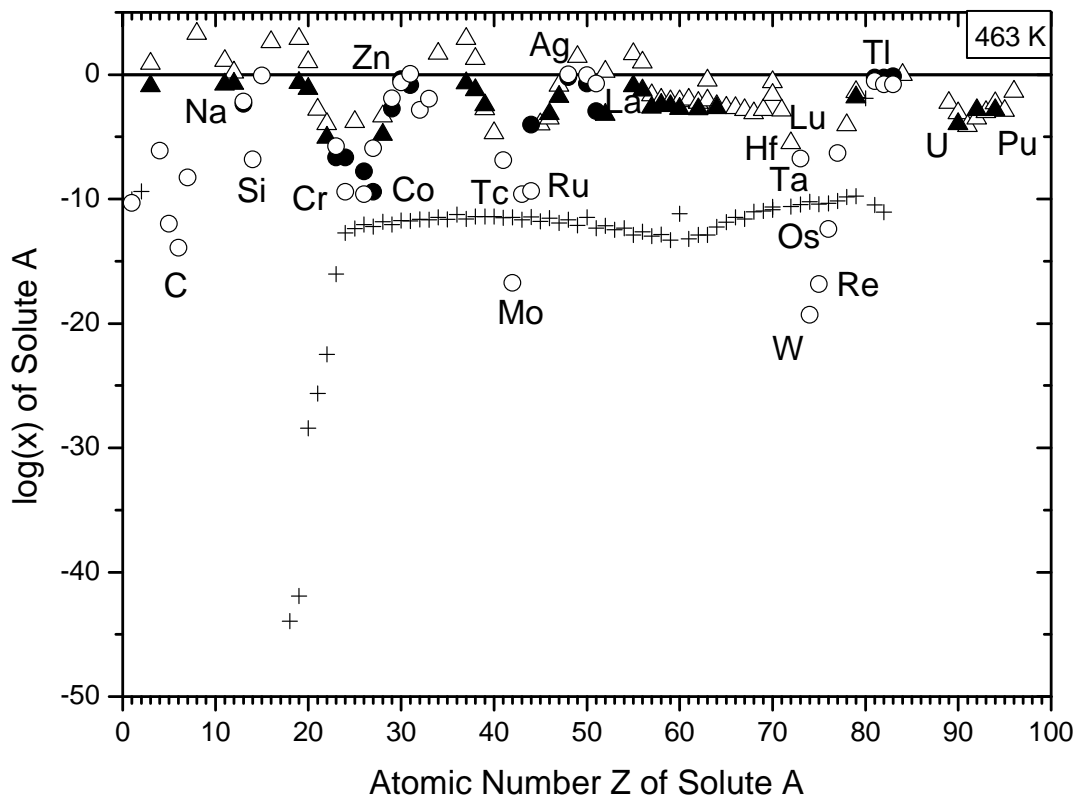
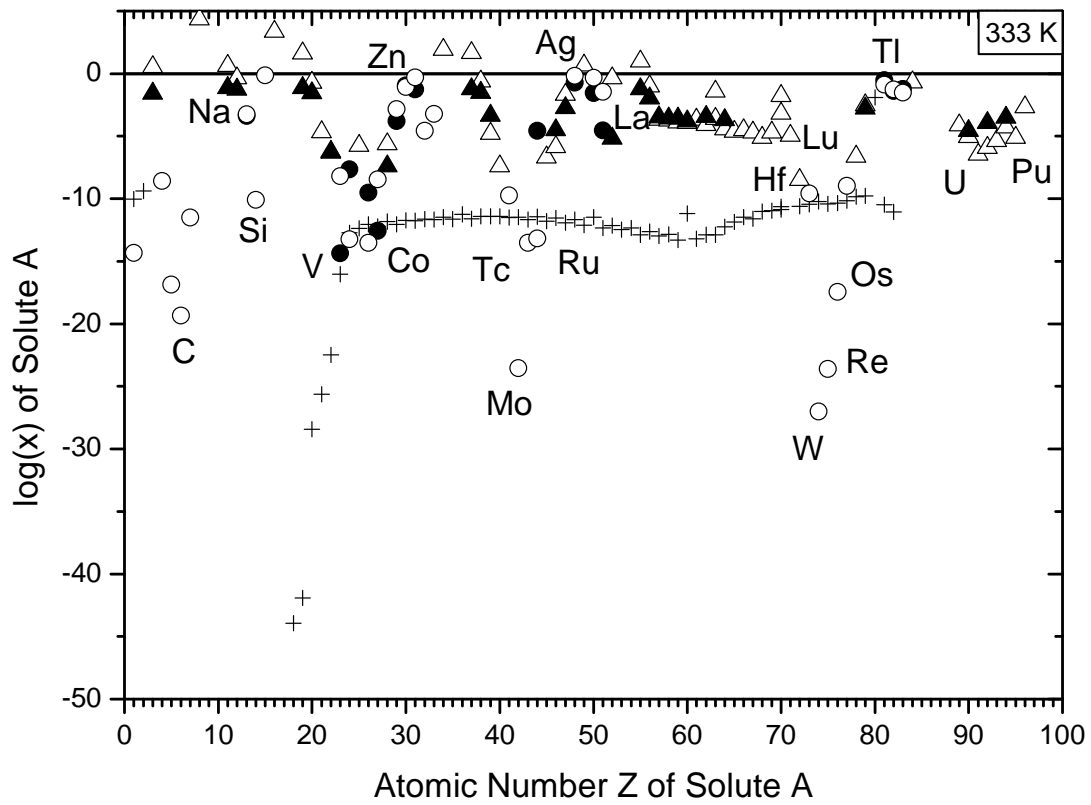


Figure 11: Comparison of literature data (solid circles and triangles) on solubility of elements in mercury [22] with calculated values for non-compound forming (open circles) and compound forming (open triangles) elements at 333 and 463 K. The expected concentrations of nuclear reaction products after 1 hour irradiation of the EURISOL target are indicated as crosses [6].

3.4. Interactions of impurities among each other

All the evaluations performed above focus on interactions of the elements with the target material only. It has already been pointed out that both literature data as well as calculated data have to be treated with caution. Additionally, interactions such as compound formation of the impurity elements among each other have been neglected completely so far. These interactions will lead to behaviour of the system that may be not comprehensible from solubility considerations alone. For example, electropositive elements that - in their pure form - are rather well soluble in mercury, may form oxides with the oxygen dissolved in the liquid metal or by reducing the oxide layers on construction materials. These oxides are most probably almost insoluble in the liquid metal. This effect could lead to precipitation of insoluble compounds and an increased attack on the construction material at the same time. Such effects naturally become more important for increased operation times, i.e. with increasing overall concentrations of the impurities. Similarly, the behaviour of impurities can be influenced by formation of intermetallic phases. A consistent and complete set of thermodynamic data for all phases/compounds and gas phase species that could possibly form in a target system is not available, as discussed in the introduction. Furthermore, determination of such a complete and consistent data set from experimental data or theoretical calculations seems unrealistic because of the complexity of the system. However, it has been proposed that one could try to obtain reasonable assumptions on the typical character of compounds formed by different elements, or at least certain groups of elements, within the target system, based on the knowledge of its total composition (construction materials and their protective layers and impurities, target material and impurities, corrosion behaviour, nuclide production) using a mass balance [63]. In this mass balance, the chemical products will be limited to binary compounds, and the latter will be formed according to their stability. In this approach, the stability of binary compounds will be judged by their enthalpies of formation. The corresponding values are calculated using the Miedema model. Because of the already large number of binaries, the fact that a binary system may comprise several compounds of different stoichiometry will be neglected. Therefore, only enthalpies of formation of equimolar composition will be calculated for the first approximation. In this report, we list values for the enthalpies of formation of these compounds $A_{0.5}B_{0.5}$, calculated using the Miedema model for the elements of group 1 to 16 of the periodic table (Appendix A). Here, some peculiarities of the Miedema models have to be discussed: The model was originally developed for the evaluation of intermetallic interactions. Over the years, semi-metallic and non-metallic elements like H, B, C, Si, Ge, N, P and As have been included in the model. This was achieved using a correction term that corresponds to the transformation of these elements to a hypothetical metallic state. As a result of this procedure, the enthalpies of formation obtained from the Miedema model for combinations of these elements correspond to solid compounds in a hypothetical metallic state rather than to formation enthalpies of realistic compounds in their standard state. For example, the "formation enthalpy" of a combination of hydrogen with itself yields a formation enthalpy of +100 kJ/mol. This value corresponds to the formation of 1 mol H in a hypothetical metallic state and not to the formation of $\frac{1}{2}$ mol H_2 in its standard state. For the same reason, for combinations of the group of elements mentioned above, often unrealistic positive values for the formation enthalpies of binary compounds are obtained that correspond to compounds in a hypothetical metallic state and not to the stable molecular compounds that exist under ambient conditions. For this reason, we exclude the enthalpy values of these binary combinations from Appendix A. For the combinations of non-metallic elements with themselves, i.e. H-H, C-C, etc., we give the standard formation enthalpy of 0 kJ/mol for the elements. Finally, we will discuss the periodicity of the calculated values of enthalpies of formation for binary compounds $A_{0.5}B_{0.5}$.

A map of heats of formation for compounds of composition $A_{0.5}B_{0.5}$ obtained in the way described above is shown in Figure 12. The periodicity of the stability of the compounds is clearly visible. For example, the chalcogenides are particularly stable. Consequently, valleys of stability are found for the atomic numbers $Z = 8$ (O), 16 (S), 34 (Se), 52 (Te) and 84 (Po), indicated by large negative enthalpies of formation (blue zones) in Figure 12. The calculated values for these enthalpies of formation of the chalcogenides become less negative with increasing atomic number of the chalcogen. This result coincides well with the well known periodic behaviour of these elements. When one looks at the enthalpies of formation of the chalcogenides with a second element as function of the atomic number of the second element, i.e. all compounds $A_{0.5}B_{0.5}$, where A is a chalcogen and B any other element ranging from $Z = 1$ to 110, one observes periodic behaviour again. Chalcogenides of electropositive elements, e.g. group 1 to 4, show exceptional high stability. When one moves to the higher group numbers 5 to 16, the enthalpies of formation become less negative (for O, S, Se and Te) or even positive (for Po). This is another example of the good qualitative correspondence of the calculational results with literature.

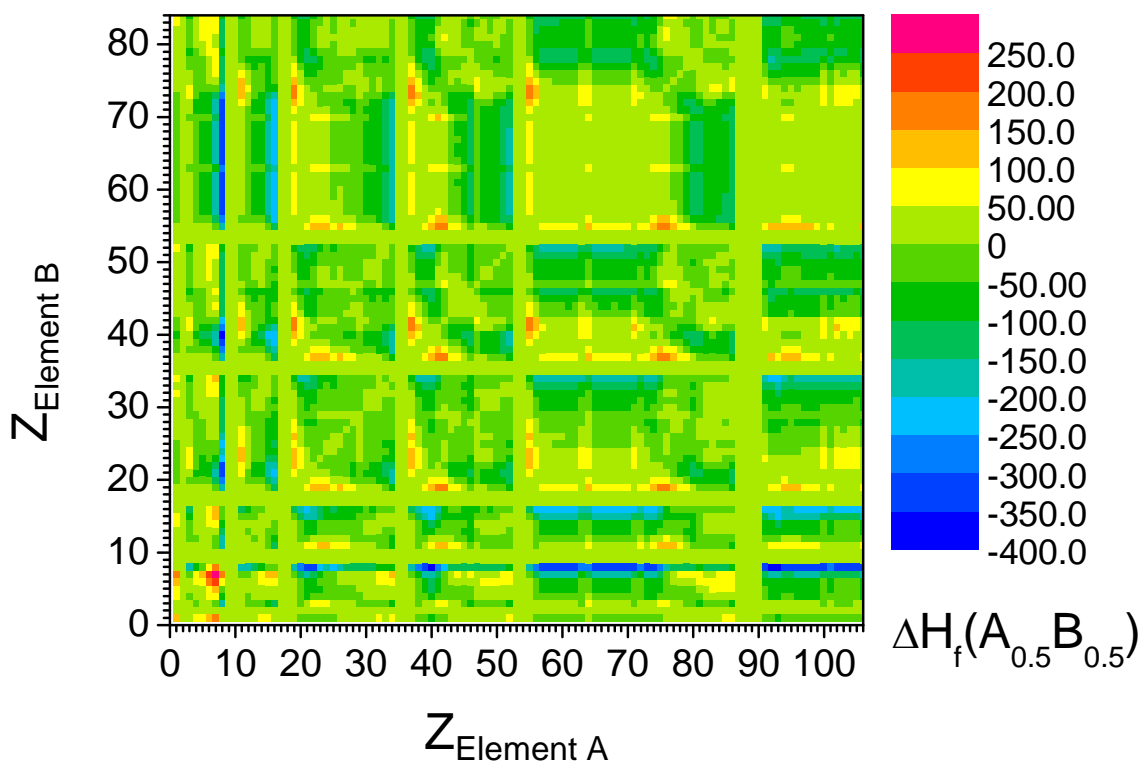


Figure 12: Stability map for all binary combinations of elements from the periodic table of the elements accessible by the Miedema model. Stability is judged by the enthalpies of formation for binary compounds of composition $A_{0.5}B_{0.5}$ calculated using the Miedema model. Values for binary combinations containing halogens and noble gases (group 17 and 18) which are not covered by the Miedema model are depicted with a formation enthalpy of 0.

In contrast to these “valleys of stability”, there are areas of very large positive values for the calculated values of formation enthalpies, indicating no stable binary compounds, e.g. for combinations of the electropositive metals of groups 1 and 2, and the refractory metals of groups 5 to 8. This behaviour is consistent with experimental results on those systems. No information on compounds in these binary systems is found in [60] and only three compounds out of 59 binary systems of those metals (all with ruthenium) are mentioned in [61]. Thus, though the results of Miedema calculations are only approximate values, they reflect the periodicity of the chemical behaviour of elements well. Furthermore, for obtaining consistent results on many

binaries in a reasonable time frame, i.e. without putting exceptional resources into experimental studies and/or computing time, the use of such a semi-empirical approach seems the only suitable choice. While the limitation to binary phases is clearly an over-simplification, it may as a first step give an indication on the specific behaviour of different elements or groups of elements. The validity of such predictions could be verified, if realistic laboratory scale experiments would be devised, or finally through experiences from existing liquid metal spallation sources such as SNS and JSNS, but also from the Post Irradiation Examination program for the MEGAPIE experiment [64].

3.5. Summary of the theoretical section

The complexity of a liquid metal spallation target system, containing numerous components – produced by nuclear reactions as well as present in form of impurities of the target and construction materials – under strongly varying conditions and a high irradiation field, makes reliable predictions on the chemical behaviour of the micro components very difficult. A rigorous thermodynamic treatment seems unrealistic, both because of the systems complexity and the lack of complete and consistent thermodynamic data. The semi-empirical Miedema model can provide approximate values for enthalpies of formation, mixing and solution for many elements of the periodic table. We used this model to assess enthalpies of solution and formation of binary systems of these elements with mercury to evaluate approximate values for the solubility of these elements in mercury.

Generally, elements can be divided in two groups: Elements that do not form stable compounds with mercury, and elements that do form stable compounds. For those two variants, equations for the description of the solubility equilibrium are developed, and solubility data are calculated based on enthalpy values obtained from the Miedema model. Values of calculated solubilities for these groups have been compiled for the lowest and highest temperatures expected in the EURISOL target for elements where a reasonable estimation is possible. Different problems of experimental determination of solubility and their calculation have been discussed. The reasons for discrepancies of the results of experimental studies and the theoretical calculations are complex and may arise from insufficiencies of the Miedema model for certain element combinations, lack of clarity in the formulation of the solubility equilibrium or even in accuracies of literature data.

For a very simplified assessment of the chemical interactions occurring among the impurities present in a liquid metal target system, the formation enthalpies of equimolar compounds in all systems within reach of the Miedema approach were calculated and their periodicity was discussed in comparison with well known facts about the properties of the elements in the periodic table.

4. Experimental studies

Radiochemical methods show several advantages with respect to the investigation of the behaviour of trace elements in liquid mercury and their separation from it. First of all, radioanalytical techniques allow one to detect and localize extremely small quantities of impurities that cannot be detected by conventional analytical methods. Furthermore, the production of impurity-doped samples by irradiation processes similar to that occurring in a real spallation target allows one to study samples that have at least a qualitative similarity to a real spallation target. The study of these samples naturally request for radiochemical studies. To a lesser extend, the study of radioactive samples allows one to work under the influence of a radiation field, which may influence the chemical behaviour of the impurities. However, because the activity limits for radiochemical laboratories this radiation field is many orders of magnitude lower compared to that of a large scale spallation target. Therefore, chemical radiolysis effects are much less pronounced in laboratory radiochemical studies.

Differences of laboratory scale radiochemical studies of liquid metals compared to a real large scale spallation target are numerous and depend on the way the impurity-doped samples are prepared. Samples prepared by direct irradiation of the liquid metal will, due to the limits of activity that can be handled, lead to much lower concentration in the samples, compared to the real target. This makes interaction of different hetero-elements much more improbable in the laboratory scale and can lead to peculiar effects of non-carrier added chemistry such as adsorption of the radionuclides on colloids or surfaces and the interaction with “conventional” impurities present in the liquid metal. Such effects are described in textbooks [65, 66] mostly for aqueous systems, but similar effects can be expected for liquid metals that contain non-carrier-added radionuclides. As an example, the presence of a very small amount of oxygen can lead to a more or less complete oxidation of some of the radiation induced impurities, a process that is known to occur in mercury containing small amounts of impurities and that may be enhanced by radiation effects. Such reactions naturally completely alter the chemical behaviour of the affected species.

The effect of extremely low concentrations can be overcome by the preparation of carrier-added samples by dedicated irradiation of the impurity components to be studied, e.g. by neutron activation, and then adding the impurities to the liquid metal in a concentration similar to that expected for a spallation target after long term irradiation. This approach generates physical as well as chemical problems that limit the use of this method. Different methods for the production of mercury samples that contain radio-tracers are discussed in more detail in the next section.

Furthermore, the setup used in a laboratory scale radiochemical experiment to study the fundamental behaviour of one or several radionuclides in liquid metal will be in general much simplified with respect to the very complex nature of a large scale spallation target, i.e. generally there will be no flow of the liquid metal and no large temperature gradients and the construction materials may differ from those used in a real target. Despite these disadvantages, one will benefit from these simplifications, since for studies leading to a fundamental understanding of the behaviour of radionuclides in mercury one wants to limit the set of parameters (and complications). Of course, the extrapolation of the results of such studies to technical scale is not trivial. In this study, we try to throw light on some interesting effects using relatively simple laboratory experiments and draw basic conclusions for the operating of a large scale target. Based on these results, much more complex intermediate scale experiments could be devised to test the validity of our results and conclusions, or alternatively, the conclusions presented here can be validated at the large scale facilities that are now under operation, i.e. SNS at ORNL and JSNS at J-PARC.

A disadvantage of radiochemical studies is that they do not allow a direct assessment of the chemical state of the impurities, e.g. structures and oxidation states. However, the study of radionuclide distribution and behaviour in liquid mercury samples under different physical and chemical conditions by radiochemical methods, together with general chemical knowledge will

allow an educated guess on the behaviour of impurities in mercury in a spallation target. The different methods for the production of Hg samples containing radioactive impurities are discussed in the next section.

4.1. Preconditioning of the mercury prior to sample preparation

For all samples prepared at PSI, mercury obtained from Merck (specification extra pure, purity 99.6-100%, impurities insoluble in $\text{HNO}_3 < 0.002\%$) was used. The liquid metal was distilled prior to sample preparation. For this purpose, a distillation apparatus was set up for the distillation of mercury in the scale of some 100 g. In this apparatus, depicted in figure 13, distillation temperatures between 200 and 250°C were achieved using a membrane pump.



Figure 13: Apparatus used for the vacuum distillation of mercury prior to the preparation of radionuclide-doped mercury samples.

4.2. Storage and handling of samples

For a fundamental study of the behaviour of radionuclides produced in irradiated mercury it is mandatory to exclude external effects that can influence their chemical state. From the known behaviour of amalgams discussed in the introductory section it was concluded that it would be of advantage to handle the samples in an inert atmosphere to reduce the possibility of oxidation effects that could influence the chemical behaviour. A highly sophisticated glove-box system that could provide such an environment is not available in our laboratory. However, a simple glove-box made from Plexiglas was on hand. As operating gas, argon was chosen. The gas was dried by running through columns of silica gel and molecular sieve prior to entering the box. During set-up, the air contained in the box was removed by inflating a large plastic bag inside the box, using the pre-dried argon, thus pressing out a large fraction of the air contained inside the box. After repeating this procedure 5 to 6 times, the box was continuously flushed with a small flow of argon over several hours to establish an inert working atmosphere. Inside the box, chemical absorbers were set-up for the continuous removal of moisture and oxygen.

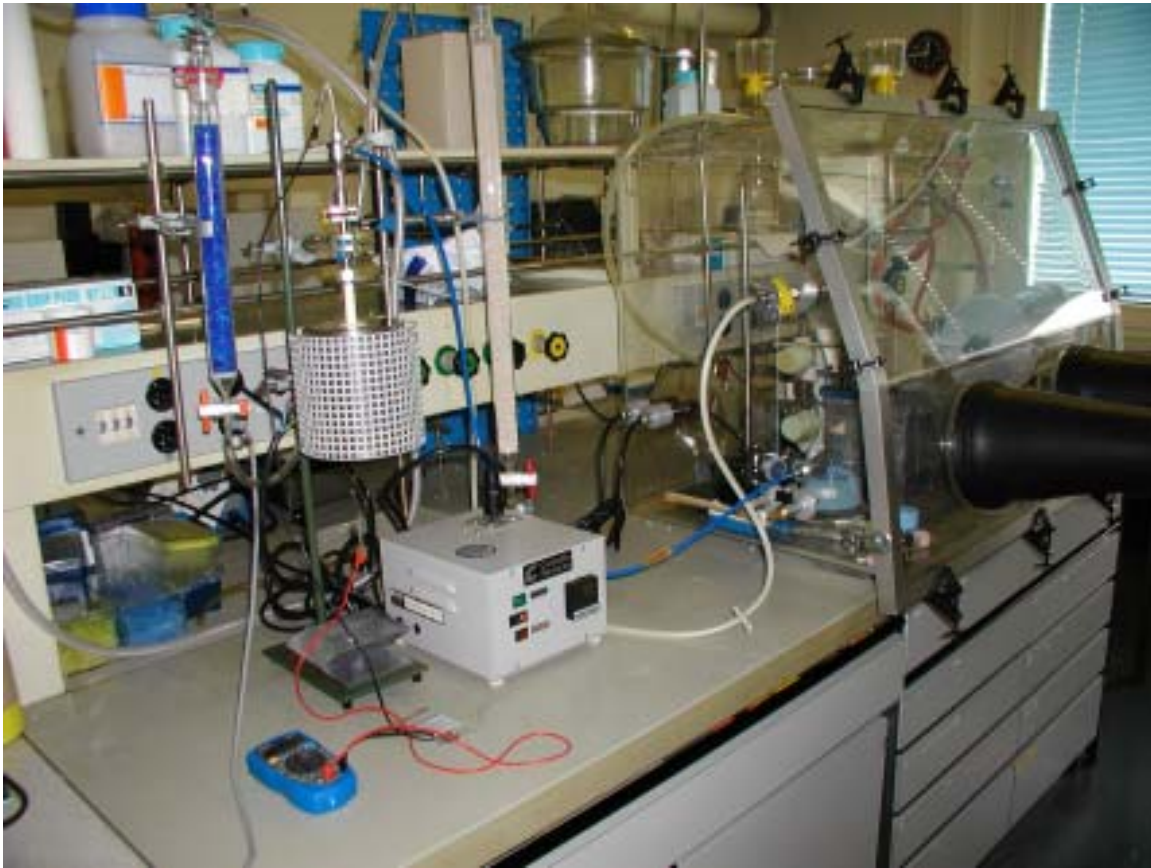


Figure 14: Glove box system. Top: outside view with gas pre-drying columns and oxygen sensor. Bottom: Inside view with lead shielding and oxygen absorber solution (left side).

For the absorption of moisture, a crystallization dish filled with SICAPENT (P_2O_5 with moisture indicator) was placed inside. Oxygen was gettered by a solution of 50 to 100 g pyrogallol in a sodium ethylene glycolide/ethylene glycol solution. This solution contains oxygen sensitive organics that bind oxygen present in the atmosphere of the box. Additional to binding the oxygen, this solution also serves as an indicator for the presence of oxygen. While the solution is nearly colourless when freshly prepared, when reacting with traces of oxygen, dark-coloured reaction products are formed. Thus, the solution gradually becomes darker and darker with the time of exposure, finally being almost black, as can be seen in figure 14 bottom. In this way, the rate of discoloration can serve as an indicator for the leak-tightness of the system.

To control the oxygen content of the glove-box system, an oxygen sensor was built from a tube of yttria-stabilized ZrO_2 . This tube was contacted with platinum wires fixed with conductive silver glue both from the inside and the outside. The inside then was connected with the gas atmosphere of the inert gas box, while the outside was in contact with ambient air. The sensor tube was placed in a tube furnace where it was heated to 600–700°C. The material of the tube becomes O^{2-} ion conducting at these temperatures. In this way, a concentration cell is obtained that allows one to determine the oxygen concentration inside the box from the electromotive force measured between the inside and outside electrodes of the cell. For our box system, we measured oxygen concentrations around 0.1% O_2 after the complete installation of the system. For the handling and storage of radioactive material, a 5 cm lead shielding was installed in the box. This setup was used to store the irradiated mercury samples obtained from CERN and perform the first series of experiments with one of these samples.

4.3. A general view on different methods for preparing Hg samples containing radionuclides

4.3.1. Direct irradiation

4.3.1.1. Irradiation of Hg with high energy protons

When mercury is hit by high energy protons, a vast variety of nuclear reaction products will be produced within the liquid metal similar to a large spallation target. Hence, the spectrum of nuclear reaction products is expected to be at least qualitatively comparable to a spallation target. Furthermore, the fact that the impurities are generated directly in the target material, as opposed to the chemical preparation methods described below, it much better resembles the actual status present in a large spallation target at least at the time of irradiation. However, already during the irradiation or during the cooling time required before the sample can be transported to the radiochemical laboratory, complex chemical processes involving the impurities can occur because of the complex composition of the sample. In general, such samples will at first be studied using γ -spectroscopy. Because of the extremely complex composition of the samples, the evaluation of spectra is equally complicated. Even a qualitative evaluation of γ -spectra of such samples is a major task. During this project, three such samples were obtained. The first one was used to study the removal of precipitated solid impurities by mechanical methods. The remaining mercury was subsequently used for the study of novel adsorption techniques for the removal of the still remaining dissolved impurities. One of the remaining samples was investigated with regard to the produced nuclides, their distribution in the irradiated sample and possible changes of this distribution with time. For the second one, additionally the removal of radionuclides by

conventional mercury purification methods such as acid washing and distillation was studied. The results of these studies will be presented below.

4.3.1.2. Irradiation of Hg with high energy neutrons at SINQ

The production of mercury containing radionuclides by its irradiation with fast neutrons in the spallation source SINQ at PSI was originally considered useful in the preparation process of the EURISOL-DS project proposal. With this method, neutron deficient mercury isotopes are produced by n,xn reactions, which subsequently decay to radioactive nuclides of elements with an atomic number a few numbers smaller than that of mercury. However, it was already shown in [67] that only very few interesting radionuclides, namely gold (^{192}Au , ^{193}Au , $^{198\text{g}}\text{Au}$, ^{199}Au) and platinum nuclides (^{188}Pt , ^{189}Pt , ^{191}Pt) can be prepared in this way in reasonable amounts. When discussing such irradiations with the responsible people, it turned out that an irradiation of liquid mercury samples is not allowed. Only solid samples are allowed to be irradiated in the SINQ neutron activation facility. However, the irradiation of solid Hg alloys does not make sense, since a separation of elemental Hg from the irradiated sample would leave the radionuclides different from mercury in the solid residue. The distilled mercury would only contain radionuclides that are built-up by the decay of radioactive mother nuclides of Hg itself. A consideration of the half-lives and production rates of these mothers lead to the conclusion that mainly gold nuclides could be produced using this method. Since gold nuclides such as ^{194}Au , dissolved in mercury, were available from other sources, this method was not used within this project.

4.3.2. Chemical procedures for the preparation of Hg samples containing radionuclides

An alternative way for obtaining samples that contain radioactive impurities is the activation of the desired impurity by neutron activation and the subsequent introduction in the liquid metal by chemical procedures. The latter can be achieved either by direct dissolution of the impurity in the liquid metal or by electrochemical deposition of the impurity onto a mercury cathode.

Neutron activated samples of various elements can be readily produced at PSI using the neutron activation facility (NAA) at SINQ. By the nature of this nuclear reaction process, these samples contain a relatively large amount of inactive carrier.

4.3.2.1. Direct dissolution of soluble radionuclides prepared by neutron activation

First of all, to produce samples of mercury containing a radio-tracer as impurity, the impurity has to be rather highly soluble in mercury, so that a sufficient amount of radioactivity can be transferred to the liquid metal at not too high temperatures with reasonable reaction times.

As a consequence of the activation procedure, mercury samples mixed with activated elements prepared in this way will contain inactive carrier of the same element. The admixture of weighable amounts of this material to mercury leads to larger concentrations of the contaminant in the liquid metal. Typically, this method leads to samples with concentrations comparable to those expected to be produced in a spallation target after decades of irradiation or even higher, but samples prepared in this way will contain only one or a few radionuclides. This makes the chemistry much less complex and facilitates a more straight forward evaluation and interpretation of experimental results. Additionally, peculiarities related to the presence of non-carrier-added nuclides with very low concentrations are expected to be non-existent or at least much less pronounced for this type of sample. However, these samples of course do not resemble a realistic

chemical composition of the spallation target environment. Thus, these samples can be used for model studies that can throw light on the fundamental behaviour of certain elements in liquid mercury. These are important in their own right, but for an assessment of the behaviour of the complete liquid metal spallation target system more complex mixtures will also have to be studied. From a fundamental science point of view, a thorough investigation of chemical phenomena that could occur in a liquid metal spallation target should proceed from simple binary systems that can be produced using the procedures described in this section, over more complex mixtures to a realistic spallation product mixture such as produced in the high energy proton irradiated samples described in a preceding section.

The samples prepared by direct mixing were mainly used to study the adsorption of rather highly soluble elements on metal surfaces. We will give here some general comments on the difficulties encountered in the production of these samples. The detailed irradiation and mixing conditions and peculiarities observed for the different elements will be given in subsections for each series of experiments below.

The impurities introduced into mercury by direct mixing should have the following properties favourable for this preparation method and the subsequent radiochemical studies:

- a) A solubility at room temperature that should allow the preparation of mixtures with concentrations comparable to those present in a liquid mercury spallation target after long term irradiation.
- b) A moderate sensitivity towards oxidation, making the handling without sophisticated inert gas equipment possible.
- c) The existence of isotopes that are readily produced by neutron activation and have decay properties that are convenient for the investigation of adsorption processes, i.e. half lives ranging from some days up to some hundred days.

Considering these prerequisites, we chose the metals Zn, Ag, Cd, Sn and Sb for our studies. After neutron activation they were mixed directly with mercury under ambient conditions in inert polyethylene (PE) containers in quantities that result in concentrations comparable to those expected for the EURISOL target at the end of irradiation. Problems and difficulties encountered using this procedure include the following:

- a) Kinetic hindrance of the dissolution: this leads to either incomplete solution or long times needed for the dissolution reaction. This effect may be enhanced by oxide layers present on the solid metals. Mechanical agitation was used to enhance the rate of dissolution. In some cases it was decided to interrupt the dissolution process on remove the remaining undissolved metal by filtration. Oxide scum remaining on the liquid after the dissolution process were removed by filtration in any case.
- b) oxygen sensitivity: a slow oxidation of the material was observed in most cases, leading to the slow formation of oxide scum during the experiment. In some cases the scum tended to float on the liquid metal surface, while in other cases a preferred adhesion to the walls of the vessel was observed. Between different series of experiments it was tried to remove this scum either by filtration or by changing the reaction vessel. It turned out that in many cases the scum contains the majority of the radioactivity. Thus it can be concluded that the results of adsorption experiments are influenced by the slow formation of this scum. Naturally, this complicates the evaluation of the results.

The details and differences of the behaviour of the different impurities will be discussed in chapter 4.5.2, together with a careful analysis of the results.

4.3.2.2. Preparation of impurity-containing mercury samples by electrochemical methods

4.3.2.2.1. Direct electrolysis

An elegant way to produce mixtures of Hg with radiotracers is electrolysis using a mercury cathode. In principle, radionuclides prepared by any irradiation method can be brought into solution and electrolyzed on a mercury cathode or anode, depending on the species contained in the solution. For complex mixtures, a selective electrolysis can be achieved by adjusting the potential. An interesting application of this procedure for the separation of radionuclides from spent nuclear fuel is discussed in [68]. We intend to use the electrolytic deposition technique for the transfer of radionuclides into liquid mercury. There are many papers that report about the use of this technique for the preparation of diluted “amalgams”, meaning diluted solutions of impurities in liquid mercury (see for example [23] for a review). Generally speaking, the electrolysis method should be advantageous over the direct mixing method because of several reasons.

- a) The solute is dispersed “atomically” in the electrolyte and will be solvated/introduced to Hg in that state through a surface reaction. Though not really comparable, this process seems to resemble the production by nuclear reactions in a spallation target since it avoids the introduction of the impurity as a bulk solid component that may result in the formation of colloidal solutions.
- b) Effects coming from surface contaminations of the impurity metals such as slow transfer into mercury solution or contamination of the metallic solution due to remaining oxide scum can be avoided
- c) the concentration of the obtained solution can be controlled by the amount of charge transferred in the electrolysis process, given the current yield is known
- d) the deposition is controlled by potential, so that more electropositive contaminations can be excluded, or elements can be selectively added or removed from the liquid metal.

The disadvantages of the method include more effort in setup of suitable equipment and choosing proper reaction conditions such as electrolyte, potential and current density. We restricted our efforts in this preparation method to a limited number of metal/mercury systems that are suitable for a deposition on mercury from aqueous solutions and that cannot easily be prepared using the simple mixing technique due to high oxygen sensitivity and/or low or slow solubility of the metal in mercury. From literature it is known that solutions of alkaline metals [69] and lanthanides [70-74] can be prepared in this way. We used aqueous solutions of ^{22}Na , ^{160}Tb and ^{192}Ir for tests of electrolysis procedures for the preparation of mercury samples containing radioactive impurities.

4.3.2.2.2. Phase exchange reactions

Another electrochemical way to prepare mercury samples containing radioactive tracers makes use of phase exchange reactions. Here, mercury containing an electropositive metal is prepared by electrolysis. This impurity containing mercury is then brought into contact with solutions of less electropositive metals. According to their position in the electrochemical potential series, the less electropositive metals will exchange with the electropositive component in the mercury, thus leading to an incorporation of the less electropositive metals into the mercury. We used this technique mainly for experiments to re-introduce into mercury the nuclear reaction products obtained in aqueous solution during the treatment of proton irradiated mercury and the respective irradiation capsule. For this, we prepared sodium and cesium amalgams by electrolysis and exposed these amalgams to solutions of the respective nuclear reaction products. An overview of these experiments is given in the corresponding section below.

4.4. Measurement and Evaluation of γ -spectra of the high energy proton irradiated samples

4.4.1. General considerations

Series of γ -measurements of the two high energy proton irradiated samples CERN 1 and CERN 2 were carried out using different detectors and time intervals in order to get as much reliable information as possible as well as to study the chemical processes inside the mercury and the separation efficiency of the chemical procedures applied.

Due to the high number of produced radionuclides and the resulting high number of expected γ -line interferences, manual spectra analysis is not possible and even high-sophisticated calculation tools meet their limits with this task. Some of the commercially available γ -analysis programs were tested already earlier concerning their ability to fulfil these special requirements. GENIE2000 from Canberra (version 3.1) proved to be best-suited for complex spectra analysis. Moreover, this software provides also special tools for a manual peak fit correction and improvement of input parameters and boundary conditions. Nevertheless, the application of standard processes given in the program was in no case possible. Nuclide libraries had to be created manually, considering all the possibly produced radionuclides by spallation processes in mercury. Due to the high number of nuclides, as well as the amount of γ -lines, the program crashed in some cases, if too much interference corrections had to be performed. Consequently, to find optimum and similar analysis conditions for all spectra was not possible; for each spectrum, individual modifications had to be performed to get best results. In the following, a detailed description of the applied tools and the analysis procedures as well as the modification of the analysis process is given.

4.4.2. Detectors

Three high-purity Germanium detectors (coaxial HPGe, Eurisys and EG&G ORTEC) - two vertically and one horizontally oriented - were used to perform the measurements. This gave the possibility to measure the same sample from the bottom and from the side. It was supposed that these measurements can differ widely from each other, due to chemical processes inside the mercury, which lead to accumulation of activity at walls and especially at the surface. This leads to different absorption of the γ -rays because of the self-shielding of mercury arising from its high atomic number. This effect is not negligible, but it cannot be corrected in a straight forward manner since the distribution of the radioactivity in the sample is not known. The absorption effects will in general lead to an underestimation of the real activities, especially for nuclides with low energy lines.

4.4.2.1. Calibration

Energy-calibration was done using a commercially available standard calibration source of ^{152}Eu in liquid form with a similar geometry like the irradiated mercury. The same source was also applied for the efficiency calibration using different distances (up to 25 cm) from the detector surface. The properties of the detectors allow a reliable efficiency calibration from about 60 keV upwards. For measurements of more than one hour, an additional low-tail correction was performed in order to correct changes of the peak shape that occur as a consequence of slight energy drifts.

To consider the self-shielding of the mercury, a special calibration tool (ISOCS/LabSOCS) is available, which changes the efficiency calibration essentially, especially in the low energy range and in case short distances from the detector are used. Additionally, the effects of self-absorption are strongly influenced by their distribution of the radioactivity in the samples. For example, when the radioactivity is measured from the bottom, the shielding of the γ -rays decreases strongly when an equal amount of radioactivity is present in a mercury sample at the bottom of the vessel, compared to when it is located in a surface layer or in homogeneous solution. A few examples of the effects of self-absorption are given below. Since we do not know the distribution of radionuclides a priori, we are not able to correct for these effects. Furthermore, the results of our investigations show that the radionuclide distribution is complex. A part of the activity is obviously preferably located on the surface of the liquid metal and adsorbed on the wall of the containers, while certain nuclides of certain elements are in homogeneous solution in mercury. It is not possible to determine the exact distribution of all the nuclides between walls and surface in a straight forward manner, using the two samples only that were also to be used for other experiments. Therefore, we do not correct our results for self-absorption effects. Thus, the activities given in this report are underestimated for those samples where self-absorption of mercury is present, i.e. all of the samples where the radioactivity is measured without separating the radionuclides from mercury.

4.4.3. Nuclide libraries

Nuclide libraries were created manually. The main problem to be solved was the tendency for a systematic crash of the computing system if the library content is too large. These crashes depend not only on the total number of the nuclides within a library, but are determined by the extent of interference corrections within the calculation procedure, and thus depend also on the total number of γ -lines. Therefore, γ -lines with less than 1% abundance were rejected, and the X-ray region up to 80 keV was not taken into consideration due to the uncertain efficiency calibration. The creation of the library was then performed iteratively. At first, the standard library was used to identify some of the common radionuclides and these assuredly identified nuclides were used as the starting point for the development of a suitable library. As the next step, a manual analysis of γ -lines from the list of unidentified peaks was performed. Those nuclides, which allow a distinct assignment, were then added to the library list and the procedure was repeated. Then, nuclides were added to the library list, which are expected to be found with high probability in the spectrum due to their production rates, measurable γ -rays and half-lives. This was also done using a step-by-step procedure because of the necessity to avoid further systematic crashes. Radionuclides, which could not be identified confidently after running the program again, were deleted from the library afterwards. The library obtained in this way is compiled in Appendix B.

4.4.4. Analysis procedure

All analysis steps were - after testing - combined to an automatically driven analysis sequence, which could then be applied to most of the spectra of the original samples. In some cases, modifications of the calibration and selection of other nuclide libraries had to be done before, and for some spectra, a special treatment had to be applied. The developed analysis sequence consisted of the following steps. The individual functions and parameters are explained in detail in the manuals of GENIE 2000:

1. Peak Locate: unidentified 2nd Diff.

A channel interval from 20 to 8192 was used with an energy tolerance of 1 keV and a significance threshold of 5.0.

2. Peak Area Sum: non-linear LSQ fit

The option "Fit singlets" was chosen with a 95% critical level test and maximum numbers of FWHM between peaks of 5.00 and 2.00 for the left and right limits, respectively.

3. Interactive peak fit

Due to the high number of detected peaks, and the resulting high number of multiplets to be fitted, the interactive peak fit tool has been used for every spectrum analysis. In many cases, the fit originally proposed by the software did not match the real data points. Variation of the region limits, the number of background points, using of fixed FWHM and low tail parameters as well as the consideration of additional peaks for the calculations could improve the fitting results in most of the cases. Usually, a deviation lower than 10σ could be reached, for the most important peaks we tried to achieve 2σ . Once more, the GENIE2000 software came here to the limits, since not in all cases such an improvement was possible. Sometimes, the program refused to fit, sometimes the program simply crashed, or, in a few cases, the library did not work anymore. Therefore, a compromise had to be found between an acceptable fit and a still working program. This procedure was iterative and, since it had to be done for every single spectrum, very time consuming.

4. Efficiency correction

The dual mode was used.

5. Tentative Nuclide Identification

This option provides an assignment of every γ -ray to nuclides included in the library. By means of this tool one can obtain an overview which γ -lines are interfered by many other lines and therefore, may cause problems. Questionable isotopes can so be identified.

6. Nuclide Identification NID w/Interfer.

This last step contains automatic nuclide identification after interference correction including quantitative calculation of the radionuclides activity. Due to the high amount of γ -lines, the high number of interferences and the already described problems with the peak identification and peak fitting, these results of the identification have to be checked carefully by use of other information (as example half-life, production rates, and probability of production). Additional information from other experiments (chemical separation of selected radionuclides, sorption studies, measurement geometries and others) can help to confirm the presence of the identified isotopes.

4.4.5. Problems of γ -spectroscopy analysis related to the high self-absorption of mercury

Mercury has a very high absorption coefficient for γ -rays, especially for those with low energy. This causes problems with the quantitative evaluation of the spectra of samples in which mercury is present. In these samples, the results very strongly depend on the geometric arrangement of the sample and the distribution of the radioactivity in the sample. The typical high energy proton irradiated samples obtained from CERN were contained in cylindrical vessels. In the following, we will consider a few simplified models for the distribution of radioactivity in such vessels and its influence on the γ -measurement with different detector-sample arrangements. For the most simple cases, the radioactivity can be homogeneously dissolved in the mercury, or it may be present as a surface layer, a bottom layer, or sticking to the side walls of the cylinder. For an illustration of the self-absorption problems encountered when working with mercury samples, we

have calculated detector efficiencies for the common sample-detector arrangements and a few different radionuclide distributions using the Geometry Composer add-on for the GENIE 2000 software. The calculated efficiencies are compared with those measured on comparable detectors using standard samples in comparable geometries. Figure 15 shows the sample-detector geometry model used for our first example. Figure 16a shows a comparison of the efficiency experimentally determined for a HPGe-detector in horizontal arrangement for an aqueous standard sample in 25 cm distance and the efficiency calculated for a sample with the dimensions of the stainless steel irradiation capsules obtained from CERN, containing 1 ml of mercury. The radioactivity is assumed to be homogeneously dissolved in mercury. One can clearly see that for the mercury sample the efficiency for low energy γ -rays is dramatically suppressed, e.g. by a factor of 100 at 100 keV. For higher γ -energies for calculated and experimentally determined efficiency curves nicely converge. Figure 16b shows the effect of a surface enrichment of the radioactivity, calculated for a surface layer of 1 μm thickness and γ -ray absorption properties similar to that of a typical oxide material. Efficiencies for varying enrichment factors between Hg and the surface layer, ranging from 1000 to 1×10^9 , have been calculated. It is shown that with increasing surface enrichment the calculated efficiency approaches the efficiency experimentally determined for the aqueous volume source. Here, it has to be pointed out that for the long sample detector distance of 25 cm the difference between a volume source (experimentally determined efficiency) and an approximately disk shaped source with a volume of Hg located beyond it (Hg sample with most of the activity in a surface layer) is comparatively small. For closer sample-detector distances, much larger differences are expected.

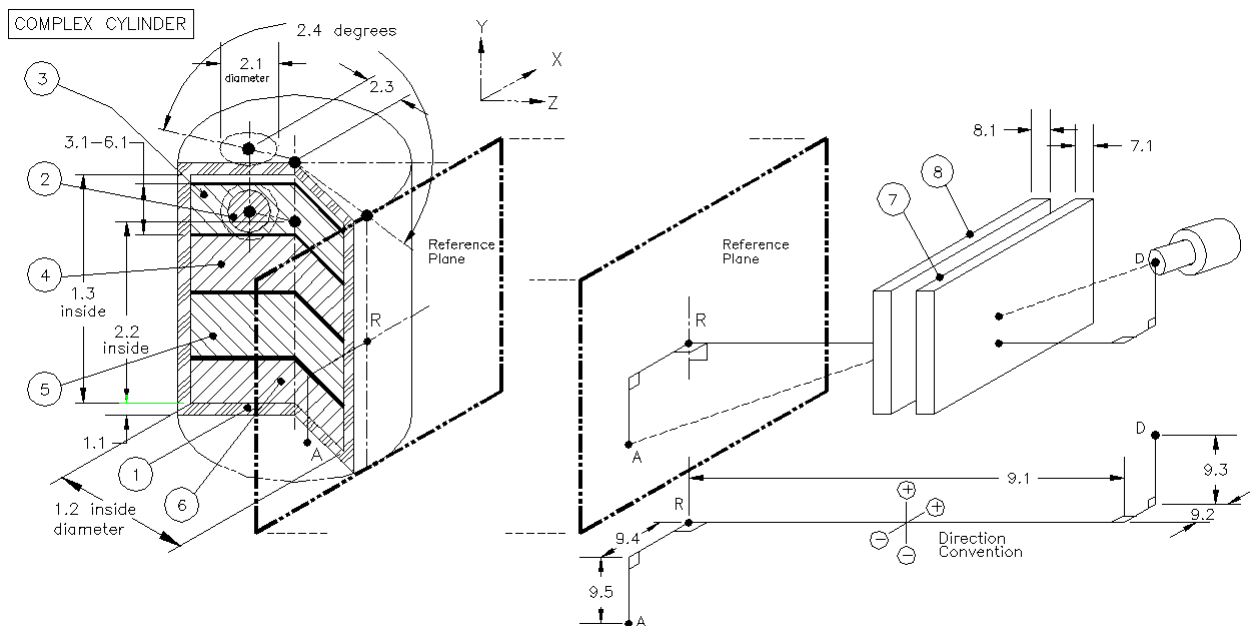
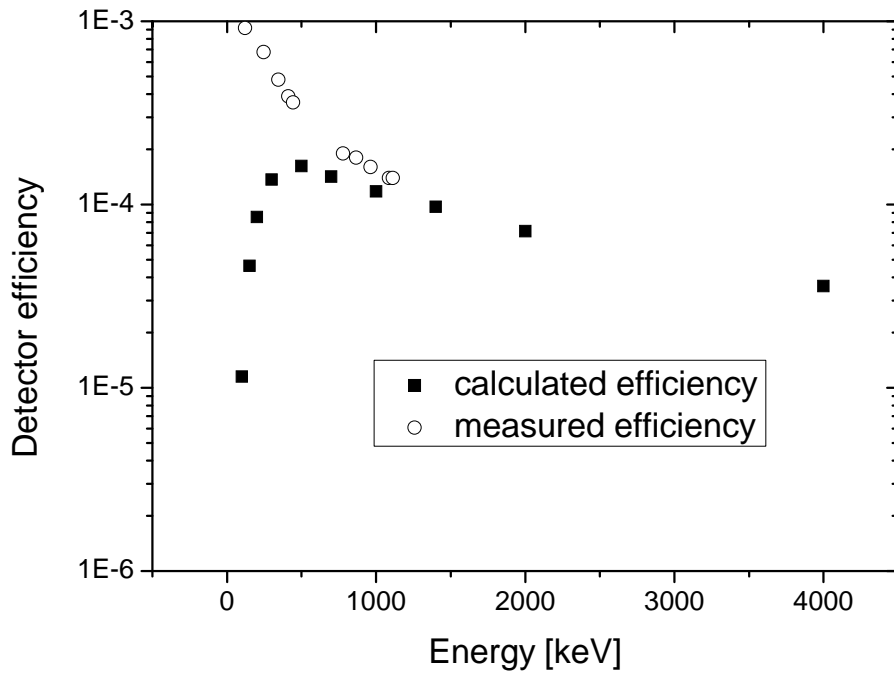
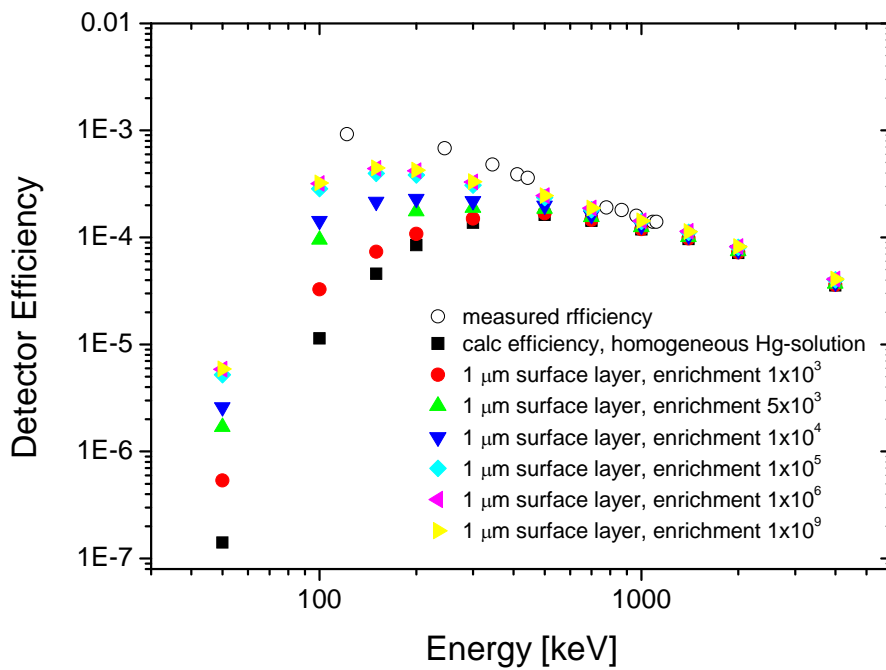


Figure 15: Geometric arrangement used for the model calculations of the efficiency for a HPGe-detector in a horizontal sample-detector arrangement. The parameters used for the calculations are the following, corresponding to the dimensions of the stainless steel irradiation capsules obtained from CERN, filled with 1 ml of Hg: sample detector distance 25 cm, container: diameter 9 mm, height 35 mm, wall thickness 2.5 mm, Hg fill height 16 mm, 1 μm surface layer of density 1.6 gcm^{-3} , cover gas argon.



a)



b)

Figure 16: a) Comparison of experimentally determined and calculated efficiency for a HPGe-detector in horizontal arrangement for a sample-detector distance of 25 cm. The experimental efficiency was measured with an aqueous standard. The calculated efficiency was obtained using the actual geometric dimensions of the stainless steel irradiation capsules, filled with 1 ml of Hg, as received from CERN, incorporating the γ -ray absorption properties of mercury. A homogenous distribution of the radioactivity in the mercury has been assumed.

b) Additionally to a), efficiencies are calculated for varying relative enrichment of the radioactivity in a surface layer of 1 μm thickness. For the surface layer, absorption properties of a typical oxide material were assumed.

In a second example, we look at the experimentally determined and calculated efficiencies for a vertical sample-detector arrangement. Figure 17 shows a graphical representation of the model used for the calculations. Figure 18 shows a comparison of the detector efficiency measured with a standard area source directly on the detector and calculated efficiencies for a cylindrical source with the dimensions of the CERN irradiation capsule, consisting of a bulk mercury phase and surface or bottom layers containing varying relative amounts of radioactivity. As expected, the efficiency calculated for a homogeneous distribution of the radioactivity in the liquid metal is much lower than that measured for a sample without the absorption effects of mercury. Especially for low energy γ -rays in the range of 100 to 200 keV, the efficiency is lowered by factors between 50 and 10 by the absorption effects of mercury. This effect naturally increases with an enrichment of the radioactivity on the mercury surface. On the other hand, the formation of a deposit on the bottom will increase the efficiency since less of the radiation is absorbed by the liquid metal. Indeed, for high enrichment of the radioactivity in the bottom layer, the sample becomes similar to an area source. This is reflected in the better agreement of the calculated efficiencies for bottom enrichment $\geq 10^3$ with the efficiency measured for the standard area source. With increasing γ -ray energies, the observed differences naturally decrease.

While the examples explained above are immediately comprehensible, they can serve only for a qualitative understanding of the absorption effects that will influence the results of the evaluation of γ -spectra of mercury samples where nuclear reaction products were induced by the wide range of nuclear reactions generated by high energy protons. Here, the situation is extremely complicated, because one has to deal with various nuclides from a large range of elements, where each element will show its individual chemical behaviour. Therefore, each element can in principle show a different distribution between bulk liquid metal phase, surface of the liquid metal, bottom and wall of the container. The material accumulated on the surfaces may even be present in form of inhomogeneous precipitates. Furthermore, the degree of inhomogeneity may change with time because of slow precipitation processes.

For a straight forward correction of the absorption effects of mercury-containing samples, the distribution of each nuclide would have to be known and simple enough for a calculation of a corrected efficiency. This is not the case for the complex samples obtained by high energy proton irradiation. Therefore, we give here for activities the values obtained by the analysis procedure described above, pointing out again that these are in most cases underestimated due to the strong γ -ray absorption of mercury. Here, the degree of underestimation is dependent on the specific γ -ray emissions of each nuclide.

In the following we will however, if possible, make use of the absorption effects discussed above to draw conclusions about the distribution of certain nuclides within the sample, using γ -measurements with different sample-detector arrangements.

General Purpose Beaker

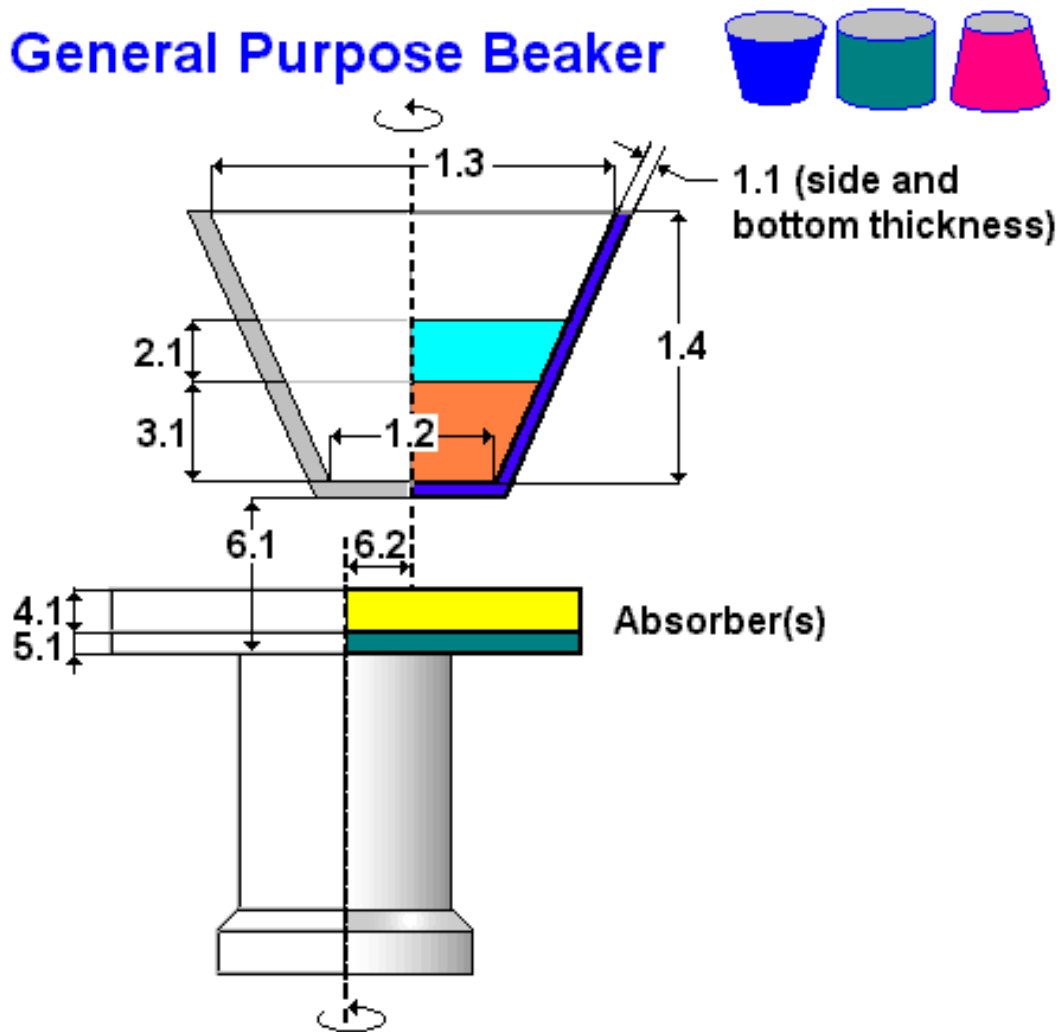


Figure 17: Geometric arrangement used for the model calculations of the efficiency for an HPGe-detector in a vertical sample-detector arrangement. The parameters used for the calculations are the following, corresponding to the dimensions of the stainless steel irradiation capsules obtained from CERN, filled with 1 ml of Hg: sample detector distance 0 cm, container: diameter 9 mm, height 35 mm, wall thickness 2.5 mm, Hg fill height 16 mm, 1 μm surface layer of density 1.6 gcm^{-3} , or 1 μm bottom layer of density 17 gcm^{-3} .

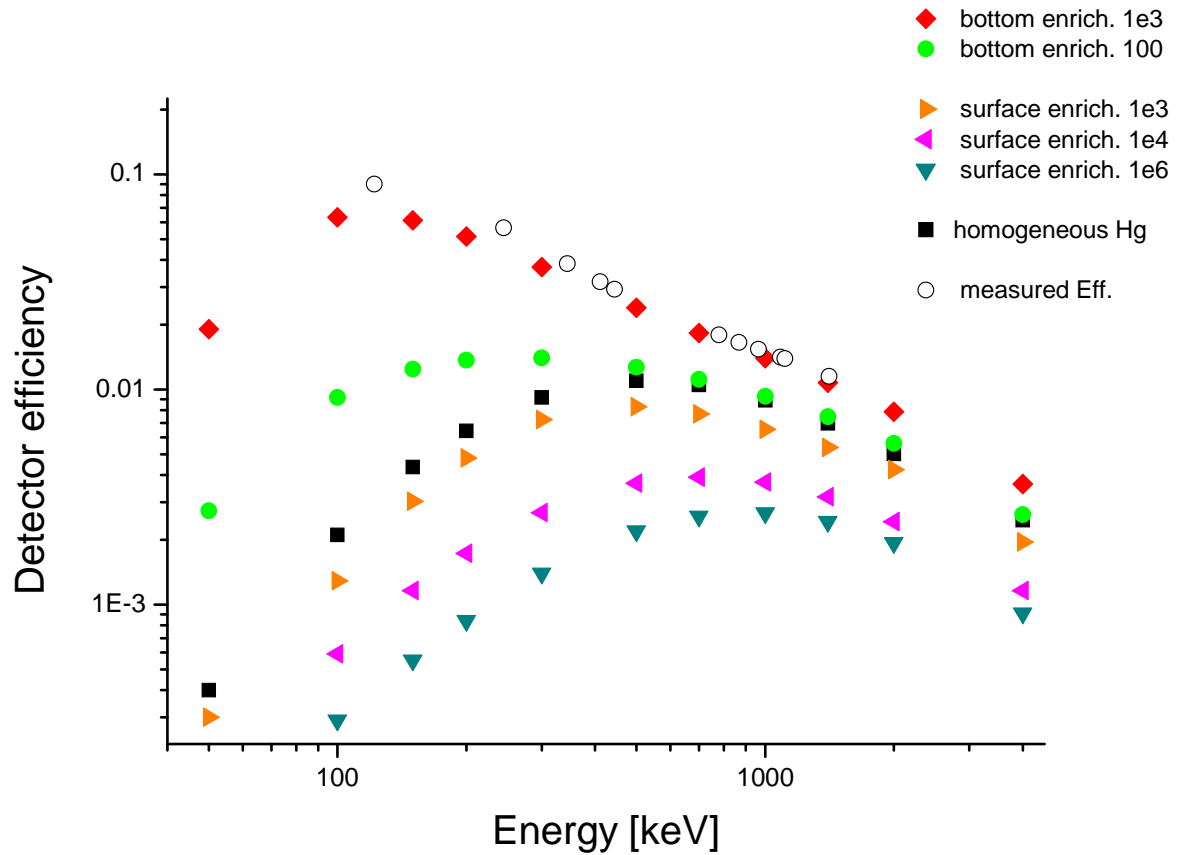


Figure 18: Comparison of experimentally determined and calculated efficiency for an HPGe-detector in vertical arrangement for a sample-detector distance of 0 cm, i.e. directly on the detector. The experimental efficiency was measured with a standard area source. The calculated efficiency was obtained using the actual geometric dimensions of the stainless steel irradiation capsules, filled with 1 ml of Hg, as received from CERN, incorporating the γ -ray absorption properties of mercury. In the calculations, a homogenous distribution of the radioactivity in the mercury and various relative enrichments in surface and bottom layers of 1 μm thickness are compared. For the surface layer, absorption properties of a typical oxide material were assumed, whereas for the bottom layer a density of tungsten was used.

4.5. Experiments and results

4.5.1. Mechanical removal of impurities

A proton irradiated mercury sample was obtained from CERN, originating from a test irradiation performed several years ago, without detailed information on the irradiation conditions. The sample will be further on called CERN0. The sample was contained in a PE container and had a mass of 31 g. A dull grey skin was observed on the surface of the liquid metal, indicating the presence of a thin oxide layer.

The sample was analyzed by γ -spectroscopy, using an HPGe-Detector in vertical orientation and conventional measuring electronics. The sample had to be measured for 15 hours in a position close to the detector to achieve good counting statistics because of its low activity. The spectrum of the sample is depicted in figure 19. Table 7 gives an account of the nuclides that could be identified in the sample.

Table 7: Radionuclides identified in the proton irradiated sample CERN0. Note that the activities given are clearly underestimated because of the neglect of the self-absorption effects of mercury.

Nuclide	Half life [d]	Activity [Bq]
^{102}Rh	207	3.9
$^{102\text{m}}\text{Rh}$	~1000	1.3
$^{110\text{m}}\text{Ag}$	249.79	0.9
^{133}Ba	3836.15	3.4
^{143}Pm	265	3.2
^{153}Gd	240.4	4.1
$^{172}\text{Hf}/^{172}\text{Lu}$	682.5	65
^{173}Lu	500	58
$^{194}\text{Hg}/^{194}\text{Au}$	189800	5.1

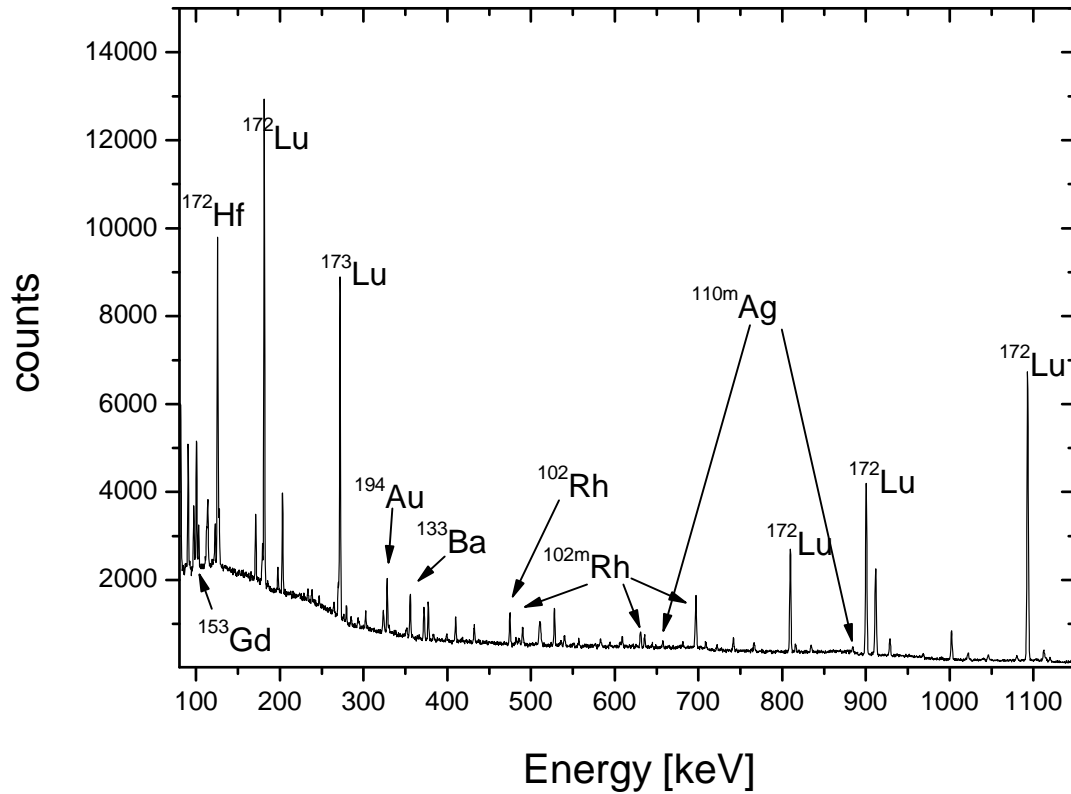


Figure 19: γ -spectrum of the sample CERN0 measured as it was received. The main lines of the identified nuclides are indicated.

The product spectrum comprises typical spallation and fission products with a half life longer than 200 d.

The dull grey appearance indicated that the sample was contaminated with impurities that during the decay time formed a thin layer on the surface. Since we expect that similar effects will occur in a spallation loop as well, the sample was a good starting point to study the distribution of radionuclides in this sample and different methods of purification of mercury useful for different types of impurities.

To study the nuclide distribution, approximately half of the mercury was separated from the bulk sample using a syringe in such a way that only material from the inner part of the Hg droplet was separated, leaving the surface layer with the remaining sample. The γ -spectrum of this fraction of Hg (see Figure 20) showed only the peaks of ^{194}Au , ^{195}Au and $^{110\text{m}}\text{Ag}$, indicating that the rest of the nuclides identified in the original sample are attached to the surface of the sample rather than dissolved in Hg. Presumably, they are oxidised, since most of the nuclides belong to metals that are rather sensitive to oxidation. Table 8 gives a summary of the found activity. ^{195}Au was not detectable in the original sample because its main γ -line is obscured by those of other nuclides.

Table 8: Radionuclides identified in a fraction of CERN0 separated with a syringe. Note that the activities given are clearly underestimated because of the neglect of the self-absorption effects of mercury.

Nuclide	Half life [d]	Activity [Bq]
$^{110\text{m}}\text{Ag}$	249.49	0.4
$^{194}\text{Hg}/^{194}\text{Au}$	189800	2
^{195}Au	186.09	1.5

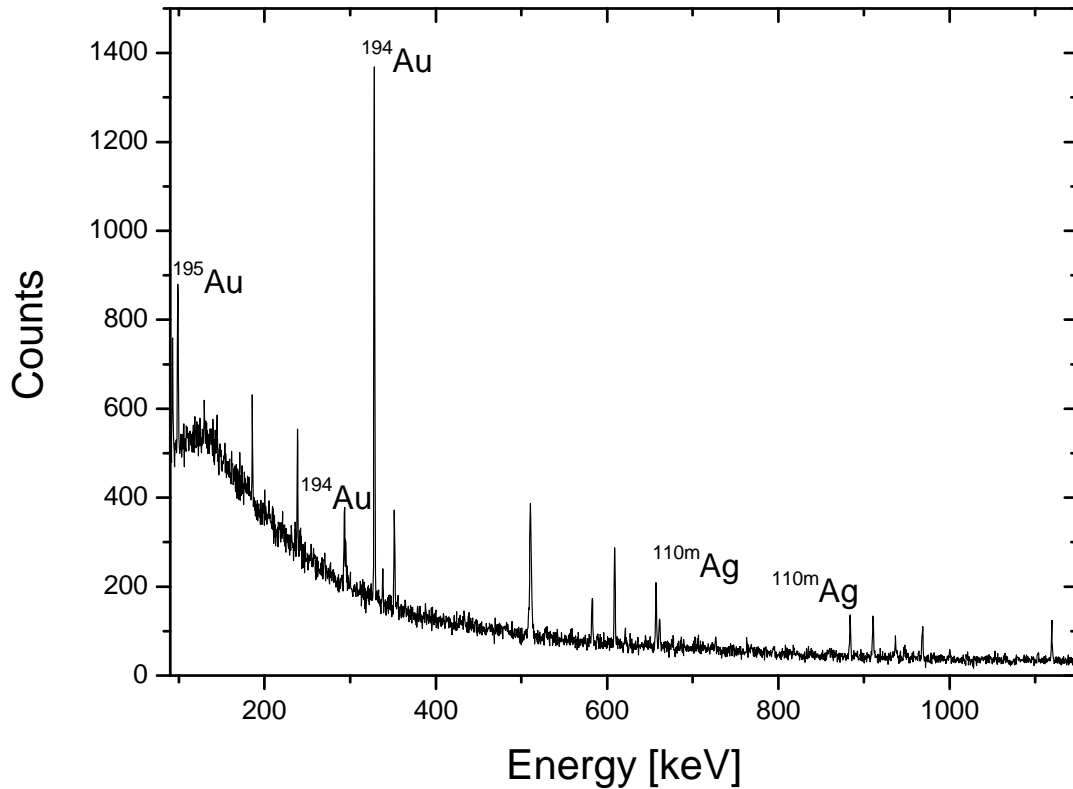


Figure 20: γ -spectrum of a fraction of sample CERN0 removed using a syringe, leaving the surface layer with the remaining Hg. The main lines of the identified nuclides are indicated.

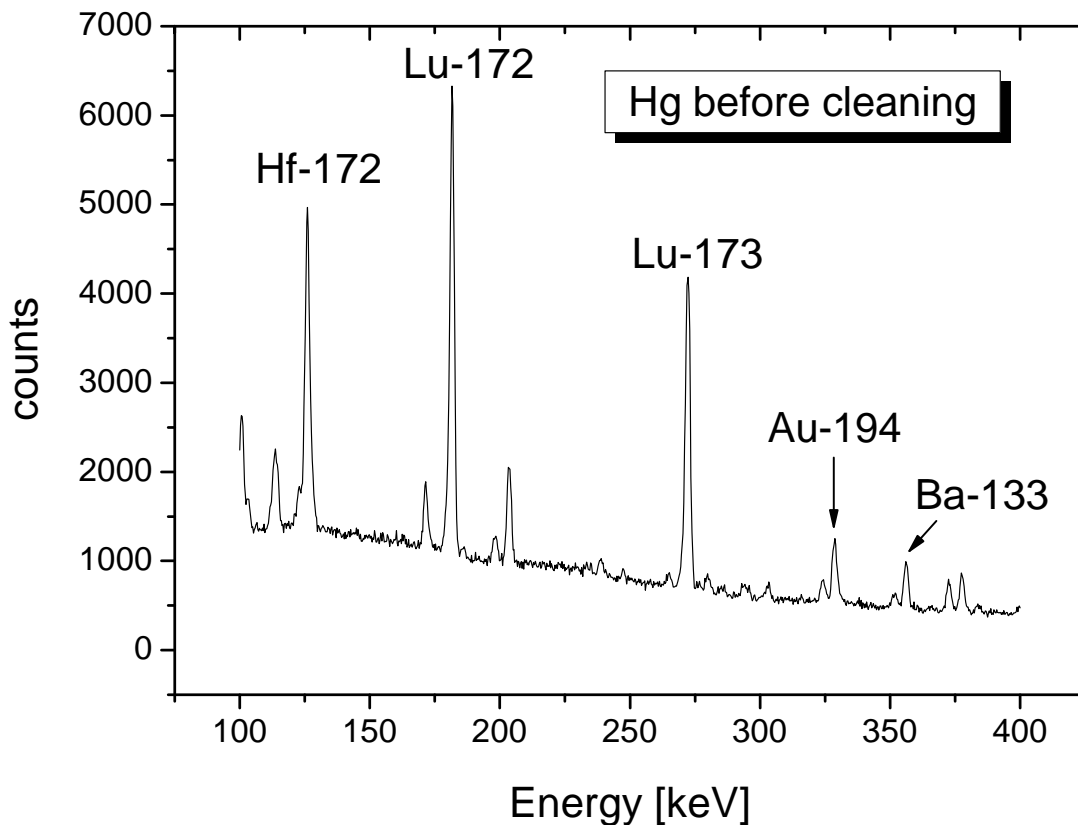
Since a spallation target system is not an ultra-pure environment, oxidation processes can be expected to occur in such a system as well. Therefore, the formation of oxide material may occur in a target system, similar as in our sample, and methods to remove these can be an efficient way to remove a part of the radionuclides formed by nuclear reactions and, possibly, making them available for other purposes. The removal of this material should also help to prevent the deposition of solid materials at unwanted places, e.g. plugging of thin pipes.

Therefore, we tested a few different methods for the removal of such surface contaminants. Unfortunately, it was impossible to divide the samples in similar fractions, because while dividing the sample, e.g. by decantation, the oxide layer tends to adhere to the remaining part of the mercury and also shows a tendency to stick to the walls of the container. We therefore decided to subsequently test several methods on the original sample after its transfer to a suitable container, trying to make sure that the most effective method is applied last.

The most simple way to remove surface contaminations described in the literature is touching the surface with some material with a high surface roughness [42]. We tried similar methods in the following way: First, the mercury was transferred to a chinaware vessel. The liquid metal was then vigorously moved to bring the surface layer into contact with the walls of the vessel. Then, the mercury was transferred to a corundum vessel, where it was treated in the same way, while the chinaware vessel was measured on the γ -spectrometer to obtain an indication on the absorption of radioactive material on the surface of the vessel. In the third step, the sample was transferred to a second corundum vessel, while the first was investigated using γ -spectroscopy. The sample surface, still showing visible impurities, was then touched from the top with a clean corundum surface. The surface was then examined by γ -spectroscopy. The latter step was repeated. For the final experiment, the sample was poured over about 1 cm³ of molecular sieve

(Molecular sieve type 13X, Alfa Aesar) placed in a small column. The column was measured using γ -spectroscopy. The mercury poured through the column was covered with a rather thick layer of solid that was obviously abraded from the molecular sieve. This material was removed by dabbing the mercury with a piece of filter paper and subsequently filtering it through a paper pinhole filter. The two pieces of filter paper and the purified mercury were also measured by γ -spectroscopy. The results of the γ -spectroscopic measurements are compiled in table 9. Figure 21 shows γ -spectra of the original mercury sample and the sample obtained after all the purification steps. Here, it should be pointed out that already after the transfer of the mercury sample to the first chinaware vessel, a substantial amount of radioactive material was stuck to the original polyethylene container. A semi-quantitative account of this sticking fraction is also given in the last column of table 9. Furthermore, about 1.0 and 0.16 g of Hg were sticking to the molecular sieve and the pinhole filter after separation, respectively, carrying a detectable amount of $^{194}\text{Hg}/\text{Au}$. This corresponds to about 5% of the total mercury contained in the sample.

In Figure 21, the spectrum recorded from the molecular sieve is also shown. Most of the nuclides are almost quantitatively removed from the mercury, whereas only nuclides of the elements gold and silver (silver is not shown in the figure) can be detected in the mercury after the cleaning procedure. The Hg sample also showed bright metallic lustre after the cleaning procedure.



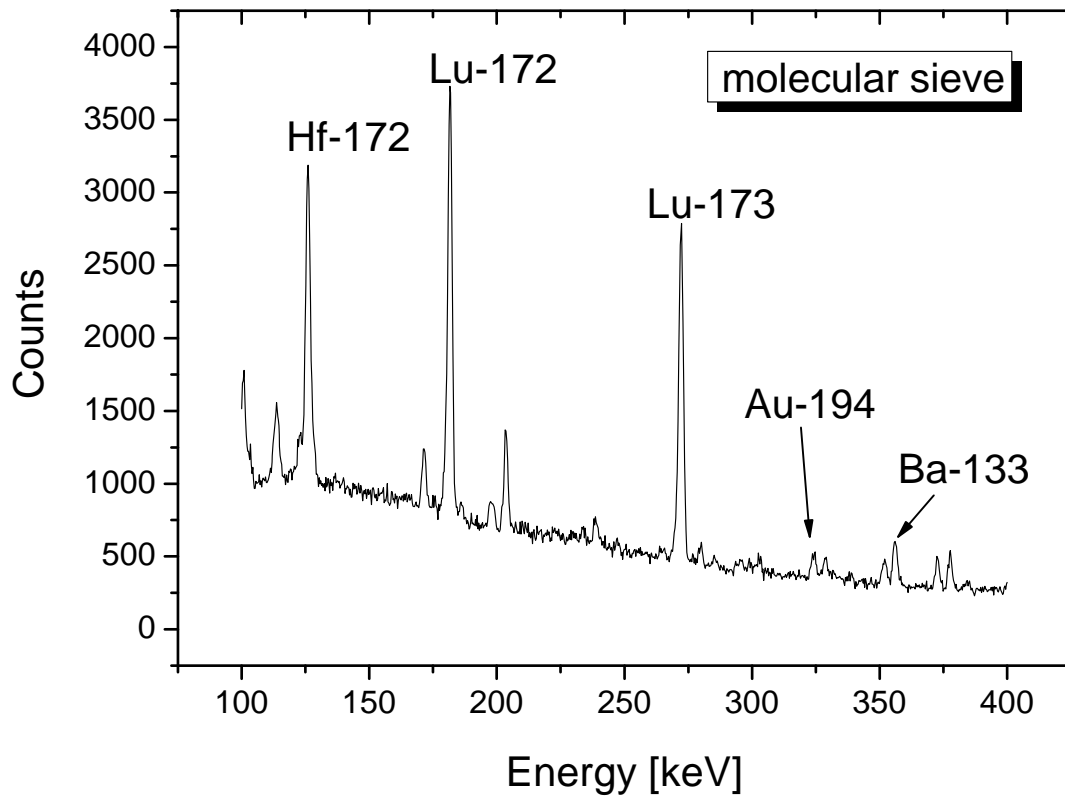
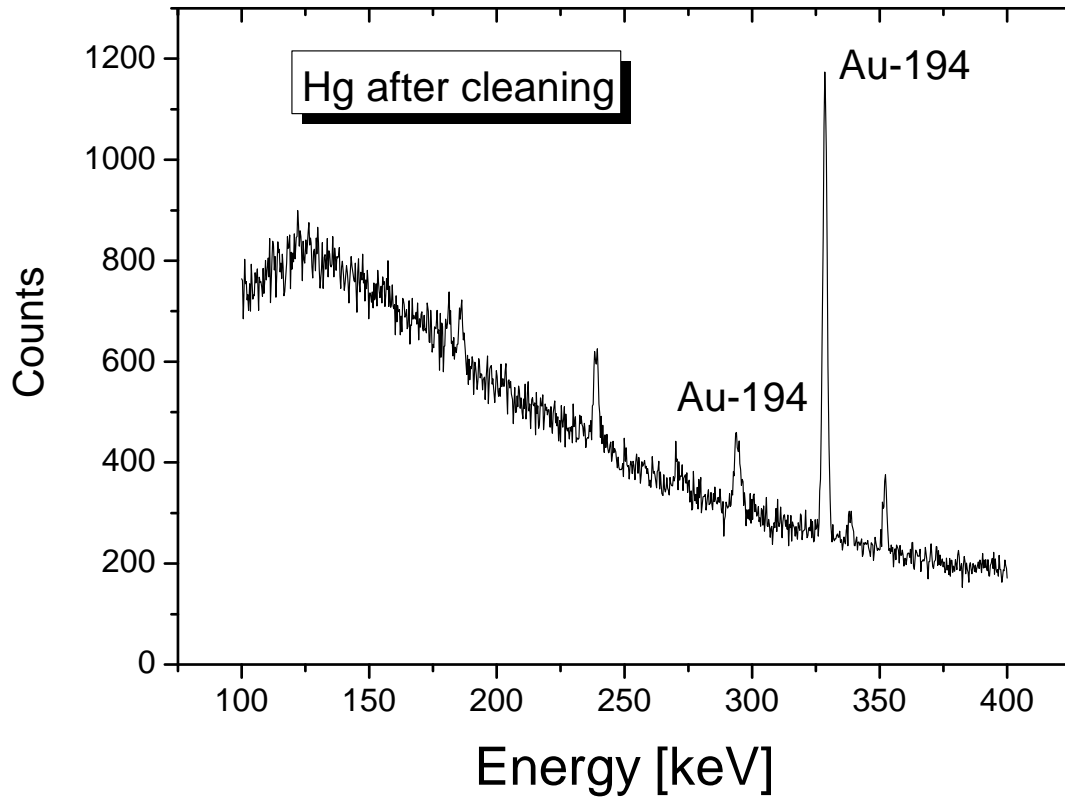


Figure 21: Comparison of the γ -spectra of the Hg sample CERN0 before and after the cleaning procedure, together with the spectrum of the molecular sieve after contact with the mercury.

Table 9: Comparison of activities measured for sample CERN0 before and after the different purification steps (see text).

Purification step		0	1	2	3	4	5	6	7	8	9
Nuclide	Half life [d]	Original Activity in Hg [Bq]	Activity on chinaware vessel [Bq]	Activity on corundum vessel [Bq]	Activity on Al ₂ O ₃ -plate [Bq]	Activity on Al ₂ O ₃ -plate [Bq]	Activity on molecular sieve [Bq]	Activity on dabbing paper [Bq]	Activity on pinhole filter [Bq]	Activity in purified mercury [Bq]	Activity on original container [Bq]
¹⁰² Rh	207	3.9	n.d.*	n.d.*	1	n.d.*	1.1	n.d.*	0.5	n.d.*	2.7
^{102m} Rh	~1000	1.3	n.d.*	n.d.*	n.d.*	n.d.*	1	n.d.*	n.d.*	n.d.*	1.4
^{110m} Ag	249.79	0.9	n.d.*	n.d.*	n.d.*	n.d.*	n.d.*	n.d.*	n.d.*	0.6	n.d.*
¹³³ Ba	3836.15	3.4	n.d.*	n.d.*	0.6	n.d.*	2	n.d.*	0.4	n.d.*	3.5
¹⁴³ Pm	265	3.2	n.d.*	n.d.*	0.3	n.d.*	1.6	n.d.*	n.d.*	n.d.*	2.6
¹⁵³ Gd	240.4	4.1	n.d.*	n.d.*	n.d.*	n.d.*	0.4	n.d.*	n.d.*	n.d.*	3.2
¹⁷² Hf/ ¹⁷² Lu	682.5	65	2.3	n.d.*	9.4	1.7	33.4	3.8	4.5	0.7	61
¹⁷³ Lu	500	58	2.8	n.d.*	8.9	1.3	30.8	3.8	5.4	n.d.*	54
¹⁸⁵ Os	93.6	n.d.*	n.d.*	n.d.*	n.d.*	n.d.*	n.d.*	n.d.*	n.d.*	0.3****	n.d.*
¹⁹⁴ Hg/ ¹⁹⁴ Au	189800	5.1	n.d.*	n.d.*	n.d.*	n.d.*	1.1**	n.d.*	1**	5.6	n.d.*
¹⁹⁵ Au**	186.09	n.d.*	n.d.*	n.d.*	n.d.*	n.d.*	n.d.*	n.d.*	n.d.*	0.8****	n.d.*

*not detected

** about 1.0 and 0.16 g of Hg were sticking to the molecular sieve and the pinhole filter after separation, carrying a detectable amount of ¹⁹⁴Hg/Au

*** only detected in the purified mercury because of interference with strong γ -lines of other nuclides in the original sample

**** only detected in the mercury by a manual search after additional separation experiments indicated its presence (see absorber experiments below)

Qualitatively, the results show that a substantial part of the macroscopic solid impurities can be removed from mercury using mechanical methods such as bringing the mercury in contact with rough surfaces, either by dabbing such a surface onto a free surface of mercury that has precipitated solid material floating on it, or introducing these surfaces into the mercury flow to remove particles carried with the liquid metal. Concerning the choice of material, no final conclusion can be drawn from the few experiments performed here. The results are dependent on parameters such as intensity of the contact between mercury and the surface and the surface area exposed to the liquid metal, all being not well comparable between the different experiments performed here. The contact surface has been largest in the final experiment using the molecular sieve. This is probably the reason why this experiment was most efficient in filtering the impurities. However, this material turned out to transfer materials from its surface to the liquid metal. Therefore, it is not suitable for a technical application because of its mechanical instability. However, mechanically more robust materials can surely be found.

4.5.2. Removal of dissolved components from liquid mercury

In principle, impurities that remain in solution after a mechanical cleaning of the liquid metal can be removed by conventional methods such as washing and/or distillation of the mercury. These methods have been discussed in preceding sections and their application to mercury containing radiotracers will be studied experimentally in one of the following sections. Alternatively, novel procedures for the removal of such elements from the liquid mercury can be developed that may prove advantageous for an application within a spallation target environment because of several reasons, e.g. the avoidance of the transfer of large amounts of radioactivity into the gas phase or the production of large amounts of water soluble radioactive waste. Furthermore, they could prove to be element-selective and in this way generated a starting point for the production of certain valuable radionuclides. One such promising technique for novel separation methods to remove radionuclides from liquid metals is their adsorption on surfaces of selected materials that show specific chemical interactions with certain elements or groups of elements or their chemical compounds. For removal of dissolved radionuclides from mercury, one needs a material that shows a higher chemical affinity to the dissolved radionuclide in its respective chemical form than mercury. Furthermore the chemical affinity of the absorber material for mercury and its solubility in mercury should be low. In principle, for the removal of dissolved metallic species metal surfaces should be suitable candidates. Some first results of such techniques for the removal of radionuclides from liquid lead are shown in [75]. The strength of intermetallic interactions can be deduced from thermodynamic data calculated with the Miedema model [38]. In this way, suitable materials can be selected. For the adsorption of oxidic materials, other oxides of different basicity or acidity could be suitable for the selective removal of certain elements by surface adsorption. Using the sample remaining from the study of mechanical cleaning procedures described above, we started to investigate different metals as candidates for an absorber that removes dissolved gold and silver from mercury.

4.5.2.1. Experimental and results on osmium, gold and silver adsorption

For our experiments, the Hg sample remaining from the mechanical separation experiments described in the preceding section was used. It contains ^{194}Au and ^{195}Au as the major radioactive component detectable by γ -spectroscopy, together with small amounts of $^{110\text{m}}\text{Ag}$ and a small amount of $^{172}\text{Hf/Lu}$ that is probably not dissolved in the liquid metals but a remainder of the previously much larger surface contamination. From an evaluation of intermetallic interactions based on semi-empirical calculations, metals of Group 4 and 5 of the periodic table should have a

higher affinity to gold than mercury. Furthermore, these metals are hardly soluble in mercury and hence be suitable materials that can be used in a liquid mercury loop without the danger of dissolution in the liquid metal. Therefore, they should be suitable candidates for absorbers. In the first experiments, Ta and Zr foils were brought into contact with mercury, but no wetting of the metal surface could be achieved. Several methods of surface treatment have been examined to facilitate wetting of the metal surfaces, e.g. mechanical scratching, etching and treatment with complexing agents. According to the results of visual inspection, none of them was successful with respect to improving the wetting of the metal foil. Nevertheless, a tantalum foil previously etched in 38 % aqueous hydrofluoric acid was kept submerged in the mercury sample for three weeks to study if long term exposure has a detectable influence on wetting. After the three weeks of exposure, visually no wetting was observed. Nevertheless, the foil was measured overnight on a γ -detector. Surprisingly, the three main γ -lines of ^{185}Os were observed in the spectrum, which is shown in figure 22. This nuclide was detected in none of the spectra originating from sample CERN0 so far. This nuclide is one of the most prominent spallation products formed in a mercury sample exposed to a high energy proton beam, and with its half life of 94 days it can be present in a detectable amount even after a few years of decay. The fact that it was not detected in any of the other measurements probably arises from an activity that is close to the detection limit, combined with the large absorption effects of mercury. The nuclide itself, enriched on the surface of the tantalum foil, without the absorption effects of mercury, is clearly detectable. The possibility of irradiation from outside sources has been excluded. After having found the nuclide on the tantalum foil, the main peak of ^{185}Os was searched manually in the spectrum of the cleaned mercury, and indeed a very weak line was found near 646 keV. The chemical origin of the attraction of osmium to the surface of the tantalum foil is unclear so far. The phenomenon has not been studied further because of the lack of additional samples. It has been found however that the removal of Os from the mercury was by far not complete. In the spectrum of the mercury, the main peak of ^{185}Os is still present after the treatment with the tantalum foil.

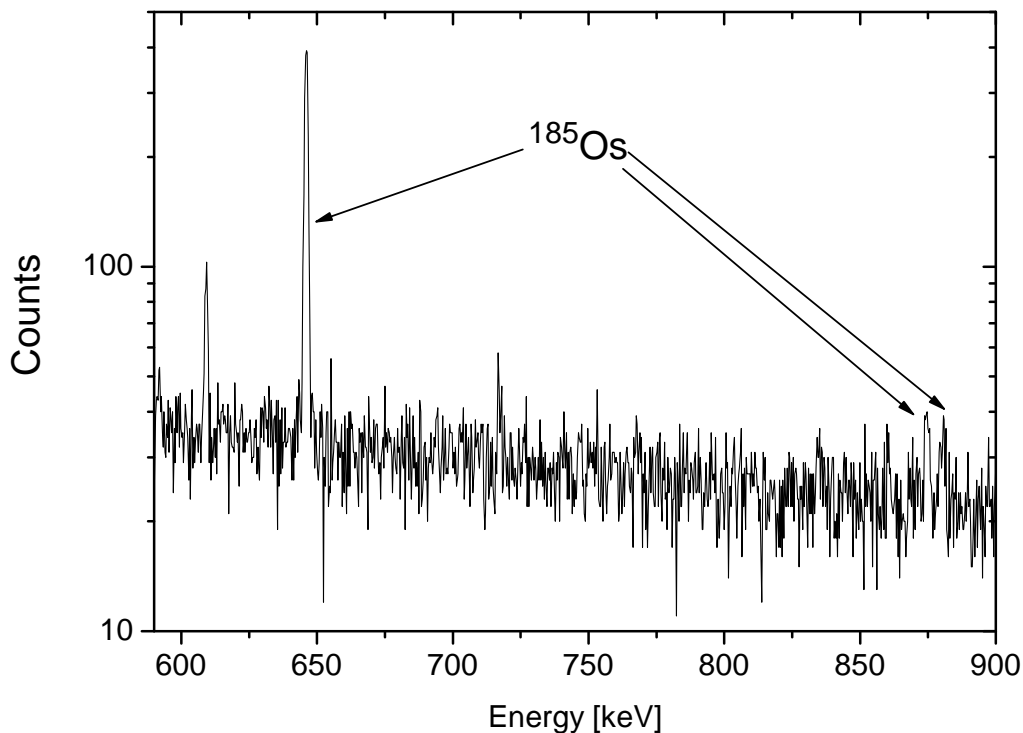


Figure 22: Spectrum of a tantalum foil previously etched in HF, stored for 3 weeks in the Hg-sample remaining from CERN0 after removal of solid precipitates. The 3 main lines of ^{185}Os are visible.

For an adsorption of the gold, silver and osmium nuclides still remaining in solution in the mercury, other candidates for metal absorbers had to be found. Copper seemed attractive since it is well known to form compounds with gold, and its solubility in mercury is fairly low. Furthermore, copper can be amalgamated fairly easily. Therefore, wetting of copper with mercury should be possible. In practice, wetting of copper is slow and incomplete when dipping a mechanically cleaned copper plate into mercury. The wetting can be enhanced by amalgamation of the copper plate. For this purpose, the copper plate is dipped in a saturated aqueous HgCl_2 -solution for several hours. After this procedure, a Cu-amalgam layer has formed at the surface of the plate. After removal of precipitated CuCl the surface shows a silvery metallic lustre. Figure 23 shows a photograph of a copper plate amalgamated in this way, together with an untreated plate.

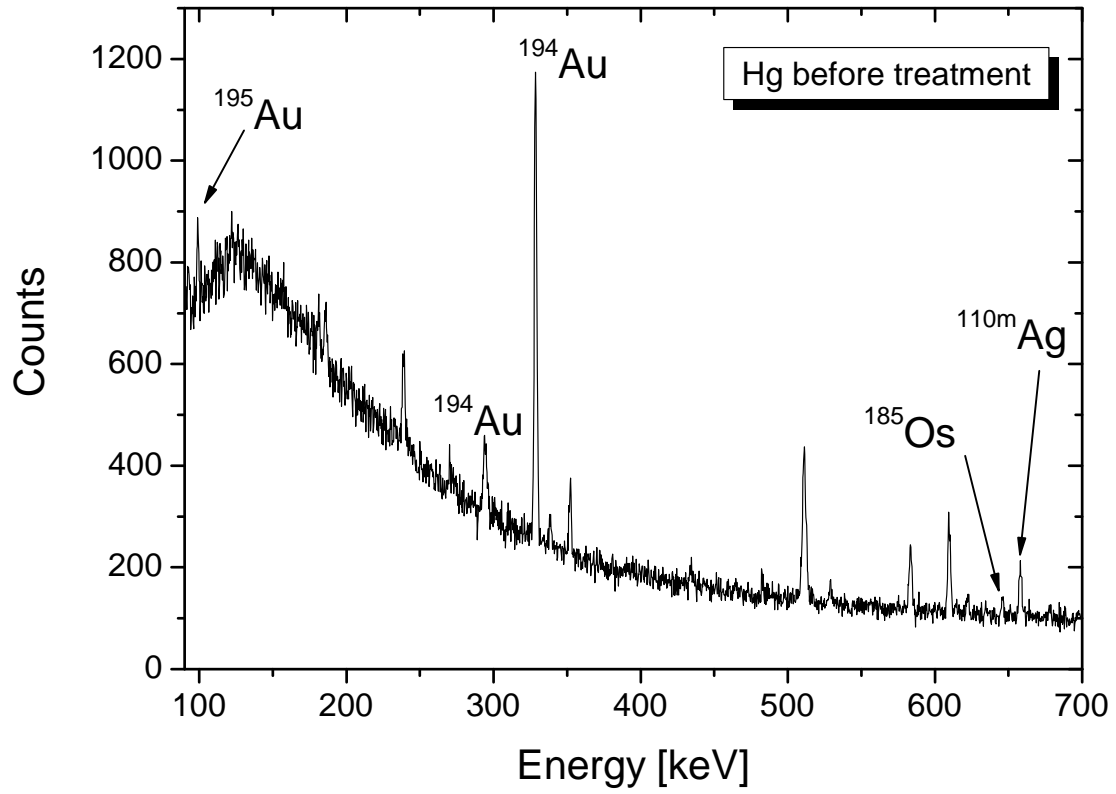
The amalgamated Cu-plate was placed in the gold and silver containing mercury sample for three days under ambient conditions. γ -spectra of the mercury sample were taken before and after the experiment. The Cu-plate was also measured on the γ -detector after the experiment.

The results of γ -spectroscopy are shown in Figure 24 and Table 10. After the treatment Au is almost quantitatively removed from Hg and adsorbed to the copper plate. The small peak of ^{194}Au detected in the spectrum of the mercury sample after the adsorption process is explained by the reproduction of this nuclide from its long lived mother, ^{194}Hg , during the 4 h measuring time.

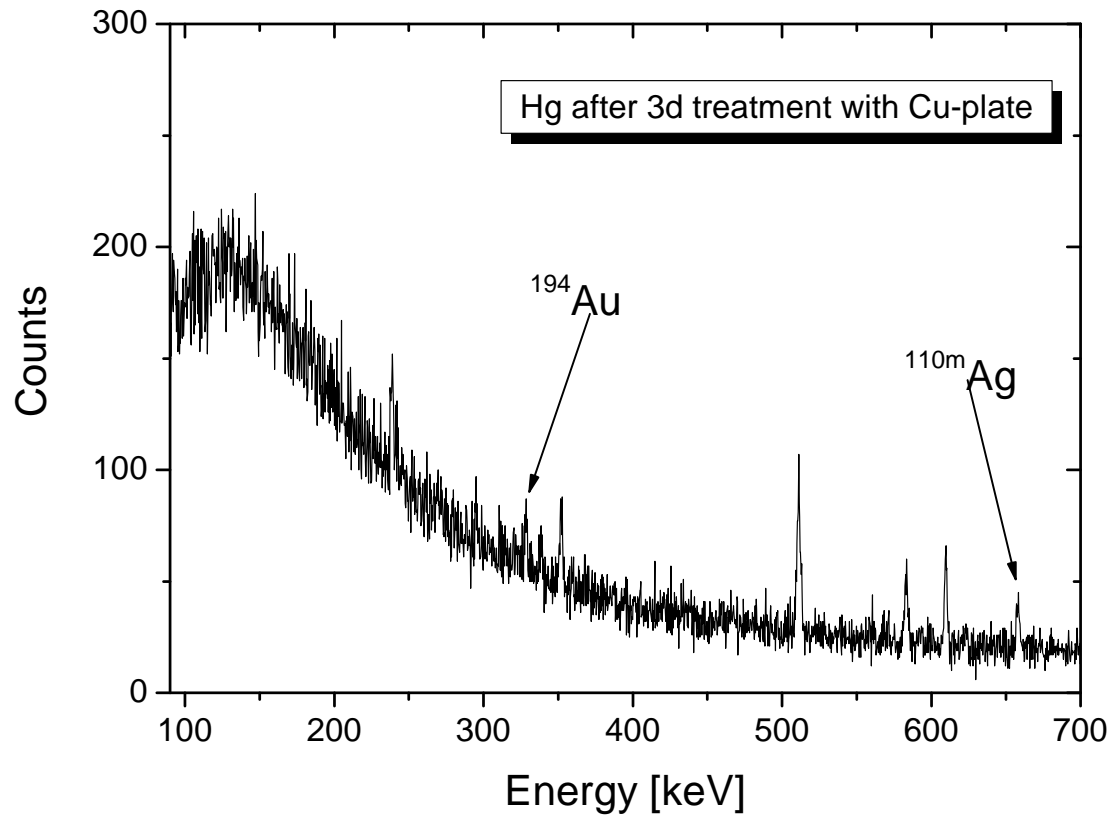
^{195}Au is not detectable anymore in the liquid metal after the treatment with the copper plate, while it is the dominating activity on the plate, together with ^{194}Au .



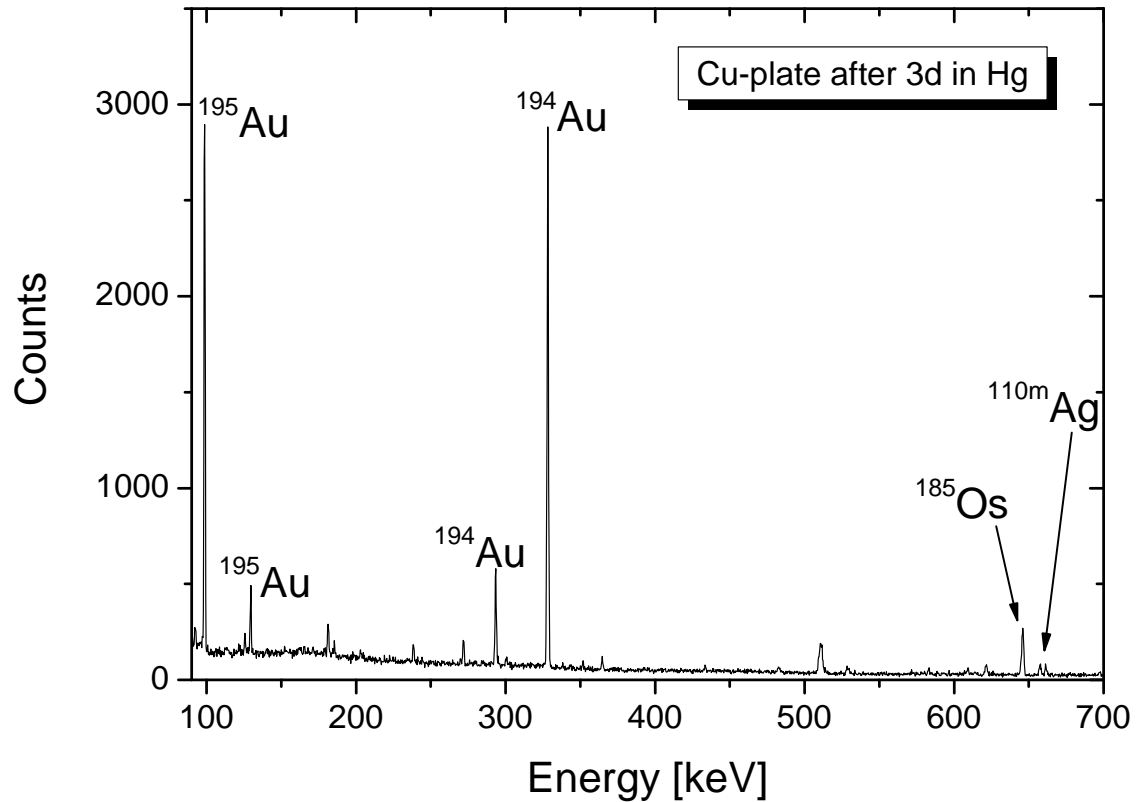
Figure 23: Untreated copper plate and copper plate amalgamated in a saturated aqueous HgCl_2 -solution, after mechanical cleaning of the surface.



a)



b)



c)

Figure 24: γ -spectra of the Hg sample before (a) and the Hg sample (b) and Cu-plate (c) after the adsorption experiment.

Table 10: Results of γ -spectroscopy of the absorption experiments for radionuclides dissolved in mercury using an amalgamated copper plate as absorber.

Nuclide	Half life [d]	Activity in Hg before treatment [Bq]	Activity in Hg after treatment [Bq]	Activity on copper plate [Bq]
^{110m}Ag	249.79	0.63	0.55	1.27
$^{172}\text{Hf}/^{172}\text{Lu}$	682.5	0.7	Not detected	3
^{173}Lu	500	Not detected	Not detected	3.8
^{185}Os	93.6	0.3	Not detected	6.2
$^{194}\text{Hg}/^{194}\text{Au}$	189800	5.1	0.47*	46.1
^{195}Au	186.09	0.8	Not detected	49.1

*from reproduction from ^{194}Hg

^{110m}Ag is only partly removed from the mercury, as it is found both in the mercury and on the copper plate after the experiments. The results indicate that most of the silver remains in the mercury. The small amount of ^{185}Os present in the mercury before it was contacted with the copper plate is removed from the mercury to quantities below the detection limit and adsorbed to the copper plate. For the Hf and Lu nuclides, the situation is not completely clear. They might be dissolved in very small amounts in the liquid metal, but more likely they are solid remainders of the incomplete mechanical cleaning procedure performed before, that stick to the copper plate after the experiment.

A look at the numerical values in table 10 nicely demonstrates the effects of self-absorption of the mercury. All of the activities found on the copper plate are substantially larger than those found in mercury. The effect is most prominent for the nuclide ^{195}Au with its low energy γ -lines at 99

and 130 keV. Still, the geometry of the copper plate deviates significantly from that of the calibration source used, and absorption effects of the copper plate itself may also play a role. Nevertheless, the activities listed for the copper plate should give a realistic estimation of the real activities present, while the values found in the mercury sample are clearly underestimated.

As a conclusion, the results obtained in this first very promising experiment suggest that metal absorbers could indeed be used to remove dissolved nuclear reaction products from a spallation target system in a selective manner. Further investigations on the time dependence of these processes and tests for various other dissolved metals are reported in the following sections.

4.5.2.1.1. Kinetic studies

In the next step, the time dependence of the process of gold adsorption to the copper plate was studied. For these experiments, the Hg sample left from the first copper absorber experiments was re-used after a three weeks long build-up period, where the ^{194}Au (half-life 38 h) was completely reproduced from the decay of its long-lived mother ^{194}Hg (half-life 520 y). After all the cleaning procedures performed before, ^{194}Au and $^{110\text{m}}\text{Ag}$ were now the only radio-active components detectable in the sample by γ -spectroscopy, apart from natural background. As absorber, the same copper plate was as in the first experiment after allowing for the decay of ^{194}Au . However, a small and roughly constant amount of ^{194}Au was always detected on this plate during this series of experiments, coming from the decay of the mercury forming the wetting layer. The copper plate also showed the activities of $^{110\text{m}}\text{Ag}$, $^{172}\text{Hf/Lu}$, ^{185}Os and ^{195}Au , still remaining from the first experiment.

In this series of experiments, the activity of the mercury sample and the copper plate was measured before each experiment. Then, the copper plate was dipped into the mercury for a certain time at room temperature and ambient atmosphere. After the copper plate was taken out of the mercury, γ -spectra of the mercury sample and the copper plate were recorded again. For the mercury sample, a measuring time of 4 hours was chosen to avoid excessive in-growth of ^{194}Au from its mother during the measurement. For the copper plate, a measuring time of 14 hours was chosen. After each experiment, the mercury sample was allowed to build up the ^{194}Au activity again during three weeks, in the same time allowing the activity of ^{194}Au deposited on the copper plate to decay.

Figure 25 shows the results for the absorption of ^{194}Au . The corresponding numerical values are compiled in table 11. The absorption of gold onto copper from a mercury solution is obviously a relatively fast process. Already after 5 minutes, one quarter of the gold is removed from the mercury solution. Accordingly, the activity deposited on the copper plate increases with exposure time until almost all of the gold is removed from the mercury. However, the activity of ^{194}Au found on the copper plate for the longest exposure time is limited by its decay. Similarly, the small amount of ^{194}Au found in the mercury after the longest exposure can be explained by its reproduction from ^{194}Hg during the 4 hours duration of the γ -measurement.

Obviously, the number of adsorption sites for gold on the copper surface is larger than the number of gold atoms present in the solution. The progression with time is steady for the increase of activity on the copper plate, but there is some scatter in the data for the removal of activity from mercury. More data should be taken here for different reaction times. The “contamination” of the plate with ^{195}Au from the first experiment does not play a role here, obviously. One reason for this becomes immediately clear when one looks at the number of atoms involved. In the first experiment, calculated from the measured activity, about 10^9 atoms of ^{195}Au were absorbed on the copper plate. The number of ^{194}Au atoms that have been adsorbed for the longest reaction times is in the range of 10^{12} . Thus, obviously many more adsorption sites for gold are present on the surface than can be occupied by the ^{195}Au atoms.

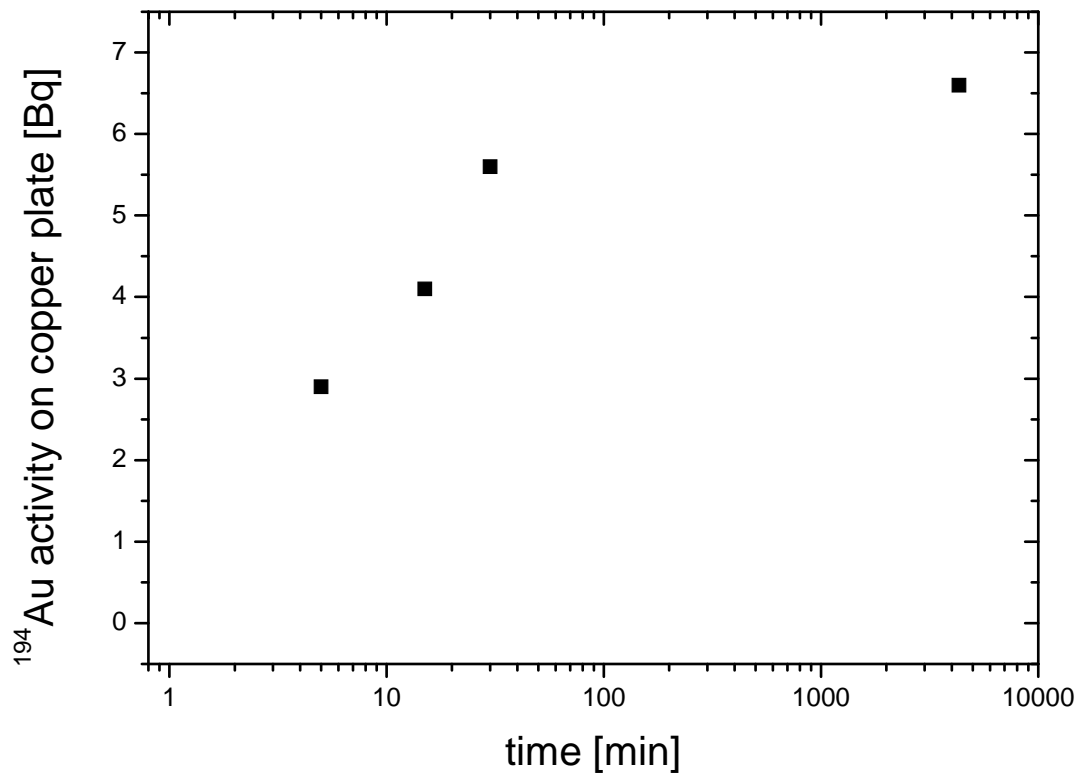
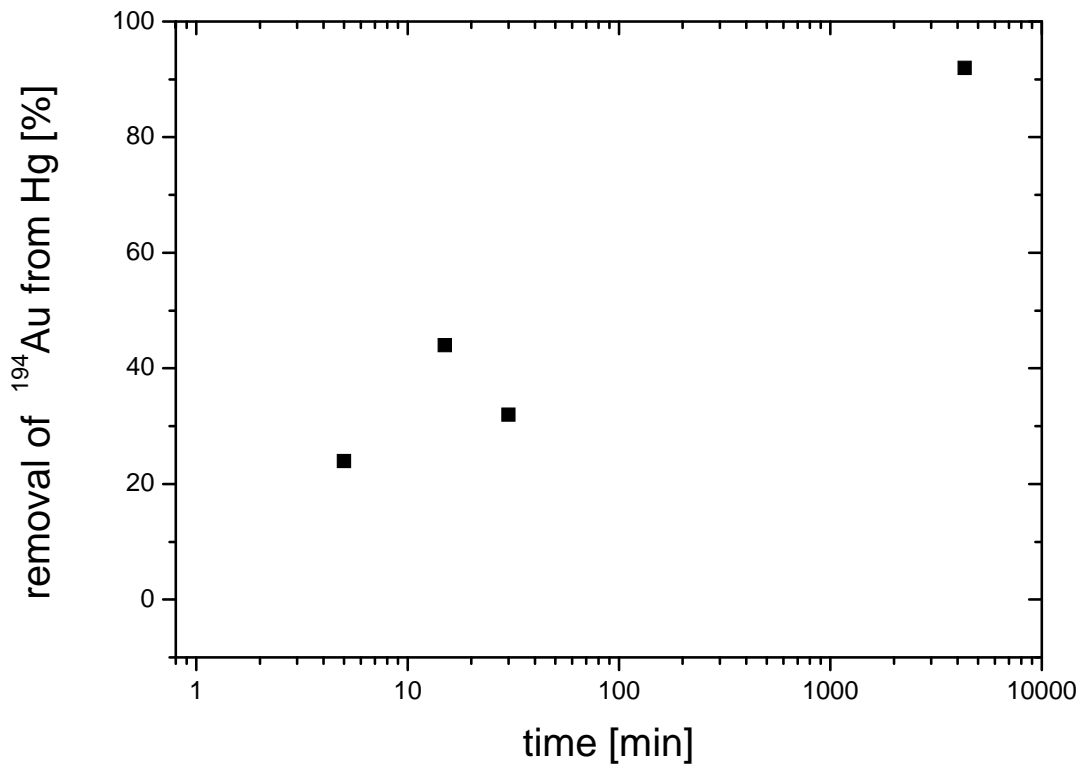


Figure 25: Removal of ^{194}Au from mercury and its adsorption on a copper plate as a function of time

Table 11: Removal of ^{194}Au from mercury and its adsorption on a copper plate as a function of time.

Time [min]	^{194}Au removal [%]	Activity ^{194}Au on Copper plate [Bq]
0	0	0
5	24	2.9
15	44	4.1
30	32	5.6
4320	92	6.6

Concerning the absorption of $^{110\text{m}}\text{Ag}$, we observed a small amount of $^{110\text{m}}\text{Ag}$ -activity on the copper plate for the long term experiment, with a large fraction of the silver remaining in the mercury. Since $^{110\text{m}}\text{Ag}$ has a half-life of about 250 days, and the time dependent experiments were started only a few weeks after the first absorber study, the copper plate used here still contained a substantial fraction of the absorbed silver. In the time dependent study we observed no significant reduction of the silver activity in mercury and no increase in the silver activity of the copper plate. An explanation could be that the silver measured on the copper plate is actually not adsorbed silver, but silver dissolved in the wetting layer of mercury present on the surface of the copper plate, thus indicating that there is no specific interaction between copper and silver. Estimating from the activity, only about 10^7 to 10^8 atoms of $^{110\text{m}}\text{Ag}$ are present in the sample, so that a saturation of adsorption sites with silver seems improbable. The adsorption behaviour of silver dissolved in mercury on a copper surface will be studied in a dedicated experiment. The results will be given in one of the following sections.

In further experiments, a non-reproducible adsorption behaviour of ^{194}Au on the copper plates was observed in some cases, leading to variations in the rate of the adsorption process. Obviously, the wetting of the copper surface varies with subtle changes in the surface preparation. Here, more detailed experiments to optimize the surface preparation are necessary.

4.5.2.2. Adsorption of various metals dissolved in mercury on copper

The first results of adsorption experiments that revealed the favourable adsorption of carrier-free gold to an amalgamated copper-plate, inspired a series of experiments, where other elements that show a rather high solubility in mercury and that are known to chemically interact with copper are studied with respect to their adsorption behaviour. We selected those elements, for which activated samples with suitable half-life can be prepared by neutron activation. After irradiation at the neutron activation system (NAA) at SINQ, small amounts of the elements were mixed with mercury. We studied the behaviour of these mixtures and the adsorption of the solute on amalgamated copper.

4.5.2.2.1. Preparation of activated samples

Samples of metallic Zn, Ag, Cd, Sn, Sb, Tb and Ir were irradiated by fast neutrons at NAA at SINQ. The amount of metal and the irradiation time was adapted in such a way that the dose rates did not exceed the allowed limits. Table 12 shows the sample and irradiation parameters. After several days of cooling, the samples were analyzed by γ -spectrometry.

Table 12: NAA irradiation of elements to be dissolved in Hg. Irradiation parameters and main nuclides produced.

Element	Mass [mg]	Irradiation time [s]	Detected Nuclides	Half-life [d]
Zn	103	3600	⁶⁵ Zn	244.26
Ag	110	180	^{110m} Ag	249.79
Cd	714	3600	¹¹¹ Ag	7.45
			^{110m} Ag	249.79
			^{106m} Ag	8.28
			¹⁰⁵ Ag	41.29
			^{115m} Cd	44.6
			¹¹⁵ Cd	2.228
Sn	90	3600	¹¹³ Sn	115.09
			^{117m} Sn	13.60
Sb	105	300	¹²⁴ Sb	60.20
Tb	20	600	¹⁶⁰ Tb	72.3
Ir	95	60	¹⁹² Ir	73.831

4.5.2.2.2. Preparation of diluted solutions of metals in mercury

Small amounts of the activated metals were mixed with Hg under ambient conditions in PE-vessels to give mixtures of mole fractions of approximately 10^{-4} (Sn) and 10^{-5} (Zn, Ag, Sb, Tb, Ir). For the Cd samples we were interested in the behaviour of non-carrier-added Ag. Therefore, we mixed the complete Cd-sample with Hg, resulting in a Cd mole fraction of 8×10^{-3} . After mixing, many samples showed visible solid precipitations on the liquid-gas interface and at the wall of the PE-vessel. The mixtures were filtrated. A part of the filtrated Hg was afterwards transferred to a new vessel, where it was exposed to amalgamated Cu-plates. γ -spectra of the mixtures, empty vessels, filters and Cu-plates were taken after each operation.

4.5.2.2.3. Behaviour of diluted solutions of metals in mercury and sorption behaviour of dissolved elements on copper

Ag: The diluted Ag-solution in mercury showed no solid precipitations on the surface for the first three weeks. Ag is obviously more or less completely dissolved in Hg. A series of adsorption experiments, running over a period of three weeks, was started, dipping a copper plate prepared

by the aqueous amalgamation method into the Ag-solution in mercury for different times and measuring the activity of the liquid metal and the copper plate before and after each dipping. The copper plate showed a small amount of activity after the first dipping, which remained constant in the following dipping experiments. It is not clear whether this activity results from a small amount of adsorbed silver, or if this silver is dissolved in the small amount of mercury that still adheres to the copper plate after its removal from the liquid metal. For the evaluation of the relative removal of Ag from Hg, the relative difference of five of the main γ -rays of ^{110m}Ag (658, 764, 885, 937 and 1505 keV) before and after the experiments were determined and averaged, and the standard deviation was calculated. The corresponding values are listed in table 13. A graphical representation is shown in figure 26.

Table 13: Evolution of the relative removal of Ag from mercury with time.

Exposure time [h]	Relative removal of Ag from Hg [%]	Standard deviation (1σ) [%]
0.01667	0.81957	3.26808
0.1	2.17722	2.98771
1.1	-2.08053	2.09923
40.5	6.55392	3.97612
167.5	-2.17189	4.055
237	1.27034	2.43416
329.4	1.72755	2.74537
498.9	2.26872	5.41886

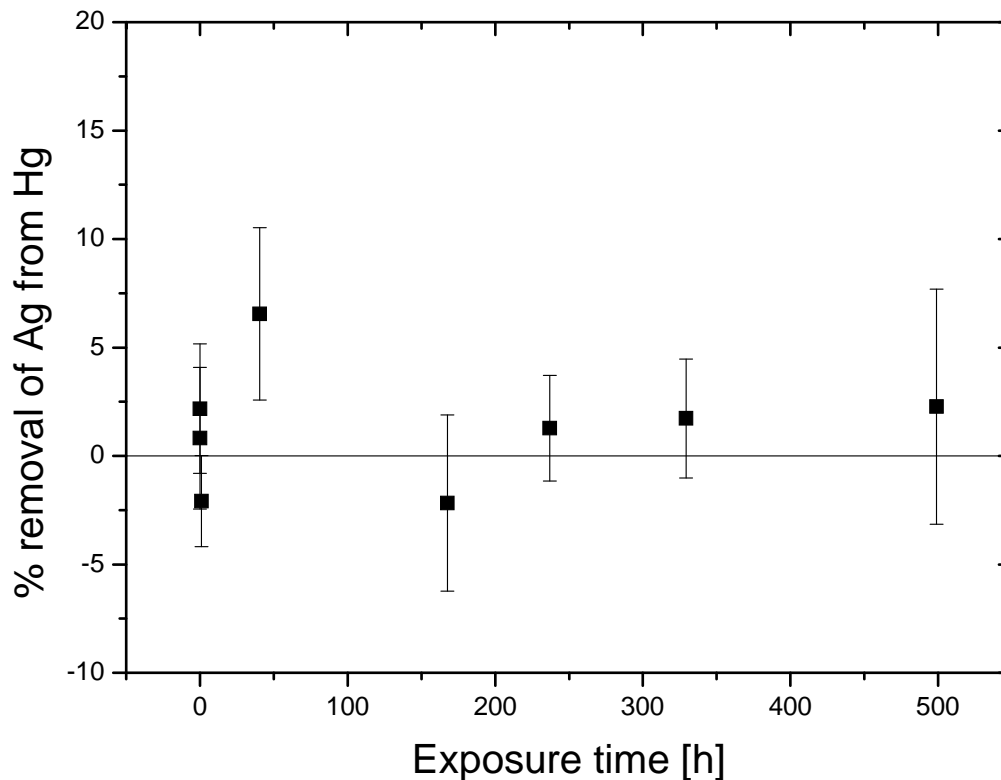


Figure 26: Graphical representation of the evolution of the relative removal of Ag from mercury with time.

It can be seen that no significant decrease of the silver activity in the mercury sample can be detected. A second long-term series of experiments was performed, only with one 10 minutes and one 4 months exposure, using a freshly prepared silver solution in mercury as well as a freshly prepared amalgamated copper plate. Here, again only a very small Ag-activity was found on the Cu-plate, and the activity decrease in the Hg was below the detection limits. We conclude that the capability of copper for the adsorption of silver from mercury is at best very small. All three experiments, including the very first tests that show a high adsorption capacity for gold, show consistent results for silver.

Cd: With the addition of the Cd-powder to the mercury, a paste-like grey mass with metallic lustre formed that remained floating on top of the liquid metal or sticking to the walls of the vessel, though according to literature data the solubility of Cd in Hg at room temperature should be about 10% [22]. The reason for the formation of such a solid could be the presence of an oxide layer on the surface of the grains of the cadmium powder that hinders dissolution and forms a paste together with adhering mercury. The sample was repeatedly shaken vigorously for a period of some days, but a complete dissolution could not be achieved. Finally, the solid was separated by filtration. After that, the Cd-solution in mercury could be used mainly to elucidate the behaviour of the non-carrier-added Ag produced by fast neutron irradiation. The activity of Cd remaining dissolved in Hg after the filtration was rather low, and consequently the evaluation of its γ -signals show relatively large errors. However, qualitative statements are possible for both elements. After the filtration, the liquid was treated with an amalgamated copper plate for various times ranging from 1 hour up to 6 weeks. In the liquid metal, no significant decrease of the activities of nuclides of both metals, Ag and Cd, was detected within this time. In some cases, even an apparent increase of activity was observed, especially for the long exposures. At the same time, the precipitation of a small amount of solid was observed with increasing time. It is presumed that this solid binds a fraction of the radionuclides. Since some of the solid sticks to the wall, radiation emitted from this solid is less influenced by the absorption by mercury and can in this way lead to increased activity in the measurement. Both the non-carrier-added Ag as well as Cd was detected on the Cu-plate in measurable amounts, but probably this is again an effect of the precipitation of the solid. The solid also sticks to some extent to the copper plate, giving rise to the increased activities observed. Finally, it can be concluded that so far we do not have an indication that silver and Cd dissolved in liquid mercury show a high affinity to be adsorbed to a copper-plate.

Sb: The amount of Sb mixed with Hg exceeded its solubility by a factor of 2. However, the surface of the Sb-solution in mercury remained visually clean, and no deposit was observed in the vessel directly after preparation of the sample. Because we exceeded the amount of antimony that should be soluble in the volume of mercury used, we decided to study the behaviour of the solution qualitatively for some time, using γ -spectroscopy, before starting the absorber experiments. This series of experiments was started on the 12.11.2007. The sample was studied over a period of about 4 days, using two γ -detectors with different geometries. For the analysis, the routine described in detail above was used, in this case based on the four most intense lines of ^{124}Sb . It was verified that an automated routine gives consistent results in the case of this sample, due to its simple composition. The automatic peak fit routine gave good results and manual corrections were not necessary. We also abstain here from a decay correction since decay effects are in the range of up to 5% only for times up to four days, and the effects shown here clearly exceed the decay effects. The results of this study are summarized in table 14. It should be noted again that the given activities are clearly underestimated for the mercury samples because of the absorption effects of mercury. On the other hand, just by this means we can draw conclusions about the distribution of the radioactivity in the sample. For a start, the sample was simply measured on a horizontally oriented detector directly after the preparation and again after standing over night. These two measurements do not show a significant difference. After this, the

sample was transferred to a vertically arranged detector and immediately measured again. Compared to the horizontally arranged detector, a much lower activity is measured using the vertical one, indicating that a large amount of the radioactivity is placed at locations where it is much more influenced by the absorption effects of mercury when measured from below compared to a measurement from the side. The most simple assumption is that a large portion of the activity is present in a thin invisible surface layer, but other inhomogeneous distributions may have a similar effect. The sample was measured in the same geometry five hours later, with no significant change. The next measurement was performed in the same geometry after letting the sample rest for 45 hours. After this time, in the bottom half of the vessel a thin black layer was observed on the surface of the PE-container. At the same time, a significant increase of the measured activity is observed, indicating that a substantial amount of the activity is associated with this layer. At this point, we decided to filter the mercury through a paper pinhole filter placed in a glass funnel. Afterwards, γ -spectra were taken of the filtered mercury, the filter paper, the empty PE vessel and the glass funnel. The mercury showed no visible contamination after the filtration. The paper filter showed some dark material on it, but hardly visible, while in the bottom part of the funnel a dark solid was clearly visible. The PE vessel still showed a thin dark layer adhering to its walls in the bottom part. The measured activities for these components correlate well with these observations. The mercury has lost around 2/3 of its original activity. The largest part of this activity is sticking to the walls of the PE container, while smaller fractions are found on the funnel and the filter paper, respectively.

Table 14: Study of a mixture of activated Sb in mercury (mole fraction $x=1.2 \times 10^{-5}$). Explanations see text.

Date of measurement	Measurement time	Sample description	Detector	Activity [Bq]
12.11.2007	17:12	Sb in Hg ($x=1.2 \times 10^{-5}$) in PE vessel	horizontal	1301
13.11.2007	08:50	Sb in Hg ($x=1.2 \times 10^{-5}$) in PE vessel	horizontal	1222
13.11.2007	09:58	Sb in Hg ($x=1.2 \times 10^{-5}$) in PE vessel	vertical	143
13.11.2007	15:19	Sb in Hg ($x=1.2 \times 10^{-5}$) in PE vessel	vertical	157
15.11.2007	12:31	Sb in Hg ($x=1.2 \times 10^{-5}$) in PE vessel Black surface layer on bottom part of PE vessel	vertical	203
15.11.2007	13:06	Hg after filtration	vertical	45
15.11.2007	14:21	Filter paper	vertical	25
15.11.2007	13:41	Original PE vessel	vertical	257
15.11.2007	15:18	Funnel with black precipitate	vertical	63

At this point, it was decided to use a part of the mercury purified by filtration for an absorber experiment. The copper plate used was freshly prepared by amalgamation using HgCl_2 -solution and afterwards cleaned by scratching off the adhering contaminations using a scoop. As in the experiments described above the activity of the mercury solution was measured before and after each experiment and the activity of the copper plate was measured accordingly. Table 15 shows the results for the first series of experiments. After one hour of exposure, the activity of ^{124}Sb in the mercury has dropped to about 30% of the original value, and correspondingly the activity of the copper plate has increased dramatically. With increasing exposure time, the activity deposited on the copper plate does not increase significantly anymore. The reason for this may be a saturation of the adsorption sites on the copper plate, since a fairly concentrated solution of antimony was used in these experiments.

Table 15: Results of first series of adsorber experiments to remove ^{124}Sb from a mercury solution.

Exposure time [h]	Measured ^{124}Sb Activity in Hg [Bq]	^{124}Sb Activity on copper plate [Bq]
0	14.3	0
1	4.1	117
1.5	5.17	111
26.2	5.2	130

In the first series, antimony showed a surprisingly fast adsorption to the copper plate. To examine shorter exposure times, it was decided to start a new series of experiments. For this series, the antimony-mercury solution remaining from the last series of experiments and a freshly prepared copper plate was used. The decision of using the remaining solution from the preceding series was based on the fact that the last series showed that there may be a saturation of adsorption sites on the copper plate. The use of a sample with lower antimony concentration should avoid this effect. In addition to the shorter exposure periods missing in the first series, we also aimed to study longer periods to clarify the effects leading to the apparent increase of the activity in the liquid metal after longer exposures.

The results of this second series are shown in table 16. Their interpretation is not simple. For the short exposure times, a decrease of the antimony activity in the liquid metal is observed. Compared to the results of the first series of experiments, the removal of antimony seems to be much slower. A comparatively fraction of the antimony remains in solution. The most sensible explanation seems to be a difference in the surface properties of the different copper plates used in the two series. These problems have already been discussed above.

For the two longer exposure times, a significant increase of the activity in the mercury is observed, indicating that the small effects observed in the first series are caused by chemical processes. On the contrary, the activity measured on the copper plate decreases in the 24 hour exposure, while it increases again dramatically after the 400 h exposure. The reasons for these effects are not clear.

Table 16: Results of second series of adsorber experiments to remove ^{124}Sb from a mercury solution.

Exposure time [h]	Measured ^{124}Sb Activity in Hg [Bq]	^{124}Sb Activity on copper plate [Bq]
0	5.2	0
0.0833	5.04	9.7
0.25	4.88	13.8
0.5	4.71	16.9
24	5.5	12.8
400	31.2	247
	Hg removed from original PE vessel	
400	1.4	
	Original PE vessel	
400	34.5	

A closer look on the mercury sample after 400 hours may help to get an idea of the processes going on in this sample as a function of time. A γ -analysis was performed on the mercury after it was separated from the original sample vessel by simple decantation. A second spectrum was taken of the emptied original vessel. The results, also listed in table 16, show that a substantial amount of the antimony is adhering to the wall of the container, but only about 25% of the

original antimony is left in the mercury. Most of the activity after 400 hours however is found on the copper plate. Obviously, depositions containing antimony are formed both on the copper plate and the polyethylene vessel. Their chemical nature is unclear. Even though the system seems relatively simple, containing macroscopic amounts of mercury, copper, polyethylene, air and small amounts of antimony, moisture and impurities in the macroscopic components, the behaviour is not predictable and to get a better understanding, intensive investigations using inert conditions, optimized pre-purifications of the components and sophisticated techniques for the preparation of reproducible adsorption surfaces would be necessary. As a conclusion, it is shown that under appropriate conditions, the extraction of antimony from liquid mercury using copper adsorption devices may be possible. The behaviour of the system also shows that even a seemingly simple system can show surprising behaviour. Extrapolating this to the complexity of a spallation target demonstrates the difficulty of making predictions on the behaviour of nuclear reaction products.

Sn: A solution of activated tin in mercury with a mole fraction of 9.6×10^{-5} , containing ^{113}Sn and $^{117\text{m}}\text{Sn}$, was prepared by direct mixing of activated tin with mercury in a PE vessel. This tin solution behaved similar to the antimony solution discussed above. The surface of the Sn-solution in mercury remained visually clean, and no deposit was observed in the vessel directly after preparation of the sample. Nevertheless, we decided to study the behaviour of the solution qualitatively for some time, using γ -spectroscopy, before starting the absorber experiments. The sample was measured on a vertical γ -detector directly after preparation and again 16 hours later. Afterwards, the solution was filtrated through a paper pinhole. The filtrate and the original PE vessel and the filter residue were measured in the same geometry again. The results are compiled in table 17.

Table 17: Study of a mixture of activated Sn in mercury (mole fraction $x=9.6 \times 10^{-5}$). Explanations see text.

Date of measurement	Measurement time	Sample description	Detector	Activity ^{113}Sn [Bq]	Activity $^{117\text{m}}\text{Sn}$ [Bq]
12.11.2007	16:44	Sn in Hg ($x=9.6 \times 10^{-5}$) in PE vessel	vertical	1772	409
13.11.2007	08:53	Sn in Hg ($x=9.6 \times 10^{-5}$) in PE vessel	vertical	1977	442
13.11.2007	10:45	Hg after filtration	vertical	1608	327
13.11.2007	12:32	Original PE vessel + filter paper	vertical	2115	1372

The measurements directly after preparation and after letting the sample set overnight do not show a significant difference. Even for the mercury solution after filtration, the differences to the original solution are small. The results of the γ -measurements of the original PE vessel and the filter reveal that a significant amount of activity sticks to these components. In the original sample, this part of the activity was presumably associated with a surface layer. Because of the relatively low energy of the predominant γ -lines of these two isotopes (^{113}Sn : 392 keV; $^{117\text{m}}\text{Sn}$: 158 keV) this activity did not contribute much to the activity of the original sample measured from below.

A part of the mercury purified by filtration was used for an absorber experiment. The copper plate used was freshly prepared by amalgamation using HgCl_2 -solution and afterwards cleaned by scratching off the adhering contaminations using a scoop. As in the experiments described before, the activity of the mercury solution was measured before and after each experiment and the activity of the copper plate was measured accordingly. Table 18 shows the results for the series of experiments using the tin solution in mercury. The activities given in the table are corrected for the decay occurring during the series of experiments.

Table 18: Results of a series of adsorber experiments to remove tin from a mercury solution.

Exposure time [h]	Measured ^{113}Sb Activity in Hg [Bq]	Measured $^{117\text{m}}\text{Sb}$ Activity in Hg [Bq]	Measured ^{113}Sn Activity on copper plate [Bq]	Measured $^{117\text{m}}\text{Sn}$ Activity on copper plate [Bq]
0	22	3.3	0	0
0.5	15	2.2	30	23
15.3	7	3.3	69	49
375	9	5.8	67	40

Similar to the results observed for antimony, it can be qualitatively stated that there is a tendency for tin to be absorbed from mercury solution onto a copper surface. For larger exposure times however, there seems to be a tendency to form precipitates that adhere to the mercury vessel. In this process, the copper absorber might be involved, leading to a transport of activity from the absorber to the mercury vessel. However, the few experiments performed here do not allow reliable statements on the details of the processes occurring in this system. The prerequisites for more detailed studies were already discussed in the section dealing with antimony and will be summarized in the conclusion of this chapter.

Zn: The diluted Zn-amalgam proved to be rather sensitive to air. Thus, solid layers show up after short time on the surface of the liquid and the walls of the vessel. The activated Zn was associated with these solids rather than the liquid phase and no substantial adsorption on Cu was detected.

Tb, Ir: For these metals, no dissolution in mercury could be detected even for very long (> 1 year) contact times. For these metals, electrochemical deposition on mercury electrodes has been tested. The results of these experiments will be reported in a separate chapter.

4.5.2.3. Conclusion on absorber experiments

It is shown that metal absorbers can be used as an option for extraction of dissolved radionuclides from liquid metals. However, these reactions have to be studied in much more detail to be transferred to a technical application. The air sensitivity of some of the samples clearly shows the necessity of an inert gas system for such experiments. Other necessary improvements include the preparation of reproducibly working metal surfaces of various elements and the pre-purification of the metals that are to be dissolved to avoid negative effects that may be caused by surface oxidation. The pre-purification may be achieved by reduction or vacuum distillation, or a combination of these methods. Considering the surface preparation, ion-beam etching could be a valuable tool for the preparation of reproducibly wetted surfaces [34]. For a technical implementation, the time dependence of the adsorption processes has to be studied, and the capacity of the materials used for adsorption has to be determined.

4.5.3. Studies on recently proton-irradiated samples from CERN

4.5.3.1. Irradiation and sample handling

Two 1 ml samples of Hg were filled in stainless steel capsules without pre-purification under an argon atmosphere. These capsules were irradiated at CERN with a proton beam of 1.5×10^{15} protons of 1.4 GeV on the 21st of April 2006. The samples took 10^{12} protons per pulse with one pulse per 18 seconds, where one such pulse was a super-cycle made up from 15 individual pulses spaced by 1.2 seconds. After some weeks of cooling the samples were transferred to PSI, where they were measured at several times over periods of some months (Sample 1) to 19 months (Sample 2) using HPGe-detectors with different geometries, equipped with standard electronics. For a detailed description of the evaluation of spectra see chapter 4.4.

One sample, in the following called CERN1, was opened in a Plexiglas glove box, which was filled with Ar. The oxygen content of the system measured using an yttria-doped ZrO_2 solid electrolyte cell was in the range of 0.1 – 1%. After opening, the Hg was removed from the steel capsule and poured into a glass vessel. γ -spectra of the steel capsule and the Hg sample were taken separately. Additionally, a part of the Hg was separated using a syringe, and a γ -spectrum of the removed fraction of Hg was measured. The main part of the Hg sample was filled into a second glass vessel and the first vessel checked for contamination. The second sample of Hg (CERN2) remained in the original irradiation capsule for 19 months, and γ -spectra were taken repeatedly to facilitate nuclide identification based on decay properties. After this period, it was opened and divided in two parts, which were then used to study the application of traditional purification methods for mercury such as leaching with oxidizing acids and/or distillation on samples containing only non-carrier added amounts of radionuclides. The results of the experiments performed using these two samples are presented in two individual chapters below. In both cases we will start the chapters with a summary on the nuclide identification and afterwards discuss the experiments performed with the samples.

4.5.3.2. CERN1 nuclide identification and experiments

The full spectrum of the sample CERN1 approximately three weeks after irradiation is shown in figure 27. It shows the full complexity of the data. The problems arising from this complexity, together with the additional difficulties caused by the strong absorption effects of mercury, have been discussed in some detail in chapter 4.4. The measuring conditions of the spectra used for nuclide identification are given in table 19. The results of the nuclide identification and analysis are compiled in table 20. It is pointed out again that the numerical data given for the activities will in most cases be significantly underestimated because of the strong absorption effects of mercury. This is especially significant for nuclides with low energy γ -rays.

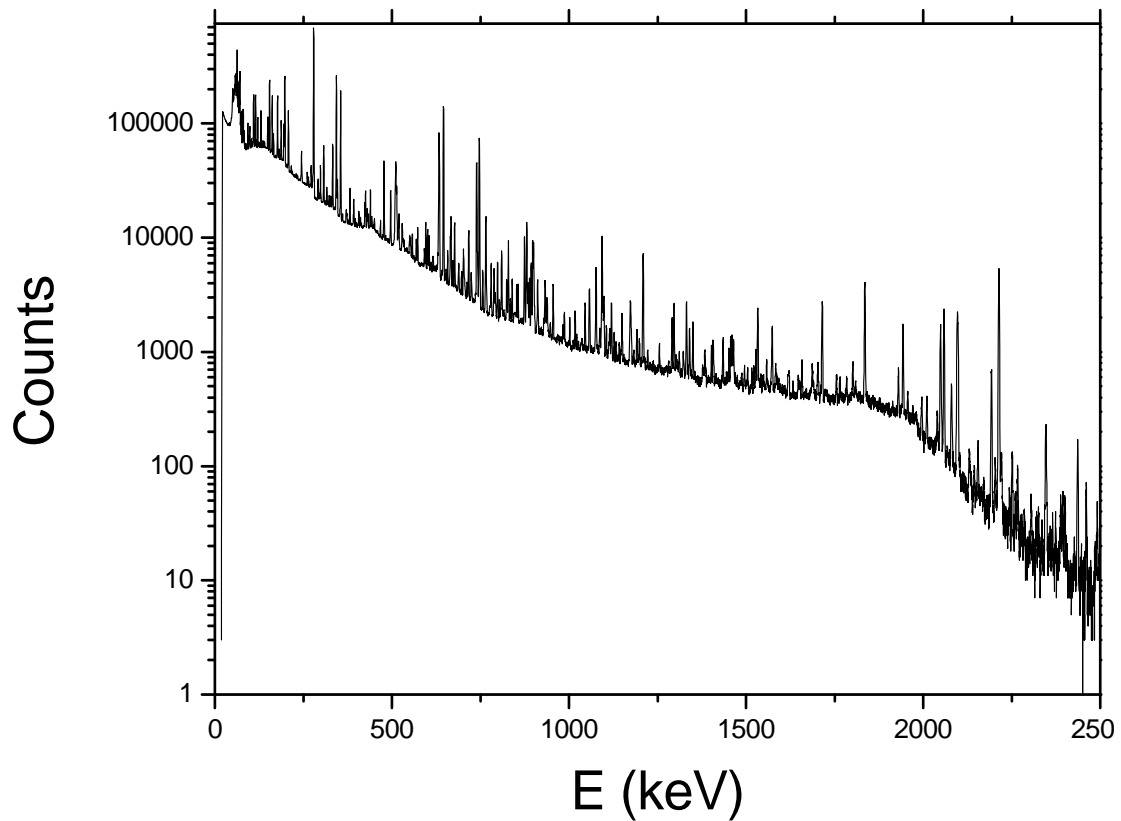


Figure 27: Full spectrum of the sample CERN1 approximately three weeks after irradiation, illustrating the immense complexity.

Table 19: Summary of the measurement parameters of the measurements used for nuclide identification in Sample Cern1 (Sample Mass 14 g, Fill height in steel container 16 mm, Volume 1 ml, Irradiated on 21.04.06, Irradiation parameters see text).

Filename	Sample composition	Acquisition start Date/time	Measuring time [s]	Detector	Geometry
Hg_Cern1 11.05.06 15h	Hg plus Steel irradiation capsule	11.05.06/ 15:32:55	54000	Det01/OIPA	Steel Capsule Horizontal arrangement, Distance 25 cm
Hg_Cern1 19.05.06 15h	Hg plus Steel irradiation capsule	19.05.06/ 13:26:06	54000	Det01/OIPA	Steel Capsule Horizontal arrangement, Distance 25 cm
Hg_Cern1 29.05.06 15h_nur_Hg	Hg removed from capsule in a glass vessel	29.05.06/ 15:40:00	54000	Det02/OIPA	Glass vessel, vertical arrangement, Distance C3
Hg_Cern1 29.05.06 1h_nur_Kapsel_ 25cm	steel irradiation capsule only	29.05.06/ 10:54:39	3600	Det01/OIPA	Steel Capsule Horizontal arrangement, Distance 25 cm
Hg_CERN1_19 -1-07	Hg in glass vessel	18.01.07/ 10:31:17	50400	Det01/OIPA	Glass vessel Horizontal arrangement, Distance 1.5 cm

A vast variety of radionuclides has been identified in sample CERN1, both produced in the steel irradiation capsule and in the mercury itself. The corresponding results are compiled in table 20. As expected from their decay properties, the rather short lived nuclides are only detected in the spectra taken shortly after the irradiation time, e.g. $^{196,198}\text{Au}$ and the directly produced ^{188}Ir and ^{172}Lu . On the contrary, in these spectra some of the long-lived nuclides are not detected because they are hidden by the background caused by the radiation of the short-lived nuclides, e.g. ^{173}Lu and ^{195}Au . In general, some of the nuclides with lower activities could not be clearly identified in some of the spectra.

It is clearly seen that after the removal of the mercury from the capsule, the activities determined for the nuclides produced in the steel capsule, e.g. ^{48}V , ^{51}Cr , $^{52,54}\text{Mn}$, and $^{57,58}\text{Co}$ are comparable to those values obtained from the measurements with the mercury inside the capsule. On the other hand, these nuclides are naturally only found in very small amounts in the liquid metal.

For the nuclear reaction products of mercury, the data in table 20 indicate that some elements, e.g. ^{109}Cd , ^{113}Sn , many of the lanthanides, ^{188}Pt and ^{202}Tl remain in the capsule after emptying to a certain extent, while other elements are mainly found in the mercury after separating it from the capsule. These are mainly the silver and gold nuclides $^{105,106\text{m},110\text{m}}\text{Ag}$ and $^{195,196}\text{Au}$, but nuclides of some alkaline metals and chalcogens show a similar behaviour. Reasonable explanations of these observations are the following: The nuclides of elements that are dissolved in mercury and do not show a large affinity to the surface of the steel capsules are preferentially found in the mercury after separation from the capsule. The remaining elements obviously form chemical species that are not soluble in mercury and are accumulated on the free mercury surface in the capsule or stick to the wall of the capsule. These materials can remain on the wall of the capsule while emptying, or they can flow out together with the mercury. In many cases, a certain fraction of a nuclide will stick to the wall, while the remainder is carried away with the mercury.

Table 20: Nuclear reaction products identified in sample CERN1. Note that the activities given for the mercury samples are underestimated because of the neglect of the absorption effects of mercury.

Nuclide	Sample Measurement date Half-life [d]	Hg in capsule 11.05.2006 A corrected to EOB* [Bq]	Hg in capsule 19.05.2006 A corrected to EOB [Bq]	Hg in glass vessel 29.05.2006 A corrected to EOB [Bq]	irradiation capsule 29.05.2006 A corrected to EOB [Bq]	Hg in glass vessel 19.01.2007 A corrected to EOB [Bq]
Be-7	5.31E+01	5.23E+04	2.46E+05	2.84E+04	2.04E+05	
Na-22	9.50E+02	1.33E+03	1.35E+03		1.30E+03	
Sc-46	8.38E+01	9.83E+04	9.80E+04	2.11E+02	8.92E+04	4.92E+02
V-48	1.60E+01	1.81E+06	2.45E+06	9.92E+02	3.19E+06	
Cr-51	2.77E+01	1.60E+06	1.91E+06		2.20E+06	
Mn-52	5.59E+00	1.30E+07	3.32E+07		1.14E+08	
Mn-54	3.12E+02	9.87E+04	4.38E+04	7.13E+01	6.90E+04	2.91E+01
Co-56	7.71E+01	2.90E+04	6.02E+04		5.23E+04	
Co-57	2.72E+02	1.46E+04	1.08E+04		9.04E+03	5.65E+00
Co-58	7.09E+01	6.55E+04	6.18E+04		7.58E+04	9.33E+03
Fe-59	4.45E+01	9.38E+02	3.56E+03			
Co-60	1.92E+03					6.32E+00
Zn-65	2.44E+02					5.82E+01
As-74	1.78E+01	1.56E+04	1.71E+04	1.11E+04		
Se-75	1.20E+02	1.04E+03	1.23E+03	1.75E+02		4.74E+02
Rb-83	8.62E+01	8.67E+02	2.01E+03	1.08E+03		1.94E+03
Rb-84	3.29E+01	3.20E+03	5.74E+03		9.07E+03	
Sr-85	6.48E+01			1.32E+03		5.83E+03
Rb-86	1.86E+01	3.22E+04	6.65E+04	2.08E+04		
Y-88	1.07E+02	2.50E+03	2.37E+03	8.93E+02		1.70E+03
Zr-88	8.34E+01	1.35E+03	1.84E+03	3.57E+02	2.91E+03	
Zr-95	6.40E+01	1.55E+03		6.12E+02		2.18E+03
Rh-101m	1.20E+03					
Rh-102	2.07E+02			7.60E+01		
Rh-102m	1.06E+03					1.35E+01
Ru-103	3.93E+01	2.37E+03	3.00E+03	2.41E+03	5.69E+03	
Ag-105	4.13E+01			2.12E+03		

Ag-106m	8.46E+00	1.71E+04		2.13E+05		
Cd-109	4.63E+02	1.60E+05	1.32E+05		1.28E+05	1.22E+02
Ag-110m	2.50E+02			2.03E+02		2.43E+02
Sn-113	1.15E+02		2.46E+03	1.47E+02	3.71E+03	8.10E+02
Te-121	1.68E+01	7.89E+03	1.38E+04	7.00E+03		
Te-121m	1.54E+02	2.44E+02		1.57E+01		7.29E+01
Ce-139	1.38E+02	1.28E+03	1.53E+03	5.24E+02	1.90E+03	1.08E+03
Pm-143	2.65E+02		6.17E+03	6.40E+02	3.39E+03	3.86E+02
Pm-144	3.63E+02			2.46E+01		1.25E+01
Eu-145	5.93E+00	3.95E+05	2.01E+06	2.80E+06		
Eu-146	4.59E+00	4.63E+06	6.06E+07	3.74E+08	9.70E+08	
Gd-146	4.83E+01	1.50E+04	1.10E+04	1.00E+04	3.39E+04	
Eu-147	2.40E+01	5.30E+04	4.68E+04	3.60E+04	6.58E+04	
Gd-149	9.40E+00	2.95E+05	5.29E+05	3.17E+05	1.14E+06	
Gd-153	2.42E+02		1.01E+03	5.03E+02		9.08E+02
Tm-167	9.25E+00	8.40E+05	1.17E+06	8.32E+05	2.88E+06	
Yb-169	3.20E+01	5.80E+04	7.34E+04	2.94E+04	1.06E+05	
Lu-171	8.24E+00	1.14E+06	2.94E+06		5.96E+06	
Hf-172	6.83E+02			1.64E+02		4.10E+02
Lu-172	6.70E+00	1.51E+05	9.49E+05	2.53E+06		
Lu-173	5.00E+02			9.04E+02	4.10E+03	7.47E+02
Hf-175	7.00E+01	2.48E+04	1.84E+04	1.14E+04	2.70E+04	5.81E+04
Re-183	7.00E+01	2.83E+04	3.13E+04	1.14E+04	4.09E+04	4.73E+04
Os-185	9.36E+01	3.36E+04	3.56E+04	1.34E+04	3.73E+04	2.24E+04
Ir-188	1.73E+00	1.00E+12				
Pt-188	1.02E+01	8.22E+05	1.41E+06	6.27E+05	3.74E+06	
Ir-190m	1.18E+01	1.76E+04	5.24E+04	3.44E+04		
Pt-191	2.90E+00	1.11E+08				
Au-195	1.86E+02			1.69E+03		3.96E+03
Au-196	6.18E+00	1.16E+06	3.41E+06	2.14E+07		
Au-198	2.69E+00	9.11E+07				
Tl-202	1.22E+01	2.66E+04	5.25E+04	2.92E+04	9.43E+04	
Hg-203	4.66E+01	1.44E+04	1.54E+04	3.82E+04		

*EOB = 21.04.2006

4.5.3.2.1. Syringe test

Figure 28 shows a small section of the γ -spectrum of Sample CERN1 approximately 3 weeks after irradiation, after the mercury was separated from the irradiation capsule and put into a standard 5 ml laboratory glass vessel. Though a substantial part of the radionuclides remained in the irradiation capsule, a large part was also carried with the mercury. The complete list of nuclides identified in the mercury after its separation from the irradiation capsule is compiled in table 20. Some of these nuclides are indicated in figure 28.

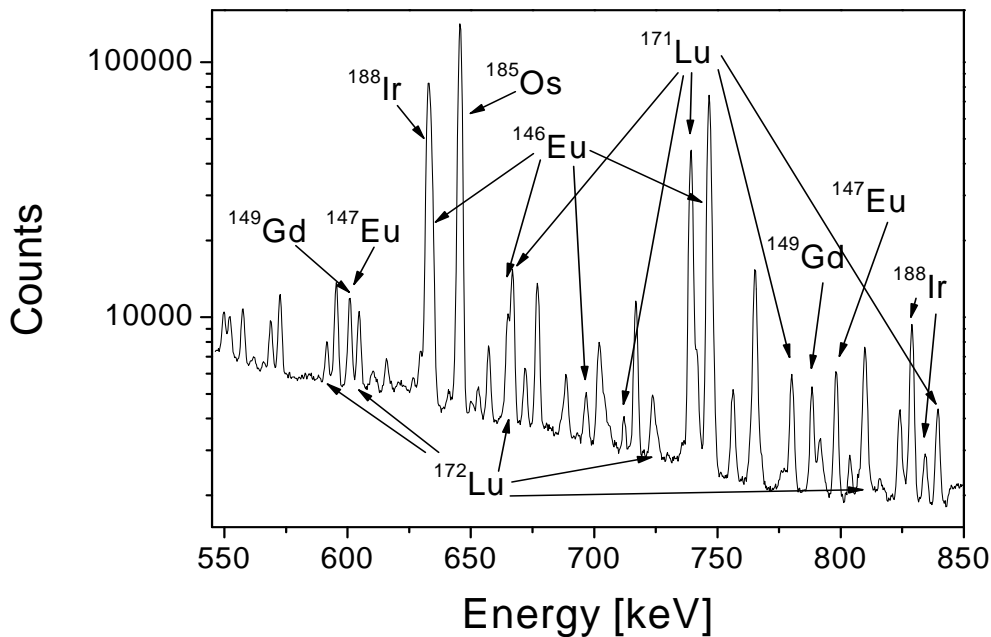


Figure 28: Section of the γ -spectrum of sample CERN1 taken approximately 3 weeks after irradiation.

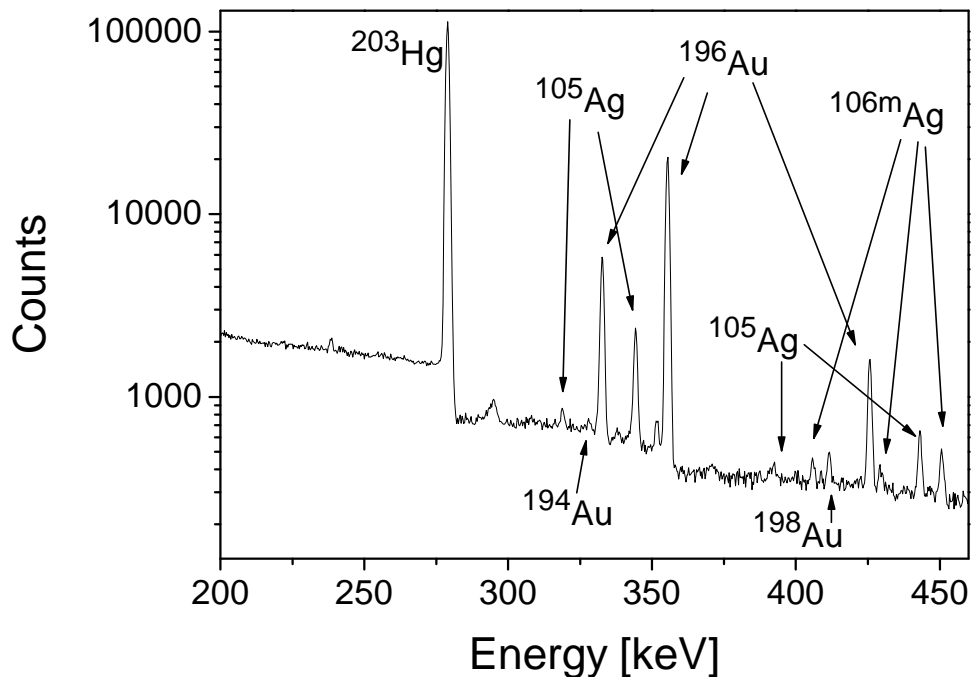


Figure 29: Section of the γ -spectrum of bulk Hg removed from sample 1 using a syringe, taken approximately 6 weeks after irradiation.

After its separation from the capsule, a part from the inner volume of the mercury was soaked into a syringe and transferred to a second glass vessel. The γ -spectrum of this fraction of Hg is shown in figure 29. A quantitative comparison of the γ -spectra of the irradiation capsule and both complete and inner part of the Hg sample is extremely difficult because of the strong absorption effect of Hg and non-sufficient knowledge of the actual distribution of the γ -emitting species. Therefore, we confine ourselves to a qualitative discussion.

The sample taken out of the inner volume of the mercury shows much less activity than expected from the spectra of the complete mercury removed from the capsule. In fact, only silver and gold isotopes could be identified in this sample. The identified nuclides are indicated in figure 29. Additional to these nuclides, also ^{195}Au was found. Since this sample was taken from the inner part of the Hg droplet, it is concluded that only Ag and Au are actually dissolved in mercury, while the radionuclides of the remaining elements are attached to the surface of the Hg droplet and were simply washed out of the irradiation capsule together with the mercury. Most of these nuclides also belong to the group of elements that partly adhere to the surface of the irradiation capsule. In comparison, Ag and Au are completely removed from the irradiation capsule together with the mercury. No Ag and Au nuclides were found in the γ -spectrum of the irradiation capsule after emptying the Hg.

The reason for this behaviour and the chemical state of the radionuclides located at the surfaces is not yet fully understood. They cannot be brought into solution by vigorous agitation. It could be that the small numbers of atoms of these nuclides present in the samples are oxidised, either by traces of oxygen present in the irradiation capsule or diffusing into it through leaks while it was exposed to ambient air, or from the reduced but not extremely low oxygen content in the atmosphere of the box. These reactions may be enhanced by radiation effects. Oxides will probably be almost insoluble and of lower density than mercury and thus will show a tendency to separate from the liquid metal and float to the top surface. It is also long-time laboratory experience that such oxidic impurities on mercury surfaces have a tendency to stick to the walls of the container. Thus, the assumption of many of the radionuclides being oxidised is in principle compatible with the observed behaviour. However, it is also known from aqueous radiochemistry that radionuclides present in carrier-free amounts often undergo adsorption processes, either on the walls of containers or on solid particles dispersed in the system [65, 66]. A rough comparison of the number of adsorption sites available in the capsule with an estimation of the total number of atoms produced during irradiation shows that substantial adsorption of radionuclides at the walls of the capsule is possible. Though the surface of the Hg samples was visually clean, a thin layer of solid material, e.g. oxide, could be present on the surface of the liquid metal. Since this material would be finely dispersed, it could also serve as a site for adsorption of carrier free radionuclides. Therefore, adsorption to such particles could be an alternative explanation for many of the radionuclides being enriched on the surface of the liquid metal. Another possible explanation would be the segregation of metals because of low solubility or the formation of insoluble intermetallic compounds. Segregation due to solubility limits seems to be a plausible explanation for the least soluble elements. For instance, for the elements Re and Os from the γ -spectrum of our Hg sample we estimate mole fraction of in the range of 10^{-11} for the radioactive nuclides ^{183}Re and ^{185}Os alone, neglecting the formation of stable nuclides. Comparing to the solubilities estimated in chapter 3, a precipitation of these elements is possible in the proton irradiated mercury. In general, also the presence of inactive carrier can play an important role in solubility considerations. Though radionuclides are present only at low concentrations in our samples, typically mole fractions of 10^{-9} to 10^{-13} , corresponding inactive carriers can be present in much larger concentrations. In this way, the solubility limit can be exceeded.

In summary, it is shown that many reasons can lead to the effects of inhomogeneous distribution of radionuclides observed in the sample CERN1. For those elements that have a high affinity to oxygen, the formation of oxides is the most probable explanation for the separation. For elements with an extremely low solubility the solubility limit could be reached. Finally, adsorption on

surfaces and colloids can also play a role. In principle, each element has its own chemical characteristics and thus will show an individual behaviour. In a complex mixture of elements as a spallation sample, all of the above effects and even more complicated reactions may occur.

4.5.3.2.2. Study of wall adsorption of radionuclides

The mercury was filled into a second 5 ml glass vessel. γ -spectra of the empty old glass vessel indicated that again a substantial amount of the radioactivity sticks to the walls of the vessel. Washing procedures were performed to remove these radionuclides from the walls of the vessel, mainly with the goal to recover the radionuclides for experiments planned to bring them back into mercury solution again, e.g. by electrolysis. The empty glass vessel was first washed with water, shaking vigorously for 5 minutes. After this, γ -spectra were recorded of the washing water and the washed glass vessel. In the next step, the glass vessel was washed for two hours with 1M HCl to remove the radionuclides still sticking to wall. Finally, a γ -spectrum was recorded of the HCl-washing solution. The results of these experiments are compiled in table 21. We observe that a substantial fraction of all nuclides but those of Hg, Au and Ag are sticking to the wall of the original vessel when the mercury is transferred to the second vessel, but also a certain fraction of all nuclides is transferred to the new vessel. A quantitative comparison of the sticking and the transferred quantities is impossible because of the absorption effects of mercury.

The washing experiments show that a fraction of the sticking nuclides are removed by a short washing procedure using water. The removal efficiency is different for each element and depends on its chemical state and the solubility of the corresponding species in water. With a few exceptions, a reasonable agreement is observed between the sum of activities found for a certain nuclide in the washing water and the vessel after washing, and the total amount of activity present in the vessel before washing. The last column shows, that a large part of the activity still remaining in the vessel after washing with water can be dissolved in 1 M HCl. For many nuclides, almost all of the activity is removed by the acid washing, while for other nuclides, e.g. those of Se, Te and Ir, the majority of the activity still remains in the glass vessel. Optimized washing procedures could be developed in case a cleaning of the mercury loop of the target system is considered necessary or useful.

Finally, the original steel irradiation capsule was shaken vigorously with freshly distilled mercury. Afterwards, the mercury was removed from the capsule, and γ -spectra were recorded of the mercury and the empty capsule. The activity of the capsule after the experiment was compared to that of the capsule before shaking with the fresh mercury. The purpose of this experiment was to find out how strong the active material is adhering to the wall and to get an idea about the possibility of its removal by the liquid metal flow during the operation of the target, simulating the flow in a very simple way by shaking. The results of this experiment are compiled in table 22 in terms of a removal factor, i.e. the percentage removed from the capsule compared to the initial contamination is given. For a qualitative comparison, we also state the activities found in the mercury used for washing, though they cannot easily be balanced against the values found for the empty capsule because of absorption effects.

The removal fractions found vary from 15 to 90% for different nuclides. No systematic trends are observed concerning the position of the corresponding elements in the periodic table and their probable chemical state and the fraction of removal found. Finally, it is found that a considerable amount of the radioactivity adhering to the wall of the irradiation capsule can be removed by vigorous mechanical contact with mercury, but still a substantial fraction remains on the wall. For an operation liquid metal target system, the conclusion is that a part of the solid material tending to separate from the liquid metal will be carried around the loop by the flowing mercury. At places where the velocity of the liquid metal is reduced, these materials will be preferentially deposited. When the liquid metal flow is stopped, e.g. before draining the loop, increased deposition is possible. The quantification of the fraction of sticking material in a real liquid metal

target system and its preferred location remain to be clarified by the experience gained from operating liquid mercury spallation sources such as SNS or JSNS.

Table 21: Main nuclides found in the empty glass vessel previously containing sample CERN1, Nuclides transferred with the mercury to the new vessel, and results of washing experiments using the old vessel.

Nuclide	Half-Life(d)	Atomic number Z	Empty glass vessel CERN1	Hg in new glass vessel	Washing water	Old glass vessel after washing with water	1 M HCl solution
Be-7	53.29	4	2093	742	423	295	211
Sc-44m	2.44	21	582	46	114	57	69
Sc-46	83.82	21	54	27	41	21	24
Se-75	119.64	34	122	32	41	63	8
Rb-86	18.631	37	592	115	424	29	6
Y-88	106.6	39	255	93	221	84	77
Zr-95	64	40	116	34	44	46	31
Ru-103	39.35	44	305	83	113	97	44
Ag-110m	249.79	47		96			
Te-121	16.8	52	109	43	32	34	19
Ce-139	137.6	58	410	46	276	173	158
Pm-143	265	61	266	102	158	118	99
Eu-146	4.51	63	1851	751	1139	654	593
Gd-146	48.3	64	2551	188	1786	938	743
Eu-147	24.6	63	1372	597	854	543	442
Gd-149	9.28	64	130	131	269	129	118
Sm-153	1.928	62	460	67	393	198	183
Yb-169	32	70	4821	473	4187	1724	1680
Lu-171	8.22	71	1211	250	504	204	192
Hf-172	682.55	72	355	41	326	274	146
Lu-172	6.7	71	494	63	428	219	212
Lu-173	500.5	71	676	207	534	387	338
Hf-175	70	72	2751	1317	1694	1774	1253
Re-183	71	75	944	150	1307	1316	562
Os-185	94	76	3259	1435	2416	1311	481
Ir-188	1.729	77	973	270	248	415	87
Pt-188	10.2	78	103	345	304	457	131
Ir-192	73.831	77	105	45	51	58	13
Au-195	186.09	79		775			
Au-196	6.183	79		630			
Tl-202	12.23	81	179	38	66	56	42
Hg-203	46.59	80		4741			

Table 22: Fractional removal of the activity sticking to the walls of the irradiation capsule of sample CERN1 by shaking with freshly distilled mercury.

Nuclide	Half-life [d]	Irradiation capsule before washing Activity corrected to EOB (21.4.06) [Bq]	Removal of nuclide [%]	Hg used for washing Activity removed with the mercury, corrected to EOB
Rb-84	3.29E+01	9.07E+03	16	1.52E+02
Zr-88	8.34E+01	2.91E+03	33	2.63E+01
Ru-103	3.93E+01	5.69E+03	62	8.57E+01
Ce-139	1.38E+02	1.90E+03	18	4.15E+01
Pm-143	2.65E+02	3.39E+03	55	3.71E+01
Gd-146	4.83E+01	3.39E+04	63	3.62E+02
Eu-147	2.40E+01	6.58E+04	65	3.85E+02
Yb-169	3.20E+01	1.06E+05	44	1.20E+03
Lu-173	5.00E+02	4.10E+03	41	Not detected
Hf-175	7.00E+01	2.70E+04	68	5.84E+02
Re-183	7.00E+01	4.09E+04	18	3.66E+01
Os-185	9.36E+01	3.73E+04	19	1.14E+03
Pt-188	1.02E+01	3.74E+06	91	8.55E+03
Ir-192	7.38E+01	1.19E+03	69	2.59E+01
Tl-202	1.22E+01	9.43E+04	88	1.04E+03

4.5.3.3. CERN2 nuclide identification and experiments

The second sample of Hg (CERN2) remained in the original irradiation capsule from April 2006 until November 2007. During this period, γ -spectra were taken repeatedly to facilitate nuclide identification based on decay properties. A summary of the measurement parameters are found in table 23. After this period, it was opened and divided in two parts, which were then used to study the application of traditional purification methods for mercury such as washing with oxidizing acid and/or distillation on samples containing non-carrier added amounts of radionuclides. The results of the experiments performed using sample CERN2 are presented in the following chapters.

Table 23: Measurement data for γ -measurements performed on sample CERN2 before opening (Mass 13.8 g, Fill height in steel container 16 mm, Volume 1 ml, irradiated on 21.04.06, Irradiation data see chapter 4.5.3.1.).

Name of spectrum	Sample composition	Acquisition start Date/time	Measuring time [s]	Detector	Geometry
Hg_Cern2 22.05.06 15h_2	Hg plus Steel irradiation capsule	22.05.06/ 12:41:49	54000	Det01/OIPA	Steel Capsule Horizontal arrangement, Distance 25 cm
Hg in Kapsel_04.08.06_ 24h	Hg plus Steel irradiation capsule	04.08.06/ 13:26:54	86400	Det01/OIPA	Steel Capsule Horizontal arrangement, Distance 10 cm
Hg_Cern2 13.09.06 15h	Hg plus Steel irradiation capsule	12.09.06/ 11:17:07	54000	Det01/OIPA	Steel Capsule Horizontal arrangement, Distance 10 cm
HG_CERN2_24_ 07_07	Hg plus Steel irradiation capsule	24.07.07/ 16:56:48	54000	Det02/OIPA	Steel Capsule vertical arrangement, Distance C0
CERN_2_mit_Ka psel_14.11.07	Hg plus Steel irradiation capsule	14.11.07/ 14:46:39	1800	Det01/OIPA	Steel capsule Horizontal arrangement, Distance 0 cm

Similar to sample CERN1, a vast variety of radionuclides has been identified in sample CERN2, both produced in the steel irradiation capsule and in the mercury itself. As expected from their decay properties, the number of short lived nuclides that are detected decreases with decay time (^{47}Sc , ^{48}V , ^{52}Mn , ^{56}Ni , ^{59}Fe , $^{145,146}\text{Eu}$, ^{149}Gd , $^{196,198,199}\text{Au}$ and many others), while a number of long lived nuclides could be detected only in the spectrum with the longest decay times because they are hidden by the background caused by the radiation of the short-lived nuclides in the spectra taken at shorter decay times, e.g. ^{133}Ba and ^{195}Au . It was expected from the experiences with sample CERN1 that a number of nuclides may accumulate on the free surface of mercury present in the irradiation capsule. Therefore, it was presumed that such nuclides show lower apparent activities on a vertically arranged measuring system because their radiation should be more influenced by the absorption resulting from mercury. In the spectrum of CERN2 measured on in a vertical arrangement, lower activities for most of the nuclides are observed compared to those measured in horizontal geometry, including those nuclides produced in the irradiation capsule. This is certainly caused by combined effects of inhomogeneous nuclide distribution, sample geometry and absorption. However, a detailed analysis of these effects for the different nuclides or elements, respectively, is not possible within the frame of this project. The results of nuclide identification are compiled in table 24.

Table 24: Nuclear reaction products identified in sample CERN2. Note that the activities given are underestimated because of the neglect of the absorption effects of mercury.

Nuclide	sample geometry Half-Life [d]	Hg in capsule 22.05.2006 horizontal geometry A corrected to EOB* [Bq]	Hg in capsule 04.08.2006 horizontal geometry A corrected to EOB [Bq]	Hg in capsule 13.09.2006 horizontal geometry A corrected to EOB [Bq]	Hg in capsule 24.07.2007 vertical geometry A corrected to EOB [Bq]	Hg in capsule 14.11.2007 horizontal geometry A corrected to EOB [Bq]
Be-7	5.31E+01	2.03E+05	8.60E+04	6.24E+04	4.83E+04	
Na-22	9.50E+02	1.47E+03	1.70E+03	1.46E+03	6.90E+02	2.59E+03
Sc-44m	2.44E+00	8.99E+06				
Sc-46	8.38E+01	8.55E+04	7.62E+04	7.68E+04	4.18E+04	1.48E+05
Sc-47	3.34E+00	9.29E+05				
V-48	1.60E+01	8.84E+05	7.97E+05	8.18E+05		
Cr-51	2.77E+01	1.18E+06	1.10E+06	9.04E+05		
Mn-52	5.59E+00	1.31E+06				
Mn-54	3.12E+02	9.03E+04	7.06E+04	8.23E+04	4.84E+04	1.73E+05
Co-56	7.71E+01	4.83E+04	4.40E+04	4.26E+04	2.32E+04	7.27E+04
Ni-56	6.10E+00	1.65E+04				
Co-57	2.72E+02	1.81E+04	2.08E+04	1.29E+04	6.45E+03	2.56E+04
Co-58	7.09E+01	6.10E+04	4.81E+04	6.29E+04	2.23E+04	2.90E+05
Fe-59	4.45E+01	2.68E+03	2.92E+03	2.76E+03		
Co-60	1.92E+03		2.70E+02	2.53E+02	9.30E+01	4.13E+02
Zn-65	2.44E+02				2.33E+02	9.85E+02
As-74	1.78E+01	9.67E+03	7.23E+03			
Se-75	1.20E+02	1.42E+03	1.27E+03	1.25E+03	6.10E+02	
Rb-83	8.62E+01	2.69E+03	4.12E+03	4.08E+03	1.23E+03	
Rb-84	3.29E+01	5.53E+03	7.42E+03	7.35E+03		
Sr-85	6.48E+01			7.62E+03	4.11E+03	
Y-88	1.07E+02	2.59E+03	3.61E+03	4.20E+03	2.88E+03	
Zr-88	8.34E+01	1.90E+03	2.53E+03	2.46E+03	1.30E+03	5.34E+03
Zr-95	6.40E+01		1.34E+03	1.42E+03		
Rh-102m	1.06E+03		1.20E+02	1.09E+02	3.35E+01	7.36E+01
Ru-103	3.93E+01	3.44E+03	3.07E+03	3.20E+03		
Ag-110m	2.50E+02		2.21E+02		6.55E+01	2.96E+02
Sn-113	1.15E+02	2.68E+03			6.90E+02	2.19E+03
Te-121	1.68E+01	6.31E+03	1.30E+04	4.12E+04		

Te-121m	1.54E+02		1.22E+02	1.05E+02	1.45E+02	
Ba-131	1.18E+01	1.05E+04				
Ba-133	3.84E+03				2.16E+01	8.80E+01
Ce-139	1.38E+02	2.13E+03	2.29E+03		6.90E+02	2.94E+03
Pm-143	2.65E+02		2.24E+03	2.46E+03	1.03E+03	3.78E+03
Eu-145	5.93E+00	1.11E+05				
Eu-146	4.59E+00	1.86E+06				
Gd-146	4.83E+01	1.14E+04	1.12E+04	1.12E+04	1.16E+04	
Eu-147	2.40E+01	3.96E+04	1.38E+04	4.98E+04		
Eu-149	9.31E+01		1.27E+04	1.49E+04	1.41E+03	
Gd-149	9.40E+00	9.67E+04				
Gd-151	1.24E+02		7.20E+03		9.95E+02	4.42E+03
Gd-153	2.42E+02	1.58E+03	1.92E+03	1.95E+03	6.30E+02	2.93E+03
Tb-155	5.32E+00	1.43E+05				
Tm-167	9.25E+00	2.06E+05				
Yb-169	3.20E+01	5.61E+04	6.41E+04	6.58E+04		
Lu-171	8.24E+00	3.97E+05				
Hf-172/Lu-172	6.83E+02		1.74E+03	1.90E+03	5.90E+02	2.88E+03
Lu-172	6.70E+00	9.39E+04				
Lu-173	5.00E+02		5.40E+03	5.34E+03	1.96E+03	6.43E+03
Hf-175	7.00E+01	3.20E+04	3.61E+04	3.75E+04	1.57E+04	1.76E+04
Lu-177	6.71E+00	3.56E+04				
Re-183	7.00E+01	3.34E+04	4.21E+04	4.23E+04	8.35E+03	3.31E+04
Os-185	9.36E+01	3.79E+04	4.05E+04	4.51E+04	1.80E+04	7.19E+04
Pt-188/Ir-188	1.02E+01	2.82E+05				
Ir-190m	1.18E+01	7.85E+03				
Ir-192	7.38E+01	1.21E+03	1.21E+03	1.22E+03		
Au-195	1.86E+02					1.82E+03
Au-196	6.18E+00	2.04E+05				
Au-198	2.69E+00	9.21E+05				
Au-199	3.14E+00	9.13E+05				
Tl-202	1.22E+01	1.48E+04	1.51E+04			
Hg-203	4.66E+01	1.37E+04	1.53E+04	1.71E+04	1.05E+04	1.99E+04

*EOB 21.04.2006

4.5.3.3.1. Test of conventional methods of mercury purification for non-carrier added samples

For testing the conventional purification methods of mercury, i.e. leaching with an oxidizing acid and distillation, using samples containing a variety of non-carrier added radionuclides, sample CERN2 was divided into two parts. To the first part, a two step purification process was applied, consisting of an acid leaching and subsequent distillation. The second part was directly purified by distillation. The experimental details and the results are presented in the following sections.

The first fraction of the sample, consisting of 9.08 g mercury contaminated with radionuclides, was brought into a 20 ml PE vessel. A γ -spectrum of the sample was recorded before the purification procedure. Then, the sample was washed for three hours with 5 ml of 2 M HNO₃ under mechanical agitation. Afterwards, the two liquids were separated and γ -spectra were recorded for the individual samples. The mass of the remaining mercury was finally determined to be 7.78 g. Consequently, a 14% loss of mercury was observed after washing with 2 M HNO₃. The lost mercury is obviously dissolved in the acid. This loss can possibly be reduced by optimizing the leaching procedure, e.g. by adjusting acid concentration, temperature and contact time, but a certain loss of mercury has to be taken into account when performing such a purification process.

After the leaching procedure, the liquid metal was transferred into a 5 ml glass flask and distilled at 200°C under a pressure of about 20 mbar, using the smallest available micro-distillation device to avoid excessive losses of mercury in the distillation apparatus. The liquid metal was collected in a 5ml flask. After the distillation, the mass of the distilled mercury was determined to be 6.92 g, resulting in a mercury loss of 11%. Small mercury droplets were visible in the top part of the distillation apparatus. Finally, γ -spectra were recorded for both distilled mercury and the distillation residue remaining in the original flask. The results of this series of experiments are compiled in table 25.

After the leaching procedure, most of the less noble elements are extracted to the HNO₃-solution and are not detectable in the mercury anymore. For ¹⁸⁵Os, ¹³⁹Ce and ^{121m}Te the major part is extracted to the acid, while a small amount of these nuclides can still be found in the liquid metal. For ^{110m}Ag, the transfer to the acid is less complete, leading to an approximately equal distribution between the acid and the mercury. The ¹⁰⁶Ru/Rh couple remains in the liquid metal and is not detected in the HNO₃-solution. Gold is also not transferred to the acid solution according to the results obtained for ¹⁹⁵Au. The activity of ¹⁹⁴Au found in the HNO₃-solution arises from the reproduction from its mother, ¹⁹⁴Hg, which was partly dissolved in the acid. The behaviour of the elements should correspond to their electrochemical potential [20, 23]. All elements with a more negative potential, compared to mercury, should be dissolved in the acid. In general, this principle is obeyed very well in our experiments with non-carrier added impurities in mercury. One exception is Ru, which has a significantly lower potential [20] than mercury and hence should be dissolved. An explanation for its deviating behaviour in our experiments may be its presence in form of an exceptionally stable compound or kinetic hindrance of the dissolution process. Another exception is ^{110m}Ag. Silver has a slightly lower electrochemical potential than mercury [20] and should be extracted into the HNO₃-phase. However, ^{110m}Ag is found in both phases to approximately equal amounts. This may be a kinetic effect, since silver is dissolved in the mercury and hence its transport out of the liquid metal may be slow and controlled by diffusion, while the remaining elements except for gold are located on the surface of the mercury droplet. The electrochemical potential of Osmium is equal to that of mercury [20]. Thus it is not surprising that it is found in both phases. Finally, of the elements present as radiotracers in our sample, only gold has a higher electrochemical potential than mercury [20] and therefore remains in the liquid metal phase. In principle, it is proven here that the conventional mercury purification method of acid leaching can be transferred to mercury samples containing non-carrier added radioactive impurities. The results of the leaching procedure are illustrated in figure 30.

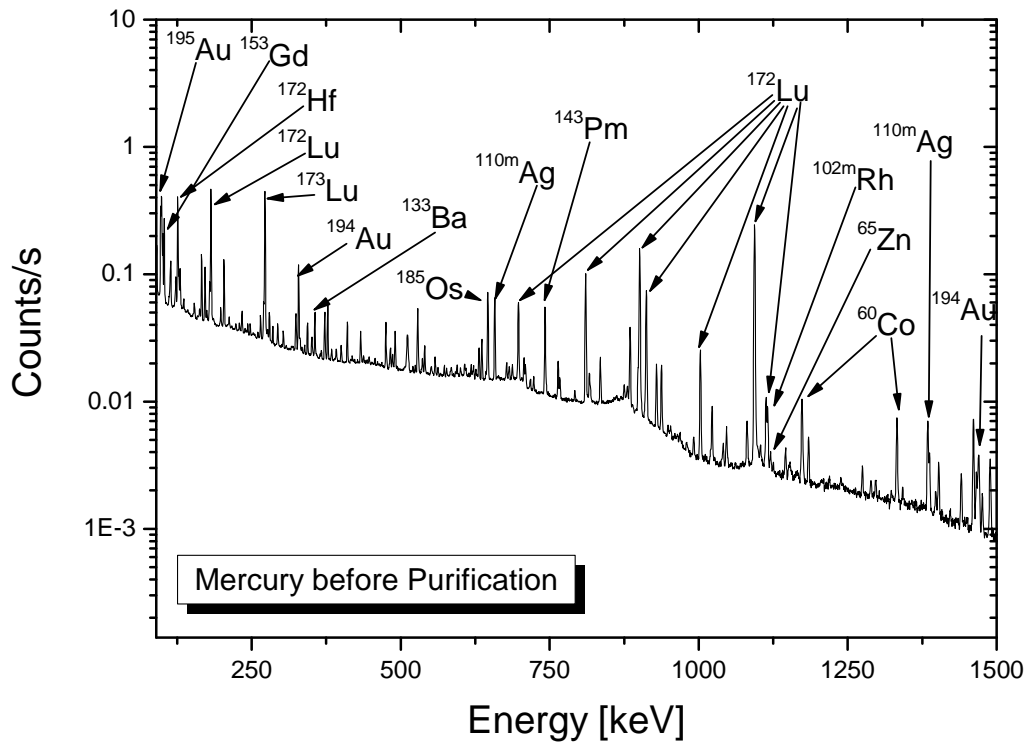
Table 25: Results of the mercury purification experiments using HNO₃-leaching and subsequent distillation. The table lists the results of γ -spectroscopic measurements on the fractions obtained by the separation procedure.

Nuclide	Half-Life [d]	Activity of mercury before purification [Bq]	Activity of mercury after HNO ₃ - leaching [Bq]	Activity of HNO ₃ - solution [Bq]	Activity of distilled mercury [Bq]	Activity of Distillation- Residue [Bq]
Mn-54	3.12E+02	1.01E+01		6.60E+00		
Co-57	2.72E+02			1.50E+00		
Co-58	7.10E+01	1.59E+01		3.50E+00		
Co-60	1.92E+03	1.11E+01		7.50E+00		
Zn-65	2.44E+02	1.35E+01		9.00E+00		
Se-75	1.20E+02	2.46E+00		3.20E+00		
Rh-102	2.07E+02	1.17E+01		2.20E+01		
Rh-102m	1.06E+03	8.30E+00		4.00E+00		
Ru-106/Rh-106	3.74E+02	8.60E+00	5.30E+00		2.40E+00	7.90E+00
Ag-110m	2.50E+02	3.39E+01	6.23E+00	1.95E+01		6.05E+00
Sn-113	1.15E+02	2.50E+00		3.00E+00		
Te-121m	1.54E+02	1.12E+00	1.80E-01	6.00E-01		3.20E-01
Ba-133	3.84E+03	1.10E+01		9.50E+00		
Ce-139	1.38E+02	1.50E+01	1.80E-01	1.24E+01		1.25E+00
Gd-146	4.83E+01	2.90E+00		3.05E+00		
Gd-153	2.40E+02	8.60E+01		8.10E+01		
Hf-172/ Lu-172	6.83E+02	2.67E+02		3.80E+02		
Lu-173	5.00E+02	3.22E+02		2.90E+02		
Hf-175	7.00E+01	2.30E+00		4.50E+00		
Re-183	7.10E+01	6.00E+00		4.00E+00		
Os-185	9.40E+01	3.90E+01	2.40E-01	4.25E+01	2.00E+00	2.00E-01
Au-194	1.90E+05	4.10E+01	5.80E+01	5.25E+00 ^a	2.83E+01 ^a	2.40E+01 ^b
Au-195	1.86E+02	2.60E+02	2.90E+02		2.90E+00	1.32E+03

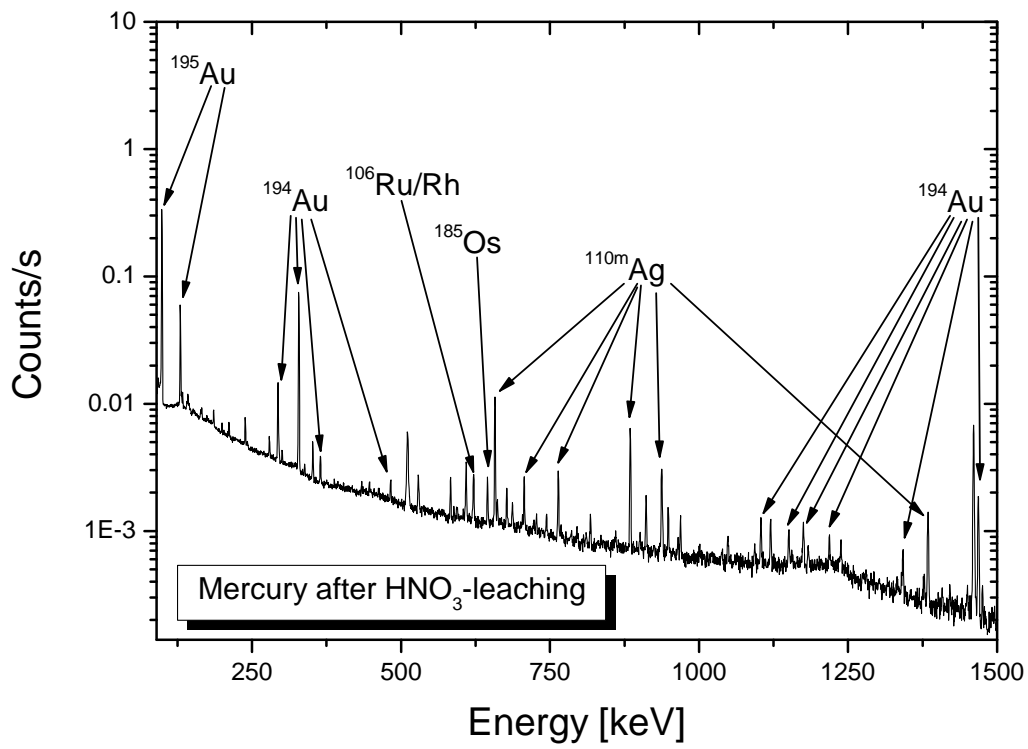
^areproduction from ¹⁹⁴Hg

^bsubstantial decay during the 4 d measurement

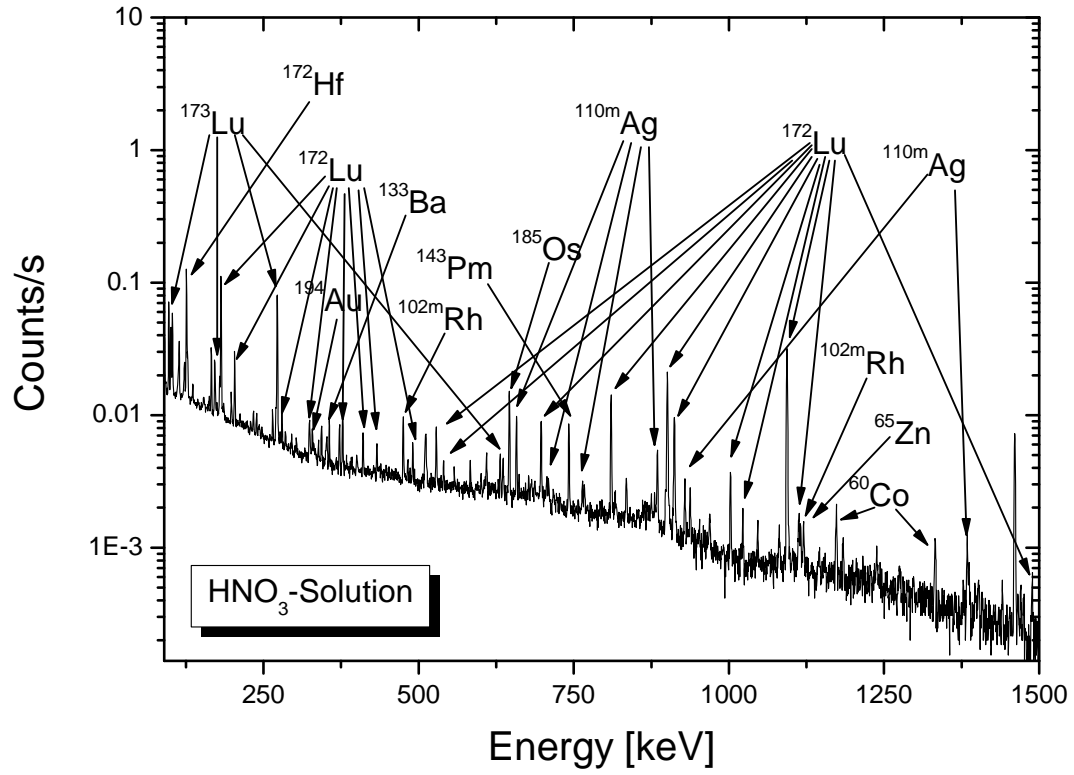
Before the distillation process, the remaining mercury contained ^{194,195}Au, ^{110m}Ag, the mother daughter couple ¹⁰⁶Ru/Rh and very small amounts of ^{121m}Te, ¹³⁹Ce and ¹⁸⁵Os. After the distillation, by far most of the activity is found in the distillation residue. The ¹⁹⁴Au-activity found in the distilled Hg arises from reproduction from ¹⁹⁴Hg. However, a very small amount of ¹⁹⁵Au was carried over with the mercury. The Te-, Ce- and Ag-nuclides remain in the residue and cannot be detected in the distilled mercury. Osmium and ruthenium partly remain in the residue, but are also in part transported in the gas phase with the mercury. It is known that these elements form volatile tetroxides when heated in air [20]. A sufficient amount of oxygen for the formation of these oxides is present in the system while performing the distillation. According to the higher stability of the osmium tetroxide, the majority of the ¹⁸⁵Os is distilled, while for ruthenium, which forms a less stable tetroxide, the majority of ¹⁰⁶Ru is detected in the distillation residue. The applicability of mercury purification by distillation on samples contaminated with non-carrier added radionuclide is demonstrated. A graphical representation of the results of distillation is shown in figure 30.



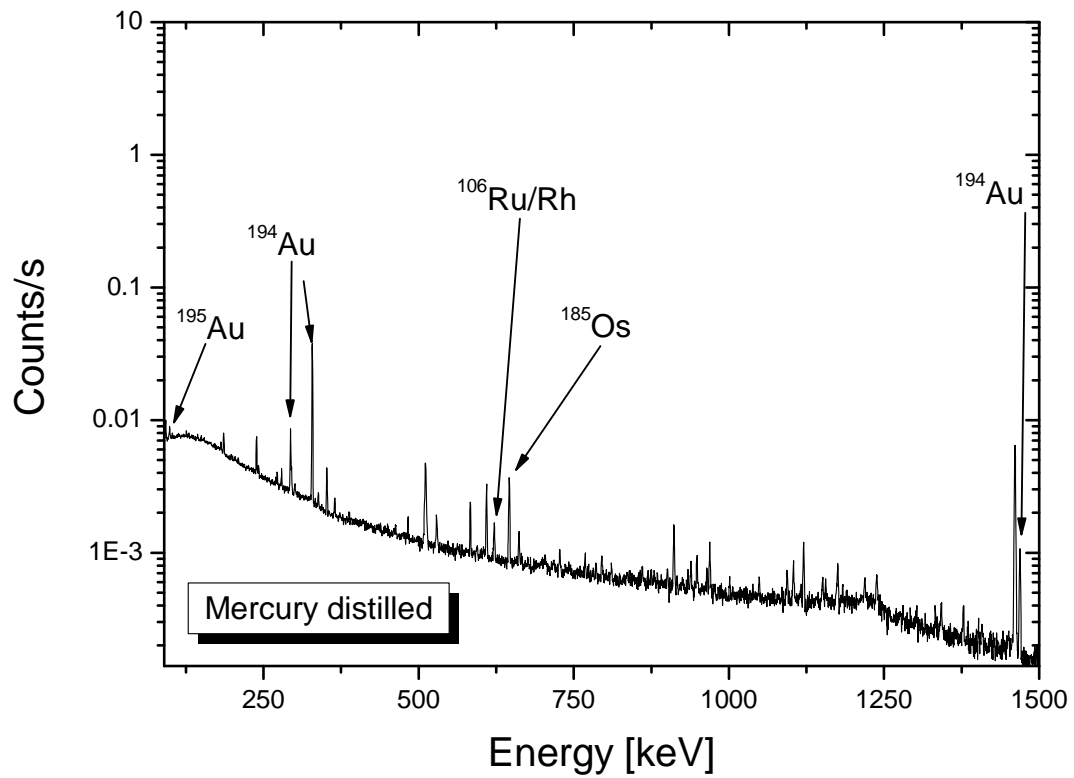
a)



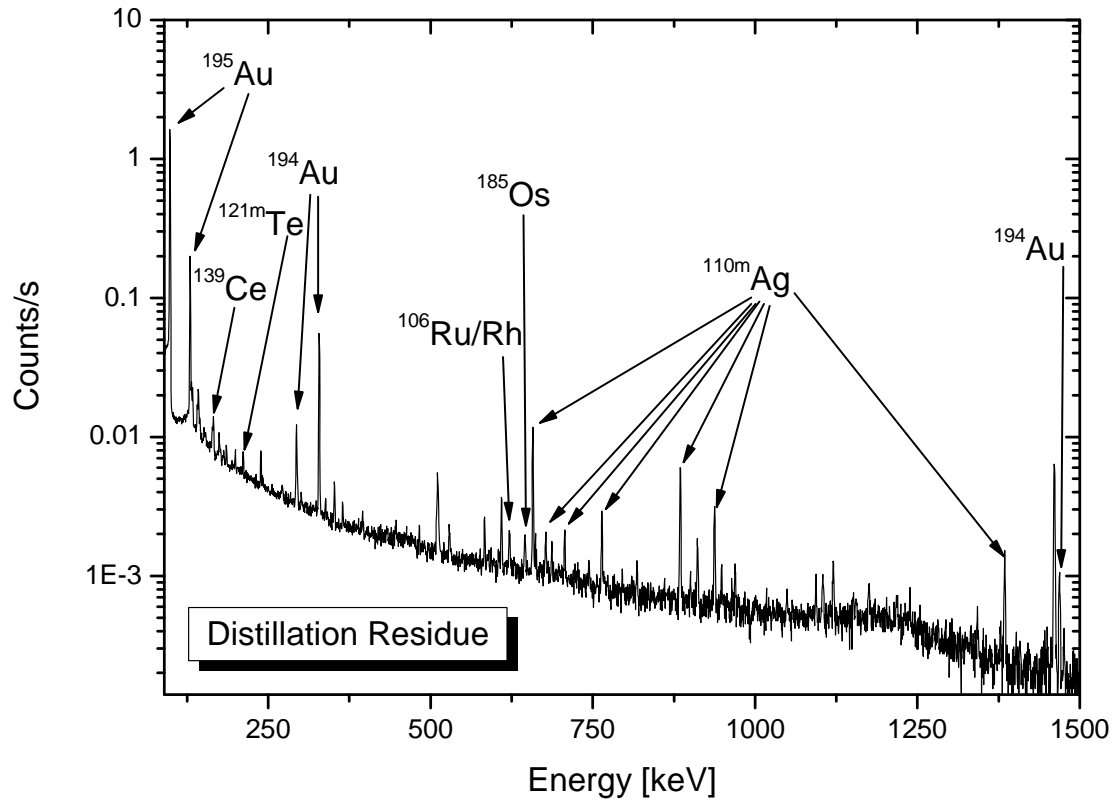
b)



c)



d)



e)

Figure 30: γ -spectra of a part of sample CERN2, illustrating the mercury purification by acid leaching and distillation. a) Mercury before purification. b) Mercury after leaching with HNO_3 (before distillation) c) HNO_3 -solution obtained from leaching process. d) Mercury after distillation. e) Distillation residue.

The second part of the mercury from sample CERN2 with a mass of 4.72 g was subjected to a one-step distillation procedure using the same conditions as above. The amount of mercury recovered was 4.12 g, corresponding to a loss of 13% of the mercury in the distillation apparatus. The results of γ -spectroscopic investigations of the fractions are compiled in table 26. Figure 31 gives a graphical representation of the results.

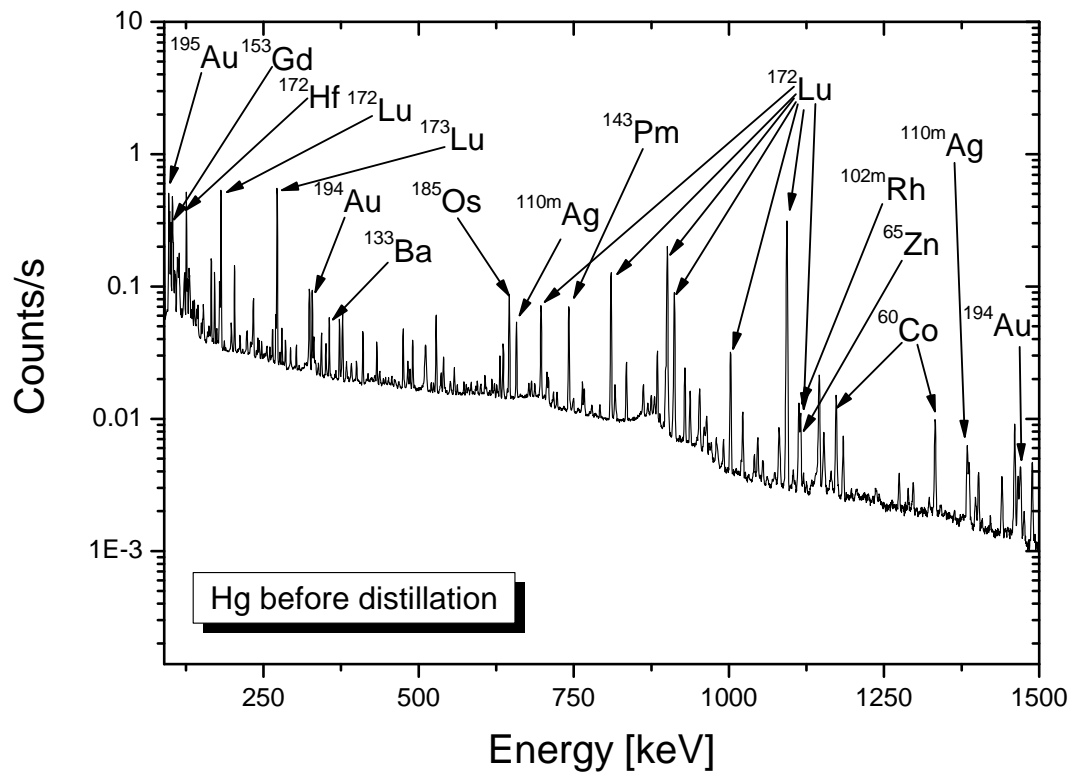
After the single-step distillation procedure, none of the nuclides except ^{106}Ru and ^{185}Os , which form volatile tetroxides, and ^{194}Au , which is reproduced from its mother ^{194}Hg , can be detected in the mercury. All other nuclides remain in the distillation residue, demonstrating that a conventional distillation procedure can be used to purify a mercury sample that contains no-carrier-added amounts of radionuclides.

Table 26: Results of the mercury purification experiments using a single-step distillation procedure. The table lists results of γ -spectroscopic measurements on the fractions obtained by the separation procedure.

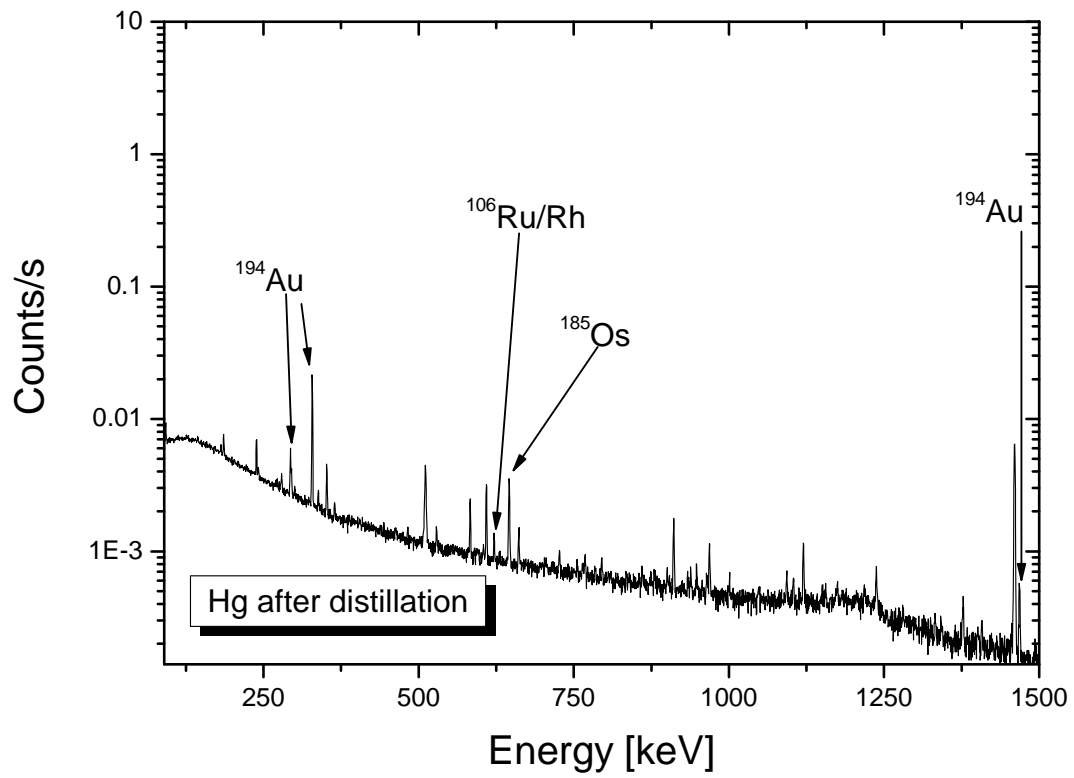
Nuclide	Half-Life [d]	Activity of Hg before distillation [Bq]	Activity of Hg after distillation [Bq]	Activity of distillation residue [Bq]
Na-22	9.50E+02	7.30E-01		6.00E-01
Mn-54	3.12E+02	4.51E+00		6.90E+00
Co-57	2.72E+02	3.60E+00		2.00E-01
Co-58	7.10E+01	4.50E+00		4.10E+00
Co-60	1.92E+03	4.03E+00		7.70E+00
Zn-65	2.44E+02	5.25E+00		9.40E+00
Rh-101	1.20E+03	1.32E+00		1.40E+00
Rh-102	2.07E+02	6.00E+00		1.98E+01
Rh-102m	1.06E+03	3.19E+00		7.98E+00
Rh-106/Ru-106	3.74E+02	2.80E+00	1.10E+00	
Ag-110m	2.50E+02	8.52E+00		1.47E+01
Sn-113	1.15E+02	1.69E+00		1.05E+01
Te-121m	1.54E+02	5.90E-01		1.12E+00
Ba-133	3.84E+03	4.75E+00		1.04E+01
Ce-139	1.38E+02	5.60E+00		1.56E+01
Pm-143	2.65E+02	3.39E+01		6.00E+01
Pm-144	3.63E+02	6.90E-01		1.40E+00
Gd-151	1.24E+02	1.30E+01		2.10E+01
Gd-153	2.40E+02	3.70E+01		1.09E+02
Tm-168	9.31E+01	1.87E+00		1.10E+00
Hf-172/Lu-172	6.83E+02	1.74E+02		3.00E+02
Lu-173	5.00E+02	1.61E+02		3.65E+02
Hf-175	7.00E+01	2.23E+00		2.60E+00
Re-183	7.10E+01	2.00E+00		2.60E+00
Os-185	9.40E+01	1.76E+01	2.04E+00	1.23E+01
Au-194	1.90E+05	2.03E+01	1.33E+01 ^a	3.40E+00 ^b
Au-195	1.86E+02	1.45E+02		2.07E+03

^areproduction from ¹⁹⁴Hg

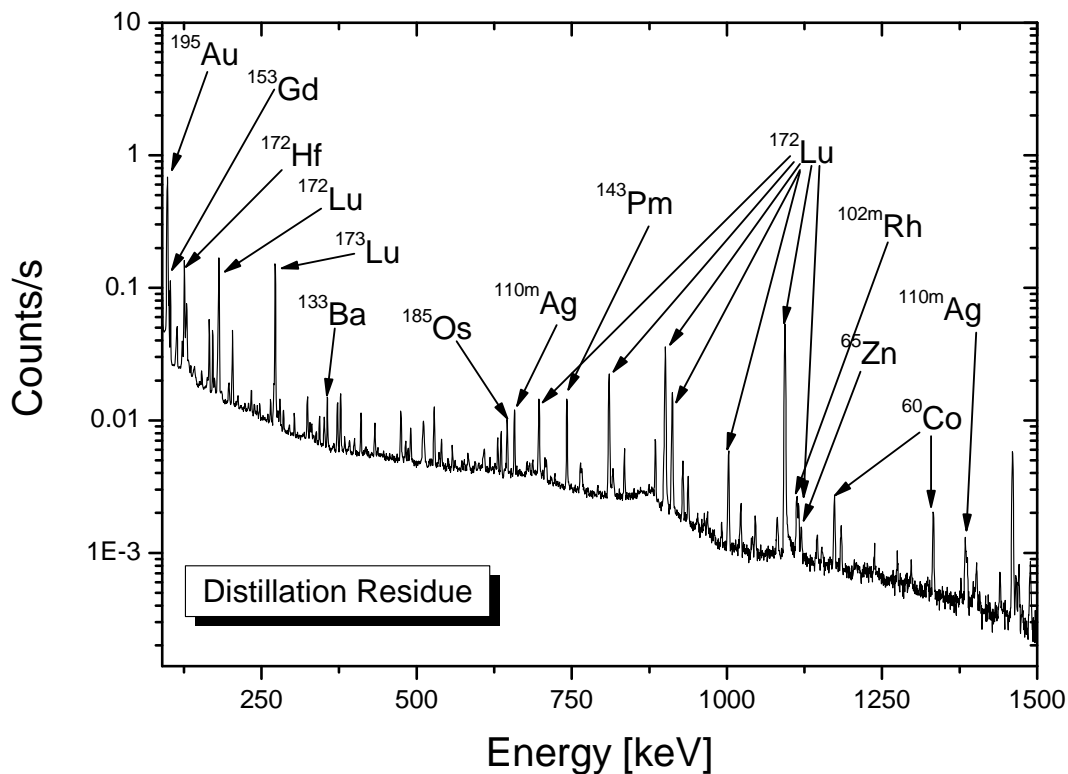
^bsubstantial decay during the 4 d measurement



a)



b)



c)

Figure 31: γ -spectra of a part of sample CERN2, illustrating the mercury purification by a single-step distillation procedure. a) Mercury before distillation. b) Mercury after distillation. c) distillation residue.

4.5.4. Electrolysis experiments

For the preparation of radiotracer-containing mercury by cathodic deposition on an Hg-Cathode a simple electrolysis apparatus was used. Teflon cylinders with a screwed-in platinum bottom were used as electrolysis vessels, which were filled with a suitable amount of mercury that covered the platinum surface at the bottom completely. The aqueous electrolyte was then poured into the vessel and a platinum net was put into the vessel from the top, acting as the counter-electrode. The electrolysis current was controlled using a DC power source and the potential was measured using a conventional multimeter. The setup is shown in figure 32.

Direct deposition of radiotracers on a mercury cathode was tried with buffered aqueous solutions of ^{22}Na , ^{160}Tb , ^{192}Ir and the aqueous solutions of complex mixtures of radionuclides obtained from leaching the CERN1 sample vessels as described in chapter 4.5.3.2.2.

During electrolysis, the activity of the aqueous phase steadily decreased with time. However, γ -spectroscopy studies of the mercury after electrolysis revealed that, similar to the samples prepared by direct proton irradiation, the radionuclides were not dissolved within the liquid metal but located on its surface.

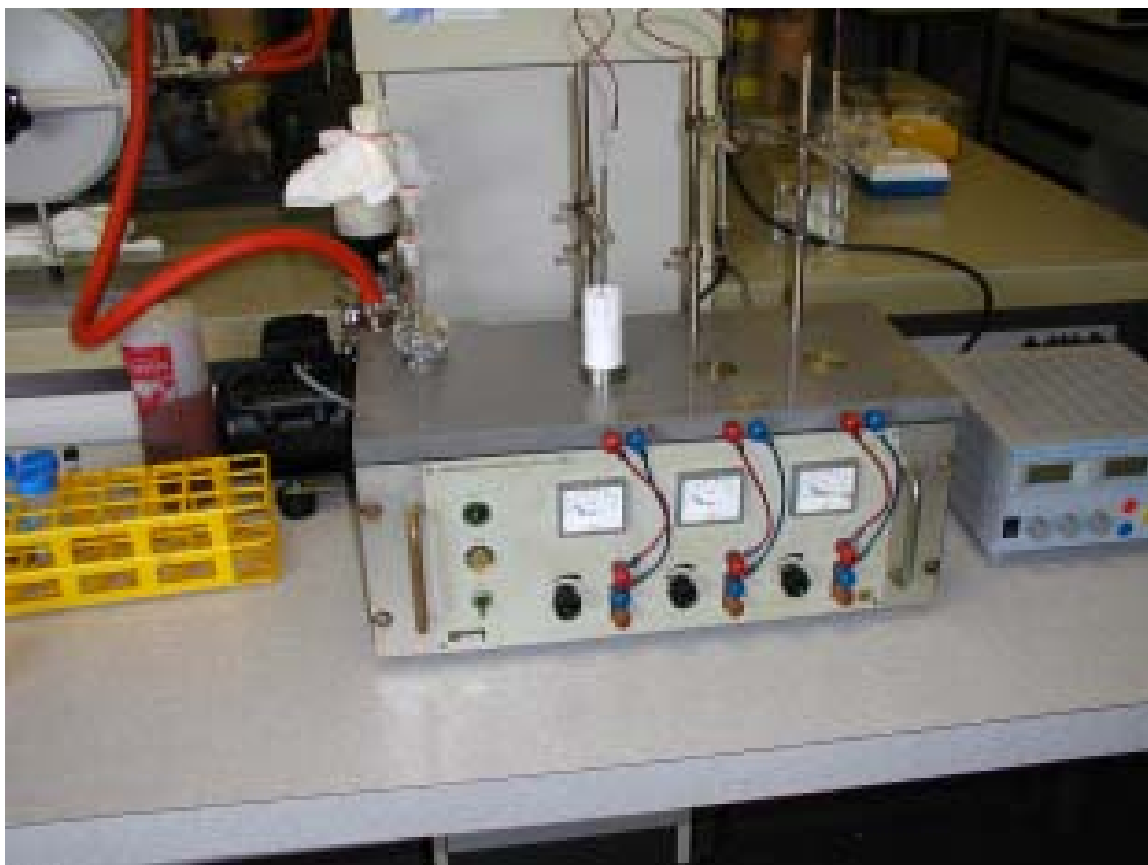


Figure 32: Setup used for electrolysis experiments

4.5.5. Phase exchange reactions with amalgams of electropositive metals

In the phase exchange reactions we tried to exploit the fact that electropositive metals dissolved in mercury exchange with less electropositive ones that are dissolved in an aqueous phase in contact with the liquid metal. Sodium and cesium amalgams containing approximately 1% of the electropositive metal were prepared by electrolysis of aqueous sodium- and cesium-solutions using the setup described above. These amalgams were exposed to aqueous solutions of ^{160}Tb , ^{192}Ir and the aqueous solution of radionuclides prepared by washing the glass vessel used to store sample CERN1. The results were similar to those of the electrolysis experiments, showing that the radionuclides are not dissolved in the liquid metal but are associated to its surface.

4.6. Discussion of the experimental results

From our results, it can be concluded that an inhomogeneous distribution of impurities induced by irradiation and also by corrosion in the loop of a spallation target system can be expected. We present results of small scale experiments on proton irradiated mercury, which show that the distribution of nuclear reaction products is far from homogeneous in these samples, but substantial amounts of these products stick to the walls of the irradiation capsules. Additionally, most nuclides adherent to the liquid metal are not homogeneously distributed in Hg as well. Highly soluble noble metals like Ag and Au are actually dissolved in the liquid metal, while the remaining elements are located at the surface of the mercury droplet.

For a liquid metal spallation target, several consequences of the effects observed in our experimental studies have to be considered. For example, shielding calculations are performed assuming a homogeneous distribution of radionuclides in the target. A deposition of radionuclides on the walls of the loop could lead to higher dose rates than expected. Such effects have been observed for example in dose measurements at JSNS. Further negative consequences for the reliable operation of a liquid metal target system may arise from plugging effects or changes in heat transfer caused by depositions.

Additionally, the radioactivity is not necessarily carried away with the liquid metal but partially remains in the loop after emptying the loop for maintenance operations. Based on the present state of knowledge, the fraction of radionuclides that remain within the loop cannot be quantified. However, from the experience gained from our investigations a substantial fraction of the radioactivity could be deposited within the loop. This deposition effect will influence the techniques that can be used for purification. In case the major part of the radioactivity, apart from the radioactive mercury itself, sticks to the wall of the loop, conventional techniques of purifying mercury will not reduce the “non-mercury” radioactivity significantly, and the liquid metal itself will not be the primary source of radionuclides. Rather, it would be necessary to study methods for cleaning the loop, if possible. It would be highly desirable and even necessary to further investigate such effects in a real Hg spallation target and loop, e.g. at SNS at ORNL or JSNS at J-PARC.

Finally, different methods for separation of nuclear reaction products from Hg have been tested on laboratory scale. The removal of solid material by high surface oxide materials and the removal of dissolved components by metal absorbers look promising. However, the absorber methods procedures are still far from a technical mature state. Conventional purification techniques for mercury such as acid leaching and distillation have been verified for the removal of non-added impurities in mercury. However, these methods will only work properly in case a substantial part of the radioactivity can be extracted from the loop while draining the mercury. These purification methods and their possible integration into a spallation target system will be discussed in chapter 5.

5. Technical and economical aspects of mercury purification in a spallation target loop

In the following section, we will discuss several methods from the point of view of their feasibility for use in a spallation target environment, their advantages and disadvantages concerning post-processing of the generated material, be it waste disposal or nuclide production. We will discuss the conventional industrial methods that are used for the purification of large amounts of mercury and their transfer to a highly radioactive environment. For the conventional distillation techniques, we will give a cost estimate based on the set-up and operational cost of conventional facilities and assumptions on the effort of transfer to a radioactive facility. We will not include here any estimations on the cost of the conditioning of the produced materials, be it for waste disposal or nuclide production. These costs strongly depend on which disposal strategy is applied or which nuclides are to be produced. Therefore, we believe that these costs are almost impossible to estimate at the present state of knowledge.

Finally we will discuss alternative methods of mercury purification in a spallation target loop, pointing out their possible advantages but also problems that remain to be solved to bring them to a technical scale application.

5.1. Cleaning of the loop

One of the most important results of our experimental studies is the fact that a substantial amount of the radioactive impurities produced in a liquid metal have the tendency to stick to the walls of the irradiation container. For the liquid metal loop of a high power liquid metal spallation target this means that a certain fraction of the radioactive components produced during operation of the target system will stick to the walls of the liquid metal loop. Similar effects have been found in the two mercury spallation sources that are currently operating [11, 12]. Concerning the fraction of the radioactive impurities that are adsorbed on the walls, no reliable quantitative statement is possible in the moment. In fact, most probably this fraction will change with operating time and increasing concentrations of the impurities. An order of magnitude of 50% sticking does not seem unrealistic. For the purification of the liquid metal, this effect is of crucial importance: In case the major part of the radioactive impurities sticks to the wall of the loop, a removal of the liquid metal from the loop and its subsequent purification in an external device does not make sense. Finally, the question of what fraction of the impurities sticks to the walls of the loop and what fraction is carried with the mercury has to be answered from the growing experience from operating liquid metal spallation target systems. When the dominant fraction of radioactive impurities is actually found to remain in the loop when draining the mercury, the only way for a removal of this radioactivity is a cleaning of the loop itself. For this purpose, two possibilities can be envisaged: Cleaning of the loop during maintenance periods when the mercury is located in the drain tank, or implementation of a second target and loop system that can be operated while the first one is cleaned using a suitable medium. As cleaning agents, oxidising and/or complexing aqueous media can be considered promising. However, the efficiency of these media has to be studied, and the question of resistivity of the loop material towards the cleaning agents has to be clarified. Both techniques would require the implementation of a system capable of flushing and drying the loop system and handling the liquids produced during the processing.

5.2. Conventional purification methods

Conventional techniques such as washing with HNO_3 and/or distillation are applied in commercial mercury purification plants. The most common way of purification is direct distillation, but there are other physical and chemical techniques such as flotation, liquid-liquid extraction (most commonly leaching with HNO_3) and electro-refining that are used to purify mercury. The standard distillation process is done at German companies such as DELA (Essen) [76], REMONDIS [77] and GMR (Gesellschaft für Metallrecycling) [78]. Bethlehem Apparatus [79], USA, the largest mercury refining company in North America, is distilling mercury four times in continuous stages under vacuum (1 - 3 mm Hg) and low temperatures [80]. They are able to produce 7N mercury quality. Their annual production rate is about 1kT/y.

GMR Leipzig [78] is also using an alternative flotation method to separate impurities less noble than mercury. Oxygen gas or air is injected into the liquid metal and the oxidized impurities are skimmed off the surface. In such a way, major contaminants as Mg, Fe, Sn, Sb, In, Pb, Bi and Zn can be removed from crude mercury. From a consideration of chemical knowledge and the experience of our laboratory experiments, this list of elements can surely be extended to all electropositive metals, such as the important lanthanides, alkaline and alkaline earth metals and many transition metals, comprising the most important spallation products. However, no noble metals can be removed in this way. Distillation is the only method suitable for this purpose, as was also demonstrated by our experiments.

A special purification unit has been developed at IPUL, Riga, where the liquid metal is pumped in counter flow through several aqueous and organic solvents [49, 81, 82], for example a sequence of aqueous sodium hydroxide solution, diluted nitric acid, ethanol and water. This technique is usually not as effective as distillation.

Concerning the scale of the plant, if we consider purification of the total amount of mercury in the EURISOL multi-MW target, we have to deal with a total amount of up to 11 tons of mercury [7]. Suitable devices for the distillation of large amounts of mercury are distributed by MRT System, Sweden [83], and major technical operation parameters can be obtained there. This company is distributing elemental mercury distillation devices for continuous fluxes from 10 kg to 2 tons per day [84]. Using the IPUL purification unit, about one ton of mercury can be processed per day using a wet technique.

Therefore, the processing of the total amount of mercury from the multi-MW target seems technically feasible within a time frame of several days to a few weeks.

There is hardly any industrial experience in the treatment of radioactive mercury. Low level radioactive waste contaminated with mercury, originating from oil refining activities, can be also reprocessed at the GMR-Leipzig company [78]. Proper shielded rotating ovens heated with thermal oil at temperatures around 300°C are used to treat aqueous contaminated sludges. This procedure is also applied to mercury contaminated soils originating from industrial plants (e.g. chlorine-alkaline electrolysis). No experience is present for highly radioactive mercury.

From the information gathered above, we conclude that in principle techniques for the large scale purification are available, but their transfer to a high power spallation target will cause much effort due to radioprotection needs caused by the radioactivity of the liquid metal, and the impurities contained therein. These radioprotection issues will lead to a vast increase of the costs.

For example, for a distillation, it has to be considered that $> 10^{16}$ Bq of mercury are transferred to the gas phase. Here, the appropriate containments, gas monitoring systems, filters and exhaust systems have to be developed, tested, installed and maintained, causing a large increase in cost.

For a wet process using e.g. HNO_3 as a leaching agent, a chemical laboratory suitable for the handling of highly active materials will have to be set-up and operated. During the operation,

a large amount of liquid waste containing large quantities of highly water soluble radioactive species is produced. While a part of these can be used for the production of useful nuclides, the majority will remain as waste. The disposal of such waste is rather problematic, since it is highly corrosive and cannot be contained in the usual cement matrix used for disposal in high concentrations. This will lead to highly increased costs.

An immense disadvantage of both distillation and aqueous techniques is the fact that mercury probably has to be transferred from the loop to an external purification plant. This does not only increase the cost, but according to our experimental results there is a high probability that only the dissolved components are transferred together with the mercury, while a major part of the impurities remain in the loop, either sticking to the walls or being deposited at certain positions, e.g. the gas- and oxide-separator or the drain tank, in this way making the purification of the transferred mercury meaningless.

The flotation method avoids both evaporation of the radioactive mercury and the formation of large amounts of solids. Furthermore, the method may be advantageous because it could be applied on-line during the operation of the target. However, the introduction of air or oxygen to the system is problematic because of the formation of explosive gas mixtures with the spallation hydrogen. We will however discuss simplified and "oxygen-free" version of this technique in the section on the alternative purification techniques.

5.3. Cost estimation

In principle, for a cost estimation of the whole purification plant, detailed knowledge of each separation step and its technical implementation is important. The detailed implementation of a suitable purification plant based on distillation or aqueous washing techniques into the EURISOL design will largely depend on the peculiarities and details of the transfer of conventional methods to a highly radioactive environment and its adaptation to the overall layout of the EURISOL facility. Furthermore, there is a complete lack of experience with the handling of large amounts of radioactive mercury. In particular, the combination of high radioactivity, chemical toxicity and volatility is special to this material and poses problems that have not been encountered before. Because of the little information available, in this report we have to confine ourselves to derive estimations for the costs of such a plant, based on the information we collected from companies that run conventional industrial purification plants. This will be combined with recommendations concerning the transfer to a radioactive environment obtained from experts in the field of radioprotection, technical radiochemistry and radioactive waste management at PSI. These estimations should give a reasonable order of magnitude for the costs that will arise from the setup and operation of a purification plant for the treatment of the complete amount of mercury within the EURISOL multi-MW target based on conventional purification techniques. It should be pointed out that very crude assumptions were taken for this estimation of the additional costs of radioprotection such as shielding, monitoring, filtering and venting systems and the costs caused by the disposal of the additional waste produced. Therefore, a relatively large error margin is possible here. A more detailed discussion of this estimation is presented below.

Finally, these assumptions led to the conclusion that a radioactive plant for mercury distillation should, in a conservative assessment, be at least 20 times as costly as a conventional one.

We will confine our estimations to those conventional purification techniques that seem feasible for an operation in a spallation target facility, i.e. distillation and washing with aqueous solutions. The flotation method with oxygen feed is ruled out by the possibility formation of explosive gas mixtures. Alternative purification methods that could be especially suitable for a spallation system are discussed in the following section. Since these methods have not been applied in an industrial scale, there is no knowledge with respect to efficiency

and economical practicability. For some of these methods, even fundamental research has to be completed before a technical up scaling can be envisaged. Therefore, we will not give any cost estimations for these methods.

For both conventional purification techniques considered, i.e. distillation and acid leaching, chemical laboratory installations allowing high levels of radioactivity are required. These have to be integrated into the hot cell of the spallation source unit. Depending on the purification method chosen, this laboratory has to be furnished with special safety equipment and installations, i.e. double enclosures, gas monitoring and mercury gas filtering systems for a distillation plant or corrosion or acid resistant systems and installations for the handling of large amounts of acid aqueous solutions in case of a wet process. Therefore, the price for devices treating high level radioactive mercury is obviously several times higher than for conventional plants. After discussion with experts, we estimate that a reasonable cost multiplier for the transfer of a conventional mercury distillation to a plant for highly radioactive mercury would lie in the range 10 to 20. For conservative cost estimation, we will use a multiplier of 20 in the following. We stress again at this point that the following estimations are not precise and give only the order of magnitude of the costs that have to be expected.

A distillation process used for separating impurities from 11 tons of radioactive mercury is favourably performed in a batch process in some 100 – 200 steps, where e.g. 100 kg batches will be processed at once [84]. A two-stage distillation should be applied [80], starting with a mercury pre-separation at low temperatures and pressure (250°C, 30 mbar) to minimize its volume, followed by a second step for the evaporation of the remaining mercury from the obtained sludge. This is done at higher temperature, i.e. around 550°C [80]. The left sludge will contain a mixture of more than 60 elements. The whole plant must be remotely controlled. The distillation vessels used in technical scale mercury purification plants are typically made from steel. In a radioactive environment, a double walled apparatus seems adequate.

Cost estimates are based on information obtained from companies that perform commercial mercury purification. The costs for a distillation of 1 ton of non-radioactive mercury range from 7000 US \$ [80] up to 10 k€ [77, 78] for a final 5N purity grade. The costs are ten times higher for a purity one order of magnitude higher. In our estimation this price would correspond to the operational costs. For the consideration of the influence of a radioactive environment in the scale of EURISOL, the cost multiplier of 20 explained above is used.

Assuming 11 tons of EURISOL mercury and a factor of 20, the total costs for a single distillation process would be around 2 M€.

A distillation system is available for a continuous distillation of up to 2 tons Hg / day for about 1M€ [84]. As the distillation procedure is planned to be a two step distillation, the small distillation system for applying high temperatures would cost around 500 k€ [76]. With the multiplier of 20, the total costs of the apparatus and its implementation into the EURISOL environment would be 30 M€. Together with the operational costs we arrive at 32 M€. These estimations are summarized in table 27.

Table 27: Preliminary cost estimation for a distillation of the complete Hg inventory of EURISOL. Due to crude simplifications, the real costs can deviate by an order of magnitude.

Distillation		
	non-radioactive	radioactive: x 20
Distillation Device		
1. step low temperature	1 M€	20 M€
2. step high temperature	0.5 M€	10 M€
total EURISOL		30 M€
Operation Costs		
distillation, 1 ton	10 k€	200 k€
total EURISOL		2 M€
TOTAL		32 M€

These estimations do not include the decommissioning costs of the plant after the shut-down of the facility and the disposal of the additional waste produced by each purification operation. These are not negligible. Since the costs for the decommissioning of 1 m³ of radioactive waste are currently about 100 kFr, i.e. 70 k€.

A wet process would probably be a little less expensive regarding the costs of installation and operation, but produces a large amount of liquid waste that is difficult and expensive to dispose. Depending on the frequency that is chosen for the purification procedure, this can lead to exorbitant costs.

5.4. Alternative cleaning methods

Alternative methods for cleaning the mercury such as filtering of the liquid metal, skimming of free surfaces, sedimentation, precipitation of materials on cold surfaces and introduction of dedicated absorbers for certain elements or groups of elements into the liquid metal loop can be applied already during the operation of the system and thus are advantageous because they avoid the installation of large scale external facilities dedicated to mercury purification. In this way, they probably generate much less cost compared to the conventional techniques. Furthermore, by facilitating an in-situ cleaning of the liquid metal within the loop, they may severely reduce the risk of operational problems arising from chemical processes during the operational period. Additionally, by applying several different methods in parallel, a pre-separation of the products can be achieved already during operation, if desired. However, the efficiency of these methods so far cannot be estimated. Some of these methods are standard purification techniques used in the chemical and metallurgical industries, but of course they have never been used in a spallation target system. Therefore, their implementation into a radioactive environment will need engineering design studies, and their efficiency in a spallation loop has to be demonstrated. For other methods, even basic research has to be performed before an up scaling to a technical scale could be undertaken. Because of the large uncertainties, we will abstain from cost estimation for these methods, but given the high costs of mercury purification using conventional methods they should be considered as alternatives. As a disadvantage of these methods, the introduction of online-separation devices will complicate the design of the target and loop system. More removable parts have to be built-in, leading to additional connections that will increase the risks of leaking. Furthermore, devices

for the remote handling of the online-separation devices have to be installed, possibly increasing the cost of the complete system. We will discuss the alternative methods in some more detail below.

5.4.1. Filtering

Filtering of liquid metals has proved to work in our simple laboratory experiments. It has also been investigated in Obninsk, Russia with respect to its technical application in liquid lead-bismuth alloy cooled reactors. While the method seems to work for in principle, obviously still effort is put into more R&D work [85]. There is also experience in filtering sodium in LMFBR [86]. However, the spectrum of impurities present in a spallation loop differs from that of a reactor loop. Therefore, the optimum choice of filter material may be different. Furthermore, because of the lack of experience with the operation of spallation loops it is unknown how much solid material, formed by various reactions of construction materials and nuclear reaction products, is formed and can be removed by filtration. Therefore, an optimal dimensioning is not possible. The number of unknown parameters makes cost estimation difficult. When more knowledge is gained from the experiences of operating liquid metal spallation sources such as SNS and JSNS, probably a reasonable estimate can be made together with the filtration experiences from other institutions such as IPPE, Obninsk.

5.4.2. Flotation and skimming

During the operation of the spallation loop it is highly probable that solid insoluble material with a lower density than mercury will accumulate in the top part of the loop and finally reach the liquid-gas interface. This material can be mechanically separated by skimming of the free surface. The development of a skimming device that is suitable for the incorporation into a spallation target loop is in principle only a question of engineering design, but important parameters like the amount of material that has to be skimmed off are unknown and will only become known with the operation of similar facilities or dedicated test facilities. A simpler alternative makes use of the gas- and oxide separator device described in [7]. The solid materials discussed here will probably accumulate in this device that is primarily designed to facilitate the separation of gaseous nuclear reaction products, but secondarily will also serve to collect those materials that tend to float on mercury. The efficiency of the device is difficult to predict, as is the amount of collected material. However, the device will definitely contribute to the separation of compounds of nuclear reaction and corrosion products from the flowing metal. If desired, with a suitable design this device could be implemented in the loop as an interchangeable device. As such, it could be retrieved periodically and exchanged with a new one, while the old device could serve as a source of radionuclides that can be obtained from the loop without complex chemical procedures. However, such a construction would require additional connections, increasing the risk of leaks.

A second place where material will be floating on the surface is the drain tank. Here, the material that has a lower density than mercury but is suspended and carried with the liquid metal during operation will separate on the mercury surface during shut-down periods. Here, a skimming device could be implemented if it is desired to separate this material for further use as source of valuable nuclides. From an operational point of view the separation of this material is not necessary because it will remain in the drain tank up to the end of operation of the facility without disturbing the operation. Here, it does not cause problems except for increasing the dose rate. It is pointed out here again that the material floating on the surface may give rise to higher dose rates compared to those calculated under the assumption of homogeneous dissolution in the liquid metal.

5.4.3. Precipitation on cold surfaces

A part of the impurities produced both by nuclear reactions and by corrosion effects which are dissolved in the liquid metal will have the tendency to precipitate on cold surfaces because of their decreasing solubility with decreasing temperature. Such precipitates may occur in various chemical states (elements or compounds) and morphologies (platings, polycrystalline, growth of large crystals etc.). In a loop without any special precautions with respect to these phenomena, such precipitations will most likely occur on the cold surfaces of the heat exchanger, where the temperature of the liquid metal drops significantly [87]. Such precipitations may severely disturb the flow of the liquid metal as well as change the heat transfer characteristics. In order to mitigate these effects, the heat exchanger should be designed in such a way that it can be easily maintained, i.e. by cleaning or exchanging the appropriate parts, during service periods. The material retrieved in this way contains radionuclides in a solid form. It can be used for radionuclide separations or be disposed as desired.

5.4.4. Sedimentation

The fraction of insoluble material that has a higher density than mercury will tend to sediment. A prominent location for this process will be the drain tank where the liquid metal will be stored during shut-down and maintenance periods. During these periods, the material with higher density compared to mercury will have time to settle and form a solid precipitation that will be deposited on the ground of the drain tank. From the operational point of view, similar to the material floating on top of the mercury, the separation of this material is not necessary because it will remain in the drain tank up to the end of operation of the facility without disturbing the operation, except for a possible increase of the dose rate. A retrieval of this material for nuclide production would involve the complete emptying and cleaning of the drain tank. This would necessitate additional installations such as a second tank to hold the remaining mercury and an installation for washing out the impurities.

5.4.5. Absorbers

As our experiments show, the adsorption of impurities on surfaces of metals and oxides could prove very useful for the removal of impurities dissolved in the liquid metal. The method has several advantages. It can be implemented as an interchangeable element within the loop, thus facilitating an online purification and easy retrieval of the adsorbed material. The appropriate choice of absorber materials can facilitate a selective removal of desired elements. The implementation of such a device will not cause much additional effort with respect to radiation safety. Furthermore, it will be the only way to remove soluble noble elements such as gold, apart from distillation. However, the technique is still in an early stage of development. Basic research is still necessary to find optimised preparation methods for the absorber surfaces and new absorber materials for the removal of various desired elements have to be studied. The method also has to be validated with respect to its removal rate and efficiency before it can be transferred to the technical scale.

5.5. An alternative concept for mercury purification in a spallation target loop

In principle, the impurities present in a spallation loop can be divided in different classes according to their physical and chemical state. First of all, one has to deal with gaseous nuclear reaction products, predominantly hydrogen, helium and the heavier noble gases. Non volatile elements can be divided in two classes: highly and less soluble. Many elements produced by nuclear reactions will undergo chemical reactions and form solid compounds, e.g. oxides or intermetallic phases, which have a low solubility in Hg. These compounds, according to their density, will tend to either float on top of the liquid metal, to sediment or to form particles dispersed in the liquid metal.

Gaseous impurities will diffuse out of the liquid metal fairly fast at the liquid-gas interface. In the present design [7], this interface is located in the gas- and oxide separator. If necessary, the heavier, condensable noble gases could be retained in cooled zeolite traps. For hydrogen, catalytic conversion to water and gettering of the latter on a drying agent has been discussed for MEGAPIE, but this approach was not realized and model studies are still pending.

For removal of dissolved components, metal absorbers could be useful, as demonstrated by the results presented above.

Since the solubility usually decreases with decreasing temperature, less soluble species can be precipitated at cold surfaces. For this purpose, the heat exchanger should be designed in such a way that the removal of precipitated material is possible.

For solid phases floating on top of the liquid gas interface, we suggest a skimming procedure, while the gas- and oxide-separator of the current design may prove sufficient for a separation of these materials. Particles carried with the liquid metal stream could be filtered out using filters, as demonstrated above for the separation of Lu and Hf from mercury. These filters probably would have to be placed in a bypass to avoid serious consequences for the flow conditions in the main loop.

Should phases with higher density than mercury be formed, they will generally tend to accumulate in the lower part of the loop. In case there are unfavourable flow conditions, these materials might accumulate at certain positions and influence the operation of the loop. In case they do not sediment but are carried by mercury, they will be either trapped by the suggested filter systems or finally sediment in the drain tank where Hg is stored during maintenance.

In general, to efficiently avoid a contamination of the loop we recommend integrating the suggested devices as close as possible to the region where the impurities are produced, i.e. directly behind the spallation target. Of course, these procedures are still not in a mature state and need much more basic research, technical development of the separation devices and finally integration in the target loop

Other possible methods for purifying mercury include distillation or treatment of Hg with oxidizing agents (e.g. oxygen or aqueous HNO_3) and removal of the oxidized impurities. Distillation would have to be carried out offline. From radioprotection considerations the evaporation of many tons of highly radioactive Hg seems undesirable. Furthermore, even if it is technically feasible, it remains questionable if this technique would be economically favourable. Oxidation with oxygen and skimming of the oxidation products could be feasible online. However, this procedure might induce larger amounts of solid oxide material that could harm the operation of the loop. The extraction of impurities using aqueous oxidizing agents will produce a large amount of liquid radioactive waste. This has disadvantages for disposal, but may be advantageous if one wants to extract carrier-free radionuclides for certain applications. The online methods using cold traps, filters, skimming and metal absorbers on the other hand do not produce additional liquid radioactivity. Furthermore, due to their chemical diversity, they will provide a certain chemical selectivity that could be very

helpful if some of the extracted radionuclides are to be exploited for medical or technical applications.

Offline methods in general have a disadvantage: They will not protect the loop from contamination. Application of the online methods suggested above, such as cold trap, skimming of expansion tank, metal absorbers and filters opens the possibility to continuously reduce the radioactive inventory and thus contamination of the loop during operation. However, the efficiency of the suggested devices cannot be judged at the present state. Another advantage of online methods is that they could provide access to nuclides with shorter half-life that may be of medical and technological interest. For this purpose, suitable remote handling techniques to replace the separation devices and appropriate chemical separation procedures would have to be developed.

6. Feasibility of the extraction of medically interesting radionuclides in EURISOL

6.1. Basic assumptions and boundary conditions

For comparability and simplicity, the basic conditions used here are taken from Appendix C of the EURISOL study [13]. The parameters of the target and its operation are as follows:

Volume of Hg 500 l; beam current 5mA; proton energy 1GeV

5 l/h extraction

Operation time 40 years; 250 d per year

The production rates used in the following are taken from chapter 8 of the cited study [13].

6.2. Main yields of chemical and physical processes

Adsorption of activity on the walls of the loop: ~ 50% (worst case)

Extraction yield (Multi-element extraction from mercury): 50%

Chemical separation of the desired radionuclide: 50%

Mass separation 5%

Labelling 30%

6.3. Possible processes

Online extraction:

The mercury flows through a by-pass (~ 1% of the total mercury per hour, i.e. 5 l/h [13]) which contains an adsorption device sensitive for the interesting radionuclides. This adsorption material has to be removed frequently for the subsequent chemical processes. The frequency of removal depends on the half-life of the desired nuclide. Selective absorbers for the desired nuclides are still to be developed. Alternatively, the methods discussed in chapter 5 can be used for the retrieval of radionuclides, e.g. from filters or the gas- and oxide separator.

Off-line extraction:

The facility is driven for a certain period, dependent on the half-life of the desired radionuclide. Then, the mercury is pumped into a separation device, or adsorption materials are put into the flow. The activity can be extracted from the entire mercury volume. In the case of very high wall absorption, the mercury can be pumped into a storage tank or a second loop and the activity is then eluted from the loop walls, e.g. by leaching with diluted HNO₃. The favourable strategy here depends on the fraction of radionuclides adsorbed to the wall.

6.4. Desired radionuclides and special problems

Radionuclides used for medical treatment require very high radiochemical purity. This means, that for directly produced radionuclides a mass separation is mandatory, because spallation reactions generate a wide spectrum of masses for every element. For generator nuclides the situation may be better, because in the treatment, the daughter nuclide only is used. The latter is separated from the mother by chemical procedures. The conditions have to be checked in detail for every desired radionuclide.

The only medically interesting α -emitter which can be produced in spallation reactions with mercury is ^{149}Tb - a radionuclide which counts as a very prospective candidate for cancer treatment [88]. It has a half-life of 4.1 h, which makes it necessary to consider also the losses due to the decay during processing. The following processing times are estimated for the different processes:

- Removing from adsorber, separation from other radionuclides
Lanthanide fractionation, final purification 6h
- Mass separation 4h
- Labelling 3h
- Quality control, shipping 3h

6.5. Calculations

The expected amounts of activity ready for application were calculated based on the assumptions described above. The production rates for the different nuclides given in tables 28 and 29 were taken from [13]. The remaining parameters listed in the tables are explained in the following paragraph:

extr. rate: extraction rate calculated from the value of 5 l/h mercury purification, together with the assumption of 50% wall absorption.

tcycle: Frequency of the extraction cycle. For online mode: collecting time, for offline mode: time for one cycle of target operation before purification. For all radionuclides, cycle times of 3 -5 half-lives are assumed.

chem.-sep: Efficiency of chemical separation including extraction yield, chemical separation, mass separation and labelling.

t-chem: time for the entire process from extraction till application of the pharmacon

Table 28: Online production

Nuclide	$T_{1/2}$	Prod.rate [1/s]	extr.rate [1/s]	tcycle [d]	chem-sep	t_chem [s]	final activity [GBq]	Availability
Tb-149	4.1 h	3.50E+13	1.39E-06	0.5	0.00375	57600	0.154	twice per day
Lu-177	6.7 d	2.40E+12	1.39E-06	30	0.00375	57600	4.14	monthly
Ir-192	74 d	1.00E+14	1.39E-06	250	0.00375	57600	310	per year
Sn-117m	13.6 d	7.00E+12	1.39E-06	60	0.00375	57600	16.6	every second month
Sr-89	50.5 d	2.10E+13	1.39E-06	250	0.00375	57600	67.5	per year
W-178	22 d	3.10E+14	1.39E-06	90	0.00375	57600	835	every third month
W-188	69 d	2.70E+12	1.39E-06	250	0.00375	57600	8.46	per year
Ge-68	288 d	3.60E+12	1.39E-06	750	0.00375	57600	11.0	every third year
Ti-44	60 y	7.00E+10	1.39E-06	2500	0.00375	57600	0.02	every 10th year

For offline-production, the extraction rate is replaced by the parameter extraction time (t-extr.). This is caused by the fact, that the activity is accumulated within the mercury. 10 h are proposed for extracting 50% of the activity off-line by adsorption, extraction or distillation processes.

Table 29: Off-line production

Nuclide	T _{1/2}	Prod.rate [1/s]	tcycle [d]	chem-sep	t _{extr.} [s]	t _{chem} [s]	final activity [GBq]	Availability
Tb-149	4.1 h	3.50E+13	0.5	0.00375	36000	57600	1.41	twice per day
Lu-177	6.7 d	2.40E+12	30	0.00375	36000	57600	7.68	monthly
Ir-192	74 d	1.00E+14	250	0.00375	36000	57600	336	per year
Sn-117m	13.6 d	7.00E+12	60	0.00375	36000	57600	23.7	every second month
Sr-89	50.5 d	2.10E+13	250	0.00375	36000	57600	75.1	per year
W-178	22 d	3.10E+14	90	0.00375	36000	57600	1060	every third month
W-188	69 d	2.70E+12	250	0.00375	36000	57600	9.20	per year
Ge-68	288 d	3.60E+12	750	0.00375	36000	57600	11.3	every third year
Ti-44	60 y	7.00E+10	2500	0.00375	36000	57600	0.02	every 10th year

6.6. Discussion

From the Tables 28 and 29 it can be seen, that off-line technology is in all cases more effective than on-line extraction. This is of special importance, when one considers the probably very high wall adsorption of radionuclides, which leads to a drastically drop of the available activity within the liquid metal. In case the major part of the activity is retained in the loop when draining, leaching the loop with HNO₃ could be the most prospective method for radionuclide production. The on-line variant could become favourable with the development of efficient extraction devices that can be operated within the loop.

It does not seem to be economical to extract long-lived and short-lived radionuclides simultaneously, because the useful cycle times for the radionuclides are very different. Therefore, a decision has to be made which types of nuclides are to be finally produced.

Some of the assumptions are quite conservative. Especially the time from extraction to a ready pharmacon is with 16 h quite long and in some cases, may be lowered. If the time can be lowered to a half (8 h), which seems to be very fast, considering the number of processes to be performed, at best a factor of 4 in the final activity for the example of ¹⁴⁹Tb can be gained.

A factor of around 50 can probably be gained for radionuclides, which serve as generator systems, and hence a mass separation is not mandatory. This could be the case for the generator nuclides listed in the tables above, leading to the values of activity production per years given in brackets: ⁴⁴Ti (100 MBq per year), ¹⁸⁸W (460 GBq per year), ¹⁷⁸W (212 TBq per year) and ⁶⁸Ge (188 GBq per year). The possibilities of process optimisations must be checked for every single nuclide.

6.7. Examples for prices

^{149}Tb : costs chemotherapy: 50 000 EURO, 10% for nuclide production

→ required activity per patient ~1 GBq (estimated)

→ 10-15 000 EURO per day → 2.5 Mio EURO per year

(There is presently no experience concerning the activity of this nuclide required for a therapy)

^{44}Ti : 185MBq 2 Mio EURO [89]

→ 1 Mio EURO per year

$^{188}\text{W}/^{188}\text{Re}$ Generator: 18.5 GBq 10 000 EURO → 250 000 EURO per year

6.8. Conclusions

With the therapeutically interesting short-lived ^{149}Tb , about 2.5 Mio EURO can be earned each year. For the other nuclides discussed here the revenues are even less. These estimations focus only on the possible income that can be generated by selling these nuclides. The costs for performing the entire separation are not estimated here. The chemical separation will require the development and up scaling of dedicated separation procedures for every desired element. In the practical application, this procedure has to be performed periodically, e.g. twice a day for ^{149}Tb , leading to additional operational costs. Because of the complexity of the source of the nuclides, no reasonable numerical estimation can be given here for the chemical processes. The following step of mass separation is also very cost intensive. Finally, the production of the pharmacon and its supply to the patient are not to be neglected. These considerations make a profitable nuclide production questionable.

If one focuses to long-lived and/or generator nuclides, maybe the outcome is higher, because separation has to be performed only around once a month and a wide variety of products can be gained.

7. Summary and conclusion

The goal of this study was to acquire knowledge to enable a decision concerning the feasibility and usefulness of the purification of the mercury of the multi-MW liquid spallation target of a future EURISOL facility. An answer to these questions requires the consideration of radioprotection, operational and commercial aspects.

From the radioprotection point of view, one has to differentiate between a reduction of the radionuclide inventory before final storage, achieved by a purification of mercury, and a reduction of the radioactivity during operation.

Concerning the final storage, a purification of the mercury will not yield substantial advantages because a large amount of the radioactivity is associated with mercury, including the long-lived isotope ^{194}Hg . This radioactivity can not be separated by chemical means.

In relation to the reduction of radioactivity during the operation period of the target, first experiences from operating mercury spallation sources indicate that dose rate reduction could be beneficial for maintenance operations. Here, increased dose rates are caused by the separation of radioactive material from the liquid metal and its deposition within the loop. To avoid this, two strategies can be applied: The radioactive material is removed continuously from the flowing liquid metal before it can deposit, using on-line techniques such as filtering, flotation or specifically developed absorber systems. A second method for avoiding increased dose rates during maintenance involves chemical cleaning of the loop after draining the mercury and before start of the maintenance operations. The optimization of these methods and their integration into the spallation target system still require additional R&D efforts. Conventional methods for cleaning the liquid metal, e.g. by distillation or acid leaching, are not helpful for this purpose.

Conventional operational problems (i.e. those not related to radioactivity) that could be caused by deposition of impurity materials include plugging and heat transfer problems. With the growing experience gained from liquid metal spallation target facilities that started to operate recently, a better understanding of the importance of such phenomena will become available. In case it turns out that it is useful or even necessary to remove impurities from the loop to avoid operational problems, the most useful purification strategy is similar to the methods described for the reduction of radioactivity during operation, using on-line techniques or periodic cleaning of the loop. The conventional techniques are again not useful here.

With respect to nuclide production, based on the current knowledge the income generated does not seem to compensate the costs generated by the purification process when conventional purification methods such as distillation are used. The situation can be substantially improved in case alternative purification techniques can be applied that lead to the separation of radionuclides without generating extensive additional costs. Additional economic benefit could arise from the development of chemical processing methods that are optimized for the production of several valuable nuclides from the material separated from the spallation system in one multi-stage processing cycle.

8. References

- [1] <http://isolde.web.cern.ch/ISOLDE/>
- [2] http://legacyweb.triumf.ca/isac/isac_home.html
- [3] www.ganil.fr/spinal
- [4] <http://www.ganil.fr/research/developments/spiral2/>
- [5] <http://www.eurisol.org>
- [6] Rapp, B., David, J.C., Blideanu, V., Doré, D., Ridikas, D., Thiollière, N.: *EURISOL DS/Task5/TN-06-09*. CEA Report (2006)
- [7] Samec, K.: *TM-34-09-01*. PSI Report (2009)
- [8] http://neutrons.ornl.gov/facilities/facilities_sns.shtml
- [9] Bayer-AG: *Purification of mercury*, United States Patent No. **3895938**, 1975.
- [10] O'Grady, A.: *Process for purifying mercury*, United States Patent No. **3639118**, 1972.
- [11] Gallmeier, F. X., SNS, Oak Ridge, TN, personal communication.
- [12] Kasugai, Y., JSNS, Tokai, Japan, personal communication.
- [13] *The EURISOL Report, Appendix C: Target and Ion Sources*. Ganil Report (2003)
- [14] Henry, R.: *Isotope Generators - Present Status and Future Development*. Journal of Nuclear Biology and Medicine **15 (4)** 105 (1972)
- [15] Knapp, F. F., Mirzadeh, S., Beets, A. L., Du, M.: *Production of therapeutic radioisotopes in the ORNL High Flux Isotope Reactor (HFIR) for applications in nuclear medicine, oncology and interventional cardiology*. Journal of Radioanalytical and Nuclear Chemistry **263 (2)** 503 (2005)
- [16] Landolt-Börnstein: *Zahlenwerte und Funktionen aus Physik, Chemie, Astronomie, Geophysik und Technik*, **Vol. 2, Part 2a**; Springer Verlag, Berlin 1960.
- [17] Wilkinson, M. C.: *Surface properties of mercury*. Chemical Reviews **72 (6)** 575 (1972)
- [18] Kasama, A., Iida, T., Morita, Z.: *Viscosity of Mercury-Based Dilute Binary-Alloys*. Transactions of the Japan Institute of Metals **16 (8)** 527 (1975)
- [19] Olsen, D. A., Bunde, R. E., Johnson, R. E., Johnson, D. C.: *Viscosity and Density of Mercury-Thallium Amalgams*. Journal of Chemical and Engineering Data **15 (1)** 190 (1970)

- [20] Holleman-Wiberg: *Lehrbuch der Anorganischen Chemie*, De Gruyter, Berlin 1985.
- [21] Fitzer, E., Fritz, W., Rohm, M., Eldeen, A. Z.: *Material Transfer in Liquid-Liquid Systems by Interfacial Convection*. *Chemie Ingenieur Technik* **39** (5-6) 319 (1967)
- [22] Guminski, C.: *Metals in Mercury*, IUPAC Solubility Data Series, **25**; Pergamon Press, Oxford 1985.
- [23] Jangg, G., Bach, H.: *Quecksilber und Amalgammetallurgie*, in G. Eger: *Handbuch der Elektrochemie*, Akademische Verlagsgesellschaft Geest & Portig KG 1961.
- [24] Dewet, J. F., Haul, R. A. W.: *Zur Löslichkeit Einiger Übergangsmetalle in Quecksilber*. *Zeitschrift Für Anorganische Und Allgemeine Chemie* **277** (1-2) 96 (1954)
- [25] Lihl, F., Demel, A.: *Herstellung Von Eisen-Zink-Legierungen Aus Amalgamen*. *Zeitschrift Fur Metallkunde* **43** (9) 307 (1952)
- [26] Barlow, M., Planting, P. J.: *Heterometallic Phenomena in Platinum-Mercury System*. *Zeitschrift Fur Metallkunde* **60** (4) 292 (1969)
- [27] Russell, A. S.: *Intermetallic compounds in mercury*. *Nature* **125** 89 (1930)
- [28] Russell, A. S., Cazalet, P. V. F., Irvin, N. M.: *Intermetallic compounds formed in mercury. Part I. The tin-copper system*. *Journal of the Chemical Society* 841 (1932)
- [29] Russell, A. S., Cazalet, P. V. F., Irvin, N. M.: *Intermetallic compounds formed in mercury. Part II. The zinc-copper system*. *Journal of the Chemical Society* 852 (1932)
- [30] Russell, A. S., Kennedy, T. R., Howitt, J., Lyons, H. A. M.: *Intermetallic compounds formed in mercury Part IV Summary of work on the Sn-Cu, Sn-Fe, Zn-Cu, Zn-Fe, Cd-Cu, Hg-Cu, Mn-Cu, and Zn-Mn systems*. *Journal of the Chemical Society* 2340 (1932)
- [31] Russell, A. S., Lyons, H. A. M.: *Intermetallic compounds formed in mercury. Part III. The Zn-Fe system and part of the Sn-Fe system*. *Journal of the Chemical Society* 857 (1932)
- [32] Jangg, G.: *Quecksilber als Hilfsstoff in der Elektrometallurgie*. *Chemie Ingenieur Technik-CIT* **36** (6) (1964)
- [33] Luborsky, F. E.: *The Kinetics of Growth of Spherical Iron Crystallites in Mercury*. *Journal of Physical Chemistry* **61** (10) 1336 (1957)
- [34] Barlow, M., Planting, P. J.: *Wetting of Metal Surfaces by Liquid Mercury*. *Zeitschrift Fur Metallkunde* **60** (10) 817 (1969)
- [35] Nejedlik, J. F., Vargo, E. J.: *Material Resistance to Mercury Corrosion*. *Electrochemical Technology* **3** (9-10) 250 (1965)
- [36] Fleitman, A. H., Romano, A. J., Klamut, C. J.: *Corrosion of Carbon Steel by High-Temperature Liquid Mercury*. *Journal of the Electrochemical Society* **110** (9) 964 (1963)

- [37] Wang, J. Y. N.: *Effect of Metallic Additives on Mercury Corrosion of Titanium*. Corrosion **21** (2) 57 (1965)
- [38] Deboer, F. R., Boom, R., Mattens, W. C. M., Miedema, A. R., Niessen, A. K.: *Cohesion in Metals*, Transition Metal Alloys, North-Holland, Amsterdam 1988.
- [39] Herbst, J. F.: *On extending Miedema's model to predict hydrogen content in binary and ternary hydrides*. Journal of Alloys and Compounds **337** 99 (2002)
- [40] Li, Chonghe, Chin, Yen Li, Wu, Ping: *Correlation between bulk modulus of ternary intermetallic compounds and atomic properties of their constituent elements*. Intermetallics **12** (1) 103 (2004)
- [41] Zhang, B. W., Jesser, W. A.: *Formation energy of ternary alloy systems calculated by an extended Miedema model*. Physica B **315** (1-3) 123 (2002)
- [42] Gordon, C. L., Wichers, E.: *Purification of Mercury and Its Physical Properties*. Annals of the New York Academy of Sciences **65** (5) 369 (1957)
- [43] Soucek, J.: *Cistení a kontrola čistoty rtuti*. Chemicke Listy **58** (10) 1203 (1964)
- [44] Bochkarev, E. P.: *Process for purifying low-melting metals from impurities*, United States Patent No. **4298380**, 1981.
- [45] Dotson, Ronald L., Simmons, Billy H.: *Process for purifying mercury*, United States Patent No. **3437476**, 1969.
- [46] Stearns, Walter V.: *Process for purifying mercury*, United States Patent No. **2032602**, 1936.
- [47] Young, Patrick J.: *Process for cleaning contaminated mercury*, United States Patent No. **3113018**, 1963.
- [48] Carlson, W. A., Borchardt, L. F.: *A complete mercury-purification system*. Industrial and Engineering Chemistry-Analytical Edition **10** 0094 (1938)
- [49] Foliforov, V. M. : *Mercury purification plant*, United States Patent No. **3596893**, 1971.
- [50] Bauer, G. S.: *ESS - Liquid Metal Target Studies, 2nd Status Report*. Report **ESS 95-33-T**, (1995)
- [51] Herrera-Martinez, A., CERN, Geneva, Switzerland, personal communication.
- [52] Miedema, A. R.: *Electronegativity Parameter for Transition-Metals - Heat of Formation and Charge-Transfer in Alloys*. Journal of the Less-Common Metals **32** (1) 117 (1973)
- [53] Neuhausen, J., Eichler, B.: *Extension of Miedema's Macroscopic Atom Model to the Elements of Group 16 (O, S, Se, Te, Po)*. Paul Scherrer Institute Report **03-13**, (2003)

- [54] Barin, I., Platzki, G.: *Thermochemical Data of Pure Substances: La-Zr*, Wiley-VCH Verlag GmbH, 1995.
- [55] Bowersox, D. F.: *Thermodynamics of Solution of Ti, V, Cr, Fe, and Co in Liquid Tin*. Metallurgical Transactions **2** (3) 916 (1971)
- [56] Evans, H. E., Watson, W. R.: *Novel Method for Determination of Solubilities of Solutes in Liquid Metals - Solubility of Antimony in Sodium from 190-550 Degrees C*. Journal of Nuclear Materials **40** (2) 195 (1971)
- [57] Kleppa, O. J., Weil, J. A.: *The Solubility of Copper in Liquid Lead Below 950°*. Journal of the American Chemical Society **73** (10) 4848 (1951)
- [58] Walker, R. A., Pratt, J. N.: *Solubilities of Bismuth and Tellurium in Liquid Sodium*. Journal of Nuclear Materials **34** (2) 165 (1970)
- [59] Guminski, C.: *Solubility of Metals in Liquid Low-Melting Metals*. Zeitschrift Fur Metallkunde **81** (2) 105 (1990)
- [60] Hultgren, R., Desai, P. D., Hawkins, D. T., Gleiser, M., Kelley, K. K.: *Selected values of the thermodynamic properties of binary alloys*, American Society for Metals, Metals Park, Ohio 1973.
- [61] Landolt-Boernstein, O.: *Madelung (Ed.), Group IV, Macroscopic and Technical Properties of Matter, New Series, vol. 5, Phase Equilibria, Crystallographic and Thermodynamic Data of Binary Alloys, Subvol. b*, Springer-Verlag, Berlin, 1991.
- [62] Shrier, L.L., Jarmin, R.A., Burstein, G. T.: *Corrosion, Metal/Environment Reactions, Chapter 2.9*, Butterworth-Heinemann Ltd, Oxford 1994.
- [63] Eichler, B., Neuhausen, J.: *Zur Wirkung chemischer Prozesse und Produkte im Pb-Bi-Target*. Paul Scherrer Institute Report **AN-18-03-01**, (2003)
- [64] <http://megapie.web.psi.ch>
- [65] Lieser, K. H.: *Nuclear and Radiochemistry: Fundamentals and Applications*, VCH, Weinheim 1997.
- [66] Majer, V., Kupsch, H.: *Grundlagen der Kernchemie*, Hanser, 1982.
- [67] Hohn, A., Eichler, R., Eichler, B.: *Investigations on adsorption and transport behaviour of carrier-free silver, gold and platinum in quartz columns under vacuum conditions*. Radiochimica Acta **92** (8) 513 (2004)
- [68] Guiragossian, Z. G., Martoyan, G. A., Demirchyan, M., Intsheyan, S. G., Nalbandyan, G. G., Tonikyan, S. G.: *New hydrometallurgical method to partition & separate actinides & fission fragments for ADS*. AREV Scientific-Industrial Institute Report (2005)
- [69] Smith, G. M., Bennett, H. C.: *The electrolytic preparation of the amalgams of the alkali and alkali-earth metals*. Journal of the American Chemical Society **31** 799 (1909)

- [70] Marsh, J. K.: *Rare-earth metal amalgams Part I The reaction between sodium amalgam and rare-earth acetate and chloride solutions*. Journal of the Chemical Society 398 (1942)
- [71] Marsh, J. K.: *Rare-earth metal amalgams Part II The separation of neodymium, samarium, and gadolinium*. Journal of the Chemical Society 523 (1942)
- [72] Marsh, J. K.: *Rare-earth metal amalgams part III The separation of ytterbium from its neighbours*. Journal of the Chemical Society 8 (1943)
- [73] Marsh, J. K.: *Rare-earth metal amalgams. Part IV The isolation of europium*. Journal of the Chemical Society 531 (1943)
- [74] Samhoun, K., David, F.: *Radiocoulometry - Its Application to Kinetics and Mechanism Studies of Amalgamation Reactions of Ba²⁺, Ca²⁺, Eu³⁺, Sm³⁺ and Cf³⁺ in Aqueous-Media*. Journal of Electroanalytical Chemistry **106 (1-2)** 161 (1980)
- [75] Zhuikov, Boris L., Kokhanyuk, Vladimir M., Konyakhin, Nikolay A., Vincent, John: *Target irradiation facility and targetry development at 160 MeV proton beam of Moscow linac*. Nuclear Instruments and Methods in Physics Research Section A: Accelerators, Spectrometers, Detectors and Associated Equipment **438 (1)** 173 (1999)
- [76] www.delagmbh.de
- [77] www.remondis-industrie-service.de
- [78] www.gmr-leipzig.de
- [79] www.bethlehemapparatus.com
- [80] Lawrence, B., Bethlehem Apparatus, Hellertown, PA, personal communication.
- [81] Foliforov, V. M.: *Device for mixing conductive liquids with reagents*, United States Patent No. **3614080**, 1971.
- [82] Foliforov, V. M., G., Sirotenko V.: *Multipurpose use of MHD devices in the production of mercury*. Magnitnaya Gidrodinamika **1** 140 (1972)
- [83] www.mrtsystem.com
- [84] Nielson, M., MRT-System, Lumavägen, Sweden, personal communication.
- [85] Чабань, А.Ю., Асхадуллин, Р.Ш., Мартынов, П.Н., Лаврова, О.В.: *Очистка теплоносителей Pb – Bi, Pb и Ga методом сорбции*, HLM Conference, Obninsk, Russia 2003.
- [86] Баринков, О.П., Коновалов, В.И., Ю.В.Привалов, Ю.Е.Штында: *Очистка натриевого теплоносителя от радионуклидов и примесей компактными ловушками*, HLM Conference, Obninsk, Russia 2003.

- [87] Latge, C.: *Cold trap for eliminating impurities from a polluted liquid metal*, United States Patent No. **4693088**, 1987.
- [88] Beyer, G. J., Miederer, M., Vranjes-duric, S., Comor, J. J., Kunzi, G., Hartley, O., Senekowitsch-Schmidtke, R., Soloviev, D., Buchegger, F.: *Targeted alpha therapy in vivo: direct evidence for single cancer cell kill using Tb-149-rituximab*. *European Journal of Nuclear Medicine and Molecular Imaging* **31 (4)** 547 (2004)
- [89] Rösch, F., Johannes Gutenberg Universität, Mainz, Germany, personal communication.

Appendix A

Enthalpies of formation for solid compounds $A_{0.5}B_{0.5}$ [kJ/mol] calculated using the Miedema model. Miedema parameters from [53] were used for the chalcogens. Parameters for the remaining elements were taken from [38].

Z	A	1	3	4	5	6	7	8	11	12	13	14	15	16
B	Element	H	Li	Be	B	C	N	O	Na	Mg	Al	Si	P	S
1	H	0	16	53	-	-	-	-	30	26	39	-	-	-
3	Li	16	0	-7	7	5	-28	-188	5	0	-5	-2	-54	-106
4	Be	53	-7	0	15	68	99	-65	24	-5	0	20	3	2
5	B	-	7	15	0	-	-	-	40	9	15	-	-	-
6	C	-	5	68	-	0	-	-	32	14	39	-	-	-
7	N	-	-28	99	-	-	0	-	-21	-24	28	-	-	-
8	O	-	-188	-65	--	-	-	0	-185	-192	-139	-	-	-
11	Na	30	5	24	40	32	-21	-185	0	16	19	25	-29	-102
12	Mg	26	0	-5	9	14	-24	-192	16	0	-3	3	-49	-96
13	Al	39	-5	0	15	39	28	-139	19	-3	0	14	-23	-48
14	Si	-	-2	20	-	-	-	--	25	3	14	0	-	-
15	P	-	-54	3	-	-	-	-	-29	-49	-23	-	0	-
16	S	-	-106	2	-	-	-	--	-102	-96	-48	-	-	0
19	K	32	16	34	49	38	-17	-182	2	29	31	34	-24	-112
20	Ca	-10	-1	-21	-19	-27	-101	-274	2	-10	-35	-38	-115	-190
21	Sc	-39	18	-54	-73	-80	-158	-340	51	-8	-68	-79	-171	-217
22	Ti	-38	50	-48	-84	-77	-129	-313	98	20	-61	-74	-162	-179
23	V	-18	55	-27	-61	-42	-66	-247	104	31	-40	-47	-117	-119
24	Cr	-3	50	-14	-45	-12	-15	-194	100	32	-30	-30	-85	-78
25	Mn	-12	28	-18	-46	-19	-33	-210	69	12	-43	-41	-95	-101
26	Fe	4	37	-8	-38	5	14	-164	88	23	-32	-26	-70	-59
27	Co	5	12	-9	-34	16	30	-144	57	1	-43	-31	-63	-54
28	Ni	5	1	-9	-33	21	39	-135	45	-8	-48	-33	-61	-52
29	Cu	27	-7	-2	2	30	22	-146	22	-7	-16	-1	-35	-54
30	Zn	39	-10	5	21	44	34	-131	9	-5	1	16	-18	-48
31	Ga	40	-12	7	23	44	26	-140	8	-6	1	16	-19	-53
32	Ge	-	-19	25	-	-	-	-	-1	-9	9	-	-	--
33	As	-	-40	10	-	-	-	-	-20	-31	-9	-	-	--
34	Se	-	-79	14	-	-	-	--	-72	-66	-25	-	-	-
37	Rb	32	18	35	50	40	-15	-179	3	32	33	34	-24	-114

Z	A	1	3	4	5	6	7	8	11	12	13	14	15	16
B	Element	H	Li	Be	B	C	N	O	Na	Mg	Al	Si	P	S
38	Sr	-8	0	-15	-12	-21	-97	-270	-3	-7	-31	-33	-111	-195
39	Y	-35	11	-47	-64	-72	-158	-340	41	-12	-69	-78	-171	-228
40	Zr	-54	41	-65	-102	-103	-179	-366	86	5	-83	-101	-203	-235
41	Nb	-27	74	-39	-79	-66	-106	-293	134	44	-44	-60	-147	-150
42	Mo	-2	70	-13	-49	-18	-26	-208	134	50	-24	-29	-93	-80
43	Tc	9	12	-7	-35	22	42	-135	67	1	-46	-33	-62	-45
44	Ru	11	7	-7	-34	26	52	-124	62	-3	-48	-32	-58	-38
45	Rh	6	-19	-12	-35	27	48	-126	27	-28	-63	-44	-63	-51
46	Pd	2	-55	-14	-33	32	51	-121	-21	-62	-84	-57	-66	-64
47	Ag	35	-23	9	21	43	23	-144	1	-16	-9	10	-21	-54
48	Cd	42	-19	16	34	52	33	-131	-4	-9	5	22	-9	-50
49	In	42	-18	22	41	54	27	-138	-8	-6	10	27	-7	-56
50	Sn	45	-25	21	40	59	39	-126	-12	-13	6	26	-2	-46
51	Sb	49	-39	26	47	73	61	-102	-29	-24	3	29	12	-30
52	Te	51	-56	24	48	84	84	-78	-49	-41	-6	26	20	-16
55	Cs	32	21	35	49	41	-10	-174	4	34	34	35	-23	-114
56	Ba	-12	0	-14	-14	-23	-101	-273	-5	-8	-35	-38	-117	-204
57	La	-34	8	-42	-59	-68	-155	-337	36	-13	-68	-76	-169	-232
58	Ce	-34	9	-44	-61	-69	-156	-338	38	-13	-68	-77	-170	-231
59	Pr	-35	10	-45	-63	-71	-157	-339	39	-12	-69	-77	-171	-230
60	Nd	-35	10	-45	-63	-71	-157	-339	39	-12	-69	-77	-170	-229
61	Pm	-36	12	-48	-66	-74	-160	-342	42	-12	-70	-79	-173	-231
62	Sm	-35	11	-47	-64	-72	-158	-340	41	-12	-69	-78	-171	-229
63	Eull	-8	-1	-17	-15	-23	-98	-270	0	-8	-32	-34	-111	-190
63	Eulll	13	59	1	-16	-24	-110	-292	89	36	-21	-30	-123	-181
64	Gd	-35	11	-47	-64	-72	-158	-340	41	-12	-69	-78	-171	-228
65	Tb	-36	13	-48	-66	-74	-158	-341	43	-11	-69	-79	-172	-228
66	Dy	-36	12	-48	-66	-74	-158	-340	43	-11	-69	-78	-171	-227
67	Ho	-35	12	-47	-65	-72	-156	-337	42	-11	-68	-77	-169	-225
68	Er	-36	14	-49	-67	-75	-159	-341	45	-11	-69	-79	-172	-226
69	Tm	-36	14	-49	-67	-75	-158	-340	44	-10	-69	-79	-171	-225
70	Ybll	-19	-1	-24	-24	-44	-138	-313	3	-11	-40	-45	-131	-215
70	Yblll	-5	32	-22	-36	-33	-96	-275	59	11	-39	-45	-127	-175

Z	A	1	3	4	5	6	7	8	11	12	13	14	15	16
B	Element	H	Li	Be	B	C	N	O	Na	Mg	Al	Si	P	S
71	Lu	-37	15	-52	-70	-78	-161	-343	47	-10	-70	-80	-174	-226
72	Hf	-47	44	-58	-94	-92	-160	-347	92	11	-75	-91	-188	-215
73	Ta	-27	71	-39	-78	-65	-105	-291	130	41	-46	-60	-147	-151
74	W	4	71	-8	-44	-8	-8	-191	139	53	-20	-23	-82	-64
75	Re	12	41	-3	-35	17	35	-144	104	28	-29	-22	-61	-39
76	Os	12	15	-6	-34	26	52	-124	73	4	-43	-29	-57	-34
77	Ir	10	-12	-11	-36	32	61	-113	40	-22	-60	-40	-58	-37
78	Pt	7	-44	-17	-39	34	64	-109	-1	-54	-82	-56	-64	-48
79	Au	35	-51	-1	8	59	69	-98	-21	-48	-37	-8	-17	-26
80	Hg	46	-28	22	41	63	48	-116	-16	-14	6	27	2	-40
81	Tl	46	-22	33	52	65	38	-125	-16	-5	16	36	6	-48
82	Pb	49	-30	35	56	73	52	-110	-26	-12	15	38	15	-37
83	Bi	50	-33	35	57	75	55	-107	-28	-14	14	38	17	-35
84	Po	56	-51	46	70	96	87	-72	-54	-28	13	46	40	-12
89	Ac	-29	2	-28	-41	-53	-140	-319	18	-13	-58	-63	-149	-220
90	Th	-43	19	-62	-82	-90	-181	-366	55	-10	-78	-91	-195	-249
91	Pa	-57	23	-62	-95	-99	-183	-369	58	-9	-89	-103	-203	-249
92	U	-41	41	-49	-84	-79	-139	-325	88	11	-69	-82	-172	-196
93	Np	-37	41	-44	-79	-71	-125	-310	87	13	-64	-75	-160	-182
94	Pu	-47	34	-54	-87	-86	-152	-337	75	4	-74	-87	-178	-209
95	Am	-38	18	-54	-74	-81	-163	-346	53	-8	-71	-82	-177	-227
96	Cm	-38	19	-55	-75	-81	-164	-348	55	-8	-71	-83	-179	-228
97	Bk	-38	17	-53	-72	-80	-161	-343	50	-9	-70	-81	-174	-224
98	CfII	-17	0	-25	-27	-45	-139	-315	8	-11	-42	-47	-136	-218
98	CfIII	-26	14	-46	-60	-56	-118	-296	42	-8	-60	-67	-148	-193
99	Es	-18	-1	-26	-27	-46	-142	-318	5	-12	-43	-48	-138	-223
100	Fm	-19	0	-28	-30	-48	-140	-317	9	-12	-44	-49	-136	-216
101	Md	-18	0	-25	-27	-45	-137	-313	8	-11	-41	-47	-133	-213
102	No	-14	1	-23	-25	-40	-128	-304	14	-9	-40	-44	-128	-202
103	Lr	-38	19	-54	-74	-80	-163	-346	54	-8	-71	-82	-178	-227

Z	A	19	20	21	22	23	24	25	26	27	28	29	30	31
B	Element	K	Ca	Sc	Ti	V	Cr	Mn	Fe	Co	Ni	Cu	Zn	Ga
1	H	32	-10	-38	-38	-18	-3	-12	4	5	5	27	39	40
3	Li	16	-1	18	50	55	50	28	37	12	1	-7	-10	-12
4	Be	34	-21	-54	-48	-27	-14	-18	-8	-9	-9	-2	5	7
5	B	49	-19	-73	-84	-61	-45	-46	-38	-34	-33	2	21	23
6	C	38	-27	-80	-77	-42	-12	-19	5	16	21	30	44	44
7	N	-17	-101	-158	-128	-66	-15	-33	14	30	39	22	34	26
8	O	-182	-274	-340	-313	-247	-194	-210	-164	-144	-135	-146	-130	-140
11	Na	2	2	51	98	104	100	69	88	58	45	22	9	8
12	Mg	29	-10	-8	20	31	32	12	23	1	-8	-7	-5	-6
13	Al	31	-35	-68	-61	-40	-30	-43	-32	-43	-48	-16	1	1
14	Si	34	-38	-79	-74	-47	-30	-41	-26	-31	-33	-1	16	16
15	P	-24	-115	-171	-162	-117	-85	-95	-70	-63	-61	-35	-17	-19
16	S	-112	-190	-217	-179	-119	-78	-101	-59	-54	-52	-54	-48	-53
19	K	0	17	82	128	127	119	86	105	72	59	33	18	17
20	Ca	17	0	26	61	62	53	27	36	3	-10	-18	-36	-47
21	Sc	82	26	0	11	11	1	-12	-17	-43	-56	-36	-52	-68
22	Ti	128	61	11	0	-3	-11	-12	-25	-42	-52	-13	-34	-51
23	V	127	62	11	-3	0	-3	-1	-11	-21	-27	7	-13	-28
24	Cr	119	53	1	-11	-3	0	3	-2	-7	-10	19	-3	-16
25	Mn	86	27	-12	-12	-1	3	0	0	-8	-12	6	-20	-34
26	Fe	105	36	-17	-25	-11	-2	0	0	-1	-2	19	-5	-18
27	Co	72	3	-43	-42	-21	-7	-8	-1	0	0	10	-18	-31
28	Ni	59	-10	-56	-52	-27	-10	-12	-2	0	0	5	-23	-37
29	Cu	33	-18	-36	-13	7	19	6	19	10	5	0	-9	-12
30	Zn	18	-36	-52	-34	-13	-3	-20	-5	-18	-23	-9	0	0
31	Ga	17	-47	-68	-51	-28	-16	-34	-18	-31	-37	-12	0	0
32	Ge	3	-61	-85	-65	-33	-13	-32	-9	-17	-20	-2	8	8
33	As	-16	-95	-129	-110	-72	-48	-65	-40	-45	-47	-23	-9	-9
34	Se	-80	-156	-177	-140	-87	-51	-75	-37	-39	-38	-33	-27	-30
37	Rb	0	22	89	132	129	120	87	106	72	59	35	19	18
38	Sr	11	1	36	75	74	64	36	47	13	-1	-12	-33	-45
39	Y	73	16	1	22	24	16	-2	-2	-31	-44	-32	-54	-73

Z	A	19	20	21	22	23	24	25	26	27	28	29	30	31
B	Element	K	Ca	Sc	Ti	V	Cr	Mn	Fe	Co	Ni	Cu	Zn	Ga
40	Zr	123	54	6	0	-6	-18	-23	-36	-60	-72	-34	-56	-77
41	Nb	169	91	27	3	-2	-11	-6	-23	-37	-45	4	-14	-30
42	Mo	162	81	16	-5	0	1	7	-3	-7	-11	28	6	-7
43	Tc	87	2	-57	-58	-32	-13	-12	-5	0	1	12	-17	-32
44	Ru	81	-5	-64	-65	-37	-17	-16	-7	-1	1	10	-19	-33
45	Rh	42	-40	-90	-78	-44	-20	-24	-8	-3	-1	-4	-36	-53
46	Pd	-12	-91	-127	-97	-53	-22	-34	-6	-2	0	-20	-59	-79
47	Ag	9	-41	-42	-2	25	40	19	42	28	23	3	-7	-10
48	Cd	1	-52	-55	-24	2	15	-8	14	-2	-8	-2	1	1
49	In	-5	-59	-58	-25	2	14	-11	12	-5	-12	-1	4	4
50	Sn	-9	-73	-81	-51	-19	-3	-27	-2	-17	-22	-6	2	1
51	Sb	-32	-99	-106	-70	-31	-9	-35	-4	-16	-20	-8	-1	-2
52	Te	-57	-129	-140	-101	-54	-25	-51	-16	-24	-26	-16	-10	-11
55	Cs	0	27	95	134	129	119	87	105	72	59	35	20	19
56	Ba	8	1	40	79	77	67	38	49	15	0	-11	-37	-50
57	La	67	12	3	28	31	24	4	6	-24	-38	-29	-54	-73
58	Ce	69	13	2	26	29	21	2	4	-26	-40	-30	-54	-73
59	Pr	71	15	2	24	26	18	0	1	-28	-42	-31	-54	-73
60	Nd	71	15	2	24	26	18	0	1	-28	-42	-31	-54	-73
61	Pm	74	17	1	22	23	15	-3	-3	-32	-46	-33	-55	-74
62	Sm	73	16	1	22	24	16	-2	-2	-31	-44	-32	-54	-73
63	Eull	14	0	31	68	68	59	32	42	9	-5	-14	-34	-45
63	Eulll	121	64	49	70	72	64	46	46	17	4	16	-6	-25
64	Gd	73	16	1	22	24	16	-2	-2	-31	-44	-32	-54	-73
65	Tb	75	18	1	20	22	13	-4	-4	-33	-46	-33	-54	-72
66	Dy	75	18	1	20	22	13	-4	-4	-33	-46	-32	-54	-72
67	Ho	74	17	1	21	23	14	-3	-3	-31	-45	-32	-53	-71
68	Er	77	19	1	18	20	11	-5	-7	-35	-48	-33	-54	-72
69	Tm	76	19	1	18	20	11	-5	-7	-35	-48	-33	-54	-71
70	Ybll	20	0	28	69	70	60	30	40	4	-12	-20	-40	-53
70	Yblll	86	37	21	36	37	30	16	15	-10	-21	-8	-26	-41
71	Lu	79	21	0	16	17	8	-8	-10	-38	-52	-35	-54	-72
72	Hf	128	57	8	0	-3	-14	-18	-30	-51	-62	-25	-48	-68

Z	A	19	20	21	22	23	24	25	26	27	28	29	30	31
B	Element	K	Ca	Sc	Ti	V	Cr	Mn	Fe	Co	Ni	Cu	Zn	Ga
73	Ta	163	86	24	2	-2	-10	-6	-22	-36	-44	3	-16	-32
74	W	168	82	14	-9	-1	1	9	0	-2	-5	33	11	-1
75	Re	129	40	-25	-38	-19	-6	-1	0	3	3	27	1	-12
76	Os	94	6	-57	-61	-35	-16	-13	-6	0	2	15	-13	-28
77	Ir	57	-32	-91	-86	-51	-27	-27	-13	-5	-2	0	-31	-47
78	Pt	12	-78	-131	-111	-68	-36	-42	-19	-11	-7	-18	-53	-73
79	Au	-13	-88	-110	-71	-29	0	-17	12	11	11	-13	-27	-34
80	Hg	-15	-68	-65	-27	3	19	-5	21	7	1	0	1	1
81	Tl	-18	-66	-54	-13	16	30	2	30	11	4	8	9	8
82	Pb	-31	-83	-73	-30	4	23	-7	25	8	2	6	7	7
83	Bi	-34	-91	-83	-41	-5	15	-14	18	2	-4	3	6	6
84	Po	-70	-123	-106	-53	-7	20	-13	27	14	10	6	4	4
89	Ac	41	1	12	48	53	47	21	30	-2	-16	-19	-49	-67
90	Th	93	29	0	11	8	-3	-17	-23	-52	-66	-43	-60	-79
91	Pa	90	31	0	7	5	-5	-17	-24	-50	-63	-38	-66	-89
92	U	120	51	5	1	0	-7	-12	-22	-41	-51	-18	-42	-62
93	Np	116	50	5	0	1	-5	-9	-18	-36	-45	-14	-38	-57
94	Pu	104	43	3	2	1	-7	-14	-23	-44	-55	-25	-49	-69
95	Am	87	26	0	13	12	3	-11	-16	-43	-56	-36	-54	-71
96	Cm	91	27	0	12	11	1	-12	-17	-44	-57	-36	-54	-72
97	Bk	83	24	0	13	13	4	-11	-14	-42	-55	-35	-53	-71
98	CfII	29	0	23	63	65	56	27	37	1	-15	-21	-41	-54
98	CfIII	70	20	0	12	12	4	-8	-11	-35	-46	-30	-46	-61
99	Es	26	0	26	67	67	58	28	38	1	-14	-22	-42	-55
100	Fm	30	1	21	59	60	51	23	32	-3	-19	-23	-42	-55
101	Md	28	0	22	62	63	54	26	36	0	-15	-21	-40	-53
102	No	37	0	17	55	59	52	25	35	2	-13	-18	-37	-49
103	Lr	89	26	0	13	12	3	-11	-15	-43	-56	-36	-54	-71

Z	A	32	33	34	37	38	39	40	41	42	43	44	45
B	Element	Ge	As	Se	Rb	Sr	Y	Zr	Nb	Mo	Tc	Ru	Rh
1	H	-	-	-	32	-8	-35	-54	-27	-2	9	11	6
3	Li	-19	-40	-79	18	0	11	41	74	70	12	7	-19
4	Be	25	10	14	35	-15	-47	-65	-39	-13	-7	-7	-12
5	B	-	-	-	49	-12	-64	-102	-79	-49	-35	-34	-35
6	C	-	-	-	40	-21	-72	-103	-66	-18	22	26	27
7	N	-	-	-	-15	-97	-157	-179	-106	-26	42	52	48
8	O	-	-	-	-179	-270	-339	-366	-293	-208	-135	-124	-126
11	Na	-1	-20	-72	3	-3	41	86	134	134	67	62	27
12	Mg	-9	-31	-66	32	-7	-12	5	44	50	1	-3	-28
13	Al	9	-9	-25	33	-31	-69	-83	-44	-24	-46	-48	-63
14	Si	-	-	-	34	-33	-78	-101	-60	-29	-33	-32	-44
15	P	-	-	-	-24	-111	-171	-203	-147	-93	-62	-58	-63
16	S	-	-	-	-114	-194	-228	-235	-150	-80	-45	-38	-51
19	K	3	-16	-80	0	11	73	123	169	162	87	81	42
20	Ca	-61	-95	-156	22	1	16	54	91	81	2	-5	-40
21	Sc	-85	-129	-177	89	36	1	6	27	16	-57	-64	-90
22	Ti	-65	-110	-140	132	75	22	0	3	-5	-58	-65	-78
23	V	-33	-72	-87	129	74	24	-6	-2	0	-32	-37	-44
24	Cr	-13	-48	-51	120	64	16	-18	-11	1	-13	-17	-20
25	Mn	-32	-65	-75	87	36	-2	-23	-6	7	-12	-16	-24
26	Fe	-9	-40	-37	106	47	-2	-36	-23	-3	-5	-7	-8
27	Co	-17	-45	-39	72	13	-31	-60	-37	-7	0	-1	-3
28	Ni	-20	-47	-38	59	-1	-44	-72	-45	-11	1	1	-1
29	Cu	-2	-23	-33	35	-12	-32	-34	4	28	12	10	-4
30	Zn	8	-9	-27	19	-33	-54	-56	-14	6	-17	-19	-36
31	Ga	8	-9	-30	18	-45	-73	-77	-30	-7	-32	-33	-53
32	Ge	0	-	-	3	-60	-88	-96	-42	-7	-14	-14	-31
33	As	-	0	-	-16	-95	-135	-149	-89	-46	-44	-42	-57
34	Se	-	-	0	-83	-162	-189	-193	-110	-49	-30	-25	-42
37	Rb	3	-16	-83	0	15	81	130	173	164	88	81	43
38	Sr	-60	-95	-162	15	0	25	69	108	96	13	6	-31
39	Y	-88	-135	-189	81	25	0	14	43	35	-42	-49	-79

Z	A	32	33	34	37	38	39	40	41	42	43	44	45
B	Element	Ge	As	Se	Rb	Sr	Y	Zr	Nb	Mo	Tc	Ru	Rh
40	Zr	-96	-149	-193	130	69	14	0	6	-9	-79	-87	-107
41	Nb	-42	-89	-110	173	108	43	6	0	-9	-54	-61	-68
42	Mo	-7	-46	-49	164	96	35	-9	-9	0	-17	-22	-23
43	Tc	-14	-44	-30	88	13	-42	-79	-54	-17	0	0	1
44	Ru	-14	-42	-25	81	6	-49	-87	-61	-22	0	0	2
45	Rh	-31	-57	-42	43	-31	-79	-107	-68	-23	1	2	0
46	Pd	-51	-75	-61	-12	-86	-123	-136	-79	-22	6	9	3
47	Ag	2	-15	-32	10	-39	-44	-31	25	56	36	35	14
48	Cd	10	-5	-28	1	-53	-61	-52	4	29	3	2	-21
49	In	11	-4	-32	-5	-61	-67	-56	5	31	0	-2	-28
50	Sn	12	-1	-24	-10	-75	-91	-86	-22	10	-13	-13	-37
51	Sb	15	5	-13	-34	-104	-119	-113	-39	3	-9	-8	-32
52	Te	13	5	-4	-60	-136	-154	-151	-69	-17	-15	-13	-34
55	Cs	4	-16	-84	0	20	87	135	174	164	88	81	43
56	Ba	-66	-102	-172	13	0	29	74	113	101	16	9	-29
57	La	-89	-136	-193	75	20	0	19	53	45	-33	-40	-72
58	Ce	-89	-135	-192	77	22	0	17	49	42	-36	-43	-75
59	Pr	-89	-135	-191	79	24	0	16	46	39	-39	-46	-77
60	Nd	-89	-135	-190	78	24	0	16	46	38	-39	-46	-77
61	Pm	-90	-136	-192	82	26	0	14	43	34	-44	-51	-81
62	Sm	-89	-135	-190	81	26	0	14	44	35	-42	-49	-79
63	Eull	-59	-93	-157	19	0	21	61	100	89	9	2	-34
63	Eulll	-41	-87	-142	129	74	48	62	92	83	6	-1	-31
64	Gd	-88	-135	-189	81	25	0	14	43	35	-42	-49	-79
65	Tb	-88	-135	-188	83	27	0	13	41	32	-45	-52	-81
66	Dy	-88	-134	-187	82	27	0	12	41	32	-44	-52	-81
67	Ho	-87	-132	-185	81	26	0	13	41	33	-43	-50	-79
68	Er	-88	-134	-186	84	29	0	11	38	29	-47	-54	-83
69	Tm	-87	-133	-185	84	29	0	11	38	29	-47	-54	-83
70	Ybll	-71	-108	-176	26	1	18	60	103	91	2	-6	-45
70	Yblll	-54	-95	-140	93	45	21	30	53	45	-20	-26	-51
71	Lu	-88	-134	-186	87	32	0	10	34	25	-51	-58	-86
72	Hf	-85	-136	-174	134	72	17	0	6	-6	-69	-77	-94

Z	A	32	33	34	37	38	39	40	41	42	43	44	45
B	Element	Ge	As	Se	Rb	Sr	Y	Zr	Nb	Mo	Tc	Ru	Rh
73	Ta	-44	-90	-112	167	103	40	4	0	-7	-52	-59	-67
74	W	1	-36	-35	170	99	35	-14	-13	0	-10	-15	-14
75	Re	1	-31	-19	130	54	-6	-52	-38	-10	0	-1	1
76	Os	-8	-37	-20	95	18	-40	-82	-59	-21	0	0	3
77	Ir	-23	-49	-29	58	-22	-78	-114	-79	-32	-2	-1	1
78	Pt	-43	-68	-45	13	-71	-122	-149	-100	-42	-5	-2	-2
79	Au	-7	-23	-16	-13	-85	-109	-111	-48	5	21	22	11
80	Hg	13	0	-20	-15	-71	-74	-61	3	35	15	14	-9
81	Tl	17	4	-25	-20	-71	-66	-47	21	50	20	19	-9
82	Pb	19	9	-17	-33	-90	-87	-69	5	42	19	18	-10
83	Bi	20	10	-15	-37	-98	-98	-82	-5	33	12	12	-16
84	Po	25	20	2	-75	-135	-124	-103	-12	38	30	32	4
89	Ac	-82	-123	-183	46	6	6	36	78	74	-5	-12	-47
90	Th	-98	-150	-206	101	41	1	6	27	12	-70	-78	-106
91	Pa	-107	-158	-209	97	43	3	4	21	8	-67	-74	-99
92	U	-76	-123	-157	125	65	15	-2	8	1	-56	-63	-79
93	Np	-68	-114	-145	121	62	14	-3	7	3	-49	-56	-71
94	Pu	-84	-131	-170	109	54	10	0	11	2	-59	-66	-85
95	Am	-88	-135	-186	95	37	1	7	29	18	-57	-65	-92
96	Cm	-89	-136	-187	99	39	2	6	28	17	-59	-66	-93
97	Bk	-87	-133	-183	91	35	1	8	30	20	-55	-63	-89
98	CfII	-71	-111	-180	36	3	14	54	97	87	-2	-9	-49
98	CfIII	-73	-114	-158	76	29	1	7	27	18	-46	-53	-76
99	Es	-73	-113	-184	33	2	16	58	101	90	-1	-9	-49
100	Fm	-72	-110	-176	37	3	12	49	91	81	-7	-14	-53
101	Md	-70	-108	-174	34	3	13	52	94	85	-2	-10	-48
102	No	-64	-102	-164	43	4	9	44	87	81	-1	-8	-45
103	Lr	-88	-135	-187	97	38	1	7	29	18	-57	-65	-92

Z	A	46	47	48	49	50	51	52	55	56	57	58	59
B	Element	Pd	Ag	Cd	In	Sn	Sb	Te	Cs	Ba	La	Ce	Pr
1	H	2	35	42	42	45	49	51	32	-12	-34	-34	-35
3	Li	-55	-23	-19	-18	-25	-39	-56	21	0	8	9	10
4	Be	-14	9	16	22	21	26	24	35	-14	-42	-44	-45
5	B	-33	21	34	41	40	47	48	49	-14	-59	-61	-63
6	C	32	43	52	54	59	73	84	41	-23	-67	-69	-71
7	N	51	23	33	27	39	61	84	-10	-100	-155	-156	-157
8	O	-121	-144	-131	-138	-126	-102	-78	-174	-273	-337	-338	-339
11	Na	-21	1	-4	-8	-12	-29	-49	4	-5	36	38	39
12	Mg	-62	-16	-9	-6	-13	-24	-41	34	-8	-13	-13	-12
13	Al	-84	-9	5	10	6	3	-6	34	-35	-68	-68	-69
14	Si	-57	10	22	27	26	29	26	35	-38	-76	-77	-77
15	P	-66	-21	-9	-7	-2	12	20	-23	-117	-169	-170	-170
16	S	-64	-54	-50	-56	-46	-30	-16	-114	-204	-231	-231	-230
19	K	-12	9	1	-5	-9	-32	-57	0	8	67	69	71
20	Ca	-91	-41	-52	-59	-73	-99	-129	27	1	12	13	15
21	Sc	-127	-42	-55	-58	-81	-106	-140	95	40	3	2	2
22	Ti	-97	-2	-24	-25	-51	-70	-101	134	79	28	26	24
23	V	-53	25	2	2	-19	-31	-54	129	77	31	29	26
24	Cr	-22	40	15	14	-3	-9	-25	119	67	24	21	18
25	Mn	-34	19	-8	-11	-27	-35	-51	87	38	4	2	0
26	Fe	-6	42	14	12	-2	-4	-16	105	49	6	4	1
27	Co	-2	28	-2	-5	-17	-16	-24	72	15	-24	-26	-28
28	Ni	0	23	-8	-12	-22	-20	-26	59	0	-37	-40	-42
29	Cu	-20	3	-2	-1	-6	-8	-16	35	-11	-29	-30	-31
30	Zn	-59	-7	1	4	2	-1	-10	20	-37	-54	-54	-54
31	Ga	-79	-10	1	4	1	-2	-11	19	-50	-73	-73	-73
32	Ge	-51	2	10	11	12	15	13	4	-66	-89	-89	-89
33	As	-75	-15	-5	-4	-1	5	5	-16	-102	-136	-135	-135
34	Se	-61	-32	-28	-32	-24	-13	-4	-84	-172	-193	-192	-191
37	Rb	-12	10	1	-5	-10	-34	-60	0	13	75	77	79
38	Sr	-86	-39	-53	-61	-75	-104	-136	20	0	20	22	24
39	Y	-123	-44	-61	-67	-91	-119	-154	87	29	0	0	0

Z	A	46	47	48	49	50	51	52	55	56	57	58	59
B	Element	Pd	Ag	Cd	In	Sn	Sb	Te	Cs	Ba	La	Ce	Pr
40	Zr	-136	-31	-52	-56	-86	-113	-151	134	74	19	17	16
41	Nb	-79	25	4	5	-22	-39	-69	174	113	53	49	46
42	Mo	-22	56	29	31	10	3	-17	164	101	45	42	39
43	Tc	6	36	3	0	-13	-9	-15	88	16	-33	-36	-39
44	Ru	9	35	2	-2	-13	-8	-13	81	9	-40	-43	-46
45	Rh	3	14	-21	-28	-37	-32	-34	43	-29	-72	-75	-77
46	Pd	0	-11	-50	-63	-69	-62	-61	-11	-85	-119	-120	-121
47	Ag	-11	0	-5	-5	-7	-8	-16	10	-39	-43	-43	-44
48	Cd	-50	-5	0	1	0	-4	-12	2	-59	-64	-63	-62
49	In	-63	-5	1	0	-1	-5	-15	-5	-69	-71	-70	-69
50	Sn	-69	-7	0	-1	0	-2	-9	-10	-84	-95	-94	-92
51	Sb	-62	-8	-4	-5	-2	0	-3	-35	-115	-124	-122	-121
52	Te	-61	-16	-12	-15	-9	-3	0	-61	-149	-160	-158	-157
55	Cs	-11	10	2	-5	-10	-35	-61	0	18	82	83	85
56	Ba	-86	-39	-59	-69	-84	-115	-149	18	0	23	25	27
57	La	-119	-43	-64	-71	-95	-124	-160	82	23	0	0	0
58	Ce	-120	-43	-63	-70	-94	-122	-158	83	25	0	0	0
59	Pr	-122	-44	-62	-69	-92	-121	-157	85	27	0	0	0
60	Nd	-121	-44	-62	-69	-92	-120	-156	85	27	0	0	0
61	Pm	-125	-45	-62	-68	-92	-120	-157	89	30	0	0	0
62	Sm	-123	-44	-62	-68	-91	-119	-155	87	29	0	0	0
63	Eull	-86	-39	-51	-59	-72	-100	-130	23	0	16	18	19
63	Eulll	-75	4	-14	-20	-43	-71	-107	135	77	48	48	48
64	Gd	-123	-44	-61	-67	-91	-119	-154	87	29	0	0	0
65	Tb	-124	-44	-61	-66	-90	-117	-153	89	31	1	0	0
66	Dy	-124	-44	-60	-66	-90	-117	-152	88	31	1	0	0
67	Ho	-121	-42	-60	-65	-88	-115	-150	87	30	1	0	0
68	Er	-125	-43	-60	-65	-88	-115	-151	90	33	1	1	0
69	Tm	-124	-43	-59	-64	-88	-115	-150	90	32	1	1	0
70	Ybll	-103	-47	-59	-66	-82	-111	-145	31	2	13	15	16
70	Yblll	-87	-17	-31	-35	-56	-79	-109	98	49	21	21	21
71	Lu	-127	-44	-59	-64	-88	-114	-150	93	35	1	1	1
72	Hf	-120	-19	-41	-45	-74	-98	-133	138	77	23	21	19

Z	A	46	47	48	49	50	51	52	55	56	57	58	59
B	Element	Pd	Ag	Cd	In	Sn	Sb	Te	Cs	Ba	La	Ce	Pr
73	Ta	-78	23	1	2	-24	-41	-71	169	108	49	46	43
74	W	-10	65	36	39	19	14	-4	170	103	46	42	39
75	Re	10	57	25	25	10	12	2	129	58	4	1	-3
76	Os	12	42	9	6	-6	-1	-6	94	21	-31	-34	-37
77	Ir	9	23	-12	-17	-27	-20	-21	58	-20	-70	-72	-75
78	Pt	3	-1	-39	-49	-57	-47	-45	13	-70	-116	-118	-120
79	Au	0	-8	-20	-21	-21	-12	-10	-13	-86	-107	-108	-109
80	Hg	-39	-3	-1	-1	0	-1	-7	-16	-78	-77	-76	-75
81	Tl	-47	2	3	1	2	-2	-11	-21	-81	-71	-69	-68
82	Pb	-46	1	2	-1	2	1	-5	-34	-100	-92	-91	-89
83	Bi	-52	0	1	-2	2	1	-4	-38	-110	-104	-102	-100
84	Po	-31	1	-2	-9	0	4	5	-79	-149	-132	-130	-127
89	Ac	-97	-37	-62	-72	-92	-120	-154	51	7	3	4	5
90	Th	-149	-52	-65	-69	-96	-126	-167	108	46	3	2	1
91	Pa	-136	-43	-69	-76	-104	-133	-170	102	47	5	5	4
92	U	-103	-11	-35	-39	-65	-87	-119	128	69	20	18	16
93	Np	-93	-5	-30	-33	-58	-78	-108	123	66	20	18	16
94	Pu	-113	-22	-46	-50	-76	-99	-132	112	58	14	13	11
95	Am	-131	-44	-58	-61	-86	-113	-148	102	41	3	2	2
96	Cm	-133	-44	-58	-61	-86	-113	-149	105	43	3	3	2
97	Bk	-129	-44	-57	-61	-85	-111	-146	96	39	2	2	1
98	CfII	-106	-46	-58	-65	-82	-113	-148	42	4	10	11	13
98	CfIII	-110	-37	-50	-53	-73	-96	-126	81	32	2	1	1
99	Es	-108	-48	-61	-68	-86	-117	-153	39	3	11	13	14
100	Fm	-108	-47	-58	-64	-81	-110	-144	42	5	8	9	10
101	Md	-104	-45	-57	-63	-80	-108	-142	40	4	9	11	12
102	No	-98	-39	-51	-56	-73	-100	-133	48	5	6	7	8
103	Lr	-131	-44	-58	-61	-86	-113	-149	103	42	3	2	2

Z	A	60	61	62	63	63	64	65	66	67	68	69	70
B	Element	Nd	Pm	Sm	Eull	Eulll	Gd	Tb	Dy	Ho	Er	Tm	Ybll
1	H	-35	-36	-35	-8	13	-35	-36	-36	-35	-36	-36	-19
3	Li	10	12	11	-1	59	11	13	12	12	14	14	-1
4	Be	-45	-48	-47	-17	1	-47	-48	-48	-47	-49	-49	-24
5	B	-63	-66	-64	-15	-16	-64	-66	-66	-65	-67	-67	-24
6	C	-71	-73	-72	-23	-24	-72	-73	-73	-72	-75	-75	-44
7	N	-157	-160	-158	-98	-110	-157	-158	-158	-156	-158	-158	-138
8	O	-339	-342	-340	-270	-292	-339	-340	-340	-337	-341	-340	-313
11	Na	39	42	41	0	89	41	43	43	42	45	44	3
12	Mg	-12	-12	-12	-8	36	-12	-11	-11	-11	-11	-10	-11
13	Al	-69	-70	-69	-32	-21	-69	-69	-69	-68	-69	-69	-40
14	Si	-77	-79	-78	-34	-30	-78	-79	-78	-77	-79	-79	-45
15	P	-170	-173	-171	-111	-123	-171	-172	-171	-169	-172	-171	-131
16	S	-229	-231	-229	-190	-181	-228	-228	-227	-224	-226	-225	-215
19	K	71	74	73	14	121	73	75	75	74	77	76	20
20	Ca	15	17	16	0	64	16	18	18	17	19	19	0
21	Sc	2	1	1	31	49	1	1	1	1	1	1	28
22	Ti	24	22	22	68	70	22	20	20	21	18	18	69
23	V	26	23	24	68	72	24	22	22	23	20	20	70
24	Cr	18	15	16	59	64	16	13	13	14	11	11	60
25	Mn	0	-3	-2	32	46	-2	-4	-4	-3	-5	-5	30
26	Fe	1	-3	-2	42	46	-2	-4	-4	-3	-7	-7	40
27	Co	-28	-32	-31	9	17	-31	-33	-33	-31	-35	-35	4
28	Ni	-42	-46	-44	-5	4	-44	-46	-46	-45	-48	-48	-12
29	Cu	-31	-33	-32	-14	16	-32	-33	-32	-32	-33	-33	-20
30	Zn	-54	-55	-54	-33	-6	-54	-54	-54	-53	-54	-54	-40
31	Ga	-73	-74	-73	-45	-25	-73	-72	-72	-71	-72	-71	-53
32	Ge	-89	-90	-89	-59	-41	-88	-88	-88	-87	-88	-87	-71
33	As	-135	-136	-135	-93	-87	-135	-134	-134	-132	-134	-133	-108
34	Se	-190	-192	-190	-157	-141	-189	-188	-187	-185	-186	-185	-176
37	Rb	78	82	81	19	129	81	83	82	81	84	84	26
38	Sr	24	26	26	0	74	25	27	27	26	29	29	1
39	Y	0	0	0	21	48	0	0	0	0	0	0	18

Z	A	60	61	62	63	63	64	65	66	67	68	69	70
B	Element	Nd	Pm	Sm	Eull	Eulll	Gd	Tb	Dy	Ho	Er	Tm	Ybll
40	Zr	16	14	14	61	62	14	13	12	13	11	11	60
41	Nb	46	43	44	100	92	43	41	41	41	38	38	103
42	Mo	38	34	35	89	83	35	32	32	33	29	29	91
43	Tc	-39	-44	-42	9	6	-42	-45	-44	-43	-47	-47	2
44	Ru	-46	-51	-49	2	-1	-49	-52	-52	-50	-54	-54	-6
45	Rh	-77	-81	-79	-34	-31	-79	-81	-81	-79	-83	-83	-45
46	Pd	-121	-125	-123	-86	-75	-123	-124	-123	-121	-125	-124	-103
47	Ag	-44	-45	-44	-39	4	-44	-44	-43	-42	-43	-43	-46
48	Cd	-62	-62	-62	-51	-14	-61	-61	-60	-60	-60	-59	-59
49	In	-69	-68	-68	-59	-20	-67	-66	-66	-65	-65	-64	-66
50	Sn	-92	-92	-91	-72	-43	-91	-90	-90	-88	-88	-88	-82
51	Sb	-120	-120	-119	-100	-71	-119	-117	-117	-115	-115	-115	-111
52	Te	-156	-157	-155	-130	-107	-154	-153	-152	-150	-151	-150	-145
55	Cs	85	89	87	23	135	87	89	88	87	91	90	31
56	Ba	27	30	29	0	77	29	31	31	30	33	32	2
57	La	0	0	0	16	48	0	1	1	1	1	1	13
58	Ce	0	0	0	18	48	0	0	0	0	1	1	15
59	Pr	0	0	0	19	48	0	0	0	0	0	0	16
60	Nd	0	0	0	19	48	0	0	0	0	0	0	16
61	Pm	0	0	0	21	48	0	0	0	0	0	0	18
62	Sm	0	0	0	21	48	0	0	0	0	0	0	18
63	Eull	19	21	21	0	69	21	22	22	22	24	24	0
63	Eulll	48	48	48	69	96	48	48	48	48	48	48	66
64	Gd	0	0	0	21	48	0	0	0	0	0	0	18
65	Tb	0	0	0	22	48	0	0	0	0	0	0	19
66	Dy	0	0	0	22	48	0	0	0	0	0	0	19
67	Ho	0	0	0	22	48	0	0	0	0	0	0	19
68	Er	0	0	0	24	48	0	0	0	0	0	0	21
69	Tm	0	0	0	24	48	0	0	0	0	0	0	21
70	Ybll	16	18	18	0	66	18	19	19	19	21	21	0
70	Yblll	21	21	21	41	69	21	21	21	21	21	21	39
71	Lu	1	0	0	26	48	0	0	0	0	0	0	23
72	Hf	19	17	17	64	65	17	15	15	16	14	14	64

Z	A	60	61	62	63	63	64	65	66	67	68	69	70
B	Element	Nd	Pm	Sm	Eull	Eulll	Gd	Tb	Dy	Ho	Er	Tm	Ybll
73	Ta	43	39	40	95	88	40	37	37	38	35	34	97
74	W	38	34	35	91	83	35	31	31	33	28	28	93
75	Re	-3	-8	-6	49	42	-6	-9	-9	-8	-13	-13	46
76	Os	-37	-42	-40	13	8	-40	-43	-43	-41	-46	-46	6
77	Ir	-75	-80	-78	-25	-30	-78	-80	-80	-78	-83	-82	-37
78	Pt	-120	-125	-122	-73	-74	-122	-124	-124	-121	-126	-125	-89
79	Au	-109	-112	-110	-84	-61	-109	-110	-110	-108	-110	-110	-99
80	Hg	-75	-75	-74	-68	-26	-74	-73	-73	-71	-71	-71	-76
81	Tl	-67	-67	-66	-67	-18	-66	-64	-64	-63	-62	-62	-74
82	Pb	-88	-88	-87	-85	-39	-87	-85	-84	-83	-83	-82	-93
83	Bi	-100	-99	-98	-93	-50	-98	-96	-96	-94	-94	-93	-102
84	Po	-127	-126	-124	-127	-76	-124	-122	-121	-120	-119	-118	-138
89	Ac	5	6	6	4	54	6	7	7	6	8	8	2
90	Th	1	1	1	35	49	1	1	1	0	0	0	32
91	Pa	4	3	3	37	51	3	2	2	2	2	2	35
92	U	16	14	15	58	63	15	13	13	13	11	11	57
93	Np	16	14	14	56	62	14	12	12	13	11	11	56
94	Pu	11	10	10	48	58	10	9	9	9	7	7	48
95	Am	2	1	1	31	49	1	1	1	1	0	0	29
96	Cm	2	1	2	33	50	2	1	1	1	1	1	30
97	Bk	1	1	1	29	49	1	1	1	1	0	0	27
98	Cfll	13	15	14	1	62	14	16	15	15	17	17	0
98	Cflll	1	1	1	24	49	1	0	0	0	0	0	22
99	Es	14	17	16	1	64	16	18	18	17	19	19	0
100	Fm	10	12	12	2	60	12	13	13	13	14	14	1
101	Md	12	14	13	1	61	13	15	15	14	16	16	0
102	No	8	10	9	2	57	9	10	10	10	12	12	0
103	Lr	2	1	1	32	49	1	1	1	1	1	1	29

Z	A	70	71	72	73	74	75	76	77	78	79	80	81
B	Element	YbIII	Lu	Hf	Ta	W	Re	Os	Ir	Pt	Au	Hg	Tl
1	H	-5	-37	-47	-27	4	12	12	10	7	35	46	46
3	Li	32	15	44	71	71	41	15	-12	-44	-51	-28	-22
4	Be	-22	-52	-58	-39	-8	-3	-6	-11	-17	-1	22	33
5	B	-36	-70	-94	-78	-44	-35	-34	-36	-39	8	41	52
6	C	-33	-77	-92	-65	-8	17	26	32	34	59	63	65
7	N	-96	-161	-160	-105	-8	35	52	61	64	69	48	38
8	O	-275	-343	-347	-291	-191	-144	-124	-113	-109	-98	-116	-125
11	Na	59	47	92	130	139	104	73	40	-1	-21	-16	-16
12	Mg	11	-10	11	41	53	28	4	-22	-54	-48	-14	-5
13	Al	-39	-70	-75	-46	-20	-29	-43	-60	-82	-37	6	16
14	Si	-45	-80	-91	-60	-23	-22	-29	-40	-56	-8	27	36
15	P	-127	-174	-188	-147	-82	-61	-57	-58	-64	-17	2	6
16	S	-175	-226	-215	-151	-64	-39	-34	-37	-48	-26	-40	-48
19	K	87	79	128	163	168	129	94	57	12	-13	-15	-18
20	Ca	37	21	57	86	82	40	6	-32	-79	-88	-68	-66
21	Sc	21	0	8	24	14	-25	-57	-91	-131	-110	-65	-54
22	Ti	36	16	0	2	-9	-38	-61	-86	-111	-71	-27	-13
23	V	37	17	-3	-2	-1	-19	-35	-51	-68	-29	3	16
24	Cr	30	8	-14	-10	1	-6	-16	-27	-36	0	19	30
25	Mn	16	-8	-18	-6	9	-1	-13	-27	-42	-17	-5	2
26	Fe	15	-10	-30	-22	0	0	-6	-13	-19	12	21	30
27	Co	-10	-38	-51	-36	-2	3	0	-5	-11	11	7	11
28	Ni	-21	-52	-62	-44	-5	3	2	-2	-7	11	1	4
29	Cu	-8	-35	-25	3	33	27	15	0	-18	-13	0	8
30	Zn	-26	-54	-48	-16	11	1	-13	-31	-53	-27	1	9
31	Ga	-41	-72	-68	-32	-1	-12	-28	-47	-73	-34	1	8
32	Ge	-54	-88	-85	-44	1	1	-8	-23	-43	-7	13	17
33	As	-95	-134	-136	-90	-36	-31	-37	-49	-68	-23	0	4
34	Se	-140	-186	-174	-112	-35	-19	-20	-29	-45	-16	-20	-25
37	Rb	93	87	134	167	170	130	95	58	13	-13	-15	-20
38	Sr	45	32	72	103	99	54	18	-22	-71	-85	-71	-71
39	Y	21	0	17	40	35	-6	-40	-78	-122	-109	-74	-66

Z	A	70	71	72	73	74	75	76	77	78	79	80	81
B	Element	YbIII	Lu	Hf	Ta	W	Re	Os	Ir	Pt	Au	Hg	Tl
40	Zr	30	10	0	4	-14	-52	-82	-114	-149	-111	-61	-47
41	Nb	53	34	6	0	-13	-38	-59	-79	-100	-48	3	21
42	Mo	45	25	-6	-7	0	-10	-21	-32	-42	5	35	50
43	Tc	-20	-51	-69	-52	-10	0	0	-2	-5	21	15	20
44	Ru	-26	-58	-77	-59	-15	-1	0	-1	-2	22	14	19
45	Rh	-51	-86	-94	-67	-14	1	3	1	-2	11	-9	-9
46	Pd	-87	-127	-120	-78	-10	10	12	9	3	0	-39	-47
47	Ag	-17	-44	-19	23	65	57	42	23	-1	-8	-3	2
48	Cd	-31	-59	-42	1	36	25	9	-12	-39	-20	-1	3
49	In	-35	-64	-45	2	39	25	6	-17	-49	-21	-1	1
50	Sn	-56	-88	-74	-24	19	10	-6	-27	-57	-21	0	2
51	Sb	-79	-114	-98	-41	14	12	-1	-20	-47	-12	-1	-2
52	Te	-109	-150	-133	-71	-4	2	-6	-21	-45	-10	-7	-11
55	Cs	98	93	138	169	170	129	94	58	13	-13	-16	-21
56	Ba	49	35	77	108	103	58	21	-20	-70	-86	-78	-81
57	La	21	1	23	49	46	4	-31	-70	-116	-107	-77	-71
58	Ce	21	1	21	46	42	1	-34	-72	-118	-108	-76	-69
59	Pr	21	1	19	43	39	-3	-37	-75	-120	-109	-75	-68
60	Nd	21	1	19	43	38	-3	-37	-75	-120	-109	-75	-67
61	Pm	21	0	17	39	34	-8	-42	-80	-125	-112	-75	-67
62	Sm	21	0	17	40	35	-6	-40	-78	-122	-110	-74	-66
63	Eull	41	26	64	95	91	49	13	-25	-73	-84	-68	-67
63	Eulll	69	48	65	88	83	42	8	-30	-74	-62	-26	-18
64	Gd	21	0	17	40	35	-6	-40	-78	-122	-109	-74	-66
65	Tb	21	0	15	37	31	-9	-43	-80	-124	-110	-73	-64
66	Dy	21	0	15	37	31	-9	-43	-80	-124	-110	-73	-64
67	Ho	21	0	16	38	33	-8	-41	-78	-121	-108	-71	-63
68	Er	21	0	14	35	28	-13	-46	-83	-126	-110	-71	-62
69	Tm	21	0	14	34	28	-13	-46	-82	-125	-110	-71	-62
70	YbII	39	23	64	97	93	46	6	-37	-89	-99	-76	-74
70	YbIII	41	21	32	50	45	10	-19	-51	-88	-75	-41	-33
71	Lu	21	0	12	31	23	-17	-50	-87	-129	-112	-71	-61
72	Hf	32	12	0	4	-10	-45	-72	-102	-134	-95	-48	-34

Z	A	70	71	72	73	74	75	76	77	78	79	80	81
B	Element	YbIII	Lu	Hf	Ta	W	Re	Os	Ir	Pt	Au	Hg	Tl
73	Ta	50	31	4	0	-11	-37	-57	-78	-98	-48	0	18
74	W	45	23	-10	-11	0	-6	-15	-23	-30	17	44	60
75	Re	10	-17	-45	-37	-6	0	-2	-5	-7	30	37	47
76	Os	-19	-50	-72	-57	-15	-2	0	-1	-1	27	21	28
77	Ir	-51	-87	-102	-78	-23	-5	-1	0	1	19	2	4
78	Pt	-88	-129	-134	-98	-30	-7	-1	1	0	7	-25	-29
79	Au	-75	-112	-95	-48	17	30	27	19	7	0	-10	-8
80	Hg	-41	-71	-48	0	44	37	21	2	-25	-10	0	1
81	Tl	-33	-61	-34	18	60	47	28	4	-29	-8	1	0
82	Pb	-51	-81	-55	2	53	44	27	5	-27	-3	2	-1
83	Bi	-60	-92	-67	-8	44	37	21	-1	-33	-4	2	-2
84	Po	-82	-117	-84	-15	53	54	41	22	-6	15	1	-9
89	Ac	27	9	41	73	76	35	-1	-40	-88	-90	-76	-75
90	Th	21	0	8	23	10	-35	-70	-109	-154	-132	-79	-65
91	Pa	22	1	5	18	5	-35	-67	-102	-142	-117	-80	-71
92	U	30	9	-1	6	-2	-33	-58	-85	-115	-80	-41	-28
93	Np	30	9	-1	6	1	-28	-51	-77	-104	-70	-34	-22
94	Pu	27	6	1	9	0	-34	-61	-90	-122	-91	-52	-42
95	Am	21	0	9	26	16	-24	-57	-93	-135	-115	-69	-57
96	Cm	21	0	8	25	15	-26	-59	-95	-137	-116	-69	-57
97	Bk	21	0	9	27	18	-22	-55	-90	-132	-113	-69	-57
98	CfII	35	19	58	92	89	42	3	-41	-94	-102	-76	-72
98	CfIII	21	0	9	24	17	-18	-46	-77	-112	-96	-59	-50
99	Es	37	22	62	96	92	44	3	-41	-95	-104	-79	-76
100	Fm	33	16	53	86	82	36	-3	-45	-97	-103	-75	-70
101	Md	34	18	56	89	87	41	2	-40	-92	-99	-73	-69
102	No	31	13	48	82	84	40	3	-37	-87	-92	-65	-61
103	Lr	21	0	9	26	17	-24	-57	-93	-135	-115	-69	-57

Z	A	82	83	84
B	Element	Pb	Bi	Po
1	H	49	50	56
3	Li	-30	-33	-51
4	Be	35	35	46
5	B	56	57	70
6	C	73	75	96
7	N	52	55	87
8	O	-110	-107	-72
11	Na	-26	-28	-54
12	Mg	-12	-14	-28
13	Al	15	14	13
14	Si	38	38	46
15	P	15	17	40
16	S	-37	-35	-12
19	K	-31	-34	-70
20	Ca	-83	-91	-123
21	Sc	-73	-83	-106
22	Ti	-30	-41	-53
23	V	4	-5	-7
24	Cr	23	15	20
25	Mn	-7	-14	-13
26	Fe	25	18	27
27	Co	8	2	14
28	Ni	2	-4	10
29	Cu	6	3	6
30	Zn	7	6	4
31	Ga	7	6	4
32	Ge	19	20	25
33	As	9	10	20
34	Se	-17	-15	2
37	Rb	-33	-37	-75
38	Sr	-90	-98	-135
39	Y	-87	-98	-124

Z	A	82	83	84
B	Element	Pb	Bi	Po
40	Zr	-69	-82	-103
41	Nb	5	-5	-12
42	Mo	42	33	38
43	Tc	19	12	30
44	Ru	18	12	32
45	Rh	-10	-16	4
46	Pd	-46	-52	-31
47	Ag	1	0	1
48	Cd	2	1	-2
49	In	-1	-2	-9
50	Sn	2	2	0
51	Sb	1	1	4
52	Te	-5	-4	5
55	Cs	-34	-38	-79
56	Ba	-100	-110	-149
57	La	-92	-104	-132
58	Ce	-91	-102	-130
59	Pr	-89	-100	-127
60	Nd	-88	-100	-127
61	Pm	-88	-99	-126
62	Sm	-87	-98	-124
63	Eull	-85	-93	-127
63	Eulll	-39	-50	-76
64	Gd	-87	-98	-124
65	Tb	-85	-96	-122
66	Dy	-84	-96	-121
67	Ho	-83	-94	-120
68	Er	-83	-94	-119
69	Tm	-82	-93	-118
70	Ybll	-93	-102	-138
70	Yblll	-51	-60	-82
71	Lu	-81	-92	-117
72	Hf	-55	-67	-84

Z	A	82	83	84
B	Element	Pb	Bi	Po
73	Ta	2	-8	-15
74	W	53	44	53
75	Re	44	37	54
76	Os	27	21	41
77	Ir	5	-1	22
78	Pt	-27	-33	-6
79	Au	-3	-4	15
80	Hg	2	2	1
81	Tl	-1	-2	-9
82	Pb	0	0	-4
83	Bi	0	0	-3
84	Po	-4	-3	0
89	Ac	-95	-106	-136
90	Th	-88	-100	-128
91	Pa	-94	-107	-131
92	U	-47	-58	-73
93	Np	-39	-50	-62
94	Pu	-61	-72	-89
95	Am	-78	-89	-113
96	Cm	-78	-89	-113
97	Bk	-78	-88	-112
98	CfII	-92	-102	-137
98	CfIII	-67	-76	-97
99	Es	-97	-106	-144
100	Fm	-90	-98	-132
101	Md	-89	-97	-132
102	No	-79	-87	-118
103	Lr	-78	-89	-113

Appendix B

Nuclide Library used for the evaluation of γ -spectra

Nuclide	Half-Life (Seconds)	Energy (keV)	Energy Uncert. (keV)	Yield (%)	Yield Uncert. (Abs.+)
Be-7	4.59E+06	477.595	0.5	10.52	0.06
Na-22	8.21E+07	1274.53	0.02	99.944	0.014
K-42	4.45E+04	1524.58	0.08	18.8	0.9
Sc-44	1.41E+04	511		188.73	0
		1157	0.05	100	20
Sc-44x	2.11E+05	271.241	0.01	86.6	0.2
		1001.82	0.03	1.39	0.022
		1126.07	0.07	1.39	0.022
		1157	0.05	1.39	0.022
Sc-46	7.24E+06	889.277	0.003	99.984	0.001
		1120.545	0.004	99.987	0.001
Ca-47	3.92E+05	489.23	0.1	6.5	0.9
		807.86	0.1	6.5	0.9
		1297.09	0.1	74	9
Sc-47	2.89E+05	159.381	0.015	67.9	1.5
V-48	1.38E+06	511		100.2	0
		944.13	0.005	7.76	0.09
		983.524	0.004	100	0.2
		1312.099	0.007	97.5	0.8
Cr-51	2.39E+06	320.084	0.001	10.08	0.23
Mn-52	4.83E+05	511		59.2	0
		744.233	0.013	90.6	0.5
		848.18	0.05	3.35	0.05
		935.544	0.012	94.9	0.5
		1246.278	0.015	4.23	0.05
		1333.649	0.017	5.07	0.04
		1434.092	0.017	100	0.5
Mn-54	2.70E+07	834.827	0.021	99.976	0.001
Co-56	6.66E+06	511		38.03	0
		846.764	0.006	99.935	0.025
		977.48	0.06	1.432	0.01
		997.33	0.16	1.409	0.02
		1037.844	0.004	14.1	0.19
		1175.099	0.008	2.3	0.4
		1238.287	0.006	68.4	0.9
		1360.206	0.006	4.32	0.06
		1771.35	0.015	15.5	0.4
		2015.179	0.011	3.18	0.07
		2034.759	0.011	8.13	0.17
Ni-56	5.27E+05	158.38	0.03	98.8	1
		269.5	0.02	36.5	0.8
		480.44	0.02	36.5	0.8
		749.95	0.03	49.5	1.2
		811.85	0.03	86	0.9

Nuclide	Half-Life (Seconds)	Energy (keV)	Energy Uncert. (keV)	Yield (%)	Yield Uncert. (Abs.+)
Ni-56	5.27E+05	1561.8	0.05	14	0.6
Co-57	2.35E+07	122.061	0	85.9	1.2
		136.474	0.001	10.33	0.1
Co-58	6.13E+06	511		29.92	0
		810.775	0.009	99.448	0.008
Fe-59	3.84E+06	142.652	0.002	1.02	0.04
		192.349	0.005	3.08	0.1
		1099.251	0.004	56.5	1.5
		1291.596	0.007	43.2	1.1
Co-60	1.66E+08	1173.237	0.004	99.9	0.02
		1332.501	0.005	99.982	0.001
Zn-65	2.11E+07	1115.546	0.004	50.7	0.13
Cu-67	2.23E+05	91.266	0.005	7	0.1
		93.311	0.005	16.1	0.2
		184.577	0.01	48.7	0.3
Ga-68	4.06E+03	1077.4	0.1	3	0.3
As-74	1.54E+06	511		58.63	0
		595.83	0.08	59	4
		634.78	0.08	15.4	1.1
Se-75	1.04E+07	96.734	0.001	3.42	0.07
		121.117	0.002	17.14	0.23
		136.001	0.001	58.3	0.6
		264.658	0.002	58.5	0.6
		279.544	0.001	24.79	0.24
		303.925	0.002	1.312	0.015
		400.66	0.001	11.37	0.12
Rb-83	7.45E+06	520.41	0.03	45	6
		529.64	0.01	30	4
		552.65	0.02	16.1	1.9
Rb-84	2.84E+06	511		51.42	0
		881.61	0.003	69	1.6
Kr-85	1.61E+04	151.17	0.03	75.4	1.8
		304.87	0.02	14	0.4
Sr-85	5.60E+06	514.007	0.002	96	4
Rb-86	1.61E+06	1077	0.4	8.64	0.04
Y-88	9.22E+06	898.042	0.003	93.7	0.3
		1836.063	0.012	99.2	0.3
Zr-88	7.21E+06	392.9	0.1	97.24	0
Zr-89	2.51E+02	511		3.03	0
		587.79	0.1	89.51	0.18
		1507.3	0.4	6.06	0.19
Y-90m	1.15E+04	202.51	0.03	96.58	0.18
		479.53	0.04	90.71	0.07
Nb-91m	5.26E+06	1204.67	0.08	2.9	1.3
Nb-92x	1.10E+15	561.1	1.1	100	0
		934.51	0.08	100	0
Nb-95	3.12E+05	204.12	0.02	2.2	0.3
		235.68	0.02	24.1	0.6

Nuclide	Half-Life (Seconds)	Energy (keV)	Energy Uncert. (keV)	Yield (%)	Yield Uncert. (Abs.+)
Zr-95	5.53E+06	724.199	0.005	44.15	0.23
		756.729	0.012	54.5	0.2
Pd-100	3.14E+05	74.77	0.08	36	3
		84	0.09	45	3
		126.07	0.19	8.1	0.6
Rh-101	1.04E+08	158.8	0.3	1.51	0.12
		127.21	0.07	73	6
		198	0.2	71	6
Rh-101x	1.04E+08	325.2	0.2	13.4	1.6
		127.21	0.07	73	6
		198	0.2	71	6
Rh-102	1.79E+07	325.2	0.2	13.4	1.6
		468.58	0.04	2.48	0.24
		475.06	0.04	39	4
Rh-102m	9.15E+07	511		29.44	0
		556.6	0.04	1.9	0.6
		628.05	0.05	3.9	0.5
		415.25	0.15	2.1	0.3
		418.52	0.18	9.4	1
		420.4	0.2	3.2	0.3
		475.06	0.04	95	4
Ru-103	3.39E+06	628.05	0.05	8.3	0.4
		631.29	0.05	56	2
		692.4	0.2	1.6	0.2
		695.6	0.3	2.9	0.4
		697.49	0.08	44	2
		766.84	0.06	34	2
		1046.59	0.07	34	2
		1103.16	0.06	4.6	0.3
		1112.84	0.07	19	1
		Ag-105	3.57E+06	497.084	0.006
610.33	0.02			5.73	0.19
Ag-105	3.57E+06	280.41	0.06	30.2	1.7
		319.14	0.06	4.35	0.21
		331.51	0.07	4.1	0.21
		344.52	0.021	41	0
		392.64	0.06	1.98	0.1
		443.37	0.07	10.5	0.5
		617.85	0.07	1.16	0.05
		644.55	0.07	11.1	0.5
		650.72	0.06	2.538	0.017
		673.21	0.06	1.05	0.06
Ag-105	3.57E+06	807.46	0.07	1.16	0.07
		1087.94	0.06	3.85	0.17

Nuclide	Half-Life (Seconds)	Energy (keV)	Energy Uncert. (keV)	Yield (%)	Yield Uncert. (Abs.+)
Ag-106x	7.31E+05	195.05	0.16	0.31	0.05
		221.701	0.015	6.6	0.3
		228.633	0.021	2.1	0.1
		328.463	0.023	1.14	0.06
		374.46	0.13	0.26	0.04
		391.04	0.03	3.68	0.18
		406.182	0.02	13.4	0.4
		418.55	0.23	0.33	0.07
		429.646	0.022	13.2	0.4
		450.976	0.022	28.2	0.8
		474.06	0.03	0.93	0.06
		511.85	0.03	88	3
		585.97	0.1	0.44	0.1
		601.17	0.07	1.61	0.09
		616.17	0.04	21.6	0.7
		646.03	0.05	1.46	0.1
		679.64	0.02	0.64	0.04
		680.42	0.01	1.54	0.08
		703.11	0.08	4.47	0.18
		717.34	0.09	28.9	0.8
		748.36	0.11	20.6	0.7
		793.17	0.1	5.9	0.3
		804.28	0.1	12.4	0.6
		808.36	0.11	4	0.5
		824.69	0.07	15.3	0.5
		847.03	0.04	2.8	0.7
		847.27	0.02	1.6	0.6
		874.81	0.18	0.33	0.05
		949.52	0.25	0.19	0.04
		956.22	0.23	0.47	0.08
		1019.72	0.15	1.04	0.16
		1045.83	0.08	29.6	1
		1050.6	0.5	0.26	0.14
		1053.77	0.21	0.96	0.14
		1121.59	0.18	0.57	0.07
		1128.02	0.07	11.8	0.6
		1136.85	0.19	0.23	0.03
		1178.07	0.21	0.19	0.03
		1199.39	0.1	11.2	0.6
		1222.88	0.12	7	0.4
		1349.5	0.6	0.12	0.05
		1394.35	0.14	1.49	0.18
		1527.65	0.19	16.3	1.4
		1565.4	0.3	0.48	0.05
		1572.35	0.15	6.6	0.6
		1722.76	0.18	1.4	0.18
		1839.05	0.1	2	0.3

Nuclide	Half-Life (Seconds)	Energy (keV)	Energy Uncert. (keV)	Yield (%)	Yield Uncert. (Abs.+)
Rh-106	3.18E+07	621.84	0	9.8	0.5
		1050.47	0	1.73	0
Rh-106m	7.80E+03	221.8	0.1	6.4	0.4
		228.6	0.3	2.1	1.4
		328.3	0.4	1.2	0.18
		390.8	0.4	3.5	0.3
		406	0.1	11.6	0.7
		429.4	0.1	13.3	2.1
		450.8	0.1	24.2	1.3
		511.7	0.1	86	5
		601.2	0.3	2.99	0.18
		616.1	0.1	20.2	1.4
		645.8	0.2	2.74	0.18
		680.6	0.3	1.88	0.09
		703.1	0.2	4.4	0.5
		717.2	0.1	28.9	1.6
		748.5	0.1	19.3	1.1
		793.8	0.2	5.6	1
		804.6	0.2	13	1.2
808.4	0.2	7.4	0.5		
825	0.1	13.6	0.8		
848	0.2	1.967	0.017		
848	0.2	1.625	0.014		
		1020.5	0.3	1.97	0.18
		1046.7	0.1	30.4	1.6
		1127.7	0.1	13.7	0.9
		1200.5	0.1	11.4	0.6
		1224.2	0.1	8.1	0.7
		1395.5	0.1	2.8	0.4
		1529.4	0.1	17.5	1.6
		1573.9	0.2	6.7	0.6
		1724.6	0.2	2.2	0.5
		1840.6	0.2	1.9	0.4
Cd-109	4.00E+07	88.034	0.001	3.61	0.1
Ag-110m	2.16E+07	446.811	0.003	3.75	0.03
		620.36	0.003	2.806	0.018
		657.762	0.002	94.6	0.4
		677.623	0.002	10.35	0.08
		687.015	0.003	6.44	0.06
		706.682	0.003	16.44	0.1
		744.277	0.003	4.73	0.03
		763.944	0.003	22.29	0.09
		818.031	0.004	7.34	0.04
		884.685	0.003	72.7	0.3
		937.493	0.004	34.36	0.12
		1384.3	0.004	24.28	0.08
		1475.788	0.006	3.995	0.017
1505.04	0.005	13.04	0.05		
1562.302	0.005	1.029	0.007		
In-111	2.42E+05	171.28	0.03	90	5

Nuclide	Half-Life (Seconds)	Energy (keV)	Energy Uncert. (keV)	Yield (%)	Yield Uncert. (Abs.+)
In-111	2.42E+05	245.35	0.04	94	5
In-113m	5.97E+03	391.69	0.008	64.23	0
Sn-113	9.94E+06	255.06	0.05	1.82	0.09
		391.688	0.015	64	2
In-114m	4.28E+06	190.27	0.03	14.74	0.07
		558.43	0.03	4	3
		725.24	0.03	4	3
Cd-115	1.93E+05	231.443	0.003	0.74	0.018
		260.896	0.003	1.94	0.04
		336.24	0.03	45.9	1
		492.351	0.004	8.03	0.19
		527.901	0.007	27.4	0.6
Cd-115x	3.85E+06	933.838	0.004	2	0.7
Sn-117m	1.18E+06	156.02	0.03	2.113	0.012
		158.56	0.02	86.4	0.4
Te-121	1.45E+06	470.472	0.013	1.41	0.05
		507.591	0.011	17.7	0.6
		573.139	0.011	80.3	2.5
Te-121x	1.33E+07	212.19	0.03	81.4	1.1
		1102.149	0.018	2.5	0.3
Sn-123m	2.41E+03	160.33	0.05	85.6	2
Te-123m	1.03E+07	159	0.03	84	0.4
Sb-124	5.20E+06	602.73	0.003	97.8	0.6
		645.855	0.002	7.38	0.07
		709.32	0.013	1.35	0.021
		713.781	0.005	2.27	0.04
		722.786	0.004	10.76	0.12
		968.201	0.004	1.888	0.022
		1045.131	0.003	1.84	0.04
		1325.512	0.005	1.62	0.04
		1355.175	0.022	1.04	0.04
		1368.164	0.006	2.62	0.05
		1436.563	0.006	1.23	0.05
		1690.98	0.004	47.3	0.7
		2090.942	0.007	5.57	0.11
Sb-125	8.62E+07	176.334	0.011	6.79	0.07
		380.435	0.02	1.52	0.019
		427.889	0.015	29.4	0.3
		463.383	0.015	10.45	0.11
		600.557	0.018	17.78	0.18
		606.641	0.019	5.02	0.06
		635.895	0.018	11.32	0.12
		671.409	0.02	1.8	0.05
Sn-125x	8.33E+05	332.1	0.05	1.31	0.06
		350.95	0.05	0.246	0.012
		469.85	0.05	1.38	0.07
		800.28	0.05	0.99	0.05
		822.48	0.05	3.99	0.19

Nuclide	Half-Life (Seconds)	Energy (keV)	Energy Uncert. (keV)	Yield (%)	Yield Uncert. (Abs.+)
Sn-125x	8.33E+05	893.4	0.05	0.271	0.02
		915.55	0.05	3.85	0.18
		934.63	0.05	0.194	0.009
		1017.4	0.05	0.298	0.014
		1067.1	0.05	9.04	0.25
		1087.7	0.1	1.11	0.06
		1089.15	0.1	4.28	0.2
		1151.23	0.05	0.107	0.005
		1173.3	0.05	0.169	0.008
		1220.88	0.1	0.25	0.012
		1419.7	0.05	0.454	0.021
		1806.3	0.05	0.138	0.007
		2001.84	0.05	1.79	0.08
2275.4	0.1	0.17	0.008		
I-126	1.13E+06	388.633	0.011	34	3
		491.243	0.011	2.85	0.22
		511	0	2.32	0
		666.331	0.012	33.1	2.5
		753.819	0.013	4.2	0.4
Xe-127	3.15E+06	145.252	0.01	4.29	0.14
		172.132	0.01	25.5	0.8
		202.86	0.01	68.3	0.4
		374.991	0.012	17.2	0.6
Cs-129	1.15E+05	318.18	0.002	2.46	0.14
		371.918	0.002	30.8	1.6
		411.49	0.002	22.5	1.2
		548.945	0.008	3.42	0.18
Te-129x	2.90E+06	695.88	0.06	3	1.1
Ba-131	1.02E+06	123.803	0.012	29.1	0.9
		133.607	0.014	2.19	0.09
		216.09	0.03	19.9	0.4
		239.63	0.03	2.41	0.08
		249.44	0.03	2.81	0.1
		373.25	0.03	13.3	1.5
		486.48	0.04	1.89	0.21
		496.28	0.03	44	4
		585.02	0.03	1.23	0.09
		620.05	0.03	1.57	0.09
Ba-133	3.32E+08	79.623	0.01	2.62	0.06
		80.997	0.003	34.1	0.3
		276.398	0.002	7.164	0.022
		302.853	0.001	18.33	0.06
		356.017	0.002	62.05	0.19
		383.851	0.003	8.94	0.03
Xe-133	4.53E+05	79.623	0.01	0.27	0.03
		80.997	0.003	38	0.7
Xe-133m	1.89E+05	233.221	0.018	10	0
Cs-134	6.51E+07	475.35	0.05	1.46	0.04
		563.227	0.015	8.38	0.05
		569.315	0.015	15.43	0.11

Nuclide	Half-Life (Seconds)	Energy (keV)	Energy Uncert. (keV)	Yield (%)	Yield Uncert. (Abs.+)
Cs-134	6.51E+07	604.699	0.015	97.6	0.4
		795.845	0.022	85.4	0.4
		801.932	0.022	8.73	0.04
		1038.57	0.03	1	0.01
		1167.94	0.03	1.8	0.03
		1365.15	0.04	3.04	0.04
Cs-137	9.47E+08	661.66	0.003	85.21	0.07
Ce-139	1.19E+07	165.853	0.007	79.886	0.015
Ce-141	2.81E+06	145.44	0.003	48.2	0.3
Pm-143	2.29E+07	741.98	0.04	38.5	2.4
Ce-144	2.46E+07	133.515	0.002	11.09	0.2
Pm-144	3.14E+07	476.78	0.03	42	0.8
		618.01	0.03	98.6	1
		696.49	0.03	99.49	0.02
		778.57	0.06	1.51	0.05
Eu-145	5.12E+05	111.087	0.024	2.01	0.1
		511		4.8	0
		542.564	0.017	4.8	0.4
		653.512	0.019	16.4	0.7
		764.775	0.018	1.77	0.08
		893.738	0.024	68.4	2.5
Eu-145	5.12E+05	1658.44	0.05	15.1	1
		1804.21	0.04	1.43	0.13
		1876.64	0.06	1.35	0.09
		1996.95	0.06	7.3	0.5
Eu-146	3.97E+05	430.53	0.14	4.74	0.11
		511		11.66	0
		633.03	0.14	43	7
		634.07	0.11	37	6
		664.65	0.14	3.3	0.8
		665.4	0.13	4.1	0.8
		702.2	0.17	4.4	0.8
		703.11	0.17	3.4	0.8
		704.9	0.2	1.7	0.05
		747.2	0.12	98.33	0.06
		888.46	0.15	1.08	0.25
		899.57	0.19	2.06	0.15
		900.93	0.19	2.25	0.21
		1057.62	0.1	2.3	0.4
		1058.71	0.1	3.9	0.4
		1297	0.2	5.37	0.13
1406.9	0.2	1.71	0.08		
1533.7	0.2	6.05	0.15		
Gd-146	4.17E+06	114.71	0.02	44	0.7
		115.51	0.02	44	0.7
		154.57	0.02	46.6	0.5
Pm-146	1.75E+08	453.88	0.2	65	2
		633.25	0.2	2.15	0.2

Nuclide	Half-Life (Seconds)	Energy (keV)	Energy Uncert. (keV)	Yield (%)	Yield Uncert. (Abs.+)
Pm-146	1.75E+08	735.93	0.2	22.5	1.5
		747.24	0.2	34	1.6
Eu-147	2.07E+06	121.25	0.05	23	3
		197.35	0.05	26	3
		601.43	0.1	6.8	1
		677.6	0.1	10.7	1.4
		798.81	0.12	5.5	0.8
		857.07	0.1	3.1	0.4
		933.11	0.12	3.6	0.5
		955.94	0.12	3.9	0.5
		1077.16	0.12	6.4	0.9
		1255.91	0.18	1.01	0.13
Nd-147	9.49E+05	91.106	0.02	27.9	1.1
		319.411	0.018	1.95	0.14
		439.895	0.022	1.2	0.1
		531.016	0.022	13.1	0.9
Eu-148	4.71E+06	241.653	0.015	1.44	0.05
		311.57	0.02	1.79	0.06
		414.028	0.012	10.3	0.4
		414.057	0.016	10.1	0.6
		432.745	0.008	2.83	0.11
		550.284	0.012	99	3
		553.231	0.014	12.9	2.2
		553.26	0.015	5	2.2
		571.962	0.007	9.6	0.3
		611.293	0.008	20.5	0.7
		629.987	0.008	71.9	2.3
		654.22	0.008	1.62	0.05
		683.153	0.007	1.28	0.04
		714.769	0.013	1.72	0.06
		725.673	0.009	12.7	0.4
		869.891	0.008	5.49	0.17
		915.331	0.008	2.6	0.09
		929.85	0.03	1.22	0.22
		930.807	0.019	1.4	0.3
		967.306	0.017	2.7	0.09
1033.986	0.014	7.77	0.23		
1146.805	0.014	1.96	0.07		
1183.208	0.016	1.66	0.06		
1328.504	0.015	1.32	0.05		
1343.87	0.03	1.69	0.15		
1344.74	0.023	1.89	0.17		
1621.51	0.02	4.64	0.15		
1650.436	0.024	3.71	0.15		
Pm-148	4.64E+05	550.27	0.03	22	0.6
		611.26	0.03	1.02	0.03
		914.85	0.03	11.5	0.3
		1465.12	0.03	22.2	0.5
Pm-148m	3.57E+06	98.48	0.03	2.46	0.05
		189.63	0.03	1.1	0.03

Nuclide	Half-Life (Seconds)	Energy (keV)	Energy Uncert. (keV)	Yield (%)	Yield Uncert. (Abs.+/-)
Pm-148m	3.57E+06	288.11	0.03	12.51	0.13
		311.63	0.03	3.9	0.06
		414.07	0.03	18.58	0.21
		432.78	0.03	5.33	0.08
		501.26	0.03	6.72	0.09
		550.27	0.03	94.5	1
		599.74	0.03	12.49	0.15
		611.26	0.03	5.46	0.1
		629.97	0.03	88.6	0.7
		725.7	0.03	32.7	0.4
		915.33	0.03	17.1	0.22
		1013.81	0.03	20.2	0.23
		Eu-149	8.04E+06	277.089	0.01
327.526	0.01			4.03	0.12
Gd-149	8.12E+05	149.72	0.01	49	4
		260.73	0.02	1.39	0.1
		272.37	0.02	2.87	0.22
		298.64	0.02	28.9	2
		346.69	0.02	23.4	2
		496.41	0.03	1.62	0.11
		516.57	0.05	2.8	0.3
		534.31	0.03	3.04	0.21
		645.39	0.05	1.56	0.13
		748.65	0.03	7.5	0.5
		788.88	0.03	7	0.5
		938.68	0.04	2.09	0.15
		Eu-150	1.13E+09	333.971	0.012
439.401	0.015			80	3
505.52	0.03			4.8	0.18
584.274	0.012			52.6	2.2
712.205	0.015			1.08	0.05
737.455	0.015			9.6	0.4
748.057	0.012			5.18	0.19
751.068	0.014			2.14	0.09
869.256	0.014			1.85	0.07
1049.04	0.03			5.4	0.3
1170.587	0.024			1.33	0.05
1197.108	0.024			1.13	0.06
1246.968	0.024			1.91	0.08
1343.777	0.022	2.59	0.11		
1485.49	0.03	1.9	0.1		
Gd-151	1.07E+07	153.57	0.06	5.1	0.8
		174.65	0.06	2.4	0.4
		243.22	0.06	4.6	0.8
Eu-152	4.27E+08	121.783	0.002	28.4	0.4
		244.699	0.001	7.49	0.13
		344.281	0.002	26.6	0.3
		411.115	0.005	2.23	0.03

Nuclide	Half-Life (Seconds)	Energy (keV)	Energy Uncert. (keV)	Yield (%)	Yield Uncert. (Abs.+)
Eu-152	4.27E+08	443.976	0.005	2.78	0.07
		778.903	0.006	12.96	0.13
		867.388	0.008	4.15	0.09
		964.131	0.009	14.34	0.2
		1085.914	0.003	9.92	0.16
		1089.7	0.015	1.71	0.025
		1112.116	0.017	13.55	0.2
		1212.95	0.012	1.399	0.018
		1299.124	0.012	1.626	0.025
		1408.011	0.014	20.87	0.11
Eu-152m	5.76E+03	89.847	0.006	69.93	0.2
Gd-153	2.09E+07	97.432	0	30.2	0.6
		103.181	0	21.4	0.7
Sm-153	1.67E+05	103.18	0.001	31.4	0.4
Eu-154	2.71E+08	123.068	0.003	40.4	0.8
		247.932	0.015	6.83	0.13
		591.76	0.03	4.91	0.09
		692.42	0.04	1.78	0.04
		722.3	0	20	0.4
		756.86	0.03	4.5	0.09
		873.2	0.03	12.09	0.22
		996.3	0.03	10.34	0.19
		1004.76	0.03	17.9	0.4
		1274.51	0.07	34.4	0.7
		1596.45	0.07	1.8	0.04
Eu-155	1.48E+08	105.306	0.002	21.8	0.6
Tb-155	4.60E+05	86.55	0.03	31.8	1.9
		105.318	0.003	24.9	1.4
		148.64	0.01	2.63	0.15
		161.29	0.01	2.73	0.16
		163.28	0.01	4.4	0.3
		180.08	0.01	7.4	0.5
		262.27	0.01	5.2	0.3
		340.67	0.01	1.17	0.07
		367.36	0.01	1.42	0.08
Tb-160	6.25E+06	197.035	0.001	5.61	0.13
		215.646	0.001	4.41	0.09
		298.58	0.002	28.9	0.6
		765.28	0.04	2.36	0.06
		879.383	0.003	32.9	0.6
		962.317	0.004	10.53	0.2
		966.171	0.003	27.2	0.5
		1002.88	0.04	1.175	0.024
		1005	1	1.175	0.024
		1115.12	0.03	1.68	0.04
		1177.962	0.004	16.2	0.3
		1199.89	0.03	2.58	0.05
		1271.88	0.008	8.13	0.15
Tm-167	7.99E+05	207.8	0.2	41	8
		531.5	0.8	1.59	0.21

Nuclide	Half-Life (Seconds)	Energy (keV)	Energy Uncert. (keV)	Yield (%)	Yield Uncert. (Abs.+)
Tm-168	8.04E+06	99.288	0.002	3.6	0.7
		184.285	0.001	17.5	0.5
		198.241	0.001	52.6	1.3
		447.515	0.003	23	0.6
		546.802	0.005	2.55	0.06
		631.703	0.003	8.85	0.21
		645.736	0.01	1.45	0.04
		720.392	0.005	11.9	0.3
		730.66	0.002	5.06	0.12
		741.356	0.003	12.3	0.3
		815.99	0.004	49	1.2
		821.164	0.005	11.5	0.3
		829.958	0.007	6.74	0.16
		914.944	0.006	2.99	0.07
1277.47	0.02	1.62	0.04		
Yb-169	2.77E+06	93.615	0	2.61	0.06
		109.78	0	17.5	0.4
		118.19	0	1.87	0.04
		130.524	0	11.31	0.21
		177.214	0	22.2	0.5
		197.958	0	35.8	0.7
		261.079	0	1.71	0.03
		307.738	0	10.05	0.19
Lu-171	7.12E+05	72.379	0.002	2	0.07
		75.891	0.002	6.08	0.19
		85.603	0.002	1.08	0.04
		667.429	0.012	11.1	0.4
		689.373	0.013	2.37	0.08
		712.681	0.014	1.14	0.04
		739.799	0.014	48.1	1.6
		780.728	0.015	4.35	0.14
		839.985	0.016	3.04	0.12
		853.095	0.006	2.55	0.08
Hf-172	5.90E+07	81.75	0.05	4.5	1.1
		114.06	0.1	2.6	0.7
		122.92	0.1	1.1	0.3
		125.82	0.05	11	3
		127.91	0.1	1.5	0.4
Lu-172	5.79E+05	90.647	0.003	4.47	0.1
		112.793	0.005	1.25	0.03
		181.53	0.004	20.5	0.8
		203.436	0.004	4.8	0.3
		270.03	0.009	1.91	0.07
		279.709	0.016	1.19	0.04
		323.887	0.023	1.53	0.04
		372.511	0.017	2.7	0.08
		377.509	0.019	3.43	0.09
		410.3	0.016	1.99	0.05
		432.544	0.016	1.68	0.04
		490.451	0.019	1.92	0.08
528.266	0.024	4.04	0.15		

Nuclide	Half-Life (Seconds)	Energy (keV)	Energy Uncert. (keV)	Yield (%)	Yield Uncert. (Abs.+)
Lu-172	5.79E+05	540.17	0.03	1.43	0.07
		697.3	0.03	6.19	0.18
		810.08	0.03	16.8	0.4
		816.34	0.03	1.16	0.04
		900.73	0.03	29.9	0.7
		912.09	0.03	15.3	0.4
		929.11	0.03	2.99	0.07
		1002.73	0.03	5.3	0.4
		1022.35	0.03	1.38	0.05
		1093.61	0.03	62.5	1.5
		1113.01	0.04	1.6	0.06
		1488.91	0.07	1.15	0.03
		1542.79	0.07	1.019	0.023
		1584.04	0.07	2.63	0.06
1621.88	0.08	2.13	0.06		
Lu-173	4.32E+07	100.696	0.011	4.5	0.5
		171.393	0.016	2.64	0.25
		179.347	0.013	1.21	0.12
		272.089	0.018	18.5	1.7
		636.07	0.04	1.25	0.12
Hf-175	6.05E+06	89.36	0	2.346	0
		343.4	0	86.86	0.07
		432.8	0	1.7	0
Lu-177	5.80E+05	112.952	0.003	6.4	0.4
		208.359	0.01	11	0.8
Lu-177m	1.39E+07	105.359	0.001	12.34	0.24
		112.95	0.005	20.4	0.4
		121.621	0.001	5.91	0.15
		128.503	0.001	15.5	0.3
		136.725	0.001	1.4	0.05
		147.164	0.001	3.51	0.14
		153.284	0.001	16.9	0.3
		171.858	0.001	4.81	0.12
		174.399	0.001	12.61	0.24
		177.001	0.001	3.43	0.12
		204.105	0.001	13.8	0.3
		208.366	0.001	57.7	1.1
		214.434	0.001	6.59	0.16
		218.104	0.001	3.28	0.12
		228.484	0.001	37	0.7
		233.861	0.001	5.58	0.14
		249.674	0.001	6.14	0.18
268.785	0.001	3.43	0.12		
281.787	0.001	14.1	0.3		
291.42	0.1	1.02	0.07		
296.458	0.001	5.08	0.14		
299.051	0.002	1.8	0.5		
305.503	0.001	1.82	0.05		

Nuclide	Half-Life (Seconds)	Energy (keV)	Energy Uncert. (keV)	Yield (%)	Yield Uncert. (Abs.+)		
Lu-177m	1.39E+07	313.725	0.021	1.26	0.05		
		319.021	0.001	10.5	0.3		
		321.316	0.002	1.2	0.06		
		327.683	0.001	18.1	0.5		
		341.643	0.001	1.69	0.06		
		367.418	0.01	3.15	0.11		
		378.503	0.001	29.7	1.2		
		385.03	0.001	3.13	0.12		
		413.664	0.001	17.4	0.6		
		418.539	0.001	21.3	0.8		
		465.842	0.001	2.35	0.12		
		Lu-177x	1.39E+07	105.36	0.02	12.2	1.3
				112.952	0.003	21.8	2.4
				121.62	0.003	6	2.1
128.48	0.02			15.5	1.8		
136.73	0.006			1.39	0.2		
147.165	0.005			3.7	1.3		
153.25	0.04			18.2	2.1		
171.868	0.008			5	1.8		
174.37	0.06			12.8	1.5		
177.05	0.08			3.4	0.4		
204.06	0.06			14.5	1.7		
208.359	0.01			62	7		
214.45	0.06			6.7	0.8		
218.097	0.011			3	1.1		
228.44	0.06			38	5		
233.83	0.06			5.7	0.7		
249.69	0.03			6.2	0.8		
268.801	0.014			3.4	1.2		
281.78	0.07			14.2	1.6		
291.42	0.1			1.02	0.15		
296.45	0.08			5.5	0.7		
299.03	0.1			1.53	0.18		
305.52	0.08			1.73	0.19		
313.69	0.08			1.29	0.15		
319.04	0.02			10	4		
321.33	0.04			1.07	0.13		
327.66	0.08	17.8	2				
341.64	0.08	1.81	0.25				
367.44	0.04	3	1.1				
378.51	0.08	28	4				
385.02	0.08	3	0.4				
413.7	0.04	17	6				
418.51	0.1	20.3	2.3				
465.96	0.12	2.4	0.3				
Hf-178m	9.78E+08	88.871	0.015	63.1	1.5		
		93.185	0.006	17.2	0.4		

Nuclide	Half-Life (Seconds)	Energy (keV)	Energy Uncert. (keV)	Yield (%)	Yield Uncert. (Abs.+)
Hf-178m	9.78E+08	213.434	0.006	81.7	1.7
		216.668	0.008	64.7	1.4
		237.38	0.013	9.3	0.3
		257.642	0.009	16.7	0.4
		277.399	0.014	1.39	0.07
		296.813	0.011	9.67	0.25
		325.556	0.007	94.1	1.8
		426.359	0.009	96.9	2
		454.048	0.013	16.6	0.5
		495.022	0.013	71.4	1.8
		535.04	0.015	9.7	0.3
Hf-179m	2.17E+06	122.7	0.07	28	1.6
		146.15	0.07	27.4	1.5
		169.78	0.07	19.6	1.2
		192.66	0.11	21.7	2.1
		217.04	0.12	9.1	0.8
		236.48	0.14	19	0.9
		257.38	0.17	3.3	0.6
		268.85	0.14	11.4	0.8
		315.93	0.14	20.5	0.8
		362.55	0.15	40.1	1.7
		409.7	0.2	21.7	1
Hf-181	3.66E+06	453.59	0.2	69	4
		133.021	0.019	43.3	0.6
		136.26	0.018	5.85	0.19
		345.93	0.06	15.12	0.13
Ta-182	9.89E+06	482.18	0.09	80.5	0.5
		100.106	0	14.1	0.3
		113.673	0	1.88	0.04
Ta-182	9.89E+06	152.431	0	6.93	0.13
		156.388	0	2.64	0.05
		179.395	0	3.08	0.06
		198.353	0	1.44	0.03
		222.11	0	7.49	0.14
		229.322	0.001	3.63	0.07
		264.075	0	3.61	0.07
		1001.695	0.002	2.07	0.04
		1121.301	0.002	34.9	0.6
		1189.05	0.002	16.2	0.3
		1221.407	0.002	27	0.5
Re-183	6.05E+06	1231.016	0.002	11.44	0.2
		1257.418	0.002	1.49	0.03
		1289.156	0.002	1.349	0.024
		99.08	0.001	2.69	0.08
		107.935	0.001	2.17	0.07
		109.73	0.001	2.87	0.09
		162.327	0.001	23.3	0.7
		208.811	0.001	2.95	0.09
		246.062	0.002	1.31	0.05

Nuclide	Half-Life (Seconds)	Energy (keV)	Energy Uncert. (keV)	Yield (%)	Yield Uncert. (Abs.+)
Re-183	6.05E+06	291.728	0.002	3.05	0.18
Re-184	3.28E+06	111.207	0.007	17.1	0.8
		252.845	0.01	3	0.3
		641.915	0.02	1.94	0.06
		792.067	0.022	37.5	1.1
		894.76	0.019	15.6	0.5
		903.282	0.019	37.9	1.1
Re-184m	1.43E+07	104.729	0.007	13.3	0.4
		111.207	0.007	5.9	0.4
		161.269	0.015	6.64	0.22
		215.326	0.012	2.84	0.12
		216.547	0.012	9.6	0.4
		226.748	0.01	1.51	0.06
		252.845	0.01	10.9	0.5
		318.008	0.01	5.88	0.19
		384.25	0.012	3.2	0.11
		536.674	0.015	3.37	0.11
		792.067	0.022	3.77	0.14
		894.76	0.019	2.81	0.13
		903.282	0.019	3.82	0.14
		920.933	0.021	8.3	0.3
		1173.77	0.03	1.24	0.08
Os-185	8.09E+06	592.066	0.01	1.33	0.04
		646.116	0.009	81	1
		717.424	0.012	4.12	0.1
		874.813	0.013	6.61	0.16
		880.523	0.013	5	0.13
Ir-188	1.49E+05	155.05	0.04	30	3
		322.91	0.04	1.62	0.15
		477.99	0.04	14.7	0.6
		632.99	0.02	18	3
		634.91	0.15	5	0.8
		672.5	0.05	1.44	0.12
		824.34	0.08	1.03	0.1
		829.42	0.06	5.1	0.5
		1017.63	0.06	1.06	0.1
		1096.54	0.06	1.46	0.14
		1174.59	0.1	1.32	0.15
		1209.77	0.06	6.9	0.7
		1435.42	0.15	1.48	0.14
		1452.28	0.15	1.06	0.1
		1457.19	0.15	1.75	0.17
		1465.24	0.15	1.35	0.15
		1574.48	0.15	2.63	0.24
		1705	0	1.04	0.16
		1715.67	0.1	6.2	0.5
		1944.08	0.2	3.9	0.4
		2049.78	0.2	5	0.4
		2059.65	0.2	7.1	0.6
		2096.9	0.4	5.7	0.8
		2099.1	0.4	4.7	0.7

Nuclide	Half-Life (Seconds)	Energy (keV)	Energy Uncert. (keV)	Yield (%)	Yield Uncert. (Abs.+)
Ir-188	1.49E+05	2193.7	0.4	2	0.4
		2214.59	0.2	18.7	1.6
Pt-188	8.81E+05	73.6	0	21.7	0.9
		140.35	0.1	2.33	0.15
		187.59	0.1	19.4	1.2
		195.05	0.1	18.6	1.2
		381.43	0.1	7.5	0.5
		423.34	0.1	4.4	0.3
Re-188	6.11E+04	71.4	0	1.01	0.08
		155.032	0.012	14.9	0.6
		477.99	0.02	1.01	0.02
		632.98	0.02	1.25	0.05
Ir-190x	1.02E+06	71.4	0	18	4
		186.68	0.04	52	3
		196.85	0.15	3.4	0.4
		198.08	0.2	1.94	0.24
		207.91	0.06	1.19	0.17
		223.81	0.05	3.74	0.22
		288.22	0.1	1.64	0.15
		294.75	0.12	6.6	0.8
		361.09	0.05	13	0.6
		371.24	0.05	22.8	0.7
		380.03	0.12	2.03	0.11
		397.36	0.06	6.5	0.3
		407.22	0.06	4.6	0.7
		407.22	0.06	23.9	1.4
		420.63	0.12	1.64	0.09
		431.62	0.07	2.74	0.18
		447.81	0.08	2.55	0.16
		477.8	0.3	1.82	0.22
		502.55	0.08	1.25	0.08
		518.55	0.07	34	1.6
557.95	0.07	30.1	1.3		
569.3	0.07	28.5	1.3		
605.14	0.07	39.9	1.9		
630.91	0.16	2.9	0.4		
656.02	0.08	1.16	0.08		
726.22	0.08	3.78	0.17		
768.57	0.08	2.21	0.12		
828.99	0.07	3.5	0.3		
839.14	0.12	1.14	0.06		
1036.05	0.2	2.42	0.16		
Pt-191	2.51E+05	82.398	0.007	4.9	0.7
		96.517	0.009	3.3	0.4
		129.4	0.007	3.2	0.5
		172.19	0.02	3.5	0.4
		178.96	0.03	1.02	0.12
		268.71	0.08	1.65	0.23
		351.17	0.03	3.4	0.4
		359.88	0.03	6	0.7
409.44	0.02	8	0.9		

Nuclide	Half-Life (Seconds)	Energy (keV)	Energy Uncert. (keV)	Yield (%)	Yield Uncert. (Abs.+)
Pt-191	2.51E+05	456.47	0.05	3.4	0.4
		538.87	0.05	13.7	1.6
		624.06	0.06	1.41	0.16
Ir-192	6.38E+06	75.7	0	2	0.05
		205.796	0	3.3	0.04
		295.958	0	28.67	0.1
		308.457	0	30	0.09
		316.508	0	82.81	0.21
		468.072	0	47.83	0.17
		484.578	0	3.18	0.03
		588.584	0.001	4.515	0.015
		604.415	0	8.23	0.06
		612.466	0	5.309	0.018
Au-194	1.37E+05	293.58	0.03	10.2	0.8
		328.5	0.03	60	5
		364.87	0.04	1.48	0.12
		482.8	0.04	1.11	0.09
		511	0	3.6	0
		528.76	0.1	1.62	0.2
		622.05	0.1	1.68	0.2
		645.18	0.03	2.11	0.15
		938.71	0.03	1.09	0.08
		948.29	0.04	2.16	0.17
		1104.06	0.05	1.98	0.16
		1150.78	0.05	1.37	0.11
		1175.34	0.05	1.98	0.16
		1218.76	0.05	1.09	0.08
		1342.15	0.1	1.2	0.11
		1468.89	0.05	6.3	0.5
		1592.4	0.1	1.08	0.14
1595.8	0.1	1.68	0.2		
1885.9	0.1	1.86	0.16		
1887	0.1	1.38	0.14		
1924.18	0.05	1.98	0.16		
2043.67	0.06	3.5	0.3		
Au-195	1.61E+07	98.88	0.02	10.9	0.9
Pt-195m	3.47E+05	98.9	0.02	11.4	0.9
		129.79	0.02	2.83	0.21
Au-196	5.34E+05	75.7	0	16.2	0.7
		333.03	0.05	22.9	0.6
		355.73	0.05	87	1
		426.1	0.08	7.2	0.13
Au-198	2.33E+05	70.819	0.002	1.38	0.12
		411.804	0.001	95.58	0.12
Au-199	2.71E+05	70.819	0.002	8.3	0.5
		80.3	0	3.63	0.22
		158.379	0	36.9	1.1
TI-202	1.06E+06	208.206	0	8.4	0.3
		80.3	0	17.1	0.4
		439.56	0.01	91.4	1
Hg-203	4.03E+06	279.197	0.001	81.46	0.13

Nuclide	Half-Life (Seconds)	Energy (keV)	Energy Uncert. (keV)	Yield (%)	Yield Uncert. (Abs.+/-)
Pb-204m	4.03E+03	374.74	0.1	89	16
		899.15	0.1	99	16
		911.74	0.15	96	16
Bi-207	1.02E+09	569.702	0.002	97.8	0.4
		1063.662	0.004	74.08	0.25
		1460	1.5	1.61	0.06
		1770.237	0.01	6.87	0.03
Bi-208	1.16E+13	2614.533	0	100	0

Totals: 134 Nuclides 885 Energy Lines